8-2013

# Structure-Function Relationship of the Ligand-Binding Domain of the Fibroblast Growth Factor Receptor

Ryan Thurman
*University of Arkansas, Fayetteville*

# Structure-Function Relationship of the Ligand-Binding Domain of the Fibroblast Growth Factor Receptor

Structure-Function Relationship of the Ligand-Binding Domain of the Fibroblast Growth Factor Receptor

A dissertation submitted in partial fulfillment
of the requirements for the degree of
Doctor of Philosophy in Chemistry

By

Ryan Thurman
University of Central Arkansas
Bachelor of Science in Chemistry, 2005

August 2013
University of Arkansas

This dissertation is approved for recommendation to the Graduate Council.

_____
Dr. Suresh K. Thallapuranam
Dissertation Director

_____
Dr. Dan Davis
Committee Member

_____
Dr. Roger Koeppe II
Committee Member

_____
Dr. James Hinton
Committee Member

_____
Dr. Frank Millett
Committee Member

**Abstract**

The interactions between FGF and fibroblast growth factor receptors are responsible for the regulation of key cellular processes. FGF is important in both germ cell and embryonic developments. FGF continues to play important roles during adulthood by regulating embryogenesis, cell differentiation, and wound healing (1-7). The regulations of these cellular events are initiated through FGF binding to the fibroblast growth factor receptors. The complex formed by FGF and the receptor involves a key interaction with heparin. Through interactions with heparin, the FGF, FGFR and Heparin form a 2:2:2 complex (8). This complex formation results in autophosphorylation in the tyrosine kinase domain in the cytoplasm. The autophosphorylation events lead to downstream signaling that result in the regulation of previously mentioned cellular processes (9, 10). Mutations within the FGF or FGFR may interfere with signaling or protein stability. Changes in the signaling efficiency by FGF or the FGFR are shown to lead to disease states There exist many point mutations in the FGF receptor that result in craniofacial, hypogonadotropic hypogonadism, anosmia, and tumor development. Using site-directed mutagenesis we have shown non-covalent interactions formed by Kallmann syndrome linked mutations result in a loss-of-binding between FGF and the FGF receptor. This evidence has shown that the non-covalent ligand binding interactions lost are due to changes in the D2 structure or binding site. Additionally, the R203C mutation, linked to breast cancer, was tested and determined to break a D2 stabilizing cation-π bond. The cation-π stabilized the binding interaction with heparin and provides stability to the D2 domain. Although the decreased stability of the D2 domain supports a loss-of-function, we are currently investigating intermolecular disulfide bond formation between adjacent receptor. This is a known mechanism among FGF receptors that may lead to signaling in the absence of a ligand.

**Table of Contents**

**List of Figures and Tables**

**List of Publications**

I. Ryan D. Thurman, Karuppanan Muthusamy Kathir, Dakshinamurthy Rajalingam, Thallapuranam K. Suresh Kumar. Molecular Basis for the Kallmann Syndrome-Linked Fibroblast Growth Factor Receptor Mutation. Biochemical and Biophysical Research Communications 425 (2012) 673–678.

## Introduction

### I. Fibroblast Growth Factor Receptor Structure

The fibroblast growth factor receptor signaling has been shown to play a critical role in embryonic development, angiogenesis, wound healing, cell differentiation and migration (11-14). The fibroblast growth factor receptors (FGFR) consist of 3 extracellular domains (D1, D2, and D3), a single transmembrane helix, juxtamembrane domain and two cytoplasmic tyrosine kinase domains. A total of four FGF receptors make up the human FGFR family. FGFR ligands, FGF and heparin are the ligands that bind to and activate the FGF receptor. The FGF receptor is activated when a 2: 2: 2 extracellular dimeric complex is formed containing two heparin molecules and two FGF molecules bound to two FGF receptors (8). Following the binding of heparin and FGF to the extracellular D2-D3 domains of the FGF receptor, autophosphorylation of the cytoplasmic tyrosine kinase domains occurs. (9, 10) Autophosphorylation of the tyrosine kinase domains is the mechanism by which signal transduction occurs in the FGFRs(15). The role of D2 on the FGFR is critical for signal transduction following the binding of FGF. Mutations that occur on the D2 domain have been associated with Kallmann syndrome, breast cancer and colon cancer (16-18). Similarly, mutations on the D3 domain have been associated with Pfeifer syndrome and Cruzon syndrome. Many of the disease-linked mutations occurring in the FGF receptors are located in the extracellular D1, D2 and D3 domains.

The D1 domain is the first of three extracellular globular domains of the FGFR. The D1 domain is a β-sandwich structure composed of 99 residues forming 10 β-strands. The D1 domain molecular weight is approximately 10.4 kDa (19). The D1 domain is linked to the D2 domain by a 24 amino acid linker domain. The linker between the D1 and D2 domain contains a patch of eleven residues formed by 9 residues that are aspartic acid or glutamic acid. This negatively

charged region in the linker domain is termed the “acid box” and along with the D1 domain are believed to play a role in an autoinhibition mechanism (20).

The D2 domain is a 13.7 kDa that consists of 12 beta strands. The beta strands of D2 form two β-sheets, which allows for a β-sandwich structure (21). Two cysteine residues form a disulfide bond between the two beta sheets and are highly conserved in the FGFRs. The D2 domain is the binding site for ligands heparin and FGF. The heparin-binding site on the D2 domain is highly conserved among the FGF receptors. The heparin-binding site on the D2 domain is made of residues K160, K163, K172, K175, and K177 (figure 1.1) (8) The five-lysine residues on the D2 domain form nine hydrogen bonds with the sulfate groups of heparin. The active dimeric complex of FGF, FGFR and heparin is a 2: 2: 2 complex (8). The requirement of heparin for FGFR signaling and autophosphorylation is highly debated and not fully understood.

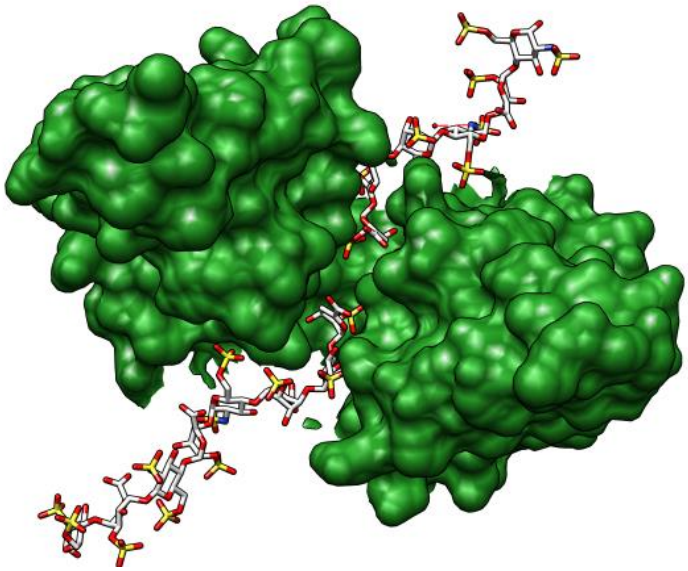

**Figure 1.1** - Shows the chimera representation of the x-ray structure of the D2 domain in complex with heparin (pdb:1EV2) (8). The figure shows the dimeric structure with the heparin molecules oriented between the two D2 domains.

FGF receptors 1-4 have been shown to interact with FGF. The structure of D2 forms a hydrophobic pocket near the C-terminal to form the FGF binding site. The beta strands of D2

making up the FGF binding site include: βA' strand and βG strand at the C-terminal end of D2. Residues located on the βA' and

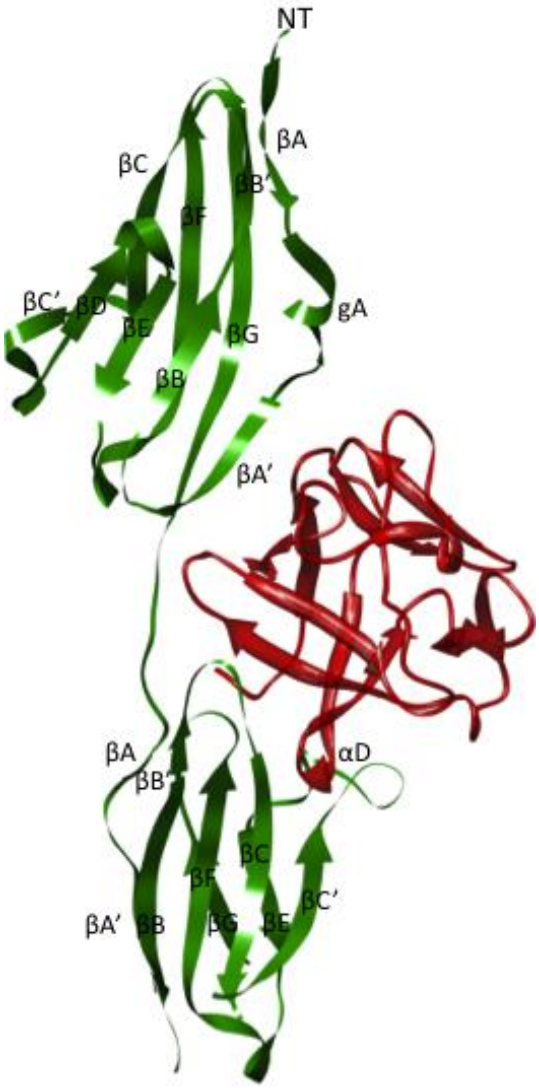


**Figure 1.2** – Chimera representation of FGFR2 D2-D3 bound to FGF-2 (pdb: 1EV2). The FGFR2 D2, D3 and linker domains are colored in green. Fibroblast growth factor 2 bound to the FGFR is colored in red. The FGF binding site on the D2 domain is located at the βA' and βG.

βG strands near the binding site are highly conserved. The D2 residues forming the binding interaction with FGF include A167, H166 and V168 (8). Valine 248 and the aliphatic portion of arginine 250 in the D2-D3 linker domain form a hydrophobic interaction with FGF. Additionally, Asp 282 in the D3 domain forms a hydrogen bond with Arg-250 further stabilizing

the FGFR-FGF interaction (8). The D2 receptor is capable of binding FGF without the D3 or linker domains (21). The FGF binding site on the D3 domain includes the βB'-βC, βC'-βE and βF-βG. Asp-320 located on the D3 domain forms a hydrogen bond with FGF. Additionally, proline 285, His 286 and Gly 315 of the D3 domain form hydrophobic interactions FGF (22). Splice variants in the FGFR's allows for variations in the binding site found on the D3 domain.

The D3 domain is the third extracellular domain located nearest to the cell membrane. A 13-residue linker domain connects the D2 domain with the D3 domain. The D3 domain is composed of 97 amino acids forming 9 beta-strands. The 9 beta strands form a beta sandwich structure containing one disulfide bond. The binding site of FGF is primarily located on the D2 domain. However, there are additional non-covalent interactions formed between FGF and the D3 domain.

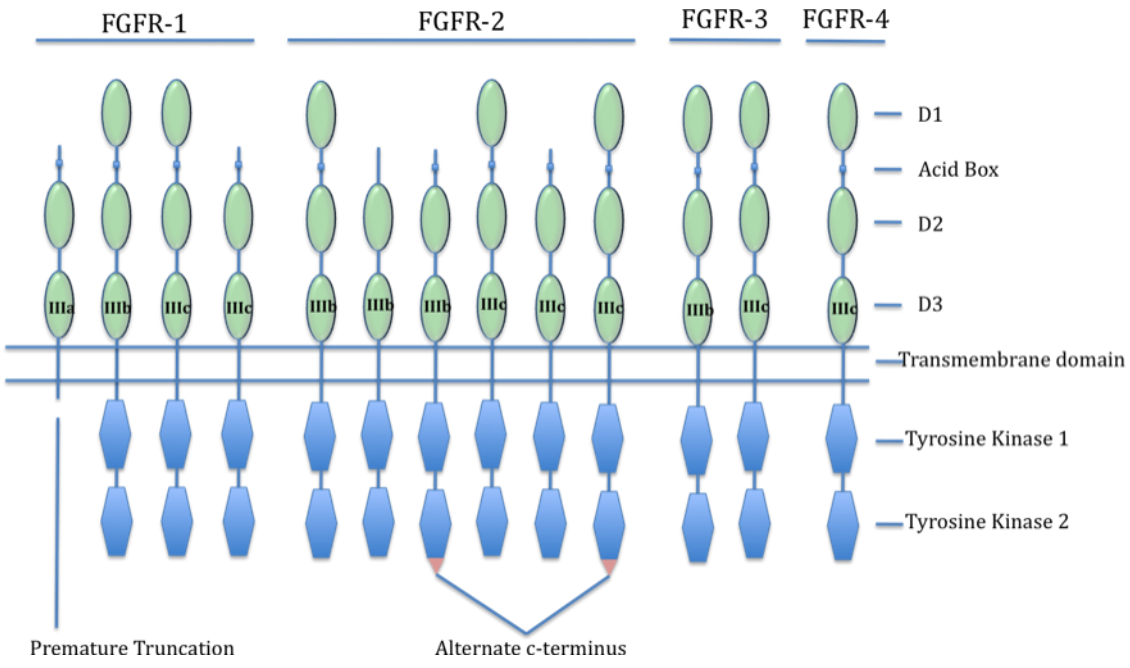


**Figure 1.3** – Splice variants that occur in FGFR's 1 – 4. FGFR's 1 and 2 are shown to exist with and without the D1 domain. Additionally, FGFR-2 variants may have an alternate c-terminus. The "acid-box" is present in all four of the FGF receptors, but may be absent one of the FGFR2 variants.

FGFR splice variants allow for an increased binding selectivity among the 22 FGF proteins expressed in humans. The possible splice variants are shown in figure 1.3. The D1 domain and the acid-box have been suggested to be required in an auto regulation mechanism. Cleavage of the D1 domain or removal of the acid-box may be a mechanism to increase signaling of the FGFR. FGF receptors 1 and 2 splice variants to include and remove the D1 domain and the acid-box**.** The D3 domain of FGFR-1, FGFR-2 and FGFR-3 encoded by the exon Ig IIIa is spliced to form the Ig IIIb or Ig IIIc variants. Exon splice variants of the FGFR includes exons a, b and c. Exon 7 (denoted exon "a") encodes from the N-terminal region of the D3 domain. Exons 8 (denoted exon "b") and exon 9 (denoted "c")

| FGF Receptor Isoform | Ligand Specificity |
|---|---|
| FGFR1b | FGF1, FGF2, FGF3, FGF10 |
| FGFR1c | FGF1, FGF2, FGF4, FGF5, FGF6 |
| FGFR2b | FGF1, FGF3, FGF7, FGF10, FGF22 |
| FGFR2c | FGF1, FGF2, FGF4, FGF6, FGF9, FGF17, FGF18 |
| FGFR3b | FGF1, FGF9 |
| FGFR3c | FGF1, FGF2, FGF4, FGF8, FGF9, FGF17, FGF18, FGF23 |
| FGFR4 | FGF1, FGF2, FGF4, FGF6, FGF8, FGF8, FGF9, FGF16, FGF17, FGF18, FGF19 |

**Table 1.4** - Ligands capable of binding to each of the FGFR isoforms. The table provides evidence that FGF1 acts as a universal binding ligand (23, 24).

encode for the c- terminal segment of the D3 domain. These isoforms are denoted by the "b" or "c" nomenclature following the FGFR. These variations allow varied specificity for the 22 FGFs as it altars the residues that form interactions with FGF.

Splice variants in the D3 domain occur in FGFRs 1, 2 and 3 but not in FGFR 4. Table 1.4 indicates the receptor – ligand specificities created by the b and c isoforms of the FGFR. Each of the receptor forms is expressed in specific tissues. The FGFR2b form is exclusively expressed in epithelial tissue. The FGFR2c isoform is exclusively found in mesenchyme tissue (25-27).The developmental roles of the FGFRs have been shown to be widely varied for specific tissue types and stages of development.

The use of knockout mice has been used to identify the roles of the FGFRs during development. The FGFR1 defect mice resulted in a disruption of cell migration through the primitive streak and ultimately embryonic death. The FGFR1c isoform disruption also results in embryonic death (28). The FGFR1b isoform disruption does not reflect the FGFR1c results – producing no identifiable changes in the phenotype {{;941 Bellusci,S. 1997;}}. Similar to the FGFR1 - the FGFR2 defect mice also resulted in embryonic death. Mice containing the disruption of the FGFR2b isoform resulted in phenotypes reflecting impaired development of the lungs and limbs. The disruption of the FGFR2c isoform resulted in a phenotype reflecting impaired skull and bone development. The FGFR2c isoform did not produce lethality in the mice. Disruption of FGFR3 and FGFR4 in mice resulted in minor phenotypic changes, but was not lethal (29-31).

**B. FGF**

**FGF Family and Structural Conservation**

Fibroblast growth factor research was initiated following the discovery of FGF1 (acidic fgf) in 1974(32). The fibroblast growth factor family consists of a total of 23 polypeptides. Twenty-two fibroblast growth factors have been identified and studied in mammals. The

fibroblast growth factors consist of 3 exons and combine to form an approximately 16 kDa protein of 150-250 amino acids (33). Variation occurs within the start codon including the placement of secondary CUG start codons(34, 35). The location of this CUG sequence is able to increase the typical size of the FGF protein from 16 kDa (FGF-1) to as many as 100 kDa (FGF-12). The FGF structures are composed of beta sheets arranged in tre-foil formation (36). The trefoil structure is composed of 12 antiparallel beta-strands. The core of the structure contains a sequence of 28 conserved amino acids. Among the 28 conserved amino acids 6 residues are identical. Conservation of these residues helps to provide only small variations to the FGFR binding site located within the 28 amino acids (37). The fibroblast growth factors are typically secreted proteins so they may act on the cell surface FGFR.

Many FGF's contain a cleavable N-terminal signal peptide (1). The N-terminal signal peptide allows for classical secretion mechanism. However, there exists a number of FGF's that are found in the extracellular space that do not contain N-terminal signal sequences. FGF1, FGF2, FGF11-FGF14 lack an N-terminal signal sequence for secretion. These FGF's have shown specific activity related to the nucleus or may be secreted via a mechanism independent of the reticulum-Golgi pathway (38, 39).The secretion mechanism of each FGF will be further discussed.

The fibroblast growth factors all bind to heparin sulfate. Within the beta barrel structure of FGF, lysine and arginine residues on beta strands β-10 and β-11 contribute to the heparin binding site of FGF (40, 41). Heparin sulfate is the side chain of cell surface proteoglycans. The binding of FGF's to HS helps to reduce proteolytic degredation of FGF. It is unclear if heparin sulfate is required for FGF to induce signaling through the FGFR (32, 42). Heparin knockout cells in proliferation studies suggest that heparin is a requirement for signaling (40). Heparin

sulfate supports dimerization of the FGFR as well as binding of FGF to the FGF receptor (43).

**General FGF Interactions**

The fibroblast growth factors each bind to FGFR1, FGFR2, FGFR3 and/or FGFR4 with varying affinities. The FGF-FGFR interface is composed largely of hydrophobic interactions. The FGF protein residues interacting with the receptor are located on the β1-strand, β1-β2 turn, β2-strand, β3-β4 loop, β8-β9 turn, β9-strand and β12-strand (8). The FGF receptor binding residues of FGF are largely hydrophobic and conserved to these locations. Only the Y24-X-X sequence motif of β1-strand is consistent in the FGF sequences (8). The binding site of FGF-FGFR is conserved on the D2 domain.

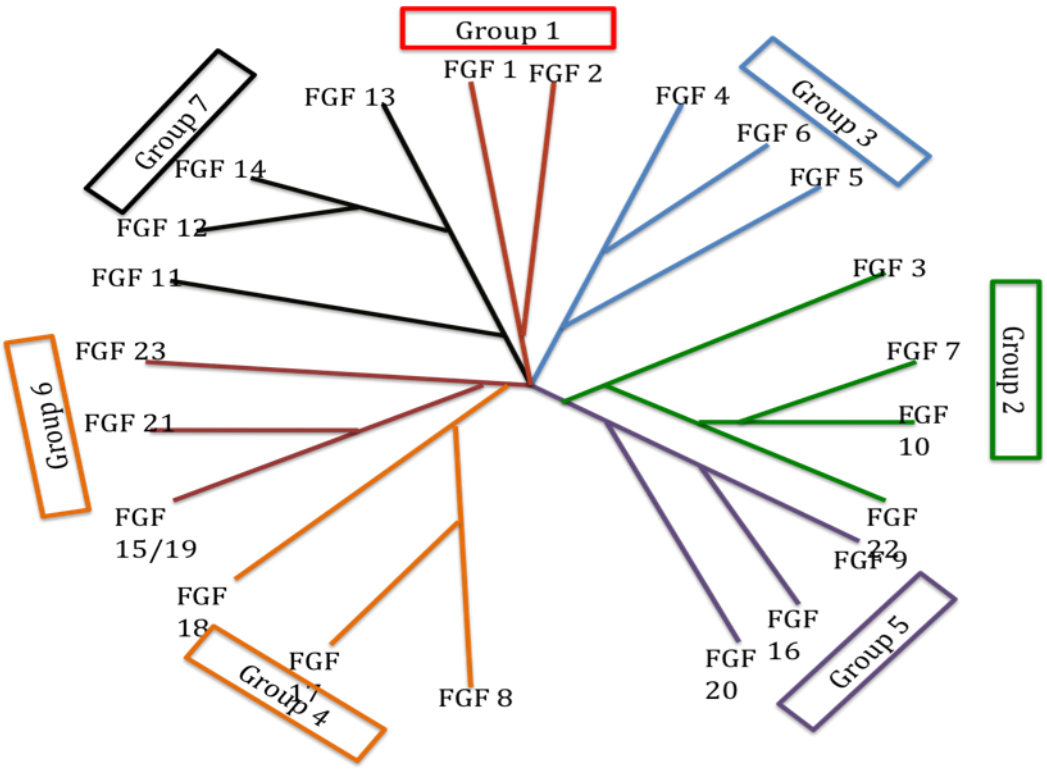


**Figure 1.5** - *Group 1 FGF's* were the first to be identified of the Fibroblast growth factors and consists of FGF-1 and FGF-2. The group-1 FGF's were first purified from bovine pituitary extracts (32, 44).

Fibroblast growth factors are sub grouped into 6 families (figure 1.5). (**Group 1**: FGF1 and FGF2; **Group 2**: FGF3, FGF7, FGF10 and FGF22; **Group 3**: FGF4, FGF5 and FGF6; **Group 4**: FGF8, FGF17 and FGF18; **Group 5**: FGF9, FGF16 and FGF20; **Group 6**: FGF19, FGF21 and FGF23) (1 - 3).

Acidic fibroblast growth factor or FGF-1 is named as such for its acidic isolectric point. Basic fibroblast growth factor or FGF-2 was given the name basic as a result of it basic isolectric point. The roles that FGF-1 and FGF-2 play in multicellular organisms has been documented as critical functions for the development of tissues. One unique character of the group-1 FGF's is they do not have a signaling peptide to allow protein delivery through classical secretion (44).

The two proposed non-classical secretion pathway for group-1 FGF's include cell damage and novel secretion methods. McNeil et. al. have shown cell damage results in the release of FGF-2(45). The types of cell damage studies include cell death, chemical injury or wound healing. FGF-2 release has also been observed in cells subjected to irradiation. Additionally, *Kathir et. al* have shown a novel FGF secretion mechanism involving an interaction with S100A13. Previous studies have shown S100A13 to act as a peptide transporter for secretion across the membrane. S100A13 was shown to bind to FGF-1 allowing for S100A13 to transport FGF's across the membrane (39).

**Ras/MAPK Signaling Pathway**

Binding fibroblast growth factors to the FGF receptors results in the autophosphorylation in the tyrosine kinase domain of the receptor. PLC-γ and Src bind to the kinase domain of the FGFR (46). Upon binding, PLC-γ and Src become phosphorylated (47). Adaptor proteins Grb2 and Shc bind to the autophosphorlyed sites. The SH3 domain of Grb2 binds to Sos (Ras guanine

nucleotide releasing factor). The Grb2-Sos complex recruits Ras in the plasma membrane. The complex is also activated by the exchange of GDP for GTP by Sos. Ras activation of a signaling cascade involving the ser/thr kinase Raf, the dual specificity MAP kinase (MEK), and MAP kinase (48). The Ras/MAP kinase pathway further regulates activities in the cell including proliferation, migration and apoptosis (49).

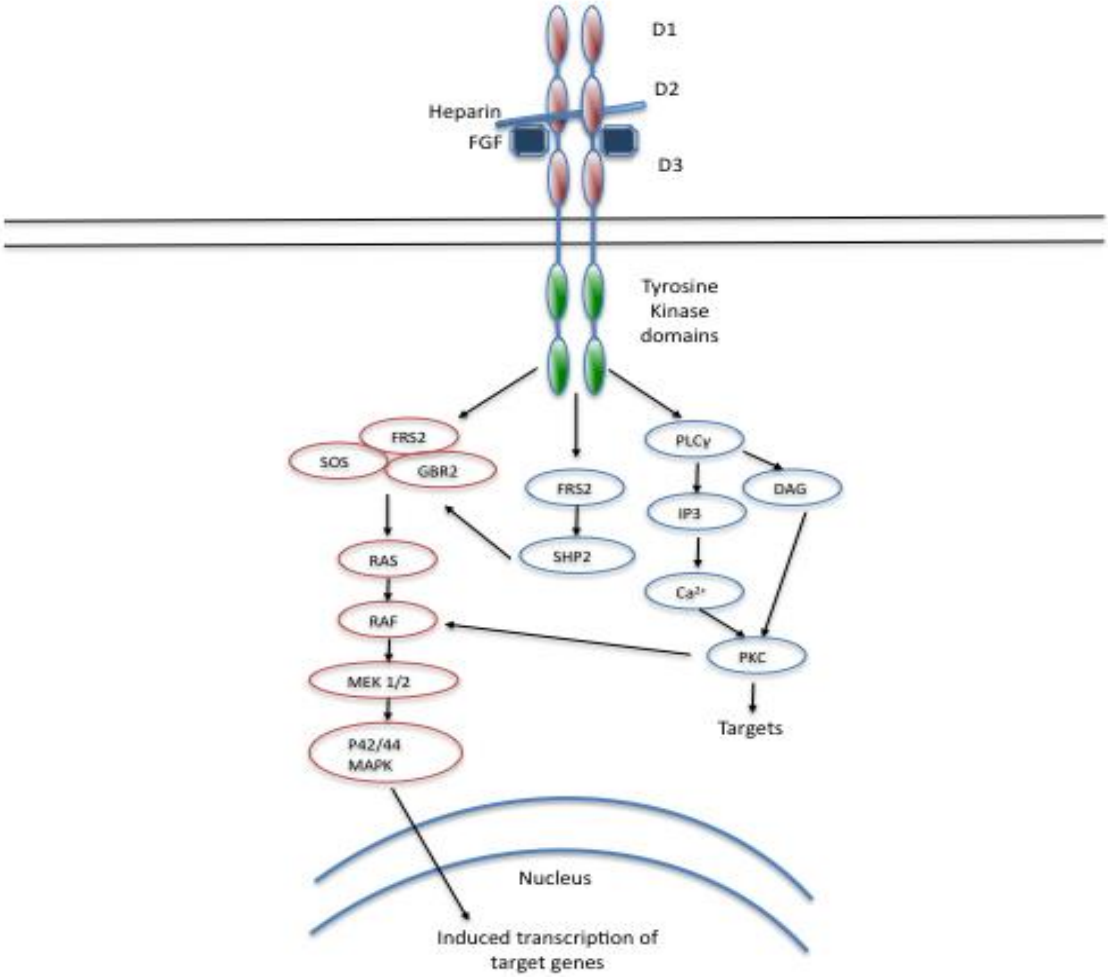


**Figure 1.6** - Shows the signaling cascade of the phosphorylated FGFR through the MAP kinase pathway. The activation of this pathway occurs through the phosphorylation of tyrosine 766 in the tyrosine kinase domain of the FGFR.

### PLCγ/$Ca^{2+}$ Signaling Pathway

Autophosphorylation of the kinase domains of the FGFR 2 and FGFR4 are able to activate

phosphatidyl inositol (Pt Ins) hydrolysis through interactions with the phosphorylated tyrosine 766 on the FGFR. Activation of PLCγ results in the hydrolysis of phophatidylinositol-4,5-diphosphate to diacylglycerol (DAG) and inositol-1,4,5-trisphosphate (IP3). Both DAG and IP3 modulate the release of $Ca^{2+}$ into the cell(50). Mutations at Y766 on the FGFR's show a little impact on the changes in mitogenic activity of a cell(51, 52). The existence of other signaling pathways that result in mitogenic activity helps to reduce the possibility of a catastrophic mutation at a single site.

**PI3 Kinase/ AKT Pathway**

The Phosphoinositol-3 Kinase pathway may be set into motion by serine-threonine kinase receptors, tyrosine kinase receptors and exchange factors that regulate heterotrimeric guanosine triphosphate binding proteins (figure 1.7). The three mechanisms by which the PI3 pathway may be induced include: P13K may bind directly to the phosphorylated tyrosine kinase domain in the FGFR, Ras may induce membrane localization as well as activation PI3K, and Gab1 may bind to FRS2 through interaction with Grb2 leading to the phosphorylation and activation of the PI3K pathway (53-56).. The binding interaction between Ras and the P110 subunit of the PI3K protein stimulates PI3K activity. Activated PI3 kinase converts the plasma membrane lipid phosphatidylinositol-4,5- bisphosphate (PI(4,5)P2) to phosphatidylinositol-3,4,5-trisphosphate (PI(3,4,5)P3) (57). The phosphatidylinositol-3-4-5 trisphosphate recruits signaling proteins containing Pleckstrin-homology domains. The recruited signaling proteins result in the phosphorylation of AKT by PDKI. Anti-apoptotic protein kinase AKT and phosphoinositide-dependent kinases are activated downstream of the PI3 kinase (58). This protein interaction pathway results in events that may control protein synthesis, actin polymerization, cell survival

and cell cycle entry.

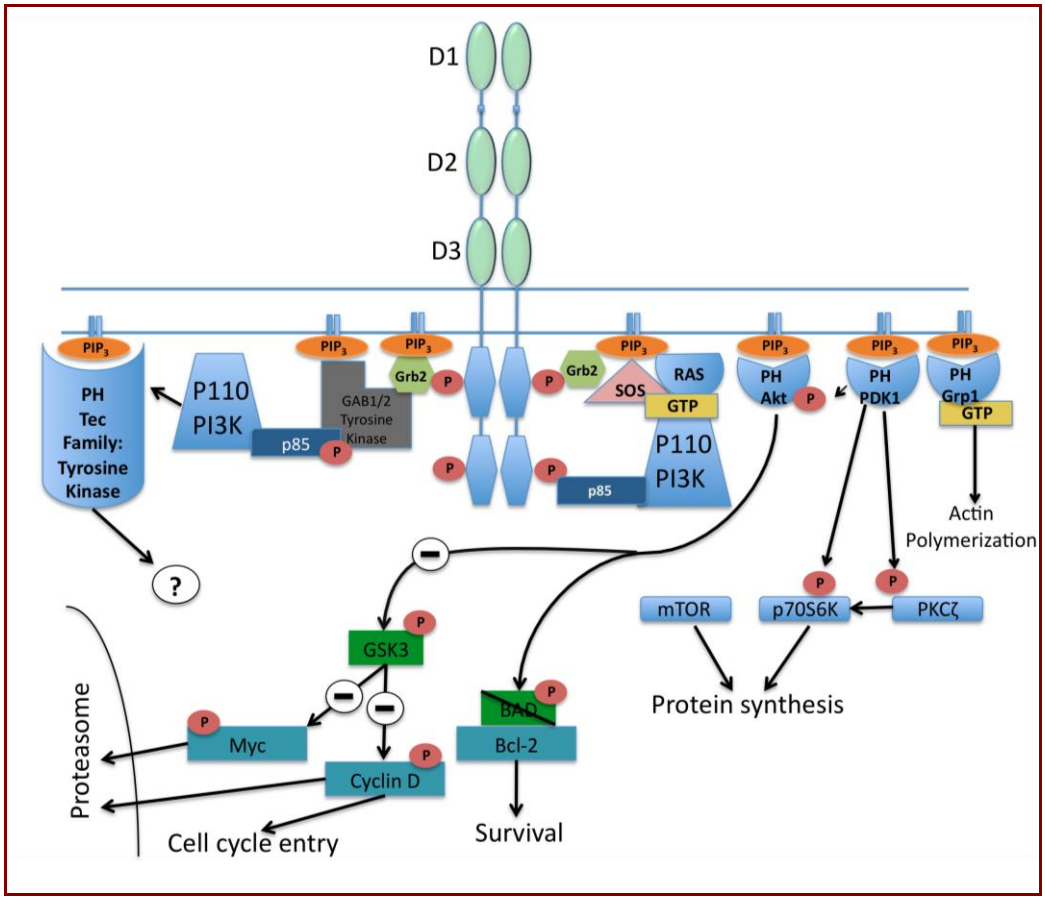


**Figure 1.7** – Intarcellular signaling pathway activated through FGFR autophosphorylation. The intracellular signaling activation results in a cascade activating the PI3 K / AKT pathway. Binding of Grb2 and p85 to the phosphorylated tyrosine kinase domain results in the recruitment of $PIP_3$ and activation of PI3 kinase. Activated PI3 Kinase phosphorylates phosphatidylinositol-3,4,5-trisphosphate (PIP3) which recruits a subset of signaling proteins with pleckstrin homology (PH). This phospoorylation of $PIP_3$ recruits signaling proteins that result in the activation protein synthesis, cell cycle entry and actin polymerzation.

**Regulation of the FGFR signaling pathway**

The FGF and FGFR activate signaling cascades including: MAPK pathway, phosphoinositol-3 kinase (PI3 kinase)/ AKT pathway and the phospholipase C gamma (PLCγ) pathway. Both up and down regulation of the FGFR signaling are important to maintain normal cellular function. The FGFR may be regulated by intercellular, extracellular and by auto

inhibition mechanisms.

The auto inhibition mechanisms of the FGFR include alternate splicing of the FGFR, selective expression of FGF, FGFR and HSPG. Heparin is a component of the extracellular matrix that is anchored to membrane bound proteins. FGFR 1 and FGFR 4 require heparin to contain 2-O-sulfates and 6-O-sulfates in order to form a binding interaction. This characteristic is not shared by FGFR2 and FGFR3 (59, 60). Alternate splicing of the receptors allows for varied affinities to the FGF's. The FGFR's may be expressed in multiple forms (61).The common splicing consists of FGFR2b or FGFR2c. The intron coding for the FGF binding site on the receptor may consist of the 2b or 2c form. In turn this provides varied affinity for FGF depending on the splice variant selected. The regions on the FGFR that are modified exist in the linker region between D2 and D3 and include residue changes in the D3 domain. The cell-specific expression of exon IIIb is largely controlled by regulatory elements IAS2 and ISAR. These elements selectively activate exonIIIb and may repress exon IIIc. Alternatively elements UISS, ESS and DISS silence exon IIIb and express exon IIIc. The associated affinities between FGF's and the isoforms of the FGF receptors are shown in figure 1.8(62-65).

This figure suggests splicing variants as mechanism of control for the affinity the FGFR may have for the various FGF families. This form of control over FGF signaling is also observed in splicing variants that occur in the D1 domain and the linker between D1- D2.

The splicing variations that occur on the FGFR result in the presence and absence of the D1 domain and the "acid box" domain located between D1 – D2. The isoforms that lack the D1 occur on FGFR1c, FGFR1b and FGFR2c. Isoforms of the FGFR that lack the "acid box" include FGFR3c.

| | FGFR1b | FGFR1c | FGFR2b | FGFR2c | FGFR3b | FGFR3c | FGFR4 |
|---|---|---|---|---|---|---|---|
| FGF1 | +++ | +++ | +++ | +++ | +++ | +++ | +++ |
| FGF2 | + | +++ | NB | + | NB | +++ | +++ |
| FGF3 | + | NB | + | NB | NB | NB | NB |
| FGF4 | NB | +++ | NB | +++ | NB | +++ | NB |
| FGF5 | NB | + | NB | + | NB | NB | NB |
| FGF6 | NB | + | NB | + | NB | NB | NB |
| FGF7 | NB | NB | ++ | NB | NB | NB | NB |
| FGF8 | NB | NB | NB | NB | NB | + | NB |
| FGF9 | NB | + | UNK | +++ | + | +++ | NB |
| FGF10 | ++ | NB | ++ | NB | UNK | UNK | NB |
| FGF11-14 | NB | NB | NB | NB | NB | NB | NB |
| FGF16 | UNK | NB | UNK | NB | UNK | UNK | NB |
| FGF17 | UNK | ++ | UNK | ++ | UNK | UNK | NB |
| FGF18 | NB | NB | NB | ++ | NB | ++ | NB |
| FGF19 | NB | NB | NB | NB | NB | NB | NB |
| FGF20 | UNK | ++ | UNK | UNK | UNK | UNK | UNK |

**Table 1.8** - "+" quantifies the mitogenic effect of FGF1-9 on BaF3 cells transfected with the respective FGF isoform. "NB" indicates no binding interaction. For the other FGF's, "+", "++" and "+++" respectively indicate the relative strength of the interaction. (66-68).

Fibroblast growth factor receptors that may lack both the D1 domain and the "acid box" include FGFR2b (27, 69, 70). The use of splicing variants as a mechanism to control FGFR activity was first demonstrated in 1993. In this study the affinity of FGF1 vs. FGFR1 with and without the D1 domain was examined. FGFR1 lacking the D1 domain showed a higher affinity for FGF-1 (71, 72).

The auto inhibition role of the "acid box" and D1 on the FGFR has been tested using both surface plasmon resonance and nuclear magnetic resonance experiments. *Kalinina et. al.* have shown that a positively charged patch of residues on the D2 domain bind to the negatively charged residues making up the acid box (73). The acid box – D2 interaction blocks the interaction of D2 with heparin. A secondary effect of this interaction is the decreased interaction of the FGFR with FGF. In this manner the expression of the splice variant of FGFR with D1 – AB may act to auto inhibit signaling of the FGFR.

**FGF Roles in Development**

Gastrulation is a process by which FGF signaling is essential in order to modulate cell migration and growth. The signaling pathways components of FGF and the FGFR including adaptor proteins FRS2/SNT-1(74, 75), Nck and Grb , Ras(76)Map kinase(77-80)Src-kinase laloo, protein tyrosine phosphatases(81, 82)MEK, ERK and transcription factors AP1 and Ets2 have shown critical for mesoderm development(83). Gastrulation defects have been the result of the inhibition of any of these pathways. Gastrulation is a process regulated by FGF by both direct and indirect signaling mechanisms. XSprouty2 has been determined to be an antagonist of FGF-dependent calcium signaling (84). Nutt et. al. showed that the overexpression of XSprouty2 inhibited convergent extension during gastrulation. The over expression of XSprouty2 did not

inhibit MAP kinase activity, mesoderm induction or mesoderm patterning (84).

FGF has also been show to indirectly regulate gastrulation. FGF has been shown to be a regulator of Xbra induction. Convergent extension is promoted by the expression of Xbra. The expression of Xbra also acts to inhibit cell migration through the inhibition of adhesion molecules on cells allowing them to bind to fibronectin (85, 86).Xbra induces the expression of Xwnt1 and prickle. These two proteins act as regulators of the Wnt-pathway, which in turn regulates convergent extension (84).

Knock-out mice have played a pivotal role in understanding the importance of FGFR signaling during gastrulation. FGFR1 $^{-/-}$ mutant mice embryos display defects in cell migration, cell specification and cell patterning resulting in embryo death (30, 87).First evidence of this appears during gastrulation in which the cells fail to make an epithelial to mesenchymal transition(88). The epithelial to mesenchymal transition is regulated by the increased expression of *m*Snail. Increased FGF results in higher expression of *m*Snail, which down regulates the expression of E-cadherin. The accumulation of E-cadherin may prevent the epithelial to mesenchymal transition. Arrest of the epithelial to mesenchymal transition may occur as a result of continued Wnt signaling. Continued expression of E-cadherin sequesters cytoplasmic β-catenin at the plasma membrane leading to the attenuation of Wnt signaling (30).

**Neural Induction**

Following gastrulation the ectodermal cells adopt a neural fate during a process termed neural induction. Ectodermal cells have two possible fates: signaling from BMP results in cells forming the epidermis or cells receive no signaling resulting in a neural fate. This process by which cells adopt a neural fate is termed the “default model”(89). The default model is

oversimplified for the process of neural induction. Several conserved proteins have shown to play a role in cell fate leading to neural induction including FGF (90).

The importance of FGF signaling during neural induction has been observed in chick embryos. Following neural induction the chick embryo undergoes the formation of a line of cells termed Hensen's node(91, 92).Using chick embryos, FGF's soaked beads are capable of inducing the formation of Hensen's node. Inhibition of FGF signaling results in the cell arrest and prevents the formation of Hensen's node (93-96). Epidermal cell fate may be indirectly controlled by the expression of FGFs. Fibroblast growth factors are shown to slowly induce the expression of Churchill (ChCh). Churchill activates the protein Sman-interacting-protein-1 (Sip1). Sip1 binds to inhibit Smad1/5, which is responsible for activating target genes – blocking BMP signaling (97). BMP signaling is capable of directing cellular development toward epidermal formation neural formation.

**Anterior/Posterior Development of the Neural Plate**

FGF signaling plays a crucial role in the anterior posterior patterning of the neural plate. The conversion of anterior neural tissue to posterior tissue is capable by FGF signaling (80, 98).The anterior to posterior patterning is observed when FGF soaked beads are imbedded within anterior neural tissue(99).The conversion of anterior to posterior neural tissue is postulated to be the result of cross talk of FGF with Wnt signaling(100-102).The overexpression of FGF3 in zebrafish continues the expansion of the posterior neural tissue while reducing the anterior neural tissue(103).The patterning of the anterior and posterior neural tissue has been shown to be related to the expression of FGF as well the expression of *Hox* genes.

*Caudals* are genes that respond to signaling by FGF's. These same genes are responsible

for regulating *Hox* gene expression(99, 104, 105).The overexpression of FGF in mouse, chick and Xenopus embryos resulted in the increased expression of *Hox* genes.

**Endoderm Formation**

FGFR knockout mice have provided evidence to the function of receptor signaling during endoderm formation. The overexpression of dominant negative FGFR2 leads to the inhibition of α-feoprotein, HNF4 and Evx1 – three endodermal markers (106). The $FGF4^{-/-}$ embryos failed to develop a mesoderm or endoderm (107). The phenotype of the $FGF4^{-/-}$ represented the phenotype observed for the embryo containing dominant negative FGFR2. FGF and the receptor are not the sole growth factors required for endoderm formation. Inhibition of other fibroblast growth factors showed no significant change in embryos. FGF's have not shown to induce the expression of endoderm genes in animal caps (108, 109).This data suggests the FGFs may be required for patterning of the endoderm and not development.

**Signaling and Angiogenesis**

The functions that FGF-1 and FGF-2 in development have been heavily studied. FGF-2 has shown to be important in the development and maintenance of the nervous system, angiogenesis, lung development, muscle, skeletal system, skin and digestive system. Angiogenesis is a key cellular process that has been the focus of novel tumor treatments (110). Angiogenesis is among the most notable processes mediated by both FGF-1 and FGF-2.

Angiogenesis is a process that must be preceded by key cellular events in order to prepare the endothelial cells for branching into new blood vessels. First, the basement membrane degradation must occur. Second, the endothelial cells begin migration and proliferation. The

endothelial cells will begin to sprout into the stromal space during proliferation. Finally, vascular loops are formed and capillary tubes develop as tight junctions bind endothelial cells to form a new basement membrane (111-113).

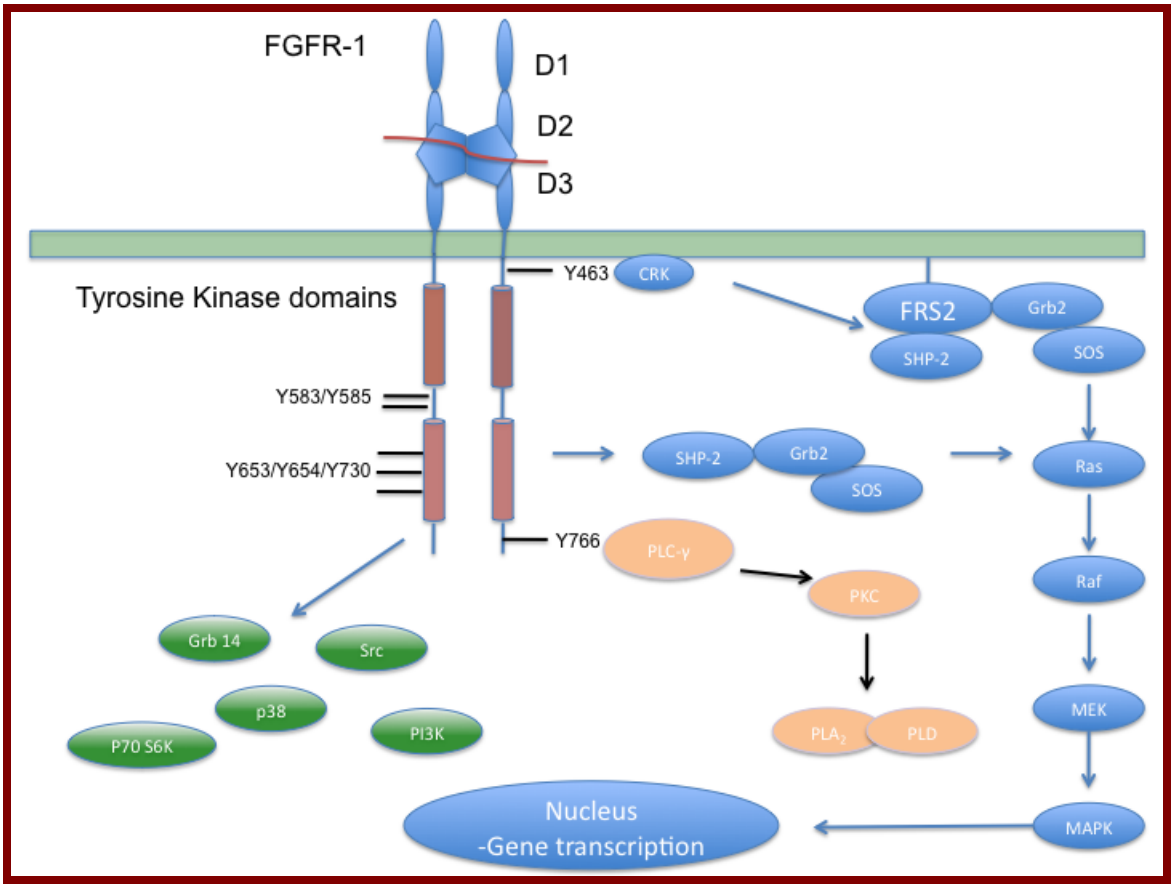


**Figure 1.9** – Schematic representation of the interactions formed following autophosphorylation events of the FGFR cytoplasmic tyrosine kinase domains. In this figure signaling through the MAPK pathway is initiated through interactions of CRK with the phosphorylated Y463. The PLC-γ activation is mediated through interactions with phosphorylated Y766. This interaction leads to the activation of PKC, which regulates the mitogenic response. The mechanism of activation of Grb-14, Src, P70 S67, P38 and PI3K is unknown. The mechanism of the SHP-2 pathway to activate Ras, which induced by FGFR1 and FGFR2 is still unknown.

FGF is a potent inducer of angiogenesis, but interactions formed by vascular endothelial growth factors (VEGF), angiopoietins, tranformaing growth factors α and β (TGFα and β), interleukins and chemokines are required for the formation of blood vessels.

Signaling through the MAPK pathway will induce cell proliferation. Activation of the

protein kinase C (PKC) pathway is required for FGF -2 to induce a full mitogenic effect. Loss of mitogenic activity as a result of reduced PKC activation may be overcome by the upregulation of the urokinase-type plasminogen activator (uPA)(115). Urokinase-type plasminogen activator upregulation is induced by FGF-2 activation of FGFR1. Following cell proliferation, it is important for extracellular matrix degradation to occur for the formation of new blood vessels.

FGF-1, FGF-2 and FGF-4 are responsible for the upregulation of uPA. These FGF's are also responsible for the upregulation of uPA receptors at the endothelial cell surface (38). In return uPA converts plasminogen into plasmin. Plasmin is a serine protease that degrades matrix-forming proteins such as fibrin (116) .uPA also activates matrix metalloproteinases MMP-1(collagenase-1), MMP-2 , MMP-3 and MMP-9 (type IV collagenase) in order to further degrade the matrix(117).The increased expression of uPA receptors induced by FGF's results in matrix degradation in a focused direction. FGF-2 has shown to stimulate surface membrane vesicle shedding. The vesicles typically contain MMP-2, MMP-9 and MMP inhibitors TIMP-1 and TIMP-2. Tarabouletti *et al.* have shown that vesicles shed stimulate capillary-like structure formation within endothelial cells (118). Extracellular matrix degradation must be followed by endothelial cell migration.

Endothelial cell migration is induced following chemotaxis and chemokinesis stimulated by FGF-1, FGF-2, FGF-8b and FGF10 (119-121). The chemotactic influence on endothelial cells has been mimicked in vitro by culturing endothelial cells within a 3D permissive matrix substrate. Using this matrix substrate, the addition of FGF-2 results in the invasion of endothelial cells into the substratum. Endothelial cells organize into capillary like structures with a hollow lumen (122). Similar results have been observed by the addition of FGF-2 to 3D fibrin gels containing endothelial cells (123). Endothelial cell migration may only lead to angiogenic

growth if lateral cell-cell adhesions and extracellular matrix interactions are formed.

Cadherin and integrin receptors direct the formation of cell-cell adhesion and extracellular matrix interactions. Cadherin and integrin ($\alpha_v$ $\beta_3$) expression is mediated by FGF-2 (124-126). Prolonged expression of FGF-2 has shown to influence the redistribution of junctional adhesion proteins, vascular and endothelial cadherins, and plakoglobin. This redistribution and cell-cell interactions formed by endothelial cell is a key step in vessel formation. Following these key interactions FGF's have been shown to be important in the development of the extracellular matrix.

Vascular endothelial growth factors (VEGF) and their receptors are required for angiogenesis development following extracellular matrix degradation. There are six VEGF's that interact with their membrane surface tyrosine kinase receptors (VEGFR). The interactions of VEGF-A with VEGFR-2 are essential in the formation of blood vessels (127). VEGF is a critical protein required for tubal formation of endothelial cells. FGF-2 interacts with vascular endothelial growth factors (VEGF) in order to modulate the induction of angiogenesis, vasculogenesis and lymphangiogenesis. The interactions between VEGF/VEGFR and FGF-2 have shown to regulate processes involved in angiogenesis. FGF-2 expressed by the cell or added to the cell has shown to induce the expression of VEGF (128). FGF-2 also plays a role with inducing VEGF receptors (129). The roles of FGF-2 and VEGF with the development of endothelial cells have been suggested to be synergistic (123, 130). This effect is observed by the differences in expression patterns observed in cells induced with FGF-2 or VEGF. Endothelial cells show an increased expression of telomerase activity and a reported induction of senescence for the cell. These modulated expressions controlled in part by FGF suggest there to be a role for fibroblasts throughout the angiogenesis process.

**Limb and Bud Formation**

Limb developments are a process by which the lateral plate mesoderm (LPM) and the ectoderm protrude in order to form a bud. From this bud cell proliferation gives rise to skeletal structures. Muscular and connective tissue are the result of the cell proliferation of mesenchymal tissue (131, 132). Cell proliferation first proceeds in a proximal to distal formation. This development forms a flattened structure along the dorsal-ventral and anterior-posterior planes. The first recognizable elements of differentiation are apparent by the development of skeletal tissue. The stylopod, found at the distal end of the limb, is among the first tissues showing development and is followed by the differentiation of other distal structures.

Initiation of limb bud outgrowth originates with the bulge of the lateral wall. Fibroblast growth factors have shown to play an important role in the initiation of the bud and outgrowth development. Induction of ectopic limb formation has been observed by the addition of FGF1, FGF2, FGF4, FGF8 and FGF10 (133-136). The method of FGF addition to the mesoderm has shown to be critical for limb formation. FGF added in a non-focal method results in the limb outgrowth in multiple locations. Each of the outgrowths eventually regresses and limb formation is not completed (136). Additionally the ectopic addition of FGF's has resulted in deletions, reductions and fusions of the proximal bones (136). Successful outgrowths and bud formations are only observed by a focused insertion of FGF. The addition of FGF by a soaked bead or pellet has been shown to lead to limb formation. Many FGF's have been shown to induce limb formation, but it is rare that induced limbs result in a functioning limb. The expression pattern in the nephronic mesoderm is has been suggested FGF 10 may be required to induce limb formation. The roles that FGF 10 plays in the induction are the result of three observations. FGF10 expression precedes the expression of FGF8 within the mesoderm. Following the

expression of FGF 10 within the mesoderm, FGF8 is subsequently expressed within the limb ectoderm. Limbs ectopically induced through the usage of FGF8 result in the expression of FGF10 rna within the mesenchyme before FGF8 rna is detected within the ectoderm (135). This data suggests that the role of FGF10 may be to act as an inducing agent for other FGF's.

The role of FGF10 has been suggested to induce the expression of FGF8 within the ectoderm. Embryos that are FGFR2 $^{\Delta IgIII}$ homozygous provide evidence for the importance of FGF 10 requirement to induce FGF 8. FGFR2 $^{\Delta IgIII}$ homozygous embryos express FGF 10 within the mesoderm. However, FGF8 fails to be expressed within the prospective limb ectoderm, as it would be in wild-type examples. Xu *et al.* have suggested that the decreased FGF8 expression is the result of a loss-of-signal transduction resulting from the FGFR2 $^{\Delta IgIII}$ homozygous embryos (27). This model proposes FGF10 expressed in the mesoderm induces the expression of FGF8 within the ectoderm through FGFR2. The expression of FGF8 is proposed to act as a positive feedback inducing FGF10. FGF8 may also act to induce Shh expression that is also required for limb formation and tissue patterning.

Tissue patterning and outgrowth originates from three distinct locations. The first limb-signaling center is the apical ectodermal ridge (AER). The apical ectodermal ridge runs from the anterior to the posterior near the distal region of the bud. FGF's originating from the AER has been shown to be required for pattern regulation along the proximal - distal axis (137, 138).The second signaling center is identified as the zone of polarizing activity (ZPA). The zpa is located posterior to the bud. Signaling from the zpa has been suggested to regulate patterning along the anterior – posterior axis (139, 140). The third signaling center is the nonridge ectoderm of the bud. FGF signaling and sonic hedgehog gene induced expression is largely responsible for acting on undifferentiated mesenchymal cells located in are region known as the "progress zone" (140).

The “progress zone” is located near the distal tip of the limb bud. Elongation of the limb is the result of cellular proliferation in the progress zone. Fibroblast growth factors perform a number of functions in the apical ectodermal ridge.

Many of the advances in our understanding of the apical ectodermal ridge have come from the study of chick limb development in ovo. The importance of FGF during limb development was observed by the addition of FGF soaked beads added to bud formation following the removal of the apical ectodermal region. Normal limb formation was observed in the chicks containing the fgf soaked beads (141, 142). The AER tissue patterning may be replaced by the addition of FGF-2, FGF-4 and FGF-8(136, 141, 142).The requirement of FGF4 and FGF8 for limb development may not be studied by null mutations because of their requirement for chick development.

Early limb development proceeds in anterior, posterior and distally from the site origin. This early development is considered to be the apical ectodermal ridge. There exists differential expression of FGF across the regions of bud formation. Tissue specific inactivation of FGF8 has been used to study the importance of FGF8 in the AER. The mutant mice skeletal abnormalaties include are observed in forelimbs, hind limbs and a lack of limb development (143). Further evidence suggests FGF’s play a significant role at the apical ectodermal ridge through the stimulation of cellular proliferation and increased expression of sonic hedgehog at the AER.

Cell proliferation has been observed as a result FGF signaling in the AER (144-146). The ectopic expression of FGF-2 results in the excess proliferation of mesenchymal cells. The increased expression results in the splitting of the skeletal primordial (147). Further evidence suggests FGF’s are required for the continued expression of *Hox* genes and Bmp2 (144, 148). The increased expression of *Hox* genes and Bmp2 may activate cell proliferation within the

mesenchymal tissue (149, 150).

The second proposed major function of FGF in the AER is to maintain the expression of Shh in the zone of polarizing activity (ZPA). Removal of the apical ectodermal ridge results in the inhibition of polarizing activity in the AER (136).Shh has been shown to be a mediator of polarizing activity in the ZPA. FGF is able to substitute the absence of an AER resulting in the continued polarizing activity. This is believed to result from the induced expression of Shh that allows for the increase polarizing activity (136, 151, 152).

Limb growth that is induced through the expression of both FGF and Shh requires an inhibitor to moderate signaling within the limb. The protein moderating FGF and Shh signaling is the Gremlin1 (Grem1) protein. Signals from FGF4, FGF8, FGF9 and FGF17 originate from the apical ectodermal ridge. The Shh and Grem 1 proteins are expressed in the underlying mesenchyme tissue (142, 144, 153-155). FGF acts to induce Shh and the Shh in turn induces the expression of FGF. The progress of limb growth and termination has been proposed by Verheyden et. al (156).

Verheyden *et al.* propose that in phase I (limb growth) and phase II (inhibitory growth) occur by two different mechanisms (156). In the growth phase FGF from expressed in the apical ectodermal ridge is too low to inhibit Grem1 efficiency. Instead FGF leads to an increased expression of Shh and BMP. In turn, higher concentration of Shh and BMP lead to an increase in the concentration of Grem1 within the distal mesenchyme tissue (157, 158). Within phase I the increased Gremlin1 protein induces the expression of FGF in the AER (159-161). The positive FGF/Shh feedback loop continues to lead to an increased expression of the two proteins.

The phase I to phase II transition occurs when the FGF expression and signaling increases to a concentration that begins to inhibit FGF signaling through an FGF/Germ1-negative

inhibitory loop. Phase II is initiated by separation of the mesenchyme tissue and apical ectodermal ridge. The mesenchyme tissue proceeds to expand distally and posteriorly (156). The mesenchyme expansion occurs until Germ1-negative diffuses past the expressed Germ1 protein. The Germ-1 negative leads to a decreased concentration of FGF, which in turn decreases the Shh expression. The decreased FGF and Shh expression is expected to result in a termination of the limb development and the end of phase II (156).

**Fibroblast Growth Factors and Disease**

Fibroblast growth factor signaling is critical for a variety of developmental, processes. Fibroblast growth factors have not been associated with disease until a mutation found in FGF 23 was determined to cause hypophosphatemic rickets in 2000. Since 2000 numerous FGF have been associated with diseases including: FGF3 in Michel aplasia; FGF 8 in hypogonadotropic hypogonadism; FGF9 in carcinoma; FGF10 in carimal/salivary aplasia; FGF14 in spinocerebellar ataxia; FGF20 in Parkinsons disease; and FGF23 in tumoral calcinosis and hypophosphatemic rickets (72, 162-164). The diseases related to the mutations across the FGF family are evidence to the variety of their functions.

**FGF3 and Michel Aplasia**

Michel aplasia is defined by an absence of developed inner ear structures including the cochlea, vestibule and semicircular canals. The loss of these structures result in hearing loss. Sometimes associated with Michel aplasia is microtia and microdentia. Microtia is defined by anteverted ears and microdentia defined by widely spaced teeth. The mutations in FGF3 that have been associated with this disease include L6P, G66C, I85M R104X, S156P and V206S

(162, 163). FGF3 and FGF10 have been inferred as important for inner ear development through knockout mice. Mice lacking FGF3 and FGF10 lack development of the cochleavestibular ganglion, impaired otic vesicles and a reduction or absence of expressed otic marker genes *Pax, Dlx4 and Sox9* (93, 165). Similar defects have been identified in FGFR2b null chicks(166).

**Kallmann Sydrome and FGF8**

Kallmann's syndrome (KS) or idiopathic hypogonadotropic hypogonadism (IHH) with is the result of absent or delayed puberty. Kallmann's syndrome is also paired with anosmia – loss of the sense of smell. Kallmann's syndrome has also been identified to occur as a result of mutations occurring in FGFR1. FGF8 mutations H14N, P26L, K100E, R127G and T229M are associated with IHH or KS (164). Structural analysis suggests these mutations may impair the interactions of FGF8 with heparin. The decreased interactions may result in a decreased signal transduction. This analysis is consistent with proposes loss-of-function mechanisms determined for the FGFr1 mutations.

**FGF8 and FGF10 in Nonsdromatic Cleft lip and/or Palate**

Cleft lip or palate is a disease by which the two halves of the craniofacies fail to fuse to complete the hard palate and/or lip. The FGF8 mutation that results in this disease is D73H. The mutation is located at the N-terminal region of FGF8 and important in the binding interactions with the D3 domain of the FGFR (147). FGF8 hypomorphic mice develop impaired survival of the neural crest cells. The neural crest cells populate the pharyngeal arches, which are required for the development of many facial structures (147).

**Spinocerebellar Ataxia and FGF14**

Spinocerebellar ataxia (SCA) is characterized by tremors, low cognitive performance and memory impairment (167). Two mutations in FGF14 have been identified to be associated with SCA. FGF14 F145S was the first mutation determined in FGF14 to be associated with SCA. A second mutation associated with SCA was determined to be a single-nucleotide deletion mutation at nucleotide 487. The result of the deletion mutation is a truncation of the FGF14 protein (167, 168). The F145S mutation is buried within the hydrophobic core of the structure. The large aromatic residue replaced by a serine results in the loss of hydrophobic interactions with surrounding residues. The significant decrease residue in volume may result in the destabilization of the FGF structure. The mutation is believed to result in a loss-of-function of FGF 14. The loss-of-function assessment is consistent with the phenotype observed in FGF 14 null mice. FGF 14 null mice develop ataxia, paroxysmal movement disorder and cognitive defects. The development of such cognitive defects is predicted to originate from neural structures where FGF14 is expressed including: hippocampal neurons, Purkinje cells and cerebellar granular neurons (169). The FGF $14^{-/-}$ mice show granular neuron morphology believed to result in ataxia and paroxysmal movement disorder (169). Additionally, FGF 14 colocalizes with voltage-gated sodium channels in the soma and beginning segment of the neuron. The colocalization is attributed through interactions of the cytoplasmic C-terminal tail of the channels α-subunit (170, 171). The source of the loss-of-function may occur through a loss of interactions formed with the C-terminal tail of the channels α-subunit. The loss of this interaction may result in the decreased neuronal excitability in the FGF $14^{-/-}$ mice.

**Parkinson's Disease and FGF20**

Parkinson disease (PD) is defined by the manifestation of a resting tremor, bradykinesia and a loss of dopaminergic neurons resulting in rigidity. FGF20 is associated with PD as a result of a single nucleotide polymorphism (SNP) at the 3' untranslated portion of the gene. The SNP located in the untranslated portion of FGF20 has been shown to increase the expression of the protein (72).The association of the increase expression FGF20 with PD is the result of both its location of expression and the resulting induction of other proteins.

FGF20 is preferentially expressed in the substantia nigra and within dopaminergic neurons (67, 172). The increased expression of FGF20 has been shown to increase the expression of α-synuclein, which is a key component in filamentous lewis bodies (173). The increased α-synuclein resulting from elevated FGF20 may be a key contributor to the deterioration of dopaminergic neurons in aging individuals.

**Hypophosphatemic Rickets and FGF23**

Autosomal dominant hypophosphatemic rickets is a disease characterized by hypophosphatemia, rickets, osteomalacia, bone pain, dental abscesses and low levels of 1,25-dihydroxyvitamine $D_3$ – resulting in renal phosphate wasting. Missense mutations R176Q, R179Q and R179W in FGF23 have been associated with ADHR (174). These mutations are expected to confer increased stability of FGF23. The increased stability in turn is inferred to result in a gain-of-function. The three mutations disrupt the RHTR amino acid sequence in FGF23. This sequence is a targeted cleavage site location for subtilisin-like protein convertase or PHEX endopeptidase (175). Increased expression of FGF23 downregulates phosphate through

the inhibition of reabsorption in renal proximal tubes. Phosphate regulation may be the result of FGF23 inhibition of $Na/P_i$ cotransporters. Therefore the expression of Npt1, Npt2a and Npt2c by the kidney is inhibited by FGF23 (176-179).

**Tumoral Calcinosis and FGF23**

Tumoral calcinosis is the result of the deposition of basic calcium phosphate crystals in the periarticular spaces including hip, elbow and shoulder (180). Within these tissues ulcerations, bone infections and contractures result in painful calcifications. Mutations H41Q, Q54K, S71G, M96T and S129F occurring in FGF23 have been associated with the tumoral calcinosis disease (181-184). $FGF23^{-/-}$ mice result in increased $1,25(OH)_2D_3$ and hyperphosphatemia – phenotypes reflected by patients with tumoral calcinosis(185). Additionally, the $FGF23^{-/-}$ mice suggest tumoral calcinosis may result from a loss-of-function mechanism. The loss-of-function may be the result of mutated FGF23 retention and lack of secretion from the golgi complex (182).

**Tumor Development and FGF Signaling**

FGF signaling has been identified as a key component in tumor pathogenesis. There exist several mechanisms by which FGF receptors are considered to encourage tumoral growth including: single-nucleotide polymorphisms (SNP); chromosomal translocation; differential expression; impaired down-regulation of FGF signaling; and mutations within the FGFR.

Single nucleotide polymorphisms (SNP) within the FGFR are related to increased malignant phenotype and increased risk of some specific types of cancer. SNP have been identified to exist adjacent to and within the FGFR2 gene. SNP adjacent to the FGFR2 gene are associated with an increased risk of breast cancer (186, 187). SNP found adjacent to the FGFR2

gene may act to alter the binding affinity for transcription factors for the FGFR2 gene. FGF receptor 2 shows increased expression in both breast cancer cell lines and breast cancer tumors (187). Current data suggests the SNP adjacent to the FGFR2 gene are related to increased expression of FGFR2 leading to sustained signal transduction (188-190). The sustained signal transduction may cause increased cell proliferation. In mice, FGFR2 acts to increase the proliferation and invasiveness of terminal end buds of developing breasts in mice (191). SNP adjacent to the FGFR2 gene provide evidence associating the SNP with increased expression and increased risk for patients with BC. Additionally SNP adjacent to FGFRs are linked to lung, skin, colon and prostate cancers (192-195).

Impaired down-regulation of the FGFR is associated with the attenuation of FGF-FGFR signaling. Following the FGF binding to the receptor and autophosphorylation, the FGFR is endocytosed and transported to lysosomes for degradation. Impairment of this down-regulation mechanism of the FGFR may occur through; alterations of the negative regulators of the FGFR and mutations preventing efficient internalization and degradation and splice variants of the FGFR that resist internalization.

The negative regulators of the FGFR include Cbl and ubiquitin ligase. Mutations or expression alterations of these proteins involved in the endocytic pathways may be related to increased lifetimes of the FGFRs. Mutations within the FGFR's may also act to prevent the endocytosis mechanisms.

Prevention of degradation and endocytosis mechanisms may also be the result of mutations within the FGFR. The FGFR3 G380R mutation is associated with bladder cancer. Analysis of this mutations shows the mutation promotes dimerization of the receptor. Additionally the FGFR3 G380R mutant avoids degradation, which is associated with prolonged signaling (195).

One component required for efficient endocytosis is the C-terminal endo of the FGFR.

FGFR2 is expressed in some tissue with a truncated C-terminal end. The endocytic motif of the FGFR is located within the C-terminal end. Truncation is shown to result in continued signaling and is related to several cancer cell lines (196).

A screen of more than 1000 somatic mutations determined exons of more than 500 kinase genes associated with 200 different forms of human cancer (197). FGF signaling pathways are the most common non-synonymous signaling pathways containing mutations (197). Fibroblast growth factors 1, 2, and 4 have been associated with cellular proliferation, differentiation, invasiveness and motility of tumor developments.

Cell survival is an important tumor defense mechanism that plays a role in the efficiency of drug treatments. Antiapoptotic proteins XIAP and Bcl-X(L) are increased in expression in small cell lung cancer cells by FGF-2(198). Additionally FGF-2 expression may form an interaction with Akt and factor κB activation, which is linked to antiapoptotic effects in breast cancer (199).

**Breast Cancer and FGFR**

Human breast cancer tissue shows an increased amplification of the 8p11-12 chromosomal regions containing the FGFR1 gene. Amplification of the 8p11-12 chromosomal regions occurs in 10% of human breast cancers. The increased expression of the 8p11-12 chromosomal regions is associated with breast cancer with a poor prognosis (200-202). FGFR1 activation in mouse and human mammary cell lines resulted in increased cell proliferation, survival and invasion (203). Although FGFR1 is associated with cell proliferation, other proteins found in the 8p11-12 regions may be capable or also required for cellular proliferation.

The ectopic expression of FGFR2 and FGFR4 is present in some breast cancer cases.

FGFR2 has been found in tumors negative for estrogen receptor, progesterone receptor and human EGFR 2/ErbB2 (HER2)(204). The FGFR2 related triple negative breast cancer tumors do not show a response to current cancer treatments. The cells showing increased expression of FGFR4 have shown increased sensitivity to chemotherapy upon the addition of antagonistic FGFR4 antibodies (205). The role of FGF receptors in the progression of breast cancer has shown to be important, but the changes induced by FGFR mutations has not yet been fully studied and will be discussed in further detail.

**Bladder Cancer and FGFR**

Fibroblast growth factor receptor 3 is found to overexpress within non-invasive urothelial cell carcinoma (UCC). UCC that initiates in the urothelial lining of the bladder and express FGFR3 account for 70% of bladder cancer types and are considered non-invasive. Approximately 70% FGFR3 found in non-invasive bladder cancer patients contain mutations (206). Common mutations in FGFR3 include R248C, S249C, G370/372C and Y373/375C. The locations of these mutants occur in the extracellular, transmembrane and cytoplasmic domain. The cysteine mutation common to each of the mutants allows for disulfide bond formation between FGFR3 dimers. Dimerization of FGFR3 would account for continued signaling (207).

FGFR3 targeted therapies are centered on antibodies for the receptor to prevent autodimerization. The SU5402 antibody inhibiting FGFR activation has shown in mice to reduce tumoral properties (208). An advance in antibody design has resulted in the development of antibodies selective for specific mutations within the FGFR. Antibody specific for FGFR3 PD173074 mutants inhibit tumor growth in mouse xenografts (209). The relative specificity of FGFR3 allows for the development of tests specific for bladder cancer by determining the

presence of FGFR3.

**Lung Cancer and FGFR**

Fibroblast growth factors and FGF receptors have been identified as playing a role in lung cancer. Mutations associated with lung cancer have been identified to occur in each of the FGF receptors. FGFR1 (G70R, T141R, P252T, P252S, P576H), FGFR2 (N211I, D283N, W290C, T370R, I380V, D530V, H544Q, R612T), FGFR3 (T79S) and FGFR4 (R183S, S232I, G388R, R616K, E681K, P712T, A729G and S772N) are suggested to play a role in lung cancer development (210-219). Normal lung development requires the expression and signaling of FGFR2, FGF7 and FGF10 (220, 221). FGFR2 W290C is a mutation associated with lung carcinomas. The W290C mutation is also found in Pfeiffer syndrome. The mutation results in ligand-independent signaling (222). The gain-of-function mechanism of action for the FGFR2 W290C accounts for increased tumoral growth. The expression of FGFR1, FGFR3 and FGFR4 and mutations occurring in these receptors are associated with lung carcinomas. The mechanism of action for each of the FGF receptors has not been clearly determined.

**Multiple Myeloma and FGFR**

Fibroblast growth factor receptor mutations associated with multiple myeloma consistently occur in FGFR3. The mutations that have been associated with multiple myeloma occurring in FGF3 include G197S, Y241C, R248C, P250R, Y373C, G380R, G382D, F384L/C, S433C, A441T, A452S, K650E, K650M, A717T and I726F (223-230). Additionally, FGFR3 is overexpressed in multiple myeloma mouse models(231). FGFR3 acts to enhance multiple myeloma cell survival and increases cell proliferation. Mutations R248C, G382D, K650M and

Y373C are associated with other disorders and result in increased kinase activity. Increased kinase activity is often the result of ligand independent signaling. The increased kinase activity is further mitigated by the increased expression of FGFR3.

Approximately 20% of multiple myeloma patients have increased FGFR3 expression. Overexpression of FGFR3 is the result of t(4:14)(p16.3;q32) translocation(232).The translocation of t(4:14)(p16.3;q32) results in the FGFR3 expression regulated by a strong IgH enhancer(233).The t(4:14) translocation is associated with a poor response to treatments(233).

**Disease States and FGFR**

Mutations in fibroblast growth factor receptors have been associated with numerous diseases related to gain-of-function and loss-of-function signaling. Among the diseases FGFRs are attributed to include: various forms of cancer, developmental disorders and skeletal disorders.

| **Cancer Type** | **Receptor** | **Up-regulated (references)** | **Down-regulated (references)** |
|---|---|---|---|
| Bladder | FGFR1 | (234-238). | |
| | FGFR2 | (234, 235). | (239). |
| | FGFR3 | (240-244). | |
| Brain | FGFR1 | (87, 245-248). | |
| | FGFR2 | (249). | (250, 251). |
| | FGFR4 | (252). | |
| Breast | FGFR1 | 60-76(253-269). | |
| | FGFR2 | (253, 257, 263, 266, 267, 269). | |
| | FGFR3 | (270-272). | |
| | FGFR4 | (267, 273, 274). | |
| Cervix | FGFR2 | (275-277). | |
| Colon | FGFR1 | (278). | (279). |
| | FGFR3 | | (280). |
| Head and neck | FGFR1 | (281-287). | |
| | FGFR2 | (287-292). | (293). |

| | | | |
|---|---|---|---|
| | FGFR3 | (290, 291, 294, 295). | |
| | FGFR4 | (91). | |
| **Cancer Type** | **Receptor** | **Up-regulated (references)** | **Down-regulated (references)** |
| Liver | FGFR2 | (297). | (298). |
| | FGFR3 | (297, 299). | |
| | FGFR4 | (297, 300, 301). | |
| Leukeamia/MPD/Lymphoma | FGFR1 | (302, 303, 303-306). | |
| | FGFR3 | (307-310). | |
| Lung | FGFR1 | (311-321). | |
| | FGFR2 | (313-316, 322-324). | |
| | FGFR3 | (313, 314, 325, 326). | |
| | FGFR4 | (313). | (327). |
| Multiple myeloma | FGFR3 | (328-343). | |
| Ovary | FGFR1 | (344-346). | |
| | FGFR2 | (347). | |
| | FGFR4 | (274). | |
| Pancreas | FGFR1 | (348-352). | |
| | FGFR2 | (353-355). | |
| | FGFR3 | (356). | |
| | FGFR4 | (356, 357). | |
| Prostate | FGFR1 | (358-365). | |
| | FGFR2 | (366-368). | |
| | FGFR4 | (358, 369, 370). | |
| Sarcoma | FGFR1 | (7, 371, 372). | |
| | FGFR2 | (7). | |
| | FGFR3 | (7). | |
| Skin | FGFR1 | (373, 374). | |
| | FGFR3 | (375, 376). | |
| | FGFR4 | (377). | |
| Soft tissue sarcoma | FGFR1 | (378).(379, 380). | |
| | FGFR2 | (381, 382). | |
| | FGFR3 | (7). | |
| | FGFR4 | (382-386). | |
| Stomach | FGFR1 | (387, 388). | |
| | FGFR2 | (387, 389-398). | |
| | FGFR4 | (387). | |
| Testis | FGFR1 | (399). | |
| Thyroid | FGFR1 | (400, 401). | |
| | FGFR2 | (402). | |
| | FGFR3 | (403). | |
| | FGFR4 | (403). | |
| Uterus | FGFR1 | (404, 405). | |
| | FGFR2 | (406-408). | |

**Table 1.11** – Identifies the myoproliferative disorders to which FGF receptors have been associated. Adjacent to each identified FGFR are the citations identifying each receptor showing

increased or decreased regulation. It is evident that the overall trend for cancer-linked mutations suggests FGFRs show up-regulation.

| Receptor | Mutation | Cancer Type | Consequence |
|---|---|---|---|
| **FGFR1** | G70R(409, 410). | Lung | |
| | R78H(411). | Prostate | |
| | S125L(412, 413). | Breast, Skin | |
| | T141R(414). | Lung | |
| | P252T(413). | Lung | Altered ligand specificity |
| | P252S(411). | Skin | |
| | A268S(411). | Stomach, Colon | |
| | A429S(415). | Colon | |
| | N546K(416). | Brain | Increased kinase activity |
| | R576W(416). | Brain | Increased kinase activity (in silico) |
| | P576H | Lung | |
| | K656E(413). | Brain | Increased kinase activity |
| | V664L(413). | Lung | |
| **FGFR2** | S24F(417). | Skin | |
| | M71T(411). | Bladder, lymphoma | |
| | V77M(417). | Skin | |
| | A97T(418). | Cervix | |
| | D101Y(418). | Endometrial | |
| | E160A(417). | Skin | Decreased HSPG interaction (in silico) |
| | R203C(413). | Breast | |
| | Q212K(419). | Brain | |
| | H213Y(417). | Skin | Decreased HSPG interaction (in silico) |
| | E219K(417). | Skin | Reduced receptor dimerization (in silico) |
| | G227E(417). | Skin | Destabilization of the D2 domain (in silico) |
| | V248D(417). | Skin | Destabilization of the D2 domain (in silico) |
| | R251Q(417). | Skin | Loss of ligand binding |
| | S252W(418). | Endometrial | Altered ligand specificity |
| | S252W(415). | Ovary | |
| | P253R(418). | Endometrial | Altered ligand specificity |
| | S267P(420). | Stomach | Ligand-independent dimerization |
| | G271E(417). | Skin | Destabilization of the D3 domain (in silico) |
| | G272V(413). | Ovary | |
| | D283N(413). | Lung | |
| | W290C(413). | Lung | Ligand-independent dimerization |
| | G305R(417). | Skin | |
| | K310R(418). | Endometrial | |
| | A314D(418). | Endometrial | |

| | | | |
|---|---|---|---|
| | A315T(421). | Endometrial | |
| | G462E(422). | Brain | |
| | W474(417). | Skin | |
| **Receptor** | **Mutation** | **Cancer Type** | **Consequence** |
| | D530N(417). | Skin | Reduced kinase activity |
| | H544Q(423). | Lung | |
| | I547V(421). | Endometrial | |
| | N549K(418). | Endometrial | Enhanced kinase activity |
| | E574K(417). | Skin | |
| | P582L(424). | Colon | |
| | R612T(413). | Lung | |
| | E636K(417). | Skin | |
| | M640I(417). | Skin | Decreased kinase activity (in silico) |
| | I642V(417). | Skin | Decreased kinase activity |
| | A648T(417). | Skin | Decreased kinase activity |
| | K659M(418). | Endometrial | |
| | K659N(418). | Endometrial | Increased kinase activity |
| | K659E(421). | Endometrial | |
| | S688F(417). | Skin | |
| | G701S(417). | Skin | Decreased kinase activity (ins silico) |
| | P708S(417). | Skin | |
| | R759X/Q(417). | Skin | |
| | L770V(417). | Skin | Inhibition of phosphorylation of Y769 |
| **FGFR3** | T79S(413). | Lung | |
| | G197S(425). | multiple myeloma | |
| | C228R(413). | Colon | |
| | Y241C(426, 427). | multiple myeloma | |
| | R248C(428). | Head and neck | |
| | R248C(429). | multiple myeloma | |
| | S249C(430). | Cervix | Ligand-independent dimerization |
| | S249C(431-433). | Bladder | |
| | S249C(434). | Head and neck | |
| | S249C(435). | Prostate | |
| | P250R(425). | Multiple myeloma | |
| | E322K(420). | Colon | |
| | G370C(427). | Bladder | Ligand-independent dimerization |
| | S371C(427). | Bladder | Ligand-independent dimerization |
| | Y373C(427). | Bladder | Ligand-independent dimerization |
| | Y373C | Multiple myeloma | |
| | I376C | Bladder | |
| | G380R(427). | Bladder | Enhanced kinase activity |

| | | | |
|---|---|---|---|
| | | Multiple | |
| | G380R | myeloma | |
| | G382D | Mult. Myeloma | Enhanced kinase activity |
| **Receptor** | **Mutation** | **Cancer Type** | **Consequence** |
| **Receptor** | **Mutation** | **Cancer Type** | **Consequence** |
| | F384L/C(425). | multiple myeloma | |
| | A391E(427). | Bladder | Dimer stabilization |
| | A391E(435). | Prostate | |
| | | Multiple | |
| | S433C(425). | Myeloma | |
| | | Multiple | |
| | A441T(425). | Myeloma | |
| | | Multiple | |
| | A452S(425). | Myeloma | |
| | E466K | Brain | |
| | D617G(428). | Head and neck | |
| | V630M(428). | Head and neck | |
| | D646Y | Bladder | |
| | K650E(413, | | |
| | 427). | Bladder | Enhanced kinase activity |
| | K650E | Testis | |
| | | Multiple | |
| | K650E | myeloma | |
| | K650Q(427). | Bladder | Enhanced kinase activity |
| | K650M | Bladder | Enhanced kinase activity |
| | K650M | Testis | |
| | K650M(425). | MM | |
| | K650T | Bladder | Enhanced kinase activity |
| | K650T | Testis | |
| | E686K(428). | Head and neck | |
| | G697C | Head and neck | Enhanced kinase activity |
| | | Multiple | |
| | A717T(425). | Myeloma | |
| | I726F(425, | Multiple | |
| | 426). | Myeloma | |
| **FGFR4** | C56S | RMS | |
| | R72L | RMS | |
| | T122A | RMS | |
| | A175T | RMS | |
| | R183S(414). | Lung | |
| | S232I(414). | Lung | |
| | R234H | RMS | |
| | Y367C(411). | Breast | Common SNP that occurs in 50% of the population |
| | G388R | Lung | |
| | G388R | Liver | |

| | | | |
|---|---|---|---|
| | G388R | Head and neck | |
| | G388R | RMS | |
| | G388R | Sarcoma | |
| | | | |
| | G388R | Colon | |
| | G388R | Breast | |
| | G388R(411). | Brain | |
| | G388R(417). | Skin | |
| | G388R | Stomach | |
| | N535D | RMS | |
| | N535K | RMS | Enhanced kinase activity |
| | V550E | RMS | Enhanced kinase activity |
| | V550L | RMS | |
| | V550M | Breast | |
| **Receptor** | **Mutation** | **Cancer Type** | **Consequence** |
| | G576D | RMS | |
| | R616G | Lung | |
| | E681K | Lung | |
| | P712T | Lung | |
| | P716R(417). | Skin | |
| | A729G(414). | Lung | |
| | S772N | Lung | |

**Table 1.12 – Mutations found in the FGF receptors and the disease for which they are associated.**

**Skeletal disorders and FGFR mutations**

The study of mutations within the FGFR started with the determination of a common mutation in FGFR3 found among 34 individuals with achondroplasia. Since 1994 and the discovery of the FGFR3 G380R mutation associated with short-limbed dwarfism, additional developmental disorders have been associated with mutations in FGF receptors. Pfeiffer syndrome, Apert, Crouzon, Beare-Stevenson, Jackson-Weiss, Meunke and Kallmann syndrome are all found to result from mutations occurring in the FGF receptors. The location of the mutations associated with theses diseases occur in the D1, D2, D3, juxtamembrane and tyrosine kinase domains.

**Apert Syndrome**

Apert syndrome (AS) is characterized by midface hypoplasia, syndactyly and visceral abnormalaties and craniosynostosis (436 - 438). Craniosynostosis is the result of premature fusion of the cranial suture. The cranial suture is composed of the periosteum, intervening mesenchyme and underlying dura matter.

The periosteum located at the surface of the cranial suture is important in cranial bone formation, wound healing and regeneration. The periosteum tissue contains fibroblast cells, mesenchymal stem cells, differentiated osteogenic progenitor cells, osteoblasts and skeletal stem cells (439-441). The stem cells and fibroblast cells found in the periosteum allows this tissue to be capable of driving the cranial fusion observed in patients with craniosynostosis (439, 440).

Fibrobast growth factor receptor 2 mutations have been associated with AS FGFR2 mutations S252W and P253R have been found in each of 40 patients analyzed for diseases and account for approximately 65% of the mutations resulting in AS (442). The FGFR2 S252W is typically expressed phenotypically with cleft palate. The FGFR2 P253R differs from the S252W phenotypes by increased syndactyly. The biological mechanism associating the S252W and P253R mutations with the phenotypes of AS are tied to their influences on cellular proliferation and differentiation. Models containing the FGFR2 S252W mutant have been shown to both increase and decrease cellular proliferation (436 - 444). The contradictory cellular proliferation studies were conducted using murine cells. More recent studies using human cell lines gathered from patients harboring the FGFR2 S252W mutation have been conducted. Mesenchymal stem cells (MSC) and fibroblast cells containing the FGFR2 S252W mutation has shown an increase

in cell proliferation activity in fibroblast cells, but not in the mesenchymal stem cells. The rate of osteogenic differentiation was increased in both MSC and fibroblast cells. Additionally, fibroblast cells were able to induce osteogenic differentiation in periosteal MSCs. Fibroblast cells do not result in osteogenic differentiation in MSC's derived from other tissue. The FGFR2 S252W mutation significantly changes the osteogenic differentiation potential in cells found in the cranial suture.

**Pfeiffer Syndrome and FGFR**

Pfeiffer syndrome is characterized by the premature fusion of the cranial sutures (craniosynostosis) during development. The cranial suture premature fusion often results in impaired cerebral blood flow, airway obstruction, impaired vision and hearing, learning difficulties and raised intracranial pressure. The rate of occurrence of Pfeiffer syndrome is approximately 1 in 2500(445). The most common mutations have been determined to result in the craniosynostosis include FGFR3 (32%), FGFR4 (25%), TWIST1 (19%) and EFNB1 (7%)(446).

Cranial suture development and morphogenesis is a cellular role postulated to be modulated by FGFR2, msx2 and transforming growth factor β 1-3. The full details of cranial suture cellular differentiation and proliferation have yet to be determined. The expression of FGFR2 has been observed in increased amounts within the cranial sutures. The presence of FGFR2 is also observed to be mutually exclusive with the increased expression of ostopontin. Osteopontin is an indicator of bone differentiation (447-449). The expression of FGR2 acts to mark cells that have not yet been differentially committed within the suture. Osteopontin acts to

commit FGFR2 expressing cells to osteogeneic differentiation. The role of the Msx2 and transforming growth factor beta 1-3 during suture development has not been fully elucidated.

Mammalian mutant studies have shed light on the mechanism of action resulting from select Pfeiffer syndrome mutations. The first Pfeiffer syndrome mutation studies were conducted using *Xenopus* oocytes/embryos. An injection of FGFR2 mutant C332Y mRNA was added to the blastomere. The resulting phenotype was an elongation of the pole ectoderm and induction of Xbra. Xbra is a marker of mesodermal expression, which acts to mimic FGF1. An antiphosphotyrosine antibody was used to determine the degree of phosphorylation of the mutant and wild-type FGFR. The FGFR C332Y mutants showed an increased phosphorylation of tyrosines when compared to FGFR (wt)(447). Additionally it was determined that the C332Y mutant was unable to bind to FGF-1. The resulting conclusion finds the PS related FGFR mutant C332Y caused a blockage of the FGF-1 binding site as well as ligand independent activation of the FGFR. The ligand independent activation is postulated to result from the disulfide dimerization of adjacent FGFR. The dimerization is the result of an opening of the FGFR, exposing additional cysteine residues (447). Pfeiffer syndrome related FGFR mutants Y349H, C342Y and S354C were transfected into NIH 3T3 cells. The findings from this study reflected the FGFR C322Y finding. Ligand independent dimerization resulted from each of the mutations (447, 448).

**Kallmann Syndrome (KS) and FGFR**

Kallmann syndrome is a human developmental disorder characterized by underdevelopment of olfactory bulbs (anosmia) and hypogonadotrophic hypogonadism. Additionally KS results (GnRH) – resulting in puberty delay. Additional phenotypes are observed in patients with

alternate mutations associated with KS. Phenotypes may include cleft palate dental agenesis and additional reproductive malformations. Mutations identified in FGFR1 have been associated with patients with the disease.

The FGF receptor mutations related to KS are attributed to loss-of-function mechanisms (1). The loss-of-function is consistent with experiments of mice containing disrupted FGFR 1 genes. The disruption of FGFR 1 in mice results in persistent cell proliferation, olfactory bulb dysplasia and decreased GnRH neurons (450). Interestingly patients containing the same FGFR1 mutations have been observed with a wide variability in phenotypes. Two Patients with identical mutations show varied phenotypes: one with isolated hyposmia without hypogonadism and the other patient with normosmic idiopathic hypogonadotrophic hypogonadism not observed in the previous patient (451). The phenotype variability observed in patients with the same mutation suggests epigenetic mechanisms or interactions with modifier genes may result in KS phenotypes. The roles of FGFR1 during development and cellular events also require interactions with both FGF proteins and FGFR regulators proteins.

Twenty-two different FGFs are found in the human genome. The mutations associated KS occur in the receptor FGFR1 IIIc. Binding specificity varies between FGF receptors. FGFR1 IIIc is capable of interacting with FGF1, FGF2, FGF8, FGF9, FGF17, FGF18 and FGF23. FGF's show tissue specific differential expression and regulate the different cellular processes. FGF8 hypomorphic mice result in a decreased number of GnRH neurons and a disruption of olfactory bulb formation (452, 453). The phenotype resulting from the FGF8 hypomorphic mice reflects the phenotype of Kallmann syndrome patients. The FGFR1 mutation L342S is found at the FGF binding site on the D3 domain. This mutation does very little to change the binding affinity of FGFR1 to FGF1 or FGF2. However, the FGF8 – FGFR1 IIIc L342S interactions is

significantly inhibited by the mutation (454). Additional mutations on the FGF8 domain have not yet been described. The interactions between FGF and the FGFR1 protein are not the single location for mutations related to KS. Although signaling requires a 2:2:2 complex of FGFR/FGF/heparin, mutations in regulating proteins are capable of producing KS.

Anosmin-1 directly interacts with FGFR1 IIIc on the cytoplasmic Ig domains II and III (455, 456). Expression of anosmin-1 is associated with FGFR1 expression as it similarly located on the KAL-1 gene associated with x-linked KS (fig. 1.13). Anosmin-1 is composed of eight domains including; cysteine rich domain (CR), whey acidic protein-like domain (WAP), four repeating domains (FnIII) and a histidine rich domain. The WAP and CR domains are the domains responsible for interacting with the D2 and D3 domains of FGFR1. The FnIII domain 1 is required to form the conformation required of the WAP and CR domains to bind to the FGFR. Surface Plasmon resonance experiments show anosmin-1 binds to the FGFR1 IIIc at 7nM affinity (457). Anosmin-1 is capable of interacting with FGFR1 IIIc with much higher affinity than the FGFR2 IIIc or FGFR3 IIIc. Additionally, anosmin-1 is induces cell proliferation in BaF3 lymphoid cells expressing FGFR1 IIIc (458). However, anosmin-1 does not increase proliferation in the same cells expressing FGFR2 IIIc or FGFR3 IIIc.

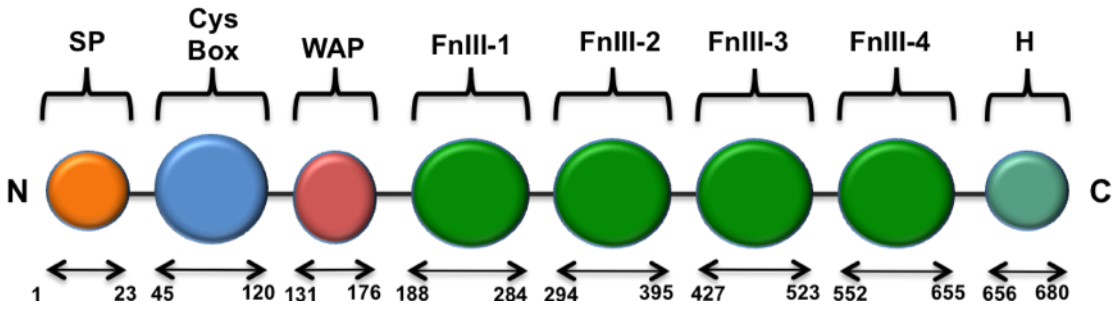


**Figure 1.13** – Cartoon representation of the domains of anosmin-1. Listed above each domain is the abbreviation of each domain including: signal peptide (sp), cystiene box (Cys Box), whey acidic protein-like (WAP), FnIII-1, FnIII-2, FnIII-3, FnIII-4 and the histidine rich domain. Below each domain is the amino acid numbering for each of the protein domains.

Missense mutations occurring in the FnIII domain of anosmin-1 results in KS phenotypes. The mutations occurring in the FnIII domain include N267K, E514K and F517L (457). The Anosmin-1 N267K mutation inhibits the interactions with FGFR1. However, mutations E514K and F517L also found in the FnIII domain result in increased interactions with the FGFR1 domain (457). Additionally, mutations found in the WAP domain are associated with KS. Mutation anosmin-1 C172R located in the WAP domain results in the disruption of a conserved disulfide bond. The disruption of the disulfide bond has shown to decrease the protein-protein interaction of anosmin-1 with FGFR. The decreased interaction of anosmin-1 C172R with FGFR1 may be the result of the increased flexibility resulting from the disrupted disulfide bond.

**Non-covalent cation-π bonds**

The FGFR's are stabilized by a variety of noncovalent interactions. The twelve beta-strands making up the FGFR D2 domain is maintained by a network of hydrogen bonds. Additionally, the beta-sandwich structure of the D2 domain allows hydrophobic interactions to stabilize the structure. In addition to the more common noncovalent interactions, cation-pi interactions have been suggested to contribute to the stability of globular proteins. Cation-π interactions may be formed from pi residue tryptophan, phenylalanine or tyrosine with cation residues lysine, arginine, or histidine. The interaction distance of cation-π interactions are limited to a distance of 3 – 8 angstroms (459). Additionally the optimum angle of interaction of the cation relative to the center of the pi residue is 90°. Cation-π interactions have been shown to stabilize beta sheets, alpha helices, protein-protein interactions and beta-hairpin structures (459-462). The energetic significance of the cation-π interaction has been exhibited in model peptide systems as well as in

protein structures through site directed mutagenesis (463). The energetic contributions of cation-π interactions are shown to contribute to β-sheet formation, β-strand interactions, turn propensity, and proper folding (464-467). Cation-π interactions involving lysine and arginine range from -3.3 ± 1.5 kcal/mol to -2.9 ± 1.4 kcal/mol (468). Typically proteins are stabilized by 5-10 kcal/mol (469). As a result it is possible that cation-pi interactions contribute significantly to the stability and functionality of a protein. However, there has been some discussion regarding the overestimation of the stabilizing potential of a cation-π interaction. One significant contributing factor to the strength of a cation-π interaction is related to the distance and orientation of the interaction.

**Characterization of cation-π interactions**

Typical cation-π interactions may be formed in a variety of angles and distances. However, there are optimal angles as well as distances to maximize the cation-π interaction. The most common cation orientations relative to the plane of the pi residue are "t-shaped" and "parallel" (468). The t-shaped interaction places the cation residue to a 90º angle relative to the aromatic pi residue. The parallel type interaction is 0º relative to the pi residue. The interaction energies determined for cation-π interaction that fall between 0º - 90º are found to have lower van der Waals and electrostatic interactions (470). Although van der Waals and electrostatic stabilizing forces are used to characterize the cation-π interaction, additional interactions have been considered.

The electrostatic contribution to the interaction between cation and π residues is supported by numerous experiments and is believed to be the major energetic factor stabilizing the interaction.

The electrostatic interactions formed between a cation and π residue is supported by: alkali metal interactions with aromatic residues, and changes in the aromatic residue.

The contribution of electrostatic energy to the cation-π bond interaction has been analyzed using alkali metals interacting with aromatic pi molecules. If electrostatics is a driving force then it is expected that the greater electrostatic potential placed over a pi residue, the stronger the cation-π bond. The cation-π energetic trend follows the electrostatic potentials in the order of $Li^+$ > $Na^+$ > $K^+$ > $Rb^+$(471). This trend would also be followed if the aromatic pi residue were replaced with a negatively charged residue.

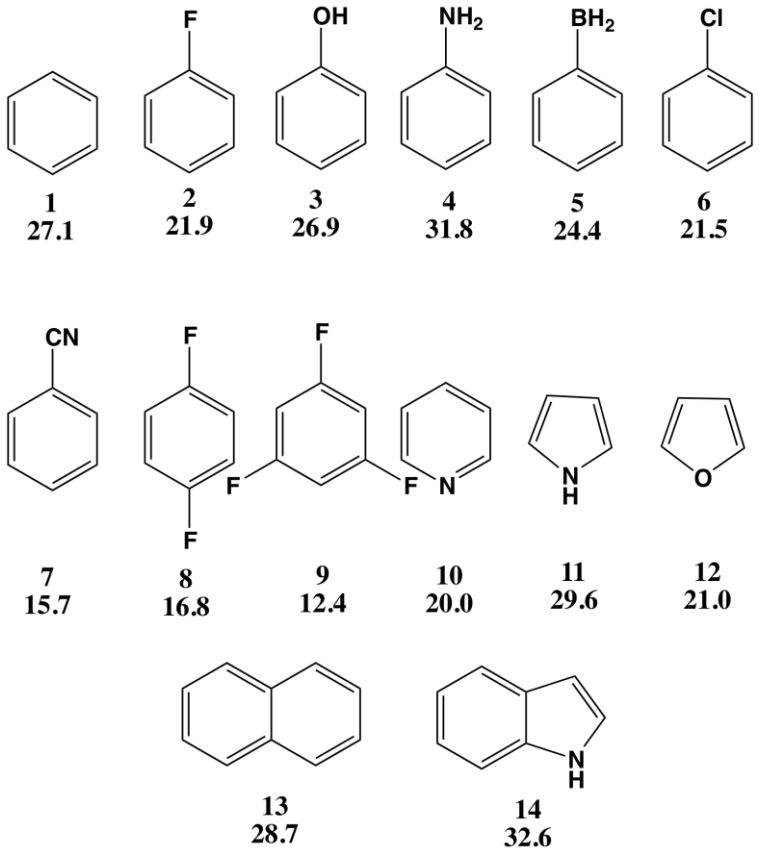


**Figure 1.14** – Structures studied by *ab initio* calculations to determine the strength of cation-π interactions formed. Binding energies are shown for each of the cation-π complexes calculated (Kcal/mol)(473).

Additional forces that must be considered are polarizability, dispersion forces and charge transfer effects (472). The contribution of electrostatic binding forces has also been established by the analysis of the aromatic residue.

The electrostatic interactions formed by a cation with an aromatic residue may be better understood by considering the cation-π bond strength through modifying the aromatic residue (figure 1.13). The electrostatic interactions of a cation-π bond formed by each of the benzene molecules clearly represent a trend. The strongest cation-π bond formed for the benzene molecules shown in figure 1.13 begins 14 > 4 > 13 > 1 > 3. This trend also suggests electron-rich heterocycles result in poor cation-π binding interactions. This trend has been observed in 1,3,5 trifluorobenze that is not capable of forming cation-π interactions and provides support for the electrostatic model (473). Although there is ample evidence for the electrostatic component in cation-π interaction, additional interactions have evidence supporting their contributions stabilizing the noncovalent bond.

Additional forces stabilizing cation-π bonds that have been included are charge-quadrupole, charge-dipole, charge-induced dipole, charge-transfer, dispersion forces and hydrophobic forces (474, 475). Benzene molecules lack a permanent dipole, but do have a permanent quadrupole. The quadrupole of benzene is the result of two dipoles aligned on the structure (476). The result is a non-spherical charge distribution allowing for a negative charge in the z plane of the benzene ring and small positive charge distributed to the hydrogen atoms of the benzene ring. The quadrupole interaction is still an electrostatic bond with a nearby cation residue. Theoretical calculations have shown point charge – quadrupolar interactions of benzene and point charges are comparable in strength to dipolar – point charge interactions (477, 478). However, the cation-π interactions that are commonly observed occur at a distance allowing for van der Waals

contacts. Additionally, distance dependence of a quadrupole – ion interaction is $1/r^3$. The distance dependence of a cation-π interaction shows a distance dependence of $1/r^n$ ($n < 2$ Å). This proximity makes it unlikely that quadrupole – cation interactions contribute significantly to the strength of the cation-π interaction (475). The complexity of protein structures allows for cation-π interactions to occur in both solvent exposed, buried locations, hydrophobic and highly electrostatic locations. Each of these variations may contribute or detract from the strength of a cation-π interaction.

**Solvation of cation-π bonds**

The peptide models used to determine the contribution a cation-π interaction provides to the stability of the peptide is most often solvent exposed. The degree of solvent exposure of the cation or the pi residue can change the strength of the interaction by at least 0.9 kcal/mol (479). Recent studies tuning the degree of solvent exposure identifies the role that solvent plays in reducing the cation-π interaction. Peptide models show a cation-π pair's allowing the aromatic pi residue to remain buried while the cation is partially solvated estimate the cation-π interaction at 0.9 kcal/mol. In contrast, solvating both the cation and pi residues results in a cation-π interaction of 0.06 kcal/mol (479). This data suggests the solvent exposed cation-π interactions are significantly less stabilized than what is observed for a buried cation-π interaction. Additionally, cation-π ineractions require that the solvated cation must undergo desolvation to bind in a hydrophobic pocket.

Desolvation of the cationic residue is considered to be a large energetic penalty of cation-π interactions. The CAPTURE program was used to determine the relative location of cation-π interactions in proteins. Roughly 60% of cation-π interactions show partial solvation (480). The strength of a cation-π interaction is energetically compared to salt bridge interactions.

However, the energetic desolvation penalty of a salt bridge interaction is double that of a cation-π interaction. The aromatic residue of a cation-π interaction shows little energetic desolvation penalties. The cation-π interaction is not strong enough to overcome the desolvation of the cationic residue. However, it is typically the summation of the non-covalent interactions provide the desolvation energy needed for the burial of cationic residues. The desolvation penalties of a lysine and arginine residue are unequal (480, 481).

The two probable interaction geometries of a cation include parallel and t-shaped orientations. The stacked orientation of arginine relative to tryptophan allows for preferential hydrogen bonding of the NH groups adjacent residues. The preferential interaction of the argnine sidechain places the epsilon carbon superficially to the indole ring. The stacked interaction of the arginine residue also provides additional van der Waals contacts with the pi residue. The van der Waals contacts of an arginine residue are not possible by any orientation of lysine over a pi residue (480, 481).

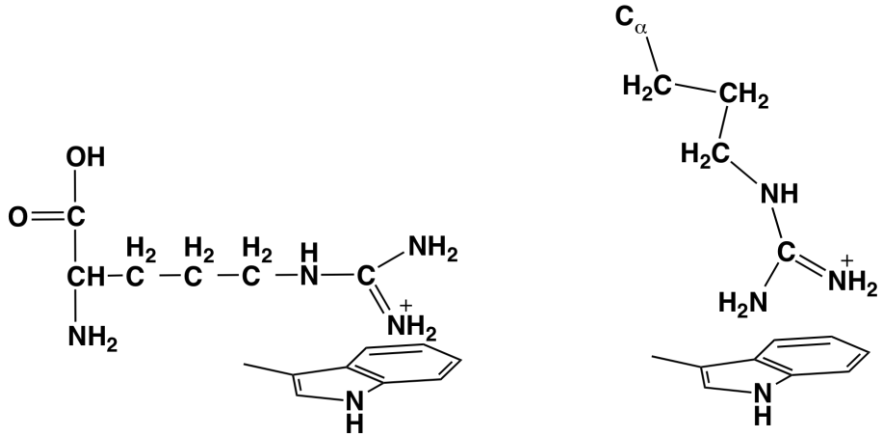


**Figure 1.15** – Shows the two major conformations of a cation relative to a pi residue. The left structure shows the arginine residue in parallel or stacked orientation relative to the plane of the tryptophan residue. The right structure shows the argnine in t-shaped orientation relative to the plane of the tryptophan.

The desolvation penalties of a lysine residue is higher that arginine. These interactions are observed in small molecule cation-π bonds. The cation-π interaction of ammonium with benzene

is stonger than the interaction of guanidinium with benzene under the same conditions (480, 481). The difference is considered to be the result of desolvation required for a cation-π interaction to form (480, 481). The van der Waals interactions as well as the electrostatic interactions are the two main parameters considered when determining the strength of a cation-π interaction.

**In silico determination of cation-π interactions**

The in silico determination of a cation-π interaction must take into consideration the contribution of several non-covalent forces contributing to a cation-π bond. The most agreed upon component of a cation-π interaction is the electrostatic force. However, the electrostatic interaction of the cationic residue is formed with an aromatic residue having no net negative. Additionally, the strength of a cation-π interaction has shown to be both distance and angle dependent. Coulombic charge interaction calculations typically used for charged interactions are only distance dependent. The second most agreed upon parameter of a cation-π interaction is the van der Waals interaction.

The van der Waals interaction is considered to contribute significantly to the cation-π interaction. The calculation required for van der Waals interactions must take into account electron correlation effects. Calculation accounting for electron correlation effects include ab *initio* – Møller-Plesset perturbation (MP2), coupled-cluster with singles, doubles and perturbative triples (CCSD(T)) or quantum Monte Carlo calculations. Additional calculations such as density functional theory (DFT) have also been used to determine van der Waals interactions. Local density approximations and generalized gradient approximations used for DFT calculations have been shown to fail in the estimation of van der Waals interactions. The

most commonly used calculation to determine cation-π interactions in a protein have been developed by Dougherty *et al.* (475).

The program cation-π trends using realistic electrostatics (CaPTURE Program) was developed by Dougherty et al. This program uses *ab initio* calculations as well as modified optimized potential for liquid surface (OPLS) calculations. Using the OPLS force field subsets, the capture program is able to estimate both electrostatic and van der Waals interactions (482). Additionally, the CaPTURE program sets distance constraints of 6Å for the determined cation-π interactions.

There are additional physical characteristics of a cation-π interaction that must be taken into account. Cation-π bonds may also be contributed to by hydrogen bonds occurring between –OH groups on tyrosine and the amino groups of lysine and arginine. Energetic penalties resulting from the solvation of cationic residues have been taken into consideration from other prediction models, but not in the CaPTURE program.

The chemical environment of a cation-pi interaction may significantly change in the strength of the interaction. Traditional gas phase studies of cation-π interactions fail to account for changes in the noncovalent interaction resulting from solvation. The chemical environment can significantly reduce or increase the cation-pi interaction. Chemical environment altering cation-π interactions include the solvent exposure of the cation or pi residue, anion coordination to the cation or pi residue and the hydrophobic environment surrounding the cation or pi residue.

**Intrinsic Fluorescence of Proteins**

The intrinsic fluorescence of proteins has served as a probe to monitor the stability of proteins through thermal denaturation, pH titrations and chemical denaturants. Additionally,

intrinsic fluorescence may be used to observed structural changes upon protein-protein or protein-ligand binding interactions. The intrinsic fluorescent probes common in proteins include amino acids tyrosine, phenylalanine and tryptophan. Although proteins are often abundant in these residues, the low quantum yields of tyrosine and phenylalanine make these intrinsic fluorophores undesirable. The high quantum yield of tryptophan has made this residue one of the most studied residues in protein fluorescence. However, there remain unique characteristics of tryptophan fluorescence that complicate the fluorescence spectrum acquired from tryptophan containing proteins. Single tryptophan containing proteins have shown unique and unpredictable characteristics that are not common among multi-tryptophan containing proteins. Tryptophan fluorescence is strongly sensitive to the local environment that may significantly influence the quantum yield ($\phi_f$), excited state lifetime ($\tau_f$) and wavelength ($\lambda_{max}$) (483). The most significant contributor to the irregularity of a fluorescence spectrum is the electrostatic landscape surrounding the tryptophan side chain. Placement of charged residues around tryptophan side chains may result in the maximum wavelength to shift to the red or blue**.** The major considerations that must be taken into account for tryptophan fluorescence intensity and lifetime include: electrostatic environment, charged residues and fluorescence quenching side chains.

Tryptophan fluorescence is initiated by the excitation of the electrons in the pyrole ring of the tryptophan side chain. The wavelength of light required for tryptophan fluorescence is 280 nm. The excited state electrons in the pyrole ring then transfer to the benzene ring of the tryptophan residue. Stabilization of the electron density shift from the pyrole to the benzene ring (ground state to the excited state $^1L_a$) may determine the degree of red shift of the wavelength maximum (483). Additionally, the intensity of the fluorescence observed for tryptophan residues is

proportional to the stabilization of the electron density shift from the indole ring as a whole to the electron acceptor during photoinduced electron transfer.

**Fluorescence lifetime**

Excited state fluorophores are able to undergo a variety of transformations that may include electron redistribution, structural changes and chemical reactions. Commonly fluorophores undergo a nonradiative loss of photoinduced energy in a process called quenching. Quenching is a process that results in a loss or decrease in the fluorescence lifetime. Quenching is a process by which energy is transferred and may occur internally by molecular vibrations or rotations or externally by transferring the energy outside the molecule. Fluorescence quenching mechanisms include internal rotation, temperature, viscosity, polarity and excited state electron transfer.

**Temperature**

The temperature of a solution may have defined effects on the observed fluorescence from the fluorophore. The solvent is among the contributors to fluorescence quenching and fluorescence lifetime as the temperature increases (106). The temperature dependence of the fluorescence lifetime is approximated by the Arrhenius equation:

$$k = Ae^{-\frac{E_a}{RT}}$$

**Figure 1.16** - Arrhenius eq. depicting the approximation temperature has on the rate of solvent quenching (K). Additional parameters include the pree-exponential factor (A ~ $10^{15}$ – $10^{17}$ $sec^{-1}$), energy of activation ($E_a$ ~ 11-13 $k_{cal}$*$mol^{-1}$), gas constant (R), and the temperature in Kelvin (T). Increasing temperature is capable of varying the $K_{sol.}$ by ~ $10^7$ $sec^{-1}$.

***Electron Transfer to the Peptide Backbone***

The peptide backbone can also be a potential quenching agent of tryptophan residues. The mechanism proposed for the tryptophan to backbone electron transfer is from the Cε of the tryptophan residue to the carbonyl carbon of the peptide backbone (484). Additional considerations that may alter the efficiency of the tryptohan to backbone electron transfer include the rotameric state and the medium between the side chain and carbonyl (485-487). The electron transfer has been described by Marcus and Sutin:

$$k_{ET}(R)=k_0 \exp(-\beta(R-R_0))$$

**Figure 1.17** - Marcus and Sutin equation for the rate of electron transfer from a sidechain to the peptide carbonyl. In the Marcus and Sutin equation the rate of electron transfer ($K_{et}$) is determined by rate constant for electron transfer from van der Waals distance of 3 Å ($K_0$), the distance between the donor and acceptor (R) and the sharpness of the distance dependence (β).

The Marcus and Sutin equation requires a series of parameters including the distance between the tryptophan and carbonyl. However, additional parameters including the rotameric states of the tryptophan side chain are required to understand the quenching mechanism.

Goldman et al have determined the possible rotameric states during electron transfer from the tryptophan residue to the carbonyl side chain (487). Classical molecular mechanics calculations were used to determine six rotameric conformations for the tryptophan side chain for electron transfer to the backbone.

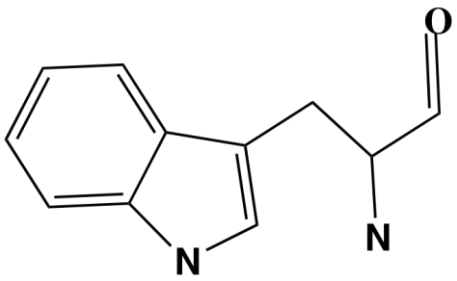


**Figure 1.18** - Structure of the tryptophan residue showing the indole and benzene rings involved in electron transfer ($C^{\varepsilon 2}$).

The semi-empirical calculations were used to determine the charge distribution and ionization potentials for each rotameric state. The two possible electron donors from the tryptophan side chain were determined to be $C^{\varepsilon 3}$ and $C^{\xi 2}$. When $C^{\xi 2}$ is the electron donor the lifetimes were between 0.1 – 10 ps, which is unrealistic slow for lifetimes (483). However, when $C^{\varepsilon 3}$ is the electron donor lifetimes were 0.11ns – 0.1ps. This is a more reasonable value that makes the $C^{\varepsilon 3}$ the more likely electron donor (487).

**Fluorescence quenching side chains**

The ability for side chains to quench tryptophan residues has been thoroughly studied. Quenching rate constants have been determined for side chains containing protonated amino groups (Lys or α-amino groups). Glutamine and asparagine are considered to be weak fluorescence quenching agents ($4 \times 10^7$ and $2.4 \times 10^7$ $M^{-1}$ $sec^{-1}$) (488). Protonated histidine residue side chains also serve as a strong electron acceptor ($K_q$ – $2.9 \times 10^9$ $M^{-1}$ $sec^{-1}$)(489, 489-491). Additionally, amino acid cysteine (including disulfide bonds) is the most efficient fluorescence quenching side chain ($K_q$ – $4 \times 10^9$ $M^{-1}$ $sec^{-1}$) Disufide bound cysteine residues is also efficient fluorescence quencher ($K_q$ ->$10^{10}$ $M^{-1}$ $sec^{-1}$) (492, 493). Additionally there are residues that have historically been mistakenly considered as fluorescent quenching residues.

There are several residues with little evidence supporting the ability to be considered to be fluorescence quenching residues. Residues that are mistakenly considered to be fluorescent quencher include glutamate, aspartate and phenylalanine. The negative charge of glutamate and aspartate make unlikely electron acceptors (494). However, the proximity of a negatively charged near a tryptophan is able to significantly increase the rate of tryptophan fluorescence without being the electron acceptor. Phenylalanine side chains have also been mistakenly considered to be a fluorescence quencher. However, the highest occupied molecular orbital of tryptophan is too low in energy and the lowest unoccupied molecular orbital is too high in energy to allow an exited state electron transfer from tryptophan (494).

**Electrostatic interactions and tryptophan quenching**

Stabilizing electrostatic interactions allow for an increase electron transfer rates that increase the quenching rate. Electron transfer from the tryptophan side chain to the electron acceptor requires the charge transfer state to be equal to the electron acceptor. The charge transfer energy may be adjusted by the location of charged residues surrounding both the tryptophan side chain and the electron acceptor. Placement of a negatively charged residue (asapartic acid or glutamic acid) near the tryptophan side chain and a positively charged residue (lysine or arginine) near the electron acceptor acts to stabilize the electron transfer (495). Stabilizing the electron transfer from the tryptophan side chain to the electron acceptor acts to significantly reduce the fluorescence intensity. Conversely, the charge transfer may be hindered by the placement of charged residues around the tryptophan side chain. Insertion of a positively charged residue (lysine or arginine) near the tryptophan side chain and a negatively charged residue (aspartic acid or glutamic acid) near the electron acceptor will hinder the charge transfer.

Inhibition of the charge transfer results in a build up of overall electron density on the benzene ring of tryptophan resulting in increased fluorescence (495). The effect of the placement of charged residues residing near the fluorescing residue to alter the charge transfer state is considered to be the *internal Stark effect.*

**Single tryptophan proteins**

Single tryptophan proteins show unique fluorescence lifetimes when compared to multiple tryptophan proteins. Single tryptophan proteins often show multiple fluorescence lifetimes. The two major considerations explaining single tryptophan fluorescence include: the existence of different states that do not interconvert on the fluorescent time scale (ground state heterogeneity) and the existence of reversible excited state dynamics of the tryptophan residue.

Ground state heterogeneity occurs as a result of multiple rotameric states of the tryptophan side chain. Each of the rotameric states possible for tryptophan do not interconvert on the nanosecond timescale (496-498). Single tryptophan protein experimental evidence has suggested the overall protein fold is unchanged while microstates for the tryptophan residues continues to change. Additionally, the different microstates possible for a single tryptophan residue allows for different quenching constants ($K_q$). The different quenching constants may be determined for a single tryptophan with as single electron acceptor. Examples of this have been observed in the single tryptophan protein colocin (499). Importantly, the timescale of the heterogenic states of tryptophan also play a significant role fluorescence lifetime observed for single tryptophan proteins. A number of case studies suggest the microstates to be on a nanosecond timescale (bacteriophage T4 lysozyme, hemoglobin and phsophofructokinase)(500-

502). The microstates determined have been suggested to be the result of rotation of the tryptophan residues about the $C^{\alpha}$ - $C^{\beta}$ and the $C^{\beta}$ - $C^{\gamma}$ bond.

Tryptophan rotameric states about the $C^{\alpha}$ - $C^{\beta}$ interconvert rapidly within protein (503). However, rotamers of tryptophan residue resulting from interconversions about the $C^{\beta}$ - $C^{\gamma}$ bond occur on a much slower timescale (504). Interconversion data suggests the rotameric states of tryptophan residues buried in proteins occur on a timescale from 0.04 ns – 0.5 ns (505). The slower predicted rotation about the $C^{\beta}$ - $C^{\gamma}$ bond was expected to contribute to the most to the multiple fluorescence lifetimes. However, experimental studies of a cyclic hexapeptide suggest the interconversion about the $C^{\alpha}$ - $C^{\beta}$ to be the major axis of rotation. Additionally, there are many structural rotameric states that complicate the possible electron acceptor – tryptophan interactions. As a result the number of unique fluorescent lifetimes may be unique to the protein and the microenvironment of the tryptophan.

**Literature Cited**


1. Ornitz, D. M. 2005. FGF signaling in the developing endochondral skeleton. Cytokine Growth Factor Rev. 16, 205-213.

2. Thisse, B. and C. Thisse 2005. Functions and regulations of fibroblast growth factor signaling during embryonic development. Dev. Biol. 287, 390-402.

3. Thisse, B. and C. Thisse 2005. Functions and regulations of fibroblast growth factor signaling during embryonic development. Dev. Biol. 287, 390-402.

4. Itoh, N. 2007. The fgf families in humans, mice, and zebrafish: Their evolutional processes and roles in development, metabolism, and disease. Biol. Pharm. Bull. 30, 1819-1825.

5. Itoh, N., R. Linhardt and M. Mohammadi 2004. Biochemical analysis of pathogenic ligand-dependent FGFR2 mutations suggests distinct pathophysiological mechanisms for craniofacial and limb abnormalities. Human Molecular 13 (19): 2313-2324.

6. Itoh, N. and D.M. Ornitz 2004. Evolution of the fgf and fgfr gene families. TRENDS in Genetics. (20) 563–569.

7. Baird, K., S. Davis, C.R. Antonescu, U.L. Harper, R.L. Walker, Y. Chen, A.A. Glatfelter, P.H. Duray and P.S. Meltzer 2005. Gene expression profiling of human sarcomas: Insights into sarcoma biology. Cancer Res. 65, 9226-9235.

8. Schlessinger J, Plotnikov AN, Ibrahimi OA, Eliseenkova AV, Yeh BK, Yayon A, Linhardt RJ and Mohammadi M 2000. Crystal structure of a ternary FGF-FGFr-heparin complex reveals a dual role for heparin in FGFr bindin and dimerization. Mol Cell. 6, 743-750.

9. Furdui, C. M., E.D. Lew, J. Schlessinger and K.S. Anderson 2006. Autophosphorylation of FGFR1 kinase is mediated by a sequential and precisely ordered reaction. Mol. Cell. 21, 711-717.

10. Mohammadi, M., I. Dikic, A. Sorokin, W.H. Burgess, M. Jaye and J. Schlessinger 1996. Identification of six novel autophosphorylation sites on fibroblast growth factor receptor 1 and elucidation of their importance in receptor activation and signal transduction. Mol. Cell. Biol. 16, 977-989.

11. Ohkubo, Y., A.O. Uchida, D. Shin, J. Partanen and F.M. Vaccarino 2004. Fibroblast growth factor receptor 1 is required for the proliferation of hippocampal progenitor cells and for hippocampal growth in mouse. J. Neurosci. 24, 6057-6069.

12. Zhao, M., D. Li, K. Shimazu, Y.X. Zhou, B. Lu and C.X. Deng 2007. Fibroblast growth factor receptor-1 is required for long-term potentiation, memory consolidation, and neurogenesis. Biol. Psychiatry. 62, 381-390.

13. Gill, J. C. and P.S. Tsai 2006. Expression of a dominant negative FGF receptor in developing GNRH1 neurons disrupts axon outgrowth and targeting to the median eminence. Biol. Reprod. 74, 463-472.

14. Gill, J. C., S.M. Moenter and P.S. Tsai 2004. Developmental regulation of gonadotropin-releasing hormone neurons by fibroblast growth factor signaling. Endocrinology. 145, 3830-3839.

15. Ibrahimi, O. A., F. Zhang, A.V. Eliseenkova, N. Itoh, R.J. Linhardt and M. Mohammadi 2004. Biochemical analysis of pathogenic ligand-dependent FGFR2 mutations suggests distinct pathophysiological mechanisms for craniofacial and limb abnormalities. Hum. Mol. Genet. 13, 2313-2324.

16. Yang, F., Y. Zhang, S.J. Ressler, M.M. Ittmann, G.E. Ayala, T.D. Dang, F. Wang and D.R. Rowley 2013. FGFR1 is essential for prostate cancer progression and metastasis. Cancer Res. April. Electronic pub.

17. Yu, K., A.B. Herr, G. Waksman and D.M. Ornitz 2000. Loss of fibroblast growth factor receptor 2 ligand-binding specificity in apert syndrome. Proc. Natl. Acad. Sci. U. S. A. 97, 14536-14541.

18. Rohmann, E., H.G. Brunner, H. Kayserili, O. Uyguner, G. Nurnberg, E.D. Lew, A. Dobbie, V.P. Eswarakumar, A. Uzumcu, M. Ulubil-Emeroglu, J.G. Leroy, Y. Li, C. Becker, K. Lehnerdt, C.W. Cremers, M. Yuksel-Apak, P. Nurnberg, C. Kubisch, J. Schlessinger, H. van Bokhoven and B. Wollnik 2006. Mutations in different components of FGF signaling in LADD syndrome. Nat. Genet. 38, 414-417.

19. Kiselyov, V. V., E. Bock, V. Berezin and F.M. Poulsen 2006. NMR structure of the first ig module of mouse FGFR1. Protein Sci. 15, 1512-1515.

20. Kalinina, J., K. Dutta, D. Ilghari, A. Beenken, R. Goetz, A.V. Eliseenkova, D. Cowburn and M. Mohammadi 2012. The alternatively spliced acid box region plays a key role in FGF receptor autoinhibition. Structure. 20, 77-88.

21. Hung KW, Kumar TK, Kathir KM, Xu P, Ni F, Ji HH, Chen MC, Yang CC, Lin FP, Chiu IM, Yu C. 2005. Solution structure of the ligand binding domain of the fibroblast growth factor receptor: Role of heparin in the activation of the receptor. Biochemistry., 15787-15798.

22. Plotnikov, A. N., J. Schlessinger, S.R. Hubbard and M. Mohammadi 1999. Structural basis for FGF receptor dimerization and activation. Cell. 98, 641-650.

23. Ornitz, D. M., J. Xu, J.S. Colvin, D.G. McEwen, C.A. MacArthur, F. Coulier, G. Gao and M. Goldfarb 1996. Receptor specificity of the fibroblast growth factor family. J. Biol. Chem. 271, 15292.

24. Yamashita, T., M. Konishi, A. Miyake, K. Inui and N. Itoh 2002. Fibroblast growth factor (FGF)-23 inhibits renal phosphate reabsorption by activation of the mitogen-activated protein kinase pathway. J. Biol. Chem. 277, 28265.

25. Orr-Urtreger, A., M.T. Bedford, T. Burakova, E. Arman, Y. Zimmer, A. Yayon, D. Givol and P. Lonai 1993. Developmental localization of the splicing alternatives of fibroblast growth factor receptor-2 (FGFR 2). Dev. Biol. 158, 475-486.

26. Umemori, H., M.W. Linhoff, D.M. Ornitz and J.R. Sanes 2004. FGF22 and its close relatives are presynaptic organizing molecules in the mammalian brain. Cell. 118, 257-270.

27. Xu, J., M. Nakahara, J.W. Crabb, E. Shi, Y. Matuo, M. Fraser, M. Kan, J. Hou and W.L. McKeehan 1992. Expression and immunochemical analysis of rat and human fibroblast growth factor receptor (flg) isoforms. J. Biol. Chem. 267, 17792-17803.

28. Partanen, J., L. Schwartz and J. Rossant 1998. Opposite phenotypes of hypomorphic and Y766 phosphorylation site mutations reveal a function for Fgfr1 in anteroposterior patterning of mouse embryos. Genes & Development. 12, 2332.

29. Bellusci, S., J. Grindley, H. Emoto, N. Itoh and B. Hogan 1997. Fibroblast growth factor 10 (FGF10) and branching morphogenesis in the embryonic mouse lung. Development. 124, 4867.

30. Deng, C. X., A. Wynshaw-Boris, M.M. Shen, C. Daugherty, D.M. Ornitz and P. Leder 1994. Murine FGFR-1 is required for early postimplantation growth and axial organization. Genes Dev. 8, 3045-3057.

31. Xu, X., M. Weinstein, L. Cuiling and C.X. Deng 1999. Fibroblast growth factor receptors (FGFRs) and their roles in limb development. Cell Tissue Res. 296, 33-43.

32. Gospodarowicz D 1974. Localization of a fibroblast growth factor and its effect alone and with hydrocortisone on 3T3 cell growth. Nature. 249, 123-127.

33. Ornitz, D. 2000. FGFs, heparan sulfate and FGFRs: Complex interactions essential for development. Bioessays. 22(2):108-12.

34. Kiefer P, Acland P, Pappin D, Peters G, Dickson C 1994. Competition between nuclear localization and secretory signals determines the subcellular fate of a single CUG-initiated form of FGF3. Embo j. 13, 4126-4136.

35. Arnaud E, Touriol C, Boutonnet C, Gensac MC, Vagner S, Prats H, Prats AC 1999. A new 34-kilodalton isoform of human fibroblast growth factor 2 is cap dependently synthesized by using a non-AUG start codon and behaves as a survival factor. Mol. Cell Biol. 19, 505-514.

36. Zhang, J. D., L.S. Cousens, P.J. Barr and S.R. Sprang 1991. Three-dimensional structure of human basic fibroblast growth factor, a structural homolog of interleukin 1 beta. Proc. Natl. Acad. Sci. U. S. A. 88, 3446-3450.

37. Plotnikov, A.N., Hubbard, S.R., Schlessinger, J., Mohammadi, M. 2000. Crystal structure of FGF2 in complex with the extracellular lignad binding domain of FGF receptor 2 (FGFR2). Cell. 101, 413-424.

38. Mignatti, P., E. Dejana, D. Hicklin and P. Bohlen 2000. Monoclonal antibody to vascular endothelial-cadherin is a potent inhibitor of angiogenesis, tumor growth, and metastasis. Cancer Res. 15;60(24):6805-10.

39. Kathir, K. M., K. Ibrahim, D. Rajalingam, I. Prudovsky, C. Yu and T.K. Kumar 2007. S100A13-lipid interactions-role in the non-classical release of the acidic fibroblast growth factor. Biochim. Biophys. Acta. 1768, 3080-3089.

40. Li LY, Safran M, Aviezer D, Bohlen P, Seddon AP, Yayon A 1994. Biochemistry. 33, 10999-11007.

41. Moy FJ, Seddon AP, Bohlen P, Powers R 1996. High-resolution solution structure of basic fibroblast growth factor determined by multidimensional heteronuclear magnetic resonance spec- troscopy. Biochemistry. 35, 13552-13561.

42. Pellegrini, L., Burke, D.F., von Delft, F., Mulloy, B. and Blundell, T.L. 2000. Crystal structure of fibroblast growth factor receptor ectodomain bound to ligand and heparin. Nature. 407, 1029-1034.

43. M. Mohammadi, I. Dikic, A. Sorokin, W.H. Burgess, M. Jaye, and J. Schlessinger 1996. Identification of six novel autophosphorylation sites on FGFR1 and elucidation of their importance in receptor activation and signal transduction. Mol. Cell. Biol. 16(3), 977-988.

44. Armelin HA 1973. Pituitary extracts and steroid hormones in the control of 3T3 cell growth. Pnas. 70, 2702-2706.

45. McNeil, P. L., L. Muthukrishnan, E. Warder and P.A. D'Amore 1989. Growth factors are released by mechanically wounded endothelial cells. J. Cell Biol. 109, 811-822.

46. Ong, S. H., G.R. Guy, Y.R. Hadari, S. Laks, N. Gotoh, J. Schlessinger and I. Lax 2000. FRS2 proteins recruit intracellular signaling pathways by binding to diverse targets on fibroblast growth factor and nerve growth factor receptors. Mol. Cell. Biol. 20, 979-989.

47. Mohammadi, M., C.A. Dionne, W. Li, N. Li, T. Spivak, A.M. Honegger, M. Jaye and J. Schlessinger 1992. Point mutation in FGF receptor eliminates phosphatidylinositol hydrolysis without affecting mitogenesis. Nature. 358, 681-684.

48. Kouhara, H., Y.R. Hadari, T. Spivak-Kroizman, J. Schilling, D. Bar-Sagi, I. Lax and J. Schlessinger 1997. A lipid-anchored Grb2-binding protein that links FGF-receptor activation to the Ras/MAPK signaling pathway. Cell. 89, 693-702.

49. Dailey, L., D. Ambrosetti, A. Mansukhani and C. Basilico 2005. Mechanisms underlying differential responses to FGF signaling. Cytokine Growth Factor Rev. 16, 233-247.

50. Peters, K. G., J. Marie, E. Wilson, H.E. Ives, J. Escobedo, M. Del Rosario, D. Mirda and L.T. Williams 1992. Point mutation of an FGF receptor abolishes phosphatidylinositol turnover and Ca2+ flux but not mitogenesis. Nature. 358, 678-681.

51. Lemmon, M. A. and J. Schlessinger 2010. Cell signaling by receptor tyrosine kinases. Cell. 141, 1117-1134.

52. Mohammadi, M., A.M. Honegger, D. Rotin, R. Fischer, F. Bellot, W. Li, C.A. Dionne, M. Jaye, M. Rubinstein and J. Schlessinger 1991. A tyrosine-phosphorylated carboxy-terminal peptide of the fibroblast growth factor receptor (flg) is a binding site for the SH2 domain of phospholipase C-gamma 1. Mol. Cell. Biol. 11, 5068-5078.

53. Ryan PJ, Paterno GD, Gillespie LL 1998. Identification of phos- phorylated proteins associated with the fibroblast growth factor receptor type I during early *xenopus* development. Biochem Biophys Res Commun. 244, 763-767.

54. Peters,Jacky Marie Emily Wilson Harfan E Ives Jaime Escobedo Mercedita Del Rosario Daniel Mirda Kevin G. and L.T. Williams 1992. Point mutations of an FGF receptor abolishes phosphatidylinositol turnover of ca 2+ flux but not mitogenesis. Nature. 358, 678-681.

55. Bottcher, R. and C. Niehrs 2005. Fibroblast growth factor signaling during early vertebrate development. Endocr. Rev. 26 (1) 63-77

56. Ornitz, D. and N. Itoh Fibroblast growth factors. Genome Biol. 2, reviews3005.1-reviews 3005.12

57. Lamothe, B., M. Yamada, U. Schaeper, W. Birchmeier, I. Lax and J. Schlessinger 2004. The docking protein Gab1 is an essential component of an indirect mechanism for fibroblast growth factor stimulation of the phosphatidylinositol 3-kinase/Akt antiapoptotic pathway. Mol. Cell. Biol. 24, 5657-5666.

58. Lamothe, B., M. Yamada, U. Schaeper, W. Birchmeier, I. Lax and J. Schlessinger 2004. The docking protein Gab1 is an essential component of an indirect mechanism for fibroblast growth factor stimulation of the phosphatidylinositol 3-kinase/Akt antiapoptotic pathway. Mol. Cell. Biol. 24, 5657-5666.

59. Guimond, S., M. Maccarana, B.B. Olwin, U. Lindahl and A.C. Rapraeger 1993. Activating and inhibitory heparin sequences for FGF-2 (basic FGF). distinct requirements for FGF-1, FGF-2, and FGF-4. J. Biol. Chem. 268, 23906-23914.

60. Kreuger, J., M. Salmivirta, L. Sturiale, G. Gimenez-Gallego and U. Lindahl 2001. Sequence analysis of heparan sulfate epitopes with graded affinities for fibroblast growth factors 1 and 2. J. Biol. Chem. 276, 30744-30752.

61. McKeehan, W. L., F. Wang and M. Kan 1998. The heparan sulfate-fibroblast growth factor family: Diversity of structure and function. Prog. Nucleic Acid Res. Mol. Biol. 59, 135-176.

62. Bonano, V., S. Oltean, R. Brazas, Garcia-Blanco MA. 2006. Imaging the alternative silencing of FGFR2 exon IIIb in vivo. Rna.12(12):2073-9.

63. Carstens, R. P., W.L. McKeehan and M.A. Garcia-Blanco 1998. An intronic sequence element mediates both activation and repression of rat fibroblast growth factor receptor 2 pre-mRNA splicing. Mol. Cell. Biol. 18, 2205-2217.

64. Del Gatto, F., A. Plet, M.C. Gesnel, C. Fort and R. Breathnach 1997. Multiple interdependent sequence elements control splicing of a fibroblast growth factor receptor 2 alternative exon. Mol. Cell. Biol. 17, 5106-5116.

65. Del Gatto-Konczak, F., C.F. Bourgeois, C. Le Guiner, L. Kister, M.C. Gesnel, J. Stevenin and R. Breathnach 2000. The RNA-binding protein TIA-1 is a novel mammalian splicing regulator acting through intron sequences adjacent to a 5' splice site. Mol. Cell. Biol. 20, 6287-6299.

66. Beer, H., L. Vindevoghel, M.J. Gait, J. Revest, D.R. Duan, I. Mason, C. Dickson and S. Werner 2000. Fibroblast growth factor (FGF) receptor 1-IIIb is a naturally occurring functional receptor for FGFs that is preferentially expressed in the skin and the brain. J. Biol. Chem. 275, 16091-16097.

67. Ohmachi, S., Y. Watanabe, T. Mikami, N. Kusu, T. Ibi, A. Akaike and N. Itoh 2000. FGF-20, a novel neurotrophic factor, preferentially expressed in the substantia nigra pars compacta of rat brain. Biochem. Biophys. Res. Commun. 277, 355-360.

68. Ornitz, D. M., J. Xu, J.S. Colvin, D.G. McEwen, C.A. MacArthur, F.o. Coulier, G. Gao and M. Goldfarb 1996. Receptor specificity of the fibroblast growth factor family. J. Biol. Chem. 271, 15292-15297.

69. Del Gatto, F., A. Plet, M.C. Gesnel, C. Fort and R. Breathnach 1997. Multiple interdependent sequence elements control splicing of a fibroblast growth factor receptor 2 alternative exon. Mol. Cell. Biol. 17, 5106-5116.

70. Shimizu, A., K. Tada, C. Shukunami, Y. Hiraki, T. Kurokawa, N. Magane and M. Kurokawa-Seo 2001. A novel alternatively spliced fibroblast growth factor receptor 3

isoform lacking the acid box domain is expressed during chondrogenic differentiation of ATDC5 cells. J. Biol. Chem. 276, 11031-11040.

71. Shi, E., M. Kan, J. Xu, F. Wang, J. Hou and W.L. McKeehan 1993. Control of fibroblast growth factor receptor kinase signal transduction by heterodimerization of combinatorial splice variants. Mol. Cell. Biol. 13, 3907-3918.

72. Wang, F., M. Kan, G. Yan, J. Xu and W.L. McKeehan 1995. Alternately spliced NH2-terminal immunoglobulin-like loop I in the ectodomain of the fibroblast growth factor (FGF) receptor 1 lowers affinity for both heparin and FGF-1. J. Biol. Chem. 270, 10231-10235.

73. Kalinina, J., K. Dutta, D. Ilghari, A. Beenken, R. Goetz, A.V. Eliseenkova, D. Cowburn and M. Mohammadi 2012. The alternatively spliced acid box region plays a key role in FGF receptor autoinhibition. Structure. 20, 77-88.

74. Akagi, K., E. Kyun Park, K. Mood and I.O. Daar 2002. Docking protein SNT1 is a critical mediator of fibroblast growth factor signaling during xenopus embryonic development. Dev. Dyn. 223, 216-228.

75. Kusakabe, M., N. Masuyama, H. Hanafusa and E. Nishida 2001. Xenopus FRS2 is involved in early embryogenesis in cooperation with the src family kinase laloo. EMBO Rep. 2, 727-735.

76. MacNicol, A. M., A.J. Muslin and L.T. Williams 1993. Raf-1 kinase is essential for early xenopus development and mediates the induction of mesoderm by FGF. Cell. 73, 571-583.

77. LaBonne, C., B. Burke and M. Whitman 1995. Role of MAP kinase in mesoderm induction and axial patterning during xenopus development. Development. 121, 1475-1486.

78. Petrovic, N., S.V. Bhagwat, W.J. Ratzan, M.C. Ostrowski and L.H. Shapiro 2003. CD13/APN transcription is induced by RAS/MAPK-mediated phosphorylation of ets-2 in activated endothelial cells. J. Biol. Chem. 278, 49358-49368.

79. Tang, T. and R. Freeman 1995. The SH2-containing protein-tyrosine phosphatase SH-PTP2 is required upstream of MAP kinase for early xenopus development. Cell. 10;80(3):473-83.

80. Umbhauer, M., A. Penzo-Mendez, L. Clavilier, J. Boucaut and J. Riou 2000. Signaling specificities of fibroblast growth factor receptors in early xenopus embryo. J. Cell. Sci. 113 ( Pt 16), 2865-2875.

81. Park, E. K., N. Warner, K. Mood, T. Pawson and I.O. Daar 2002. Low-molecular-weight protein tyrosine phosphatase is a positive component of the fibroblast growth factor receptor signaling pathway. Mol. Cell. Biol. 22, 3404-3414.

82. Weinstein, D. C., J. Marden, F. Carnevali and A. Hemmati-Brivanlou 1998. FGF-mediated mesoderm induction involves the src-family kinase laloo. Nature. 394, 904-908.

83. Dong, Z., R.H. Xu, J. Kim, S.N. Zhan, W.Y. Ma, N.H. Colburn and H. Kung 1996. AP-1/jun is required for early xenopus development and mediates mesoderm induction by fibroblast growth factor but not by activin. J. Biol. Chem. 271, 9942-9946.

84. Nutt, S. L., K.S. Dingwell, C.E. Holt and E. Amaya 2001. Xenopus Sprouty2 inhibits FGF-mediated gastrulation movements but does not affect mesoderm induction and patterning. Genes Dev. 15, 1152-1166.

85. Heisenberg, C. P., M. Tada, G.J. Rauch, L. Saude, M.L. Concha, R. Geisler, D.L. Stemple, J.C. Smith and S.W. Wilson 2000. Silberblick/Wnt11 mediates convergent extension movements during zebrafish gastrulation. Nature. 405, 76-81.

86. Takeuchi, M., J. Nakabayashi, T. Sakaguchi, T.S. Yamamoto, H. Takahashi, H. Takeda and N. Ueno 2003. The prickle-related gene in vertebrates is essential for gastrulation cell movements. Curr. Biol. 13, 674-679.

87. Yamaguchi, T. P., K. Harpal, M. Henkemeyer and J. Rossant 1994. Fgfr-1 is required for embryonic growth and mesodermal patterning during mouse gastrulation. Genes Dev. 8, 3032-3044.

88. Ciruna, B. G., L. Schwartz, K. Harpal, T.P. Yamaguchi and J. Rossant 1997. Chimeric analysis of fibroblast growth factor receptor-1 (Fgfr1) function: A role for FGFR1 in morphogenetic movement through the primitive streak. Development. 124, 2829-2841.

89. Weinstein, D. C. and A. Hemmati-Brivanlou 1997. Neural induction in xenopus laevis: Evidence for the default model. Curr. Opin. Neurobiol. 7, 7-12.

90. Lemaire, P., V. Bertrand and C. Hudson 2002. Early steps in the formation of neural tissue in ascidian embryos. Dev. Biol. 252, 151-169.

91. Streit, A., A.J. Berliner, C. Papanayotou, A. Sirulnik and C.D. Stern 2000. Initiation of neural induction by FGF signalling before gastrulation. Nature. 406, 74-78.

92. Wilson, S. I., E. Graziano, R. Harland, T.M. Jessell and T. Edlund 2000. An early requirement for FGF signalling in the acquisition of neural cell fate in the chick embryo. Curr. Biol. 10, 421-429.

93. Alvarez, I. S., M. Araujo and M.A. Nieto 1998. Neural induction in whole chick embryo cultures by FGF. Dev. Biol. 199, 42-54.

94. Rodriguez-Gallardo, L., V. Climent, V. Garcia-Martinez, G.C. Schoenwolf and I.S. Alvarez 1997. Targeted over-expression of FGF in chick embryos induces formation of ectopic neural cells. Int. J. Dev. Biol. 41, 715-723.

95. Storey, K. G., A. Goriely, C.M. Sargent, J.M. Brown, H.D. Burns, H.M. Abud and J.K. Heath 1998. Early posterior neural tissue is induced by FGF in the chick embryo. Development. 125, 473-484.

96. Muhr, J., E. Graziano, S. Wilson, T.M. Jessell and T. Edlund 1999. Convergent inductive signals specify midbrain, hindbrain, and spinal cord identity in gastrula stage chick embryos. Neuron. 23, 689-702.

97. Sheng, G., M. dos Reis and C.D. Stern 2003. Churchill, a zinc finger transcriptional activator, regulates the transition between gastrulation and neurulation. Cell. 115, 603-613.

98. Ribisi, S.,Jr, F.V. Mariani, E. Aamar, T.M. Lamb, D. Frank and R.M. Harland 2000. Ras-mediated FGF signaling is required for the formation of posterior but not anterior neural tissue in xenopus laevis. Dev. Biol. 227, 183-196.

99. Pownall, M. E., H.V. Isaacs and J.M. Slack 1998. Two phases of hox gene regulation during early xenopus development. Curr. Biol. 8, 673-676.

100. Domingos, P. M., N. Itasaki, C.M. Jones, S. Mercurio, M.G. Sargent, J.C. Smith and R. Krumlauf 2001. The Wnt/beta-catenin pathway posteriorizes neural tissue in xenopus by an indirect mechanism requiring FGF signalling. Dev. Biol. 239, 148-160.

101. Kazanskaya, O., A. Glinka and C. Niehrs 2000. The role of xenopus dickkopf1 in prechordal plate specification and neural patterning. Development. 127, 4981-4992.

102. Kudoh, T., S.W. Wilson and I.B. Dawid 2002. Distinct roles for fgf, wnt and retinoic acid in posteriorizing the neural ectoderm. Development. 129, 4335-4346.

103. Koshida, S., M. Shinya, M. Nikaido, N. Ueno, S. Schulte-Merker, A. Kuroiwa and H. Takeda 2002. Inhibition of BMP activity by the FGF signal promotes posterior neural development in zebrafish. Dev. Biol. 244, 9-20.

104. Bel-Vialar, S., N. Itasaki and R. Krumlauf 2002. Initiating hox gene expression: In the early chick neural tube differential sensitivity to FGF and RA signaling subdivides the HoxB genes in two distinct groups. Development. 129, 5103-5115.

105. Isaacs, H. V., M.E. Pownall and J.M. Slack 1998. Regulation of hox gene expression and posterior development by the xenopus caudal homologue Xcad3. Embo j. 17, 3413-3427.

106. Chen, Y., X. Li, V.P. Eswarakumar, R. Seger and P. Lonai 2000. Fibroblast growth factor (FGF) signaling through PI 3-kinase and Akt/PKB is required for embryoid body differentiation. Oncogene. 19, 3750-3756.

107. Arman, E., R. Haffner-Krausz, Y. Chen, J.K. Heath and P. Lonai 1998. Targeted disruption of fibroblast growth factor (FGF) receptor 2 suggests a role for FGF signaling in pregastrulation mammalian development. Proc. Natl. Acad. Sci. U. S. A. 95, 5082-5087.

108. Hudson, C., D. Clements, R.V. Friday, D. Stott and H.R. Woodland 1997. Xsox17alpha and -beta mediate endoderm formation in xenopus. Cell. 91, 397-405.

109. Sasai, Y., B. Lu, S. Piccolo and E.M. De Robertis 1996. Endoderm induction by the organizer-secreted factors chordin and noggin in xenopus animal caps. Embo j. 15, 4547-4555.

110. Papetti, M. and I.M. Herman 2002. Mechanisms of normal and tumor-derived angiogenesis. Am. J. Physiol. Cell. Physiol. 282, C947-70.

111. van Oostrom, M. C., O. van Oostrom, P.H. Quax, M.C. Verhaar and I.E. Hoefer 2008. Insights into mechanisms behind arteriogenesis: What does the future hold? J. Leukoc. Biol. 84, 1379-1391.

112. Carmeliet, P. 2000. Mechanisms of angiogenesis and arteriogenesis. Nat. Med. 6, 389-395.

113. Hanahan, D. and J. Folkman 1996. Patterns and emerging mechanisms of the angiogenic switch during tumorigenesis. Cell. 86, 353-364.

114. Mattila MM, Ruohoola JK, Valve EM, Tasanen MJ, Seppanen JA, Harkonen PL. 2001. FGF-8b increases angiogenic capacity and tumor growth of androgen-regulated S115 breast cancer cells. Oncogene. 20, 2791-2804.

115. Dell'Era, P., M. Mohammadi and M. Presta 1999. Different tyrosine autophosphorylation requirements in fibroblast growth factor receptor-1 mediate urokinase-type plasminogen activator induction and mitogenesis. Mol. Biol. Cell. 10, 23-33.

116. Liotta, L. A., P.S. Steeg and W.G. Stetler-Stevenson 1991. Cancer metastasis and angiogenesis: An imbalance of positive and negative regulation. Cell. 64, 327-336.

117. Hiraoka, N., E. Allen, I.J. Apel, M.R. Gyetko and S.J. Weiss 1998. Matrix metalloproteinases regulate neovascularization by acting as pericellular fibrinolysins. Cell. 95, 365-377.

118. Taraboletti, G., S. D'Ascenzo, P. Borsotti, R. Giavazzi, A. Pavan and V. Dolo 2002. Shedding of the matrix metalloproteinases MMP-2, MMP-9, and MT1-MMP as membrane vesicle-associated components by endothelial cells. Am. J. Pathol. 160, 673-680.

119. Terranova VP, Diflorio R. Lyall RM, Hic S, Friesel R, Maciag T. 1985. Human endothelial cells are chemotactic to endothelial cell growth factor and heparin. J. Cell Biol. 101, 2330-2334.

120. Stokes CL, Rupnick MA, Williams SK, Lauffenburger DA 1990. Chemotaxis of human microvessel endothelial cells in response to acidic fibroblast growth factor. Lab Invest. 63, 657-668.

121. Gillis, P., U. Savla, O.V. Volpert, B. Jimenez, C.M. Waters, R.J. Panos and N.P. Bouck 1999. Keratinocyte growth factor induces angiogenesis and protects endothelial barrier function. J. Cell. Sci. 112 ( Pt 12), 2049-2057.

122. Montesano R, Orci L, Vassalli P. 1983. In vitro rapid organization of endothelial cells into capillary-like networks is promoted by collagen matrices. J. Cell Biol. 97, 1648-1652.

123. Peppers MS, Belin D, Montesano R, Orci L, Vassalli JD. 1990. Transforming growth factor-beta 1 modulates basic fibroblast growth factor induced proteolytic and angiogenic properties of endothelial cells in vitro. J. Cell Biol. 111, 743-755.

124. Underwood PA, Bean PA, Gamble JR 2002.Rate of endothelial expansion is controlled by cell:cell adhesion J. Biochem Cell Biol. 34, 55-69.

125. Zhou L, Dosanjh A, Chen H, Kaarasek M. 2000. Divergent effects of extracellular oxygen on the growth, morphology and function of human skin microvascular endothelial cells. J. Cell Physiol. 182, 134-140.

126. Collo G, P. M. 1999. Endothelial cell integrin alpha5 beta1 expression is modulated by cytokines and during migration in vitro. J. Cell Sci. 112, 569-578.

127. Ferrara N, Gerber HP, LeCouter J. 2003. The biology of VEGF and its receptors. Nat Med. 9, 669-676.

128. Seghezzi, G., S. Patel, C.J. Ren, A. Gualandris, G. Pintucci, E.S. Robbins, R.L. Shapiro, A.C. Galloway, D.B. Rifkin and P. Mignatti 1998. Fibroblast growth factor-2 (FGF-2) induces vascular endothelial growth factor (VEGF) expression in the endothelial cells of forming capillaries: An autocrine mechanism contributing to angiogenesis. J. Cell Biol. 141, 1659-1673.

129. Gabler, C., A. Plath-Gabler, G.J. Killian, B. Berisha and D. Schams 2004. Expression pattern of fibroblast growth factor (FGF) and vascular endothelial growth factor (VEGF) system members in bovine corpus luteum endothelial cells during treatment with FGF-2, VEGF or oestradiol. Reprod. Domest. Anim. 39, 321-327.

130. Castellon, R., H.K. Hamdi, I. Sacerio, A.M. Aoki, M.C. Kenney and A.V. Ljubimov 2002. Effects of angiogenic growth factor combinations on retinal endothelial cells. Exp. Eye Res. 74, 523-535.

131. Chevallier, A., M. Kieny and A. Mauger 1977. Limb-somite relationship: Origin of the limb musculature. J. Embryol. Exp. Morphol. 41, 245-258.

132. Christ, B., H.J. Jacob and M. Jacob 1977. Experimental analysis of the origin of the wing musculature in avian embryos. Anat. Embryol. (Berl). 150, 171-186.

133. Cohn, M. J., J.C. Izpisua-Belmonte, H. Abud, J.K. Heath and C. Tickle 1995. Fibroblast growth factors induce additional limb development from the flank of chick embryos. Cell. 80, 739-746.

134. Crossley, P., G. Minowada, C.A. MacArthur and G.R. Martin 1995. The mouse Fgf8 gene encodes a family of polypeptides and is expressed in regions that direct outgrowth and patterning in the developing embryo. Development. 121, 439-451.

135. Ohuchi, H., T. Nakagawa, A. Yamamoto, A. Araga, T. Ohata, Y. Ishimaru, H. Yoshioka, T. Kuwana, T. Nohno, M. Yamasaki, N. Itoh and S. Noji 1997. The mesenchymal factor, FGF10, initiates and maintains the outgrowth of the chick limb bud through interaction with FGF8, an apical ectodermal factor. Development. 124, 2235-2244.

136. Vogel, A., C. Rodriguez and J.C. Izpisua-Belmonte 1996. Involvement of FGF-8 in initiation, outgrowth and patterning of the vertebrate limb. Development. 122, 1737-1750.

137. Summerbell, D. 1974. A quantitative analysis of the effect of excision of the AER from the chick limb-bud. J. Embryol. Exp. Morphol. 32, 651-660.

138. Rubin, L. and J. Saunders 1972. Ectodermal-mesodermal interactions in the growth of limb buds in the chick embryo: Constancy and temporal limits of the ectodermal induction* 1. Dev. Biol. 28, 94-112.

139. Echelard, Y., D.J. Epstein, B. St-Jacques, L. Shen, J. Mohler, J.A. McMahon and A.P. McMahon 1993. Sonic hedgehog, a member of a family of putative signaling molecules, is implicated in the regulation of CNS polarity. Cell. 75, 1417-1430.

140. Chang, D. T., A. Lopez, D.P. von Kessler, C. Chiang, B.K. Simandl, R. Zhao, M.F. Seldin, J.F. Fallon and P.A. Beachy 1994. Products, genetic linkage and limb patterning activity of a murine hedgehog gene. Development. 120, 3339-3353.

141. Fallon, J. F., A. Lopez, M.A. Ros, M.P. Savage, B.B. Olwin and B.K. Simandl 1994. FGF-2: Apical ectodermal ridge growth signal for chick limb development. Science. 264, 104-107.

142. Niswander, L., S. Jeffrey, G.R. Martin and C. Tickle 1994. A positive feedback loop coordinates growth and patterning in the vertebrate limb. Nature. 371, 609-612.

143. Meyers, E. N., M. Lewandoski and G.R. Martin 1998. An Fgf8 mutant allelic series generated by cre-and flp-mediated recombination. Nat. Genet. 18, 136-141.

144. Niswander, L., C. Tickle, A. Vogel, I. Booth and G.R. Martin 1993. FGF-4 replaces the apical ectodermal ridge and directs outgrowth and patterning of the limb. Cell. 75, 579-587.

145. Dealy, C. N., M.R. Seghatoleslami, D. Ferrari and R.A. Kosher 1997. FGF-stimulated outgrowth and proliferation of limb mesoderm is dependent on syndecan-3. Dev. Biol. 184, 343-350.

146. Aono, H. and H. Ide 1988. A gradient of responsiveness to the growth-promoting activity of ZPA (zone of polarizing activity) in the chick limb bud* 1. Dev. Biol. 128, 136-141.

147. Riley, B. B., M.P. Savage, B.K. Simandl, B.B. Olwin and J.F. Fallon 1993. Retroviral expression of FGF-2 (bFGF) affects patterning in chick limb bud. Development. 118, 95-104.

148. Laufer, E., C.E. Nelson, R.L. Johnson, B.A. Morgan and C. Tabin 1994. Sonic hedgehog and fgf-4 act through a signaling cascade and feedback loop to integrate growth and patterning of the developing limb bud. Cell. 79, 993-1003.

149. Ohsugi, K., D.M. Gardiner and S.V. Bryant 1997. Cell cycle length affects gene expression and pattern formation in limbs. Dev. Biol. 189, 13-21.

150. Duboule, D. 1995. Vertebrate hox genes and proliferation: An alternative pathway to homeosis? Current Opinion in Genetics & Development. 5, 525-528.

151. Chan, D. and A. Wynshaw-Boris 1995. Formin isoforms are differentially expressed in the mouse embryo and are required for normal expression of fgf-4 and shh in the limb bud. Development. 121. 3151-3162.

152. Kuhlman, J. and L. Niswander 1997. Limb deformity proteins: Role in mesodermal induction of the apical ectodermal ridge. Development. 124, 133-139

153. Panman, L., A. Galli, N. Lagarde, O. Michos, G. Soete, A. Zuniga and R. Zeller 2006. Differential regulation of gene expression in the digit forming area of the mouse limb bud by SHH and gremlin 1/FGF-mediated epithelial-mesenchymal signalling. Development. 133, 3419.

154. Pizette, S. and L. Niswander 1999. BMPs negatively regulate structure and function of the limb apical ectodermal ridge. Development. 126(5):883-94.

155. Sun, X., M. Lewandoski, E.N. Meyers, Y.H. Liu, R.E. Maxson and G.R. Martin 2000. Conditional inactivation of Fgf4 reveals complexity of signalling during limb bud development. Nat. Genet. 25, 83-86.

156. Verheyden, J. M. and X. Sun 2008. An Fgf/Gremlin inhibitory feedback loop triggers termination of limb bud outgrowth. Nature. 454, 638-641.

157. Capdevila, J., T. Tsukui, C.R. Esteban, V. Zappavigna and J.C.I. Belmonte 1999. Control of vertebrate limb outgrowth by the proximal factor Meis2 and distal antagonism of BMPs by gremlin. Mol. Cell. 4, 839-849.

158. Panman, L., A. Galli, N. Lagarde, O. Michos, G. Soete, A. Zuniga and R. Zeller 2006. Differential regulation of gene expression in the digit forming area of the mouse limb bud by SHH and gremlin 1/FGF-mediated epithelial-mesenchymal signalling. Development. 133, 3419-28

159. Scherz, P. J., B.D. Harfe, A.P. McMahon and C.J. Tabin 2004. The limb bud shh-fgf feedback loop is terminated by expansion of former ZPA cells. Science. 305, 396-399.

160. Selever, J., W. Liu, M.F. Lu, R.R. Behringer and J.F. Martin 2004. Bmp4 in limb bud mesoderm regulates digit pattern by controlling AER development. Dev. Biol. 276, 268-279.

161. Bandyopadhyay, A., K. Tsuji, K. Cox, B.D. Harfe, V. Rosen and C.J. Tabin 2006. Genetic analysis of the roles of BMP2, BMP4, and BMP7 in limb patterning and skeletogenesis. PLoS Genetics. 2, e216.

162. Tekin, M., B.O. Hismi, S. Fitoz, H. Ozdag, F.B. Cengiz, A. Sirmaci, I. Aslan, B. Inceoglu, E.B. Yuksel-Konuk, S.T. Yilmaz, O. Yasun and N. Akar 2007. Homozygous mutations in fibroblast growth factor 3 are associated with a new form of syndromic deafness characterized by inner ear agenesis, microtia, and microdontia. Am. J. Hum. Genet. 80, 338-344.

163. Alsmadi, O., B.F. Meyer, F. Alkuraya, S. Wakil, F. Alkayal, H. Al-Saud, K. Ramzan and M.A. Al-Sayed 2008. Syndromic congenital sensorineural deafness, microtia and microdontia resulting from a novel homoallelic mutation in fibroblast growth factor 3 (FGF3). European Journal of Human Genetics. 17, 14-21.

164. Falardeau, J., W.C.J. Chung, A. Beenken, T. Raivio, L. Plummer, Y. Sidis, E.E. Jacobson-Dickman, A.V. Eliseenkova, J. Ma and A. Dwyer 2008. Decreased FGF8 signaling causes deficiency of gonadotropin-releasing hormone in humans and mice. J. Clin. Invest. 118, 2822-2831.

165. Wright, T. J., E.P. Hatch, H. Karabagli, P. Karabagli, G.C. Schoenwolf and S.L. Mansour 2003. Expression of mouse fibroblast growth factor and fibroblast growth factor receptor genes during early inner ear development. Developmental Dynamics. 228, 267-272.

166. Vendrell, V., E. Carnicero, F. Giraldez, M.T. Alonso and T. Schimmang 2000. Induction of inner ear fate by FGF3. Development. 127(10):2011-9.

167. Swieten, J. C. V., E. Brusse, B.M.D. Graaf, E. Krieger, R.V.d. Graaf, I.D. Koning, A. Maat-Kievit, P. Leegwater, D. Dooijes and B.A. Oostra 2003. A mutation in the fibroblast growth factor 14 gene is associated with autosomal dominant cerebral ataxia. The American Journal of Human Genetics. 72, 191-199.

168. Dalski, A., J. Atici, F.R. Kreuz, Y. Hellenbroich, E. Schwinger and C. Z\uhlke 2005. Mutation analysis in the fibroblast growth factor 14 gene: Frameshift mutation and

polymorphisms in patients with inherited ataxias. European Journal of Human Genetics. 13, 118-120.

169. Goldfarb, M., J. Schoorlemmer, A. Williams, S. Diwakar, Q. Wang, X. Huang, J. Giza, D. Tchetchik, K. Kelley and A. Vega 2007. Fibroblast growth factor homologous factors control neuronal excitability through modulation of voltage-gated sodium channels. Neuron. 55, 449-463.

170. Liu, C., S.D. Dib-Hajj and S.G. Waxman 2001. Fibroblast growth factor homologous factor 1B binds to the C terminus of the tetrodotoxin-resistant sodium channel rNav1. 9a (NaN). J. Biol. Chem. 276(22):18925-33.

171. Wittmack, E. K., A.M. Rush, M.J. Craner, M. Goldfarb, S.G. Waxman and S.D. Dib-Hajj 2004. Fibroblast growth factor homologous factor 2B: Association with Nav1. 6 and selective colocalization at nodes of ranvier of dorsal root axons. The Journal of Neuroscience. 24(30):6765-75.

172. Murase, S. and R.D. McKay 2006. A specific survival response in dopamine neurons at most risk in parkinson's disease. The Journal of Neuroscience. 26(38):9750-60.

173. Spillantini, M. G., M.L. Schmidt, M.Y.L. Virginia, J.Q. Trojanowski, R. Jakes and M. Goedert 1997. Î±-Synuclein in lewy bodies. Nature. 388, 839-840.

174. Shimada, T., H. Hasegawa, Y. Yamazaki, T. Muto, R. Hino, Y. Takeuchi, T. Fujita, K. Nakahara, S. Fukumoto and T. Yamashita 2004. FGF23 is a potent regulator of vitamin D metabolism and phosphate homeostasis. Journal of Bone and Mineral Research. 19, 429-435.

175. White, K. E., G. Carn, B. Lorenz-Depiereux, A. Benet-Pages, T.M. Strom and M.J. Econs 2001. Autosomal-dominant hypophosphatemic rickets (ADHR) mutations stabilize FGF-23. Kidney Int. 60, 2079-2086.

176. Bai, X., D. Miao, J. Li, D. Goltzman and A.C. Karaplis 2004. Transgenic mice overexpressing human fibroblast growth factor 23 (R176Q) delineate a putative role for parathyroid hormone in renal phosphate wasting disorders. Endocrinology. 145(11):5269-79.

177. Dunstan, C. R., H. Zhou and M.J. Seibel 2004. Fibroblast growth factor 23: A phosphatonin regulating phosphate homeostasis? Endocrinology. 145(7):3084-6.

178. Inoue, Y., H. Segawa, I. Kaneko, S. Yamanaka, K. Kusano, E. Kawakami, J. Furutani, M. Ito, M. Kuwahata and H. Saito 2005. Role of the vitamin D receptor in FGF23 action on phosphate metabolism. Biochem. J. 390(Pt 1):325-31.

179. Liu, S., R. Guo, L.G. Simpson, Z.S. Xiao, C.E. Burnham and L.D. Quarles 2003. Regulation of fibroblastic growth factor 23 expression but not degradation by PHEX. J. Biol. Chem. 278(39):37419-26.

180. Palmer, P. 1966. Tumoural calcinosis. Br. J. Radiol. 39, 518-525.

181. Larsson, T., R. Marsell, E. Schipani, C. Ohlsson,. Ljunggren, H.S. Tenenhouse, and K.B. Jonsson 2004. Transgenic mice expressing fibroblast growth factor 23 under the control of the alpha1(I) collagen promoter exhibit growth retardation, osteomalacia, and disturbed phosphate homeostasis.. Endocrinology. 145, 3087-94

182. Garringer, H. J., M. Malekpour, F. Esteghamat, S.M.J. Mortazavi, S.I. Davis, E.G. Farrow, X. Yu, D.E. Arking, H.C. Dietz and K.E. White 2008. Molecular genetic and biochemical analyses of FGF23 mutations in familial tumoral calcinosis. American Journal of Physiology-Endocrinology and Metabolism. 295, E929.

183. Benet-Pages, A., P. Orlik, T.M. Strom and B. Lorenz-Depiereux 2005. An FGF23 missense mutation causes familial tumoral calcinosis with hyperphosphatemia. Hum. Mol. Genet. 14(3):385-90

184. Araya, K., S. Fukumoto, R. Backenroth, Y. Takeuchi, K. Nakayama, N. Ito, N. Yoshii, Y. Yamazaki, T. Yamashita and J. Silver 2005. A novel mutation in fibroblast growth factor 23 gene as a cause of tumoral calcinosis. Journal of Clinical Endocrinology & Metabolism. 90(10):5523-7.

185. Shimada, T., S. Mizutani, T. Muto, T. Yoneya, R. Hino, S. Takeda, Y. Takeuchi, T. Fujita, S. Fukumoto and T. Yamashita 2001. Cloning and characterization of FGF23 as a causative factor of tumor-induced osteomalacia. Proceedings of the National Academy of Sciences. 98(11):6500-5.

186. Jia, C., Y. Cai, Y. Ma and D. Fu 2010. Quantitative assessment of the effect of FGFR2 gene polymorphism on the risk of breast cancer. Breast Cancer Res. Treat. 124, 521-528.

187. Adnane, J., P. Gaudray, C.A. Dionne, G. Crumley, M. Jaye, J. Schlessinger, P. Jeanteur, D. Birnbaum and C. Theillet 1991. BEK and FLG, two receptors to members of the FGF family, are amplified in subsets of human breast cancers. Oncogene. 6, 659-663.

188. Grose, R. and C. Dickson 2005. Fibroblast growth factor signaling in tumorigenesis. Cytokine Growth Factor Rev. 16, 179-186.

189. Moffa, A. B. and S.P. Ethier 2007. Differential signal transduction of alternatively spliced FGFR2 variants expressed in human mammary epithelial cells. J. Cell. Physiol. 210, 720-731.

190. Moffa, A. B., S.L. Tannheimer and S.P. Ethier 2004. Transforming potential of alternatively spliced variants of fibroblast growth factor receptor 2 in human mammary epithelial cells. Mol. Cancer. Res. 2, 643-652.

191. Lu, P., A.J. Ewald, G.R. Martin and Z. Werb 2008. Genetic mosaic analysis reveals FGF receptor 2 function in terminal end buds during mammary gland branching morphogenesis. Dev. Biol. 321, 77-87.

192. Bange, J., D. Prechtl, Y. Cheburkin, K. Specht, N. Harbeck, M. Schmitt, T. Knyazeva, S. Muller, S. Gartner, I. Sures, H. Wang, E. Imyanitov, H.U. Haring, P. Knayzev, S. Iacobelli, H. Hofler and A. Ullrich 2002. Cancer progression and tumor cell motility are associated with the FGFR4 arg(388) allele. Cancer Res. 62, 840-847.

193. Sugiyama, N., M. Varjosalo, P. Meller, J. Lohi, M. Hyytiainen, S. Kilpinen, O. Kallioniemi, S. Ingvarsen, L.H. Engelholm, J. Taipale, K. Alitalo, J. Keski-Oja and K. Lehti 2010. Fibroblast growth factor receptor 4 regulates tumor invasion by coupling fibroblast growth factor signaling to extracellular matrix degradation. Cancer Res. 70, 7851-7861.

194. Spinola, M., V. Leoni, C. Pignatiello, B. Conti, F. Ravagnani, U. Pastorino and T.A. Dragani 2005. Functional FGFR4 Gly388Arg polymorphism predicts prognosis in lung adenocarcinoma patients. J. Clin. Oncol. 23, 7307-7311.

195. Spinola, M., V.P. Leoni, J. Tanuma, A. Pettinicchio, M. Frattini, S. Signoroni, R. Agresti, R. Giovanazzi, S. Pilotti, L. Bertario, F. Ravagnani and T.A. Dragani 2005. FGFR4 Gly388Arg polymorphism and prognosis of breast and colorectal cancer. Oncol. Rep. 14, 415-419.

196. Cha, J. Y., S. Maddileti, N. Mitin, T.K. Harden and C.J. Der 2009. Aberrant receptor internalization and enhanced FRS2-dependent signaling contribute to the transforming activity of the fibroblast growth factor receptor 2 IIIb C3 isoform. J. Biol. Chem. 284, 6227-6240.

197. Greenman, C., P. Stephens, R. Smith, G.L. Dalgliesh, C. Hunter, G. Bignell, H. Davies, J. Teague, A. Butler and C. Stevens 2007. Patterns of somatic mutation in human cancer genomes. Nature. 446, 153-158.

198. Pardo, O. E., C. Wellbrock, U.K. Khanzada, M. Aubert, I. Arozarena, S. Davidson, F. Bowen, P.J. Parker, V. Filonenko and I.T. Gout 2006. FGF-2 protects small cell lung cancer cells from apoptosis through a complex involving PKC & epsiv;, B-raf and S6K2. Embo j. 25, 3078-3088.

199. Vandermoere, F., I.E. Yazidi-Belkoura, E. Adriaenssens, J. Lemoine and H. Hondermarck 2005. The antiapoptotic effect of fibroblast growth factor-2 is mediated through nuclear factor-ÎºB activation induced via interaction between akt and IÎºB kinase-Î² in breast cancer cells. Oncogene. 24, 5482-5491.

200. Gelsi-Boyer, V., B. Orsetti, N. Cervera, P. Finetti, F. Sircoulomb, C. Rouge, L. Lasorsa, A. Letessier, C. Ginestier, F. Monville, S. Esteyries, J. Adelaide, B. Esterni, C. Henry, S.P. Ethier, F. Bibeau, M.J. Mozziconacci, E. Charafe-Jauffret, J. Jacquemier, F. Bertucci, D.

Birnbaum, C. Theillet and M. Chaffanet 2005. Comprehensive profiling of 8p11-12 amplification in breast cancer. Mol. Cancer. Res. 3, 655-667.

201. Chin, K., S. DeVries, J. Fridlyand, P.T. Spellman, R. Roydasgupta, W.L. Kuo, A. Lapuk, R.M. Neve, Z. Qian, T. Ryder, F. Chen, H. Feiler, T. Tokuyasu, C. Kingsley, S. Dairkee, Z. Meng, K. Chew, D. Pinkel, A. Jain, B.M. Ljung, L. Esserman, D.G. Albertson, F.M. Waldman and J.W. Gray 2006. Genomic and transcriptional aberrations linked to breast cancer pathophysiologies. Cancer. Cell. 10, 529-541.

202. Letessier, A., F. Sircoulomb, C. Ginestier, N. Cervera, F. Monville, V. Gelsi-Boyer, B. Esterni, J. Geneix, P. Finetti, C. Zemmour, P. Viens, E. Charafe-Jauffret, J. Jacquemier, D. Birnbaum and M. Chaffanet 2006. Frequency, prognostic impact, and subtype association of 8p12, 8q24, 11q13, 12p13, 17q12, and 20q13 amplifications in breast cancers. BMC Cancer. 6, 245.

203. Xian, W., L. Pappas, D. Pandya, L.M. Selfors, P.W. Derksen, M. de Bruin, N.S. Gray, J. Jonkers, J.M. Rosen and J.S. Brugge 2009. Fibroblast growth factor receptor 1-transformed mammary epithelial cells are dependent on RSK activity for growth and survival. Cancer Res. 69, 2244-2251.

204. Turner, N., M.B. Lambros, H.M. Horlings, A. Pearson, R. Sharpe, R. Natrajan, F.C. Geyer, M. van Kouwenhove, B. Kreike, A. Mackay, A. Ashworth, M.J. van de Vijver and J.S. Reis-Filho 2010. Integrative molecular profiling of triple negative breast cancers identifies amplicon drivers and potential therapeutic targets. Oncogene. 29, 2013-2023.

205. Roidl, A., H.J. Berger, S. Kumar, J. Bange, P. Knyazev and A. Ullrich 2009. Resistance to chemotherapy is associated with fibroblast growth factor receptor 4 up-regulation. Clin. Cancer Res. 15, 2058-2066.

206. Pandith, A. A., Z.A. Shah and M.A. Siddiqi 2010. Oncogenic role of fibroblast growth factor receptor 3 in tumorigenesis of urinary bladder cancer. Urol. Oncol. 31(4):398-406

207. Cappellen, D., C. De Oliveira, D. Ricol, S. de Medina, J. Bourdin, X. Sastre-Garau, D. Chopin, J.P. Thiery and F. Radvanyi 1999. Frequent activating mutations of FGFR3 in human bladder and cervix carcinomas. Nat. Genet. 23, 18-20.

208. Qing, J., X. Du, Y. Chen, P. Chan, H. Li, P. Wu, S. Marsters, S. Stawicki, J. Tien, K. Totpal, S. Ross, S. Stinson, D. Dornan, D. French, Q.R. Wang, J.P. Stephan, Y. Wu, C. Wiesmann and A. Ashkenazi 2009. Antibody-based targeting of FGFR3 in bladder carcinoma and t(4;14)-positive multiple myeloma in mice. J. Clin. Invest. 119, 1216-1229.

209. Qing, J., X. Du, Y. Chen, P. Chan, H. Li, P. Wu, S. Marsters, S. Stawicki, J. Tien, K. Totpal, S. Ross, S. Stinson, D. Dornan, D. French, Q.R. Wang, J.P. Stephan, Y. Wu, C. Wiesmann and A. Ashkenazi 2009. Antibody-based targeting of FGFR3 in bladder carcinoma and t(4;14)-positive multiple myeloma in mice. J. Clin. Invest. 119, 1216-1229.

210. Ding, L., G. Getz, D.A. Wheeler, E.R. Mardis, M.D. McLellan, K. Cibulskis, C. Sougnez, H. Greulich, D.M. Muzny, M.B. Morgan, L. Fulton, R.S. Fulton, Q. Zhang, M.C. Wendl, M.S. Lawrence, D.E. Larson, K. Chen, D.J. Dooling, A. Sabo, A.C. Hawes, H. Shen, S.N. Jhangiani, L.R. Lewis, O. Hall, Y. Zhu, T. Mathew, Y. Ren, J. Yao, S.E. Scherer, K. Clerc, G.A. Metcalf, B. Ng, A. Milosavljevic, M.L. Gonzalez-Garay, J.R. Osborne, R. Meyer, X. Shi, Y. Tang, D.C. Koboldt, L. Lin, R. Abbott, T.L. Miner, C. Pohl, G. Fewell, C. Haipek, H. Schmidt, B.H. Dunford-Shore, A. Kraja, S.D. Crosby, C.S. Sawyer, T. Vickery, S. Sander, J. Robinson, W. Winckler, J. Baldwin, L.R. Chirieac, A. Dutt, T. Fennell, M. Hanna, B.E. Johnson, R.C. Onofrio, R.K. Thomas, G. Tonon, B.A. Weir, X. Zhao, L. Ziaugra, M.C. Zody, T. Giordano, M.B. Orringer, J.A. Roth, M.R. Spitz, I.I. Wistuba, B. Ozenberger, P.J. Good, A.C. Chang, D.G. Beer, M.A. Watson, M. Ladanyi, S. Broderick, A. Yoshizawa, W.D. Travis, W. Pao, M.A. Province, G.M. Weinstock, H.E. Varmus, S.B. Gabriel, E.S. Lander, R.A. Gibbs, M. Meyerson and R.K. Wilson 2008. Somatic mutations affect key pathways in lung adenocarcinoma. Nature. 455, 1069-1075.

211. Davies, H., C. Hunter, R. Smith, P. Stephens, C. Greenman, G. Bignell, J. Teague, A. Butler, S. Edkins, C. Stevens, A. Parker, S. O'Meara, T. Avis, S. Barthorpe, L. Brackenbury, G. Buck, J. Clements, J. Cole, E. Dicks, K. Edwards, S. Forbes, M. Gorton, K. Gray, K. Halliday, R. Harrison, K. Hills, J. Hinton, D. Jones, V. Kosmidou, R. Laman, R. Lugg, A. Menzies, J. Perry, R. Petty, K. Raine, R. Shepherd, A. Small, H. Solomon, Y. Stephens, C. Tofts, J. Varian, A. Webb, S. West, S. Widaa, A. Yates, F. Brasseur, C.S. Cooper, A.M. Flanagan, A. Green, M. Knowles, S.Y. Leung, L.H. Looijenga, B. Malkowicz, M.A. Pierotti, B.T. Teh, S.T. Yuen, S.R. Lakhani, D.F. Easton, B.L. Weber, P. Goldstraw, A.G. Nicholson, R. Wooster, M.R. Stratton and P.A. Futreal 2005. Somatic mutations of the protein kinase gene family in human lung cancer. Cancer Res. 65, 7591-7595.

212. Davies, H., C. Hunter, R. Smith, P. Stephens, C. Greenman, G. Bignell, J. Teague, A. Butler, S. Edkins, C. Stevens, A. Parker, S. O'Meara, T. Avis, S. Barthorpe, L. Brackenbury, G. Buck, J. Clements, J. Cole, E. Dicks, K. Edwards, S. Forbes, M. Gorton, K. Gray, K. Halliday, R. Harrison, K. Hills, J. Hinton, D. Jones, V. Kosmidou, R. Laman, R. Lugg, A. Menzies, J. Perry, R. Petty, K. Raine, R. Shepherd, A. Small, H. Solomon, Y. Stephens, C. Tofts, J. Varian, A. Webb, S. West, S. Widaa, A. Yates, F. Brasseur, C.S. Cooper, A.M. Flanagan, A. Green, M. Knowles, S.Y. Leung, L.H. Looijenga, B. Malkowicz, M.A. Pierotti, B.T. Teh, S.T. Yuen, S.R. Lakhani, D.F. Easton, B.L. Weber, P. Goldstraw, A.G. Nicholson, R. Wooster, M.R. Stratton and P.A. Futreal 2005. Somatic mutations of the protein kinase gene family in human lung cancer. Cancer Res. 65, 7591-7595.

213. Dutt, A., H.B. Salvesen, T.H. Chen, A.H. Ramos, R.C. Onofrio, C. Hatton, R. Nicoletti, W. Winckler, R. Grewal, M. Hanna, N. Wyhs, L. Ziaugra, D.J. Richter, J. Trovik, I.B. Engelsen, I.M. Stefansson, T. Fennell, K. Cibulskis, M.C. Zody, L.A. Akslen, S. Gabriel, K.K. Wong, W.R. Sellers, M. Meyerson and H. Greulich 2008. Drug-sensitive FGFR2 mutations in endometrial carcinoma. Proc. Natl. Acad. Sci. U. S. A. 105, 8713-8717.

214. Dutt, A., H.B. Salvesen, T.H. Chen, A.H. Ramos, R.C. Onofrio, C. Hatton, R. Nicoletti, W. Winckler, R. Grewal, M. Hanna, N. Wyhs, L. Ziaugra, D.J. Richter, J. Trovik, I.B. Engelsen, I.M. Stefansson, T. Fennell, K. Cibulskis, M.C. Zody, L.A. Akslen, S. Gabriel, K.K. Wong,

W.R. Sellers, M. Meyerson and H. Greulich 2008. Drug-sensitive FGFR2 mutations in endometrial carcinoma. Proc. Natl. Acad. Sci. U. S. A. 105, 8713-8717.

215. Jaakkola, S., P. Salmikangas, S. Nylund, J. Partanen, E. Armstrong, S. Pyrhonen, P. Lehtovirta and H. Nevanlinna 1993. Amplification of fgfr4 gene in human breast and gynecological cancers. Int. J. Cancer. 54, 378-382.

216. Weiss, J., M.L. Sos, D. Seidel, M. Peifer, T. Zander, J.M. Heuckmann, R.T. Ullrich, R. Menon, S. Maier, A. Soltermann, H. Moch, P. Wagener, F. Fischer, S. Heynck, M. Koker, J. Schottle, F. Leenders, F. Gabler, I. Dabow, S. Querings, L.C. Heukamp, H. Balke-Want, S. Ansen, D. Rauh, I. Baessmann, J. Altmuller, Z. Wainer, M. Conron, G. Wright, P. Russell, B. Solomon, E. Brambilla, C. Brambilla, P. Lorimier, S. Sollberg, O.T. Brustugun, W. Engel-Riedel, C. Ludwig, I. Petersen, J. Sanger, J. Clement, H. Groen, W. Timens, H. Sietsma, E. Thunnissen, E. Smit, D. Heideman, F. Cappuzzo, C. Ligorio, S. Damiani, M. Hallek, R. Beroukhim, W. Pao, B. Klebl, M. Baumann, R. Buettner, K. Ernestus, E. Stoelben, J. Wolf, P. Nurnberg, S. Perner and R.K. Thomas 2010. Frequent and focal FGFR1 amplification associates with therapeutically tractable FGFR1 dependency in squamous cell lung cancer. Sci. Transl. Med. 2, 62ra93.

217. Falvella, F. S., E. Frullanti, A. Galvan, M. Spinola, S. Noci, L. De Cecco, M. Nosotti, L. Santambrogio, M. Incarbone, M. Alloisio, E. Calabro, U. Pastorino, V. Skaug, A. Haugen, E. Taioli and T.A. Dragani 2009. FGFR4 Gly388Arg polymorphism may affect the clinical stage of patients with lung cancer by modulating the transcriptional profile of normal lung. Int. J. Cancer. 124, 2880-2885.

218. Sasaki, H., K. Okuda, O. Kawano, H. Yukiue, M. Yano and Y. Fujii 2008. Fibroblast growth factor receptor 4 mutation and polymorphism in japanese lung cancer. Oncol. Rep. 20, 1125-1130.

219. Spinola, M., V. Leoni, C. Pignatiello, B. Conti, F. Ravagnani, U. Pastorino and T.A. Dragani 2005. Functional FGFR4 Gly388Arg polymorphism predicts prognosis in lung adenocarcinoma patients. J. Clin. Oncol. 23, 7307-7311.

220. Kumar, V. H. and R.M. Ryan 2004. Growth factors in the fetal and neonatal lung. Front. Biosci. 9, 464-480.

221. Warburton, D., A. El-Hashash, G. Carraro, C. Tiozzo, F. Sala, O. Rogers, S. De Langhe, P.J. Kemp, D. Riccardi, J. Torday, S. Bellusci, W. Shi, S.R. Lubkin and E. Jesudason 2010. Lung organogenesis. Curr. Top. Dev. Biol. 90, 73-158.

222. Lajeunie, E., S. Heuertz, V. El Ghouzzi, J. Martinovic, D. Renier, M. Le Merrer and J. Bonaventure 2006. Mutation screening in patients with syndromic craniosynostoses indicates that a limited number of recurrent FGFR2 mutations accounts for severe forms of pfeiffer syndrome. Eur. J. Hum. Genet. 14, 289-298.

223. Claudio, J. O., F. Zhan, L. Zhuang, R. Khaja, Y.X. Zhu, K. Sivananthan, S. Trudel, E. Masih-Khan, R. Fonseca, P.L. Bergsagel, S.W. Scherer, J. Shaughnessy and A.K. Stewart 2007. Expression and mutation status of candidate kinases in multiple myeloma. Leukemia. 21, 1124-1127.

224. Onwuazor, O. N., X.Y. Wen, D.Y. Wang, L. Zhuang, E. Masih-Khan, J. Claudio, B. Barlogie, J.D. Shaughnessy Jr and A.K. Stewart 2003. Mutation, SNP, and isoform analysis of fibroblast growth factor receptor 3 (FGFR3) in 150 newly diagnosed multiple myeloma patients. Blood. 102, 772-773.

225. Soverini, S., C. Terragna, N. Testoni, D. Ruggeri, P. Tosi, E. Zamagni, C. Cellini, M. Cavo, M. Baccarani, S. Tura and G. Martinelli 2002. Novel mutation and RNA splice variant of fibroblast growth factor receptor 3 in multiple myeloma patients at diagnosis. Haematologica. 87, 1036-1040.

226. Intini, D., L. Baldini, S. Fabris, L. Lombardi, G. Ciceri, A.T. Maiolo and A. Neri 2001. Analysis of FGFR3 gene mutations in multiple myeloma patients with t(4;14). Br. J. Haematol. 114, 362-364.

227. Naski, M. C., Q. Wang, J. Xu and D.M. Ornitz 1996. Graded activation of fibroblast growth factor receptor 3 by mutations causing achondroplasia and thanatophoric dysplasia. Nat. Genet. 13, 233-237.

228. Ronchetti, D., A. Greco, S. Compasso, G. Colombo, P. Dell'Era, T. Otsuki, L. Lombardi and A. Neri 2001. Deregulated FGFR3 mutants in multiple myeloma cell lines with t(4;14): Comparative analysis of Y373C, K650E and the novel G384D mutations. Oncogene. 20, 3553-3562.

229. Chesi, M., L.A. Brents, S.A. Ely, C. Bais, D.F. Robbiani, E.A. Mesri, W.M. Kuehl and P.L. Bergsagel 2001. Activated fibroblast growth factor receptor 3 is an oncogene that contributes to tumor progression in multiple myeloma. Blood. 97, 729-736.

230. Chesi, M., E. Nardini, L.A. Brents, E. Schrock, T. Ried, W.M. Kuehl and P.L. Bergsagel 1997. Frequent translocation t(4;14)(p16.3;q32.3) in multiple myeloma is associated with increased expression and activating mutations of fibroblast growth factor receptor 3. Nat. Genet. 16, 260-264.

231. Plowright, E. E., Z. Li, P.L. Bergsagel, M. Chesi, D.L. Barber, D.R. Branch, R.G. Hawley and A.K. Stewart 2000. Ectopic expression of fibroblast growth factor receptor 3 promotes myeloma cell proliferation and prevents apoptosis. Blood. 95, 992-998.

232. Keats, J. J., T. Reiman, A.R. Belch and L.M. Pilarski 2006. Ten years and counting: So what do we know about t(4;14)(p16;q32) multiple myeloma. Leuk. Lymphoma. 47, 2289-2300.

233. Keats, J. J., T. Reiman, C.A. Maxwell, B.J. Taylor, L.M. Larratt, M.J. Mant, A.R. Belch and L.M. Pilarski 2003. In multiple myeloma, t(4;14)(p16;q32) is an adverse prognostic factor irrespective of FGFR3 expression. Blood. 101, 1520-1529.

234. Marzioni, D., T. Lorenzi, R. Mazzucchelli, L. Capparuccia, M. Morroni, R. Fiorini, C. Bracalenti, A. Catalano, G. David, M. Castellucci, G. Muzzonigro and R. Montironi 2009. Expression of basic fibroblast growth factor, its receptors and syndecans in bladder cancer. Int. J. Immunopathol. Pharmacol. 22, 627-638.

235. De Boer, W. I., A.B. Houtsmuller, V. Izadifar, B. Muscatelli-Groux, T.H. Van der Kwast and D.K. Chopin 1997. Expression and functions of EGF, FGF and TGFbeta-growth-factor family members and their receptors in invasive human transitional-cell-carcinoma cells. Int. J. Cancer. 71, 284-291.

236. Simon, R., J. Richter, U. Wagner, A. Fijan, J. Bruderer, U. Schmid, D. Ackermann, R. Maurer, G. Alund, H. Knonagel, M. Rist, K. Wilber, M. Anabitarte, F. Hering, T. Hardmeier, A. Schonenberger, R. Flury, P. Jager, J.L. Fehr, P. Schraml, H. Moch, M.J. Mihatsch, T. Gasser and G. Sauter 2001. High-throughput tissue microarray analysis of 3p25 (RAF1) and 8p12 (FGFR1) copy number alterations in urinary bladder cancer. Cancer Res. 61, 4514-4519.

237. Veltman, J. A., J. Fridlyand, S. Pejavar, A.B. Olshen, J.E. Korkola, S. DeVries, P. Carroll, W.L. Kuo, D. Pinkel, D. Albertson, C. Cordon-Cardo, A.N. Jain and F.M. Waldman 2003. Array-based comparative genomic hybridization for genome-wide screening of DNA copy number in bladder tumors. Cancer Res. 63, 2872-2880.

238. Tomlinson, D. C., F.R. Lamont, S.D. Shnyder and M.A. Knowles 2009. Fibroblast growth factor receptor 1 promotes proliferation and survival via activation of the mitogen-activated protein kinase pathway in bladder cancer. Cancer Res. 69, 4613-4620.

239. Diez de Medina, S. G., D. Chopin, A. El Marjou, A. Delouvee, W.J. LaRochelle, A. Hoznek, C. Abbou, S.A. Aaronson, J.P. Thiery and F. Radvanyi 1997. Decreased expression of keratinocyte growth factor receptor in a subset of human transitional cell bladder carcinomas. Oncogene. 14, 323-330.

240. Nord, H., U. Segersten, J. Sandgren, K. Wester, C. Busch, U. Menzel, J. Komorowski, J.P. Dumanski, P.U. Malmstrom and T. Diaz de Stahl 2010. Focal amplifications are associated with high grade and recurrences in stage ta bladder carcinoma. Int. J. Cancer. 126, 1390-1402.

241. Romanenko, A. M., K. Morimura, A. Kinoshita, H. Wanibuchi, S. Takahashi, W.K. Zaparin, W.I. Vinnichenko, A.F. Vozianov and S. Fukushima 2006. Upregulation of fibroblast growth factor receptor 3 and epidermal growth factor receptors, in association with raf-1, in urothelial dysplasia and carcinoma in situ after the chernobyl accident. Cancer. Sci. 97, 1168-1174.

242. Mhawech-Fauceglia, P., G. Fischer, V. Alvarez Jr, A. Ahmed and F.R. Herrmann 2007. Predicting outcome in minimally invasive (T1a and T1b) urothelial bladder carcinoma using a panel of biomarkers: A high throughput tissue microarray analysis. BJU Int. 100, 1182-1187.

243. Gomez-Roman, J. J., P. Saenz, M. Molina, J. Cuevas Gonzalez, K. Escuredo, S. Santa Cruz, C. Junquera, L. Simon, A. Martinez, J.L. Gutierrez Banos, M. Lopez-Brea, C. Esparza and J.F. Val-Bernal 2005. Fibroblast growth factor receptor 3 is overexpressed in urinary tract carcinomas and modulates the neoplastic cell growth. Clin. Cancer Res. 11, 459-465.

244. Tomlinson, D. C., O. Baldo, P. Harnden and M.A. Knowles 2007. FGFR3 protein expression and its relationship to mutation status and prognostic variables in bladder cancer. J. Pathol. 213, 91-98.

245. Suzui, H., J.A. Takahashi, M. Fukumoto, N. Hashimoto, N. Itoh, M. Hatanaka and H. Kikuchi 1994. Immunohistochemical study for basic fibroblast growth factor and fibroblast growth factor receptor I in pituitary adenomas. Neurosci. Lett. 171, 192-196.

246. Ueba, T., J.A. Takahashi, M. Fukumoto, M. Ohta, N. Ito, Y. Oda, H. Kikuchi and M. Hatanaka 1994. Expression of fibroblast growth factor receptor-1 in human glioma and meningioma tissues. Neurosurgery. 34, 221-5; discussion 225-6.

247. Morrison, R. S., F. Yamaguchi, H. Saya, J.M. Bruner, A.M. Yahanda, L.A. Donehower and M. Berger 1994. Basic fibroblast growth factor and fibroblast growth factor receptor I are implicated in the growth of human astrocytomas. J. Neurooncol. 18, 207-216.

248. Allerstorfer, S., G. Sonvilla, H. Fischer, S. Spiegl-Kreinecker, C. Gauglhofer, U. Setinek, T. Czech, C. Marosi, J. Buchroithner, J. Pichler, R. Silye, T. Mohr, K. Holzmann, B. Grasl-Kraupp, B. Marian, M. Grusch, J. Fischer, M. Micksche and W. Berger 2008. FGF5 as an oncogenic factor in human glioblastoma multiforme: Autocrine and paracrine activities. Oncogene. 27, 4180-4190.

249. Cancer Genome Atlas Research Network 2008. Comprehensive genomic characterization defines human glioblastoma genes and core pathways. Nature. 455, 1061-1068.

250. Suzuki, T., M. Maruno, K. Wada, N. Kagawa, Y. Fujimoto, N. Hashimoto, S. Izumoto and T. Yoshimine 2004. Genetic analysis of human glioblastomas using a genomic microarray system. Brain Tumor Pathol. 21, 27-34.

251. Sasaki, T., H. Arai, T. Beppu and K. Ogasawara 2003. Detection of gene amplification and deletion in high-grade gliomas using a genome DNA microarray (GenoSensor array 300). Brain Tumor Pathol. 20, 59-63.

252. Yamada, S. M., S. Yamada, Y. Hayashi, H. Takahashi, A. Teramoto and K. Matsumoto 2002. Fibroblast growth factor receptor (FGFR) 4 correlated with the malignancy of human astrocytomas. Neurol. Res. 24, 244-248.

253. Kadota, M., M. Sato, B. Duncan, A. Ooshima, H.H. Yang, N. Diaz-Meyer, S. Gere, S. Kageyama, J. Fukuoka, T. Nagata, K. Tsukada, B.K. Dunn, L.M. Wakefield and M.P. Lee 2009. Identification of novel gene amplifications in breast cancer and coexistence of gene amplification with an activating mutation of PIK3CA. Cancer Res. 69, 7357-7365.

254. Gruel, N., C. Lucchesi, V. Raynal, M.J. Rodrigues, G. Pierron, R. Goudefroye, P. Cottu, F. Reyal, X. Sastre-Garau, A. Fourquet, O. Delattre and A. Vincent-Salomon 2010. Lobular invasive carcinoma of the breast is a molecular entity distinct from luminal invasive ductal carcinoma. Eur. J. Cancer. 46, 2399-2407.

255. Turner, N., A. Pearson, R. Sharpe, M. Lambros, F. Geyer, M.A. Lopez-Garcia, R. Natrajan, C. Marchio, E. Iorns, A. Mackay, C. Gillett, A. Grigoriadis, A. Tutt, J.S. Reis-Filho and A. Ashworth 2010. FGFR1 amplification drives endocrine therapy resistance and is a therapeutic target in breast cancer. Cancer Res. 70, 2085-2094.

256. Elbauomy Elsheikh, S., A.R. Green, M.B. Lambros, N.C. Turner, M.J. Grainge, D. Powe, I.O. Ellis and J.S. Reis-Filho 2007. FGFR1 amplification in breast carcinomas: A chromogenic in situ hybridisation analysis. Breast Cancer Res. 9, R23.

257. Courjal, F., M. Cuny, J. Simony-Lafontaine, G. Louason, P. Speiser, R. Zeillinger, C. Rodriguez and C. Theillet 1997. Mapping of DNA amplifications at 15 chromosomal localizations in 1875 breast tumors: Definition of phenotypic groups. Cancer Res. 57, 4360-4367.

258. Letessier, A., F. Sircoulomb, C. Ginestier, N. Cervera, F. Monville, V. Gelsi-Boyer, B. Esterni, J. Geneix, P. Finetti, C. Zemmour, P. Viens, E. Charafe-Jauffret, J. Jacquemier, D. Birnbaum and M. Chaffanet 2006. Frequency, prognostic impact, and subtype association of 8p12, 8q24, 11q13, 12p13, 17q12, and 20q13 amplifications in breast cancers. BMC Cancer. 6, 245.

259. Jacquemier, J., J. Adelaide, P. Parc, F. Penault-Llorca, J. Planche, O. deLapeyriere and D. Birnbaum 1994. Expression of the FGFR1 gene in human breast-carcinoma cells. Int. J. Cancer. 59, 373-378.

260. Theillet, C., J. Adelaide, G. Louason, F. Bonnet-Dorion, J. Jacquemier, J. Adnane, M. Longy, D. Katsaros, P. Sismondi and P. Gaudray 1993. FGFRI and PLAT genes and DNA amplification at 8p12 in breast and ovarian cancers. Genes Chromosomes Cancer. 7, 219-226.

261. Reis-Filho, J. S., P.T. Simpson, N.C. Turner, M.B. Lambros, C. Jones, A. Mackay, A. Grigoriadis, D. Sarrio, K. Savage, T. Dexter, M. Iravani, K. Fenwick, B. Weber, D. Hardisson, F.C. Schmitt, J. Palacios, S.R. Lakhani and A. Ashworth 2006. FGFR1 emerges as a potential therapeutic target for lobular breast carcinomas. Clin. Cancer Res. 12, 6652-6662.

262. Andre, F., B. Job, P. Dessen, A. Tordai, S. Michiels, C. Liedtke, C. Richon, K. Yan, B. Wang, G. Vassal, S. Delaloge, G.N. Hortobagyi, W.F. Symmans, V. Lazar and L. Pusztai 2009. Molecular characterization of breast cancer with high-resolution oligonucleotide comparative genomic hybridization array. Clin. Cancer Res. 15, 441-451.

263. Kwek, S. S., R. Roy, H. Zhou, J. Climent, J.A. Martinez-Climent, J. Fridlyand and D.G. Albertson 2009. Co-amplified genes at 8p12 and 11q13 in breast tumors cooperate with two major pathways in oncogenesis. Oncogene. 28, 1892-1903.

264. Gelsi-Boyer, V., B. Orsetti, N. Cervera, P. Finetti, F. Sircoulomb, C. Rouge, L. Lasorsa, A. Letessier, C. Ginestier, F. Monville, S. Esteyries, J. Adelaide, B. Esterni, C. Henry, S.P. Ethier, F. Bibeau, M.J. Mozziconacci, E. Charafe-Jauffret, J. Jacquemier, F. Bertucci, D. Birnbaum, C. Theillet and M. Chaffanet 2005. Comprehensive profiling of 8p11-12 amplification in breast cancer. Mol. Cancer. Res. 3, 655-667.

265. Chin, K., S. DeVries, J. Fridlyand, P.T. Spellman, R. Roydasgupta, W.L. Kuo, A. Lapuk, R.M. Neve, Z. Qian, T. Ryder, F. Chen, H. Feiler, T. Tokuyasu, C. Kingsley, S. Dairkee, Z. Meng, K. Chew, D. Pinkel, A. Jain, B.M. Ljung, L. Esserman, D.G. Albertson, F.M. Waldman and J.W. Gray 2006. Genomic and transcriptional aberrations linked to breast cancer pathophysiologies. Cancer. Cell. 10, 529-541.

266. Adnane, J., P. Gaudray, C.A. Dionne, G. Crumley, M. Jaye, J. Schlessinger, P. Jeanteur, D. Birnbaum and C. Theillet 1991. BEK and FLG, two receptors to members of the FGF family, are amplified in subsets of human breast cancers. Oncogene. 6, 659-663.

267. Penault-Llorca, F., F. Bertucci, J. Adelaide, P. Parc, F. Coulier, J. Jacquemier, D. Birnbaum and O. deLapeyriere 1995. Expression of FGF and FGF receptor genes in human breast cancer. Int. J. Cancer. 61, 170-176.

268. Neve, R. M., K. Chin, J. Fridlyand, J. Yeh, F.L. Baehner, T. Fevr, L. Clark, N. Bayani, J.P. Coppe, F. Tong, T. Speed, P.T. Spellman, S. DeVries, A. Lapuk, N.J. Wang, W.L. Kuo, J.L. Stilwell, D. Pinkel, D.G. Albertson, F.M. Waldman, F. McCormick, R.B. Dickson, M.D. Johnson, M. Lippman, S. Ethier, A. Gazdar and J.W. Gray 2006. A collection of breast cancer cell lines for the study of functionally distinct cancer subtypes. Cancer. Cell. 10, 515-527.

269. Forozan, F., R. Veldman, C.A. Ammerman, N.Z. Parsa, A. Kallioniemi, O.P. Kallioniemi and S.P. Ethier 1999. Molecular cytogenetic analysis of 11 new breast cancer cell lines. Br. J. Cancer. 81, 1328-1334.

270. Adelaide, J., P. Finetti, I. Bekhouche, L. Repellini, J. Geneix, F. Sircoulomb, E. Charafe-Jauffret, N. Cervera, J. Desplans, D. Parzy, E. Schoenmakers, P. Viens, J. Jacquemier, D. Birnbaum, F. Bertucci and M. Chaffanet 2007. Integrated profiling of basal and luminal breast cancers. Cancer Res. 67, 11565-11575.

271. Heiskanen, M., J. Kononen, M. Barlund, J. Torhorst, G. Sauter, A. Kallioniemi and O. Kallioniemi 2001. CGH, cDNA and tissue microarray analyses implicate FGFR2 amplification in a small subset of breast tumors. Anal. Cell. Pathol. 22, 229-234.

272. Turner, N., M.B. Lambros, H.M. Horlings, A. Pearson, R. Sharpe, R. Natrajan, F.C. Geyer, M. van Kouwenhove, B. Kreike, A. Mackay, A. Ashworth, M.J. van de Vijver and J.S. Reis-Filho 2010. Integrative molecular profiling of triple negative breast cancers identifies amplicon drivers and potential therapeutic targets. Oncogene. 29, 2013-2023.

273. Kuroso, K., Y. Imai, M. Kobayashi, K. Yanagimoto, T. Suzuki, M. Kojima and Y. Ueda 2010. Immunohistochemical detection of fibroblast growth factor receptor 3 in human breast cancer: Correlation with clinicopathological/molecular parameters and prognosis. Pathobiology. 77, 231-240.

274. Jaakkola, S., P. Salmikangas, S. Nylund, J. Partanen, E. Armstrong, S. Pyrhonen, P. Lehtovirta and H. Nevanlinna 1993. Amplification of fgfr4 gene in human breast and gynecological cancers. Int. J. Cancer. 54, 378-382.

275. Kurban, G., T. Ishiwata, M. Kudo, M. Yokoyama, Y. Sugisaki and Z. Naito 2004. Expression of keratinocyte growth factor receptor (KGFR/FGFR2 IIIb) in human uterine cervical cancer. Oncol. Rep. 11, 987-991.

276. Kawase, R., T. Ishiwata, Y. Matsuda, M. Onda, M. Kudo, T. Takeshita and Z. Naito 2010. Expression of fibroblast growth factor receptor 2 IIIc in human uterine cervical intraepithelial neoplasia and cervical cancer. Int. J. Oncol. 36, 331-340.

277. Hudelist, G., K. Czerwenka, C. Singer, K. Pischinger, E. Kubista and M. Manavi 2005. cDNA array analysis of cytobrush-collected normal and malignant cervical epithelial cells: A feasibility study. Cancer Genet. Cytogenet. 158, 35-42.

278. Jang, J. H. 2005. Reciprocal relationship in gene expression between FGFR1 and FGFR3: Implication for tumorigenesis. Oncogene. 24, 945-948.

279. Jayson, G. C., C. Vives, C. Paraskeva, K. Schofield, J. Coutts, A. Fleetwood and J.T. Gallagher 1999. Coordinated modulation of the fibroblast growth factor dual receptor mechanism during transformation from human colon adenoma to carcinoma. Int. J. Cancer. 82, 298-304.

280. Sonvilla, G., S. Allerstorfer, C. Heinzle, S. Stattner, J. Karner, M. Klimpfinger, F. Wrba, H. Fischer, C. Gauglhofer, S. Spiegl-Kreinecker, B. Grasl-Kraupp, K. Holzmann, M. Grusch, W. Berger and B. Marian 2010. Fibroblast growth factor receptor 3-IIIc mediates colorectal cancer growth and migration. Br. J. Cancer. 102, 1145-1156.

281. Sugiura, K., S. Ozawa, Y. Kitagawa, M. Ueda and M. Kitajima 2007. Co-expression of aFGF and FGFR-1 is predictive of a poor prognosis in patients with esophageal squamous cell carcinoma. Oncol. Rep. 17, 557-564.

282. Douwes Dekker, P. B., N.J. Kuipers-Dijkshoorn, H.J. Baelde, A.G. van der Mey, P.C. Hogendoorn and C.J. Cornelisse 2007. Basic fibroblast growth factor and fibroblastic growth factor receptor-1 may contribute to head and neck paraganglioma development by an autocrine or paracrine mechanism. Hum. Pathol. 38, 79-85.

283. Freier, K., C. Schwaenen, C. Sticht, C. Flechtenmacher, J. Muhling, C. Hofele, B. Radlwimmer, P. Lichter and S. Joos 2007. Recurrent FGFR1 amplification and high FGFR1 protein expression in oral squamous cell carcinoma (OSCC). Oral Oncol. 43, 60-66.

284. Ishizuka, T., C. Tanabe, H. Sakamoto, K. Aoyagi, M. Maekawa, N. Matsukura, A. Tokunaga, T. Tajiri, T. Yoshida, M. Terada and H. Sasaki 2002. Gene amplification profiling of esophageal squamous cell carcinomas by DNA array CGH. Biochem. Biophys. Res. Commun. 296, 152-155.

285. Myoken, Y., Y. Myoken, T. Okamoto, J.D. Sato, M. Kan, W.L. McKeehan, M. Nakahara and K. Takada 1996. Immunohistochemical study of overexpression of fibroblast growth factor-1 (FGF-1), FGF-2, and FGF receptor-1 in human malignant salivary gland tumours. J. Pathol. 178, 429-436.

286. Iida, S., O. Katoh, A. Tokunaga and M. Terada 1994. Expression of fibroblast growth factor gene family and its receptor gene family in the human upper gastrointestinal tract. Biochem. Biophys. Res. Commun. 199, 1113-1119.

287. Dellacono, F. R., J. Spiro, R. Eisma and D. Kreutzer 1997. Expression of basic fibroblast growth factor and its receptors by head and neck squamous carcinoma tumor and vascular endothelial cells. Am. J. Surg. 174, 540-544.

288. Iida, S., O. Katoh, A. Tokunaga and M. Terada 1994. Expression of fibroblast growth factor gene family and its receptor gene family in the human upper gastrointestinal tract. Biochem. Biophys. Res. Commun. 199, 1113-1119.

289. Yoshino, M., T. Ishiwata, M. Watanabe, T. Matsunobu, O. Komine, Y. Ono, T. Yamamoto, T. Fujii, K. Matsumoto, A. Tokunaga and Z. Naito 2007. Expression and roles of keratinocyte growth factor and its receptor in esophageal cancer cells. Int. J. Oncol. 31, 721-728.

290. Vairaktaris, E., V. Ragos, C. Yapijakis, S. Derka, S. Vassiliou, E. Nkenke, A. Yannopoulos, S. Spyridonidou, A. Vylliotis, V. Papakosta, S. Loukeri, A. Lazaris, C. Tesseromatis, C. Tsigris and E. Patsouris 2006. FGFR-2 and -3 play an important role in initial stages of oral oncogenesis. Anticancer Res. 26, 4217-4221.

291. Wakulich, C., L. Jackson-Boeters, T.D. Daley and G.P. Wysocki 2002. Immunohistochemical localization of growth factors fibroblast growth factor-1 and fibroblast growth factor-2 and receptors fibroblast growth factor receptor-2 and fibroblast

growth factor receptor-3 in normal oral epithelium, epithelial dysplasias, and squamous cell carcinoma. Oral Surg. Oral Med. Oral Pathol. Oral Radiol. Endod. 93, 573-579.

292. Janot, F., A.K. el-Naggar, R.S. Morrison, T.J. Liu, D.L. Taylor and G.L. Clayman 1995. Expression of basic fibroblast growth factor in squamous cell carcinoma of the head and neck is associated with degree of histologic differentiation. Int. J. Cancer. 64, 117-123.

293. Zhang, Y., H. Wang, S. Toratani, J.D. Sato, M. Kan, W.L. McKeehan and T. Okamoto 2001. Growth inhibition by keratinocyte growth factor receptor of human salivary adenocarcinoma cells through induction of differentiation and apoptosis. Proc. Natl. Acad. Sci. U. S. A. 98, 11336-11340.

294. Henson, B. J. and S.M. Gollin 2010. Overexpression of KLF13 and FGFR3 in oral cancer cells. Cytogenet. Genome Res. 128, 192-198.

295. Vekony, H., B. Ylstra, S.M. Wilting, G.A. Meijer, M.A. van de Wiel, C.R. Leemans, I. van der Waal and E. Bloemena 2007. DNA copy number gains at loci of growth factors and their receptors in salivary gland adenoid cystic carcinoma. Clin. Cancer Res. 13, 3133-3139.

296. Kin, M., M. Sata, T. Ueno, T. Torimura, S. Inuzuka, R. Tsuji, K. Sujaku, M. Sakamoto, H. Sugawara, S. Tamaki and K. Tanikawa 1997. Basic fibroblast growth factor regulates proliferation and motility of human hepatoma cells by an autocrine mechanism. J. Hepatol. 27, 677-687.

297. Gauglhofer, C., Sagmeister, S., Schrottmaier, W., Fischer, C., Rodgarkia-Dara, C., Mohr, T., Stattner, S., Bichler, C., Kandioler, D. and Wrba, F. 2010. Up-regulation of the fibroblast growth factor 8 subfamily in human hepatocellular carcinoma for cell survival and neoangiogenesis. Hepatology. 53, 854-864.

298. Amann, T., F. Bataille, T. Spruss, K. Dettmer, P. Wild, C. Liedtke, M. Muhlbauer, P. Kiefer, P.J. Oefner, C. Trautwein, A.K. Bosserhoff and C. Hellerbrand 2010. Reduced expression of fibroblast growth factor receptor 2IIIb in hepatocellular carcinoma induces a more aggressive growth. Am. J. Pathol. 176, 1433-1442.

299. Qiu, W. H., B.S. Zhou, P.G. Chu, W.G. Chen, C. Chung, J. Shih, P. Hwu, C. Yeh, R. Lopez and Y. Yen 2005. Over-expression of fibroblast growth factor receptor 3 in human hepatocellular carcinoma. World J. Gastroenterol. 11, 5266-5272.

300. Ho, H. K., S. Pok, S. Streit, J.E. Ruhe, S. Hart, K.S. Lim, H.L. Loo, M.O. Aung, S.G. Lim and A. Ullrich 2009. Fibroblast growth factor receptor 4 regulates proliferation, anti-apoptosis and alpha-fetoprotein secretion during hepatocellular carcinoma progression and represents a potential target for therapeutic intervention. J. Hepatol. 50, 118-127.

301. Tsou, A. P., K.M. Wu, T.Y. Tsen, C.W. Chi, J.H. Chiu, W.Y. Lui, C.P. Hu, C. Chang, C.K. Chou and S.F. Tsai 1998. Parallel hybridization analysis of multiple protein kinase genes:

Identification of gene expression patterns characteristic of human hepatocellular carcinoma. Genomics. 50, 331-340.

302. Brusa, G., E. Zuffa, C.M. Hattinger, M. Serra, D. Remondini, G. Castellani, S. Righi, C. Campidelli, S. Pileri, P.L. Zinzani, A. Gabriele, M. Mancini, P. Corrado, E. Barbieri and M.A. Santucci 2007. Genomic imbalances associated with secondary acute leukemias in hodgkin lymphoma. Oncol. Rep. 18, 1427-1434.

303. Gutierrez, N. C., R. Lopez-Perez, J.M. Hernandez, I. Isidro, B. Gonzalez, M. Delgado, E. Ferminan, J.L. Garcia, L. Vazquez, M. Gonzalez and J.F. San Miguel 2005. Gene expression profile reveals deregulation of genes with relevant functions in the different subclasses of acute myeloid leukemia. Leukemia. 19, 402-409.

304. Mao, X., Z. Onadim, E.A. Price, F. Child, D.M. Lillington, R. Russell-Jones, B.D. Young and S. Whittaker 2003. Genomic alterations in blastic natural killer/extranodal natural killer-like T cell lymphoma with cutaneous involvement. J. Invest. Dermatol. 121, 618-627.

305. Mao, X., G. Orchard, D.M. Lillington, R. Russell-Jones, B.D. Young and S. Whittaker 2003. Genetic alterations in primary cutaneous CD30+ anaplastic large cell lymphoma. Genes Chromosomes Cancer. 37, 176-185.

306. Mao, X., G. Orchard, D.M. Lillington, R. Russell-Jones, B.D. Young and S.J. Whittaker 2003. Amplification and overexpression of JUNB is associated with primary cutaneous T-cell lymphomas. Blood. 101, 1513-1519.

307. Larson, A. and J.R. Cook 2008. Fibroblast growth factor receptor 3 (FGFR3) expression in malignant lymphomas. Appl. Immunohistochem. Mol. Morphol. 16, 322-325.

308. Larson, A. and J.R. Cook 2008. Fibroblast growth factor receptor 3 (FGFR3) expression in malignant lymphomas. Appl. Immunohistochem. Mol. Morphol. 16, 322-325.

309. Dvorak, P., D. Dvorakova, M. Doubek, J. Faitova, J. Pacholikova, A. Hampl and J. Mayer 2003. Increased expression of fibroblast growth factor receptor 3 in CD34+ BCR-ABL+ cells from patients with chronic myeloid leukemia. Leukemia. 17, 2418-2425.

310. Joos, S., M. Granzow, H. Holtgreve-Grez, R. Siebert, L. Harder, J.I. Martin-Subero, J. Wolf, M. Adamowicz, T.F. Barth, P. Lichter and A. Jauch 2003. Hodgkin's lymphoma cell lines are characterized by frequent aberrations on chromosomes 2p and 9p including REL and JAK2. Int. J. Cancer. 103, 489-495.

311. Donnem, T., K. Al-Shibli, S. Al-Saad, L.T. Busund and R.M. Bremnes 2009. Prognostic impact of fibroblast growth factor 2 in non-small cell lung cancer: Coexpression with VEGFR-3 and PDGF-B predicts poor survival. J. Thorac. Oncol. 4, 578-585.

312. Weiss, J., M.L. Sos, D. Seidel, M. Peifer, T. Zander, J.M. Heuckmann, R.T. Ullrich, R. Menon, S. Maier, A. Soltermann, H. Moch, P. Wagener, F. Fischer, S. Heynck, M. Koker, J.

Schottle, F. Leenders, F. Gabler, I. Dabow, S. Querings, L.C. Heukamp, H. Balke-Want, S. Ansen, D. Rauh, I. Baessmann, J. Altmuller, Z. Wainer, M. Conron, G. Wright, P. Russell, B. Solomon, E. Brambilla, C. Brambilla, P. Lorimier, S. Sollberg, O.T. Brustugun, W. Engel-Riedel, C. Ludwig, I. Petersen, J. Sanger, J. Clement, H. Groen, W. Timens, H. Sietsma, E. Thunnissen, E. Smit, D. Heideman, F. Cappuzzo, C. Ligorio, S. Damiani, M. Hallek, R. Beroukhim, W. Pao, B. Klebl, M. Baumann, R. Buettner, K. Ernestus, E. Stoelben, J. Wolf, P. Nurnberg, S. Perner and R.K. Thomas 2010. Frequent and focal FGFR1 amplification associates with therapeutically tractable FGFR1 dependency in squamous cell lung cancer. Sci. Transl. Med. 2, 62ra93.

313. Berger, W., U. Setinek, T. Mohr, I. Kindas-Mugge, M. Vetterlein, G. Dekan, F. Eckersberger, C. Caldas and M. Micksche 1999. Evidence for a role of FGF-2 and FGF receptors in the proliferation of non-small cell lung cancer cells. Int. J. Cancer. 83, 415-423.

314. Fischer, H., N. Taylor, S. Allerstorfer, M. Grusch, G. Sonvilla, K. Holzmann, U. Setinek, L. Elbling, H. Cantonati, B. Grasl-Kraupp, C. Gauglhofer, B. Marian, M. Micksche and W. Berger 2008. Fibroblast growth factor receptor-mediated signals contribute to the malignant phenotype of non-small cell lung cancer cells: Therapeutic implications and synergism with epidermal growth factor receptor inhibition. Mol. Cancer. Ther. 7, 3408-3419.

315. Marek, L., K.E. Ware, A. Fritzsche, P. Hercule, W.R. Helton, J.E. Smith, L.A. McDermott, C.D. Coldren, R.A. Nemenoff, D.T. Merrick, B.A. Helfrich, P.A. Bunn Jr and L.E. Heasley 2009. Fibroblast growth factor (FGF) and FGF receptor-mediated autocrine signaling in non-small-cell lung cancer cells. Mol. Pharmacol. 75, 196-207.

316. Behrens, C., H.Y. Lin, J.J. Lee, M.G. Raso, W.K. Hong, I.I. Wistuba and R. Lotan 2008. Immunohistochemical expression of basic fibroblast growth factor and fibroblast growth factor receptors 1 and 2 in the pathogenesis of lung cancer. Clin. Cancer Res. 14, 6014-6022.

317. Zhao, X., B.A. Weir, T. LaFramboise, M. Lin, R. Beroukhim, L. Garraway, J. Beheshti, J.C. Lee, K. Naoki, W.G. Richards, D. Sugarbaker, F. Chen, M.A. Rubin, P.A. Janne, L. Girard, J. Minna, D. Christiani, C. Li, W.R. Sellers and M. Meyerson 2005. Homozygous deletions and chromosome amplifications in human lung carcinomas revealed by single nucleotide polymorphism array analysis. Cancer Res. 65, 5561-5570.

318. Guddo, F., G. Fontanini, C. Reina, A.M. Vignola, A. Angeletti and G. Bonsignore 1999. The expression of basic fibroblast growth factor (bFGF) in tumor-associated stromal cells and vessels is inversely correlated with non-small cell lung cancer progression. Hum. Pathol. 30, 788-794.

319. Volm, M., R. Koomagi, J. Mattern and G. Stammler 1997. Prognostic value of basic fibroblast growth factor and its receptor (FGFR-1) in patients with non-small cell lung carcinomas. Eur. J. Cancer. 33, 691-693.

320. Takanami, I., F. Tanaka, T. Hashizume, K. Kikuchi, Y. Yamamoto, T. Yamamoto and S. Kodaira 1996. The basic fibroblast growth factor and its receptor in pulmonary adenocarcinomas: An investigation of their expression as prognostic markers. Eur. J. Cancer. 32A, 1504-1509.

321. Bass, A. J., H. Watanabe, C.H. Mermel, S. Yu, S. Perner, R.G. Verhaak, S.Y. Kim, L. Wardwell, P. Tamayo, I. Gat-Viks, A.H. Ramos, M.S. Woo, B.A. Weir, G. Getz, R. Beroukhim, M. O'Kelly, A. Dutt, O. Rozenblatt-Rosen, P. Dziunycz, J. Komisarof, L.R. Chirieac, C.J. Lafargue, V. Scheble, T. Wilbertz, C. Ma, S. Rao, H. Nakagawa, D.B. Stairs, L. Lin, T.J. Giordano, P. Wagner, J.D. Minna, A.F. Gazdar, C.Q. Zhu, M.S. Brose, I. Cecconello, U.R. Jr, S.K. Marie, O. Dahl, R.A. Shivdasani, M.S. Tsao, M.A. Rubin, K.K. Wong, A. Regev, W.C. Hahn, D.G. Beer, A.K. Rustgi and M. Meyerson 2009. SOX2 is an amplified lineage-survival oncogene in lung and esophageal squamous cell carcinomas. Nat. Genet. 41, 1238-1242.

322. Giatromanolaki, A., M.I. Koukourakis, E. Sivridis, K. O'Byrne, G. Cox, P.E. Thorpe, K.C. Gatter and A.L. Harris 2000. Coexpression of MUC1 glycoprotein with multiple angiogenic factors in non-small cell lung cancer suggests coactivation of angiogenic and migration pathways. Clin. Cancer Res. 6, 1917-1921.

323. Levina, V., A.M. Marrangoni, R. DeMarco, E. Gorelik and A.E. Lokshin 2008. Drug-selected human lung cancer stem cells: Cytokine network, tumorigenic and metastatic properties. PLoS One. 3, e3077.

324. Yamayoshi, T., T. Nagayasu, K. Matsumoto, T. Abo, Y. Hishikawa and T. Koji 2004. Expression of keratinocyte growth factor/fibroblast growth factor-7 and its receptor in human lung cancer: Correlation with tumour proliferative activity and patient prognosis. J. Pathol. 204, 110-118.

325. Woenckhaus, M., L. Klein-Hitpass, U. Grepmeier, J. Merk, M. Pfeifer, P. Wild, M. Bettstetter, P. Wuensch, H. Blaszyk, A. Hartmann, F. Hofstaedter and W. Dietmaier 2006. Smoking and cancer-related gene expression in bronchial epithelium and non-small-cell lung cancers. J. Pathol. 210, 192-204.

326. Ohira, T., S. Akutagawa, J. Usuda, T. Nakamura, T. Hirano, M. Tsuboi, K. Nishio, F. Taguchi, N. Ikeda, H. Nakamura, C. Konaka, N. Saijo and H. Kato 2002. Up-regulated gene expression of angiogenesis factors in post-chemotherapeutic lung cancer tissues determined by cDNA macroarray. Oncol. Rep. 9, 723-728.

327. Nakamura, N., T. Iijima, K. Mase, S. Furuya, J. Kano, Y. Morishita and M. Noguchi 2004. Phenotypic differences of proliferating fibroblasts in the stroma of lung adenocarcinoma and normal bronchus tissue. Cancer. Sci. 95, 226-232.

328. Otsuki, T., O. Yamada, K. Yata, H. Sakaguchi, J. Kurebayashi, N. Nakazawa, M. Taniwaki, Y. Yawata and A. Ueki 1999. Expression of fibroblast growth factor and FGF-receptor

family genes in human myeloma cells, including lines possessing t(4;14)(q16.3;q32. 3) and FGFR3 translocation. Int. J. Oncol. 15, 1205-1212.

329. Chandesris, M. O., J. Soulier, S. Labaume, A. Crinquette, L. Repellini, K. Chemin, M. Malphettes, C. Fieschi, B. Asli, Y. Uzunhan, J.P. Fermand, J.C. Bories and B. Arnulf 2007. Detection and follow-up of fibroblast growth factor receptor 3 expression on bone marrow and circulating plasma cells by flow cytometry in patients with t(4;14) multiple myeloma. Br. J. Haematol. 136, 609-614.

330. Krejci, P., P.B. Mekikian and W.R. Wilcox 2006. The fibroblast growth factors in multiple myeloma. Leukemia. 20, 1165-1168.

331. Chang, H., A.K. Stewart, X.Y. Qi, Z.H. Li, Q.L. Yi and S. Trudel 2005. Immunohistochemistry accurately predicts FGFR3 aberrant expression and t(4;14) in multiple myeloma. Blood. 106, 353-355.

332. Fabris, S., L. Agnelli, M. Mattioli, L. Baldini, D. Ronchetti, F. Morabito, D. Verdelli, L. Nobili, D. Intini, V. Callea, C. Stelitano, L. Lombardi and A. Neri 2005. Characterization of oncogene dysregulation in multiple myeloma by combined FISH and DNA microarray analyses. Genes Chromosomes Cancer. 42, 117-127.

333. Onwuazor, O. N., X.Y. Wen, D.Y. Wang, L. Zhuang, E. Masih-Khan, J. Claudio, B. Barlogie, J.D. Shaughnessy Jr and A.K. Stewart 2003. Mutation, SNP, and isoform analysis of fibroblast growth factor receptor 3 (FGFR3) in 150 newly diagnosed multiple myeloma patients. Blood. 102, 772-773.

334. Keats, J. J., T. Reiman, C.A. Maxwell, B.J. Taylor, L.M. Larratt, M.J. Mant, A.R. Belch and L.M. Pilarski 2003. In multiple myeloma, t(4;14)(p16;q32) is an adverse prognostic factor irrespective of FGFR3 expression. Blood. 101, 1520-1529.

335. Sibley, K., J.A. Fenton, A.M. Dring, A.J. Ashcroft, A.C. Rawstron and G.J. Morgan 2002. A molecular study of the t(4;14) in multiple myeloma. Br. J. Haematol. 118, 514-520.

336. Rasmussen, T., H.R. Hudlebusch, L.M. Knudsen and H.E. Johnsen 2002. FGFR3 dysregulation in multiple myeloma: Frequency and prognostic relevance. Br. J. Haematol. 117, 626-628.

337. Zhan, F., J. Hardin, B. Kordsmeier, K. Bumm, M. Zheng, E. Tian, R. Sanderson, Y. Yang, C. Wilson, M. Zangari, E. Anaissie, C. Morris, F. Muwalla, F. van Rhee, A. Fassas, J. Crowley, G. Tricot, B. Barlogie and J. Shaughnessy Jr 2002. Global gene expression profiling of multiple myeloma, monoclonal gammopathy of undetermined significance, and normal bone marrow plasma cells. Blood. 99, 1745-1757.

338. Intini, D., L. Baldini, S. Fabris, L. Lombardi, G. Ciceri, A.T. Maiolo and A. Neri 2001. Analysis of FGFR3 gene mutations in multiple myeloma patients with t(4;14). Br. J. Haematol. 114, 362-364.

339. Ho, P. J., R.D. Brown, G.J. Pelka, A. Basten, J. Gibson and D.E. Joshua 2001. Illegitimate switch recombinations are present in approximately half of primary myeloma tumors, but do not relate to known prognostic indicators or survival. Blood. 97, 490-495.

340. Nakazawa, N., K. Nishida, A. Tamura, M. Kobayashi, T. Iwai, S. Horiike, H. Nishigaki, T. Otsuki, Y. Tomiyama, H. Fujii, K. Kashima and M. Taniwaki 2000. Interphase detection of t(4;14)(p16.3;q32.3) by in situ hybridization and FGFR3 overexpression in plasma cell malignancies. Cancer Genet. Cytogenet. 117, 89-96.

341. Avet-Loiseau, H., J.Y. Li, T. Facon, C. Brigaudeau, N. Morineau, F. Maloisel, M.J. Rapp, P. Talmant, F. Trimoreau, A. Jaccard, J.L. Harousseau and R. Bataille 1998. High incidence of translocations t(11;14)(q13;q32) and t(4;14)(p16;q32) in patients with plasma cell malignancies. Cancer Res. 58, 5640-5645.

342. Richelda, R., D. Ronchetti, L. Baldini, L. Cro, L. Viggiano, R. Marzella, M. Rocchi, T. Otsuki, L. Lombardi, A.T. Maiolo and A. Neri 1997. A novel chromosomal translocation t(4; 14)(p16.3; q32) in multiple myeloma involves the fibroblast growth-factor receptor 3 gene. Blood. 90, 4062-4070.

343. Chesi, M., E. Nardini, L.A. Brents, E. Schrock, T. Ried, W.M. Kuehl and P.L. Bergsagel 1997. Frequent translocation t(4;14)(p16.3;q32.3) in multiple myeloma is associated with increased expression and activating mutations of fibroblast growth factor receptor 3. Nat. Genet. 16, 260-264.

344. Theillet, C., J. Adelaide, G. Louason, F. Bonnet-Dorion, J. Jacquemier, J. Adnane, M. Longy, D. Katsaros, P. Sismondi and P. Gaudray 1993. FGFRI and PLAT genes and DNA amplification at 8p12 in breast and ovarian cancers. Genes Chromosomes Cancer. 7, 219-226.

345. Gorringe, K. L., S. Jacobs, E.R. Thompson, A. Sridhar, W. Qiu, D.Y. Choong and I.G. Campbell 2007. High-resolution single nucleotide polymorphism array analysis of epithelial ovarian cancer reveals numerous microdeletions and amplifications. Clin. Cancer Res. 13, 4731-4739.

346. Crickard, K., J.L. Gross, U. Crickard, M. Yoonessi, S. Lele, W.F. Herblin and K. Eidsvoog 1994. Basic fibroblast growth factor and receptor expression in human ovarian cancer. Gynecol. Oncol. 55, 277-284.

347. Steele, I. A., R.J. Edmondson, J.N. Bulmer, B.S. Bolger, H.Y. Leung and B.R. Davies 2001. Induction of FGF receptor 2-IIIb expression and response to its ligands in epithelial ovarian cancer. Oncogene. 20, 5878-5887.

348. Kornmann, M., T. Ishiwata, K. Matsuda, M.E. Lopez, K. Fukahi, G. Asano, H.G. Beger and M. Korc 2002. IIIc isoform of fibroblast growth factor receptor 1 is overexpressed in human

pancreatic cancer and enhances tumorigenicity of hamster ductal cells. Gastroenterology. 123, 301-313.

349. Motoda, N., Y. Matsuda, M. Onda, T. Ishiwata, E. Uchida and Z. Naito 2011. Overexpression of fibroblast growth factor receptor 4 in high-grade pancreatic intraepithelial neoplasia and pancreatic ductal adenocarcinoma. Int. J. Oncol. 38, 133-143.

350. Liu, Z., T. Ishiwata, S. Zhou, S. Maier, D. Henne-Bruns, M. Korc, M. Bachem and M. Kornmann 2007. Human fibroblast growth factor receptor 1-IIIb is a functional fibroblast growth factor receptor expressed in the pancreas and involved in proliferation and movement of pancreatic ductal cells. Pancreas. 35, 147-157.

351. Leung, H. Y., W.J. Gullick and N.R. Lemoine 1994. Expression and functional activity of fibroblast growth factors and their receptors in human pancreatic cancer. Int. J. Cancer. 59, 667-675.

352. Kobrin, M. S., Y. Yamanaka, H. Friess, M.E. Lopez and M. Korc 1993. Aberrant expression of type I fibroblast growth factor receptor in human pancreatic adenocarcinomas. Cancer Res. 53, 4741-4744.

353. Nomura, S., H. Yoshitomi, S. Takano, T. Shida, S. Kobayashi, M. Ohtsuka, F. Kimura, H. Shimizu, H. Yoshidome, A. Kato and M. Miyazaki 2008. FGF10/FGFR2 signal induces cell migration and invasion in pancreatic cancer. Br. J. Cancer. 99, 305-313.

354. Cho, K., T. Ishiwata, E. Uchida, N. Nakazawa, M. Korc, Z. Naito and T. Tajiri 2007. Enhanced expression of keratinocyte growth factor and its receptor correlates with venous invasion in pancreatic cancer. Am. J. Pathol. 170, 1964-1974.

355. Ishiwata, T., H. Friess, M.W. Buchler, M.E. Lopez and M. Korc 1998. Characterization of keratinocyte growth factor and receptor expression in human pancreatic cancer. Am. J. Pathol. 153, 213-222.

356. Leung, H. Y., W.J. Gullick and N.R. Lemoine 1994. Expression and functional activity of fibroblast growth factors and their receptors in human pancreatic cancer. Int. J. Cancer. 59, 667-675.

357. Kobrin, M. S., Y. Yamanaka, H. Friess, M.E. Lopez and M. Korc 1993. Aberrant expression of type I fibroblast growth factor receptor in human pancreatic adenocarcinomas. Cancer Res. 53, 4741-4744.

358. Sahadevan, K., S. Darby, H.Y. Leung, M.E. Mathers, C.N. Robson and V.J. Gnanapragasam 2007. Selective over-expression of fibroblast growth factor receptors 1 and 4 in clinical prostate cancer. J. Pathol. 213, 82-90.

359. Devilard, E., F. Bladou, O. Ramuz, G. Karsenty, J.P. Dales, G. Gravis, C. Nguyen, F. Bertucci, L. Xerri and D. Birnbaum 2006. FGFR1 and WT1 are markers of human prostate cancer progression. BMC Cancer. 6, 272.

360. Gravdal, K., O.J. Halvorsen, S.A. Haukaas and L.A. Akslen 2006. Expression of bFGF/FGFR-1 and vascular proliferation related to clinicopathologic features and tumor progress in localized prostate cancer. Virchows Arch. 448, 68-74.

361. Edwards, J., N.S. Krishna, C.J. Witton and J.M. Bartlett 2003. Gene amplifications associated with the development of hormone-resistant prostate cancer. Clin. Cancer Res. 9, 5271-5281.

362. Valve, E. M., M.T. Nevalainen, M.J. Nurmi, M.K. Laato, P.M. Martikainen and P.L. Harkonen 2001. Increased expression of FGF-8 isoforms and FGF receptors in human premalignant prostatic intraepithelial neoplasia lesions and prostate cancer. Lab. Invest. 81, 815-826.

363. Giri, D., F. Ropiquet and M. Ittmann 1999. Alterations in expression of basic fibroblast growth factor (FGF) 2 and its receptor FGFR-1 in human prostate cancer. Clin. Cancer Res. 5, 1063-1071.

364. Leung, H. Y., P. Mehta, L.B. Gray, A.T. Collins, C.N. Robson and D.E. Neal 1997. Keratinocyte growth factor expression in hormone insensitive prostate cancer. Oncogene. 15, 1115-1120.

365. Hamaguchi, A., I. Tooyama, T. Yoshiki and H. Kimura 1995. Demonstration of fibroblast growth factor receptor-I in human prostate by polymerase chain reaction and immunohistochemistry. Prostate. 27, 141-147.

366. Valve, E. M., M.T. Nevalainen, M.J. Nurmi, M.K. Laato, P.M. Martikainen and P.L. Harkonen 2001. Increased expression of FGF-8 isoforms and FGF receptors in human premalignant prostatic intraepithelial neoplasia lesions and prostate cancer. Lab. Invest. 81, 815-826.

367. Giri, D., F. Ropiquet and M. Ittmann 1999. Alterations in expression of basic fibroblast growth factor (FGF) 2 and its receptor FGFR-1 in human prostate cancer. Clin. Cancer Res. 5, 1063-1071.

368. Leung, H. Y., P. Mehta, L.B. Gray, A.T. Collins, C.N. Robson and D.E. Neal 1997. Keratinocyte growth factor expression in hormone insensitive prostate cancer. Oncogene. 15, 1115-1120.

369. Gowardhan, B., D.A. Douglas, M.E. Mathers, A.B. McKie, S.R. McCracken, C.N. Robson and H.Y. Leung 2005. Evaluation of the fibroblast growth factor system as a potential target for therapy in human prostate cancer. Br. J. Cancer. 92, 320-327.

370. Ropiquet, F., D. Giri, B. Kwabi-Addo, A. Mansukhani and M. Ittmann 2000. Increased expression of fibroblast growth factor 6 in human prostatic intraepithelial neoplasia and prostate cancer. Cancer Res. 60, 4245-4250.

371. Schaefer, K. L., D.H. Wai, C. Poremba, E. Korsching, F. van Valen, T. Ozaki, W. Boecker and B. Dockhorn-Dworniczak 2002. Characterization of the malignant melanoma of soft-parts cell line GG-62 by expression analysis using DNA microarrays. Virchows Arch. 440, 476-484.

372. Bovee, J. V., L.J. van den Broek, A.M. Cleton-Jansen and P.C. Hogendoorn 2000. Up-regulation of PTHrP and bcl-2 expression characterizes the progression of osteochondroma towards peripheral chondrosarcoma and is a late event in central chondrosarcoma. Lab. Invest. 80, 1925-1934.

373. Straume, O. and L.A. Akslen 2002. Importance of vascular phenotype by basic fibroblast growth factor, and influence of the angiogenic factors basic fibroblast growth factor/fibroblast growth factor receptor-1 and ephrin-A1/EphA2 on melanoma progression. Am. J. Pathol. 160, 1009-1019.

374. Xerri, L., Z. Battyani, J.J. Grob, P. Parc, J. Hassoun, J.J. Bonerandi and D. Birnbaum 1996. Expression of FGF1 and FGFR1 in human melanoma tissues. Melanoma Res. 6, 223-230.

375. Hida, Y., Y. Kubo, Y. Nishio, S. Murakami, D. Fukumoto, K. Sayama, K. Hashimoto and S. Arase 2009. Malignant acanthosis nigricans with enhanced expression of fibroblast growth factor receptor 3. Acta Derm. Venereol. 89, 435-437.

376. Hida, Y., Y. Kubo and S. Arase 2009. Activation of fibroblast growth factor receptor 3 and oncogene-induced senescence in skin tumours. Br. J. Dermatol. 160, 1258-1263.

377. Streit, S., D.S. Mestel, M. Schmidt, A. Ullrich and C. Berking 2006. FGFR4 Arg388 allele correlates with tumour thickness and FGFR4 protein expression with survival of melanoma patients. Br. J. Cancer. 94, 1879-1886.

378. Missiaglia, E., J. Selfe, M. Hamdi, D. Williamson, G. Schaaf, C. Fang, J. Koster, B. Summersgill, B. Messahel, R. Versteeg, K. Pritchard-Jones, M. Kool and J. Shipley 2009. Genomic imbalances in rhabdomyosarcoma cell lines affect expression of genes frequently altered in primary tumors: An approach to identify candidate genes involved in tumor development. Genes Chromosomes Cancer. 48, 455-467.

379. Goldstein, M., I. Meller and A. Orr-Urtreger 2007. FGFR1 over-expression in primary rhabdomyosarcoma tumors is associated with hypomethylation of a 5' CpG island and abnormal expression of the AKT1, NOG, and BMP4 genes. Genes Chromosomes Cancer. 46, 1028-1038.

380. Woolley, P. V., S.M. Gollin, W. Riskalla, S. Finkelstein, D.F. Stefanik, L. Riskalla, W.P. Swaney, L. Weisenthal and R.J. McKenna Jr 2000. Cytogenetics, immunostaining for

fibroblast growth factors, p53 sequencing, and clinical features of two cases of cystosarcoma phyllodes. Mol. Diagn. 5, 179-190.

381. Cottoni, F., S. Ceccarelli, M.V. Masala, M.A. Montesu, R. Satta, C. Pirodda, S. Rotolo, L. Frati, C. Marchese and A. Angeloni 2009. Overexpression of the fibroblast growth factor receptor 2-IIIc in kaposi's sarcoma. J. Dermatol. Sci. 53, 65-68.

382. Wachtel, M., M. Dettling, E. Koscielniak, S. Stegmaier, J. Treuner, K. Simon-Klingenstein, P. Buhlmann, F.K. Niggli and B.W. Schafer 2004. Gene expression signatures identify rhabdomyosarcoma subtypes and detect a novel t(2;2)(q35;p23) translocation fusing PAX3 to NCOA1. Cancer Res. 64, 5539-5545.

383. Khan, J., J.S. Wei, M. Ringner, L.H. Saal, M. Ladanyi, F. Westermann, F. Berthold, M. Schwab, C.R. Antonescu, C. Peterson and P.S. Meltzer 2001. Classification and diagnostic prediction of cancers using gene expression profiling and artificial neural networks. Nat. Med. 7, 673-679.

384. Yu, S. J., L. Zheng, M. Ladanyi, S.L. Asa and S. Ezzat 2004. Sp1-mediated transcriptional control of fibroblast growth factor receptor 4 in sarcomas of skeletal muscle lineage. Clin. Cancer Res. 10, 6750-6758.

385. Schaaf, G. J., J.M. Ruijter, F. van Ruissen, D.A. Zwijnenburg, R. Waaijer, L.J. Valentijn, J. Benit-Deekman, A.H. van Kampen, F. Baas and M. Kool 2005. Full transcriptome analysis of rhabdomyosarcoma, normal, and fetal skeletal muscle: Statistical comparison of multiple SAGE libraries. Faseb j. 19, 404-406.

386. Davicioni, E., F.G. Finckenstein, V. Shahbazian, J.D. Buckley, T.J. Triche and M.J. Anderson 2006. Identification of a PAX-FKHR gene expression signature that defines molecular classes and determines the prognosis of alveolar rhabdomyosarcomas. Cancer Res. 66, 6936-6946.

387. Shin, E. Y., B.H. Lee, J.H. Yang, K.S. Shin, G.K. Lee, H.Y. Yun, Y.J. Song, S.C. Park and E.G. Kim 2000. Up-regulation and co-expression of fibroblast growth factor receptors in human gastric cancer. J. Cancer Res. Clin. Oncol. 126, 519-528.

388. Gong, J., A. Morishita, K. Kurokohchi, J. Tani, K. Kato, H. Miyoshi, H. Inoue, M. Kobayashi, S. Liu, M. Murota, A. Muramatsu, K. Izuishi, Y. Suzuki, H. Yoshida, N. Uchida, K. Deguchi, H. Iwama, I. Ishimaru and T. Masaki 2010. Use of protein array to investigate receptor tyrosine kinases activated in gastric cancer. Int. J. Oncol. 36, 101-106.

389. Hattori, Y., H. Itoh, S. Uchino, K. Hosokawa, A. Ochiai, Y. Ino, H. Ishii, H. Sakamoto, N. Yamaguchi, K. Yanagihara, S. Hirohashi, T. Sugimura and M. Terada 1996. Immunohistochemical detection of K-sam protein in stomach cancer. Clin. Cancer Res. 2, 1373-1381.

390. Hara, T., A. Ooi, M. Kobayashi, M. Mai, K. Yanagihara and I. Nakanishi 1998. Amplification of c-myc, K-sam, and c-met in gastric cancers: Detection by fluorescence in situ hybridization. Lab. Invest. 78, 1143-1153.

391. Peng, D. F., H. Sugihara, K. Mukaisho, Y. Tsubosa and T. Hattori 2003. Alterations of chromosomal copy number during progression of diffuse-type gastric carcinomas: Metaphase- and array-based comparative genomic hybridization analyses of multiple samples from individual tumours. J. Pathol. 201, 439-450.

392. Matsunobu, T., T. Ishiwata, M. Yoshino, M. Watanabe, M. Kudo, K. Matsumoto, A. Tokunaga, T. Tajiri and Z. Naito 2006. Expression of keratinocyte growth factor receptor correlates with expansive growth and early stage of gastric cancer. Int. J. Oncol. 28, 307-314.

393. Tsujimoto, H., H. Sugihara, A. Hagiwara and T. Hattori 1997. Amplification of growth factor receptor genes and DNA ploidy pattern in the progression of gastric cancer. Virchows Arch. 431, 383-389.

394. Yoshida, T., H. Sakamoto and M. Terada 1993. Amplified genes in cancer in upper digestive tract. Semin. Cancer Biol. 4, 33-40.

395. Mor, O., G.N. Ranzani, Y. Ravia, G. Rotman, M. Gutman, A. Manor, D. Amadori, J. Houldsworth, M. Hollstein, M. Schwab and Y. Shiloh 1993. DNA amplification in human gastric carcinomas. Cancer Genet. Cytogenet. 65, 111-114.

396. Toyokawa, T., M. Yashiro and K. Hirakawa 2009. Co-expression of keratinocyte growth factor and K-sam is an independent prognostic factor in gastric carcinoma. Oncol. Rep. 21, 875-880.

397. Ueki, T., T. Koji, S. Tamiya, P.K. Nakane and M. Tsuneyoshi 1995. Expression of basic fibroblast growth factor and fibroblast growth factor receptor in advanced gastric carcinoma. J. Pathol. 177, 353-361.

398. Kunii, K., L. Davis, J. Gorenstein, H. Hatch, M. Yashiro, A. Di Bacco, C. Elbi and B. Lutterbach 2008. FGFR2-amplified gastric cancer cell lines require FGFR2 and Erbb3 signaling for growth and survival. Cancer Res. 68, 2340-2348.

399. Suzuki, K., A. Tokue, T. Kamiakito, K. Kuriki, K. Saito and A. Tanaka 2001. Predominant expression of fibroblast growth factor (FGF) 8, FGF4, and FGF receptor 1 in nonseminomatous and highly proliferative components of testicular germ cell tumors. Virchows Arch. 439, 616-621.

400. St Bernard, R., L. Zheng, W. Liu, D. Winer, S.L. Asa and S. Ezzat 2005. Fibroblast growth factor receptors as molecular targets in thyroid carcinoma. Endocrinology. 146, 1145-1153.

401. Shingu, K., M. Fujimori, K. Ito, Y. Hama, Y. Kasuga, S. Kobayashi, N. Itoh and J. Amano 1998. Expression of fibroblast growth factor-2 and fibroblast growth factor receptor-1 in thyroid diseases: Difference between neoplasms and hyperplastic lesions. Endocr. J. 45, 35-43.

402. Arora, N., T. Scognamiglio, C.C. Lubitz, T.A. Moo, M.A. Kato, B. Zhu, R. Zarnegar, Y.T. Chen and T.J. Fahey 3rd 2009. Identification of borderline thyroid tumors by gene expression array analysis. Cancer. 115, 5421-5431.

403. St Bernard, R., L. Zheng, W. Liu, D. Winer, S.L. Asa and S. Ezzat 2005. Fibroblast growth factor receptors as molecular targets in thyroid carcinoma. Endocrinology. 146, 1145-1153.

404. O'Toole, S. A., E. Dunn, B.L. Sheppard, H. Klocker, J. Bektic, P. Smyth, C. Martin, O. Sheils and J.J. O'Leary 2006. Genome-wide analysis of deoxyribonucleic acid in endometrial cancer using comparative genomic hybridization microarrays. Int. J. Gynecol. Cancer. 16, 834-842.

405. Mayr, D., V. Kanitz, B. Anderegg, B. Luthardt, J. Engel, U. Lohrs, G. Amann and J. Diebold 2006. Analysis of gene amplification and prognostic markers in ovarian cancer using comparative genomic hybridization for microarrays and immunohistochemical analysis for tissue microarrays. Am. J. Clin. Pathol. 126, 101-109.

406. Ishikawa, A., M. Kudo, N. Nakazawa, M. Onda, T. Ishiwata, T. Takeshita and Z. Naito 2008. Expression of keratinocyte growth factor and its receptor in human endometrial cancer in cooperation with steroid hormones. Int. J. Oncol. 32, 565-574.

407. Ishikawa, A., M. Kudo, N. Nakazawa, M. Onda, T. Ishiwata, T. Takeshita and Z. Naito 2008. Expression of keratinocyte growth factor and its receptor in human endometrial cancer in cooperation with steroid hormones. Int. J. Oncol. 32, 565-574.

408. Siegfried, S., F. Pekonen, T. Nyman, M. Ammala and E.M. Rutanen 1997. Distinct patterns of expression of keratinocyte growth factor and its receptor in endometrial carcinoma. Cancer. 79, 1166-1171.

409. Weiss, J., M.L. Sos, D. Seidel, M. Peifer, T. Zander, J.M. Heuckmann, R.T. Ullrich, R. Menon, S. Maier, A. Soltermann, H. Moch, P. Wagener, F. Fischer, S. Heynck, M. Koker, J. Schottle, F. Leenders, F. Gabler, I. Dabow, S. Querings, L.C. Heukamp, H. Balke-Want, S. Ansen, D. Rauh, I. Baessmann, J. Altmuller, Z. Wainer, M. Conron, G. Wright, P. Russell, B. Solomon, E. Brambilla, C. Brambilla, P. Lorimier, S. Sollberg, O.T. Brustugun, W. Engel-Riedel, C. Ludwig, I. Petersen, J. Sanger, J. Clement, H. Groen, W. Timens, H. Sietsma, E. Thunnissen, E. Smit, D. Heideman, F. Cappuzzo, C. Ligorio, S. Damiani, M. Hallek, R. Beroukhim, W. Pao, B. Klebl, M. Baumann, R. Buettner, K. Ernestus, E. Stoelben, J. Wolf, P. Nurnberg, S. Perner and R.K. Thomas 2010. Frequent and focal FGFR1 amplification associates with therapeutically tractable FGFR1 dependency in squamous cell lung cancer. Sci. Transl. Med. 2, 62ra93.

410. Ding, L., G. Getz, D.A. Wheeler, E.R. Mardis, M.D. McLellan, K. Cibulskis, C. Sougnez, H. Greulich, D.M. Muzny, M.B. Morgan, L. Fulton, R.S. Fulton, Q. Zhang, M.C. Wendl, M.S. Lawrence, D.E. Larson, K. Chen, D.J. Dooling, A. Sabo, A.C. Hawes, H. Shen, S.N. Jhangiani, L.R. Lewis, O. Hall, Y. Zhu, T. Mathew, Y. Ren, J. Yao, S.E. Scherer, K. Clerc, G.A. Metcalf, B. Ng, A. Milosavljevic, M.L. Gonzalez-Garay, J.R. Osborne, R. Meyer, X. Shi, Y. Tang, D.C. Koboldt, L. Lin, R. Abbott, T.L. Miner, C. Pohl, G. Fewell, C. Haipek, H. Schmidt, B.H. Dunford-Shore, A. Kraja, S.D. Crosby, C.S. Sawyer, T. Vickery, S. Sander, J. Robinson, W. Winckler, J. Baldwin, L.R. Chirieac, A. Dutt, T. Fennell, M. Hanna, B.E. Johnson, R.C. Onofrio, R.K. Thomas, G. Tonon, B.A. Weir, X. Zhao, L. Ziaugra, M.C. Zody, T. Giordano, M.B. Orringer, J.A. Roth, M.R. Spitz, I.I. Wistuba, B. Ozenberger, P.J. Good, A.C. Chang, D.G. Beer, M.A. Watson, M. Ladanyi, S. Broderick, A. Yoshizawa, W.D. Travis, W. Pao, M.A. Province, G.M. Weinstock, H.E. Varmus, S.B. Gabriel, E.S. Lander, R.A. Gibbs, M. Meyerson and R.K. Wilson 2008. Somatic mutations affect key pathways in lung adenocarcinoma. Nature. 455, 1069-1075.

411. Ruhe, J. E., S. Streit, S. Hart, C.H. Wong, K. Specht, P. Knyazev, T. Knyazeva, L.S. Tay, H.L. Loo, P. Foo, W. Wong, S. Pok, S.J. Lim, H. Ong, M. Luo, H.K. Ho, K. Peng, T.C. Lee, M. Bezler, C. Mann, S. Gaertner, H. Hoefler, S. Iacobelli, S. Peter, A. Tay, S. Brenner, B. Venkatesh and A. Ullrich 2007. Genetic alterations in the tyrosine kinase transcriptome of human cancer cell lines. Cancer Res. 67, 11368-11376.

412. Stephens, P., S. Edkins, H. Davies, C. Greenman, C. Cox, C. Hunter, G. Bignell, J. Teague, R. Smith, C. Stevens, S. O'Meara, A. Parker, P. Tarpey, T. Avis, A. Barthorpe, L. Brackenbury, G. Buck, A. Butler, J. Clements, J. Cole, E. Dicks, K. Edwards, S. Forbes, M. Gorton, K. Gray, K. Halliday, R. Harrison, K. Hills, J. Hinton, D. Jones, V. Kosmidou, R. Laman, R. Lugg, A. Menzies, J. Perry, R. Petty, K. Raine, R. Shepherd, A. Small, H. Solomon, Y. Stephens, C. Tofts, J. Varian, A. Webb, S. West, S. Widaa, A. Yates, F. Brasseur, C.S. Cooper, A.M. Flanagan, A. Green, M. Knowles, S.Y. Leung, L.H. Looijenga, B. Malkowicz, M.A. Pierotti, B. Teh, S.T. Yuen, A.G. Nicholson, S. Lakhani, D.F. Easton, B.L. Weber, M.R. Stratton, P.A. Futreal and R. Wooster 2005. A screen of the complete protein kinase gene family identifies diverse patterns of somatic mutations in human breast cancer. Nat. Genet. 37, 590-592.

413. Greenman, C., P. Stephens, R. Smith, G.L. Dalgliesh, C. Hunter, G. Bignell, H. Davies, J. Teague, A. Butler, C. Stevens, S. Edkins, S. O'Meara, I. Vastrik, E.E. Schmidt, T. Avis, S. Barthorpe, G. Bhamra, G. Buck, B. Choudhury, J. Clements, J. Cole, E. Dicks, S. Forbes, K. Gray, K. Halliday, R. Harrison, K. Hills, J. Hinton, A. Jenkinson, D. Jones, A. Menzies, T. Mironenko, J. Perry, K. Raine, D. Richardson, R. Shepherd, A. Small, C. Tofts, J. Varian, T. Webb, S. West, S. Widaa, A. Yates, D.P. Cahill, D.N. Louis, P. Goldstraw, A.G. Nicholson, F. Brasseur, L. Looijenga, B.L. Weber, Y.E. Chiew, A. DeFazio, M.F. Greaves, A.R. Green, P. Campbell, E. Birney, D.F. Easton, G. Chenevix-Trench, M.H. Tan, S.K. Khoo, B.T. Teh, S.T. Yuen, S.Y. Leung, R. Wooster, P.A. Futreal and M.R. Stratton 2007. Patterns of somatic mutation in human cancer genomes. Nature. 446, 153-158.

414. Jaakkola, S., P. Salmikangas, S. Nylund, J. Partanen, E. Armstrong, S. Pyrhonen, P. Lehtovirta and H. Nevanlinna 1993. Amplification of fgfr4 gene in human breast and gynecological cancers. Int. J. Cancer. 54, 378-382.

415. Bardelli, A., D.W. Parsons, N. Silliman, J. Ptak, S. Szabo, S. Saha, S. Markowitz, J.K. Willson, G. Parmigiani, K.W. Kinzler, B. Vogelstein and V.E. Velculescu 2003. Mutational analysis of the tyrosine kinome in colorectal cancers. Science. 300, 949.

416. Rand, V., J. Huang, T. Stockwell, S. Ferriera, O. Buzko, S. Levy, D. Busam, K. Li, J.B. Edwards, C. Eberhart, K.M. Murphy, A. Tsiamouri, K. Beeson, A.J. Simpson, J.C. Venter, G.J. Riggins and R.L. Strausberg 2005. Sequence survey of receptor tyrosine kinases reveals mutations in glioblastomas. Proc. Natl. Acad. Sci. U. S. A. 102, 14344-14349.

417. Gartside, M. G., H. Chen, O.A. Ibrahimi, S.A. Byron, A.V. Curtis, C.L. Wellens, A. Bengston, L.M. Yudt, A.V. Eliseenkova, J. Ma, J.A. Curtin, P. Hyder, U.L. Harper, E. Riedesel, G.J. Mann, J.M. Trent, B.C. Bastian, P.S. Meltzer, M. Mohammadi and P.M. Pollock 2009. Loss-of-function fibroblast growth factor receptor-2 mutations in melanoma. Mol. Cancer. Res. 7, 41-54.

418. Dutt, A., H.B. Salvesen, T.H. Chen, A.H. Ramos, R.C. Onofrio, C. Hatton, R. Nicoletti, W. Winckler, R. Grewal, M. Hanna, N. Wyhs, L. Ziaugra, D.J. Richter, J. Trovik, I.B. Engelsen, I.M. Stefansson, T. Fennell, K. Cibulskis, M.C. Zody, L.A. Akslen, S. Gabriel, K.K. Wong, W.R. Sellers, M. Meyerson and H. Greulich 2008. Drug-sensitive FGFR2 mutations in endometrial carcinoma. Proc. Natl. Acad. Sci. U. S. A. 105, 8713-8717.

419. Cancer Genome Atlas Research Network 2008. Comprehensive genomic characterization defines human glioblastoma genes and core pathways. Nature. 455, 1061-1068.

420. Jang, J. H., K.H. Shin and J.G. Park 2001. Mutations in fibroblast growth factor receptor 2 and fibroblast growth factor receptor 3 genes associated with human gastric and colorectal cancers. Cancer Res. 61, 3541-3543.

421. Pollock, P. M., M.G. Gartside, L.C. Dejeza, M.A. Powell, M.A. Mallon, H. Davies, M. Mohammadi, P.A. Futreal, M.R. Stratton, J.M. Trent and P.J. Goodfellow 2007. Frequent activating FGFR2 mutations in endometrial carcinomas parallel germline mutations associated with craniosynostosis and skeletal dysplasia syndromes. Oncogene. 26, 7158-7162.

422. Hansen, R. M., A. Goriely, S.A. Wall, I.S. Roberts and A.O. Wilkie 2005. Fibroblast growth factor receptor 2, gain-of-function mutations, and tumourigenesis: Investigating a potential link. J. Pathol. 207, 27-31.

423. Ding, L., G. Getz, D.A. Wheeler, E.R. Mardis, M.D. McLellan, K. Cibulskis, C. Sougnez, H. Greulich, D.M. Muzny, M.B. Morgan, L. Fulton, R.S. Fulton, Q. Zhang, M.C. Wendl, M.S. Lawrence, D.E. Larson, K. Chen, D.J. Dooling, A. Sabo, A.C. Hawes, H. Shen, S.N. Jhangiani, L.R. Lewis, O. Hall, Y. Zhu, T. Mathew, Y. Ren, J. Yao, S.E. Scherer, K. Clerc,

G.A. Metcalf, B. Ng, A. Milosavljevic, M.L. Gonzalez-Garay, J.R. Osborne, R. Meyer, X. Shi, Y. Tang, D.C. Koboldt, L. Lin, R. Abbott, T.L. Miner, C. Pohl, G. Fewell, C. Haipek, H. Schmidt, B.H. Dunford-Shore, A. Kraja, S.D. Crosby, C.S. Sawyer, T. Vickery, S. Sander, J. Robinson, W. Winckler, J. Baldwin, L.R. Chirieac, A. Dutt, T. Fennell, M. Hanna, B.E. Johnson, R.C. Onofrio, R.K. Thomas, G. Tonon, B.A. Weir, X. Zhao, L. Ziaugra, M.C. Zody, T. Giordano, M.B. Orringer, J.A. Roth, M.R. Spitz, I.I. Wistuba, B. Ozenberger, P.J. Good, A.C. Chang, D.G. Beer, M.A. Watson, M. Ladanyi, S. Broderick, A. Yoshizawa, W.D. Travis, W. Pao, M.A. Province, G.M. Weinstock, H.E. Varmus, S.B. Gabriel, E.S. Lander, R.A. Gibbs, M. Meyerson and R.K. Wilson 2008. Somatic mutations affect key pathways in lung adenocarcinoma. Nature. 455, 1069-1075.

424. Hansen, R. M., A. Goriely, S.A. Wall, I.S. Roberts and A.O. Wilkie 2005. Fibroblast growth factor receptor 2, gain-of-function mutations, and tumourigenesis: Investigating a potential link. J. Pathol. 207, 27-31.

425. Claudio, J. O., F. Zhan, L. Zhuang, R. Khaja, Y.X. Zhu, K. Sivananthan, S. Trudel, E. Masih-Khan, R. Fonseca, P.L. Bergsagel, S.W. Scherer, J. Shaughnessy and A.K. Stewart 2007. Expression and mutation status of candidate kinases in multiple myeloma. Leukemia. 21, 1124-1127.

426. Onwuazor, O. N., X.Y. Wen, D.Y. Wang, L. Zhuang, E. Masih-Khan, J. Claudio, B. Barlogie, J.D. Shaughnessy Jr and A.K. Stewart 2003. Mutation, SNP, and isoform analysis of fibroblast growth factor receptor 3 (FGFR3) in 150 newly diagnosed multiple myeloma patients. Blood. 102, 772-773.

427. Tomlinson, D. C., O. Baldo, P. Harnden and M.A. Knowles 2007. FGFR3 protein expression and its relationship to mutation status and prognostic variables in bladder cancer. J. Pathol. 213, 91-98.

428. Chou, A., N. Dekker and R.C. Jordan 2009. Identification of novel fibroblast growth factor receptor 3 gene mutations in actinic cheilitis and squamous cell carcinoma of the lip. Oral Surg. Oral Med. Oral Pathol. Oral Radiol. Endod. 107, 535-541.

429. Soverini, S., C. Terragna, N. Testoni, D. Ruggeri, P. Tosi, E. Zamagni, C. Cellini, M. Cavo, M. Baccarani, S. Tura and G. Martinelli 2002. Novel mutation and RNA splice variant of fibroblast growth factor receptor 3 in multiple myeloma patients at diagnosis. Haematologica. 87, 1036-1040.

430. Cappellen, D., C. De Oliveira, D. Ricol, S. de Medina, J. Bourdin, X. Sastre-Garau, D. Chopin, J.P. Thiery and F. Radvanyi 1999. Frequent activating mutations of FGFR3 in human bladder and cervix carcinomas. Nat. Genet. 23, 18-20.

431. Lindgren, D., S. Gudjonsson, K.J. Jee, F. Liedberg, S. Aits, A. Andersson, G. Chebil, A. Borg, S. Knuutila, T. Fioretos, W. Mansson and M. Hoglund 2008. Recurrent and multiple bladder tumors show conserved expression profiles. BMC Cancer. 8, 183.

432. Miyake, M., K. Sugano, K. Kawashima, H. Ichikawa, K. Hirabayashi, T. Kodama, H. Fujimoto, T. Kakizoe, Y. Kanai, K. Fujimoto and Y. Hirao 2007. Sensitive detection of FGFR3 mutations in bladder cancer and urine sediments by peptide nucleic acid-mediated real-time PCR clamping. Biochem. Biophys. Res. Commun. 362, 865-871.

433. Sibley, K., D. Cuthbert-Heavens and M.A. Knowles 2001. Loss of heterozygosity at 4p16.3 and mutation of FGFR3 in transitional cell carcinoma. Oncogene. 20, 686-691.

434. Shotelersuk, V., C. Ittiwut, K. Shotelersuk, S. Triratanachat, Y. Poovorawan and A. Mutirangura 2001. Fibroblast growth factor receptor 3 S249C mutation in virus associated squamous cell carcinomas. Oncol. Rep. 8, 1301-1304.

435. Hernandez, S., S. de Muga, L. Agell, N. Juanpere, R. Esgueva, J.A. Lorente, S. Mojal, S. Serrano and J. Lloreta 2009. FGFR3 mutations in prostate cancer: Association with low-grade tumors. Mod. Pathol. 22, 848-856.

436. Anderson, P. J., C.M. Hall, R.D. Evans, B.M. Jones and R.D. Hayward 1998. The feet in pfeiffer's syndrome. J. Craniofac. Surg. 9, 83-87.

437. Gripp, K. W., C.A. Stolle, D.M. McDonald-McGinn, R.I. Markowitz, S.P. Bartlett, J.A. Katowitz, M. Muenke and E.H. Zackai 1998. Phenotype of the fibroblast growth factor receptor 2 Ser351Cys mutation: Pfeiffer syndrome type III. Am. J. Med. Genet. 78, 356-360.

438. Murnaghan, L. M., C.H. Thurgur, B.B. Forster, B.J. Sawatzky, R. Hawkins and S.J. Tredwell 2007. A clinicoradiologic study of the shoulder in apert syndrome. J. Pediatr. Orthop. 27, 838-843.

439. Ito, Y., A. Sanyal, J.S. Fitzsimmons, M.A. Mello and S.W. O'Driscoll 2001. Histomorphological and proliferative characterization of developing periosteal neochondrocytes in vitro. J. Orthop. Res. 19, 405-413.

440. Allen, M. R., J.M. Hock and D.B. Burr 2004. Periosteum: Biology, regulation, and response to osteoporosis therapies. Bone. 35, 1003-1012.

441. Squier, C. A., S. Ghoneim and C.R. Kremenak 1990. Ultrastructure of the periosteum from membrane bone. J. Anat. 171, 233-239.

442. Ibrahimi, O. A., A.V. Eliseenkova, A.N. Plotnikov, K. Yu, D.M. Ornitz and M. Mohammadi 2001. Structural basis for fibroblast growth factor receptor 2 activation in apert syndrome. Proc. Natl. Acad. Sci. U. S. A. 98, 7182-7187.

443. Yang, F., Y. Wang, Z. Zhang, B. Hsu, E.W. Jabs and J.H. Elisseeff 2008. The study of abnormal bone development in the apert syndrome Fgfr2+/S252W mouse using a 3D hydrogel culture model. Bone. 43, 55-63.

444. Lomri, A., J. Lemonnier, M. Hott, N. de Parseval, E. Lajeunie, A. Munnich, D. Renier and P.J. Marie 1998. Increased calvaria cell differentiation and bone matrix formation induced by fibroblast growth factor receptor 2 mutations in apert syndrome. J. Clin. Invest. 101, 1310-1317.

445. Lajeunie, E., M. Le Merrer, C. Bonaiti-Pellie, D. Marchac and D. Renier 1995. Genetic study of nonsyndromic coronal craniosynostosis. Am. J. Med. Genet. 55, 500-504.

446. Wilkie, A. O., J.C. Byren, J.A. Hurst, J. Jayamohan, D. Johnson, S.J. Knight, T. Lester, P.G. Richards, S.R. Twigg and S.A. Wall 2010. Prevalence and complications of single-gene and chromosomal disorders in craniosynostosis. Pediatrics. 126, e391-400.

447. Neilson, K. M. and R.E. Friesel 1995. Constitutive activation of fibroblast growth factor receptor-2 by a point mutation associated with crouzon syndrome. J. Biol. Chem. 270, 26037-26040.

448. Galvin, B. D., K.C. Hart, A.N. Meyer, M.K. Webster and D.J. Donoghue 1996. Constitutive receptor activation by crouzon syndrome mutations in fibroblast growth factor receptor (FGFR)2 and FGFR2/Neu chimeras. Proc. Natl. Acad. Sci. U. S. A. 93, 7894-7899.

449. Iseki, S., A.O. Wilkie, J.K. Heath, T. Ishimaru, K. Eto and G.M. Morriss-Kay 1997. Fgfr2 and osteopontin domains in the developing skull vault are mutually exclusive and can be altered by locally applied FGF2. Development. 124, 3375-3384.

450. Hebert, J. M., M. Lin, J. Partanen, J. Rossant and S.K. McConnell 2003. FGF signaling through FGFR1 is required for olfactory bulb morphogenesis. Development. 130, 1101-1111.

451. Pitteloud, N., J.S. Acierno Jr, A. Meysing, A.V. Eliseenkova, J. Ma, O.A. Ibrahimi, D.L. Metzger, F.J. Hayes, A.A. Dwyer, V.A. Hughes, M. Yialamas, J.E. Hall, E. Grant, M. Mohammadi and W.F. Crowley Jr 2006. Mutations in fibroblast growth factor receptor 1 cause both kallmann syndrome and normosmic idiopathic hypogonadotropic hypogonadism. Proc. Natl. Acad. Sci. U. S. A. 103, 6281-6286.

452. Falardeau, J., W.C. Chung, A. Beenken, T. Raivio, L. Plummer, Y. Sidis, E.E. Jacobson-Dickman, A.V. Eliseenkova, J. Ma, A. Dwyer, R. Quinton, S. Na, J.E. Hall, C. Huot, N. Alois, S.H. Pearce, L.W. Cole, V. Hughes, M. Mohammadi, P. Tsai and N. Pitteloud 2008. Decreased FGF8 signaling causes deficiency of gonadotropin-releasing hormone in humans and mice. J. Clin. Invest. 118, 2822-2831.

453. Meyers, E. N., M. Lewandoski and G.R. Martin 1998. An Fgf8 mutant allelic series generated by cre- and flp-mediated recombination. Nat. Genet. 18, 136-141.

454. Pitteloud, N., R. Quinton, S. Pearce, T. Raivio, J. Acerno, A. Dwyer, L. Plummer, V. Hughes, S. Seminara, Y. Cheng, W. Li, G. Maccoll, A.V. Eliseenkova, S.K. Olsen, O. Ibrahimi, F.J. Hayes, P. Boepple, J.E. Hall, P. Bouloux, M. Mohammadi and W.J. Crowley

2007. Digenic mutations account for variable phenotypes in idiopathic hypogonadotropic hypogonadism. J. Clin. Invest. 117, 457-463.

455. Gonzalez-Martinez, D., S.H. Kim, Y. Hu, S. Guimond, J. Schofield, P. Winyard, G.B. Vannelli, J. Turnbull and P.M. Bouloux 2004. Anosmin-1 modulates fibroblast growth factor receptor 1 signaling in human gonadotropin-releasing hormone olfactory neuroblasts through a heparan sulfate-dependent mechanism. J. Neurosci. 24, 10384-10392.

456. Bribian, A., M.J. Barallobre, N. Soussi-Yanicostas and F. de Castro 2006. Anosmin-1 modulates the FGF-2-dependent migration of oligodendrocyte precursors in the developing optic nerve. Mol. Cell. Neurosci. 33, 2-14.

457. Hu, Y., S.E. Guimond, P. Travers, S. Cadman, E. Hohenester, J.E. Turnbull, S.H. Kim and P.M. Bouloux 2009. Novel mechanisms of fibroblast growth factor receptor 1 regulation by extracellular matrix protein anosmin-1. J. Biol. Chem. 284, 29905-29920.

458. Romanelli, R. G., T. Barni, M. Maggi, M. Luconi, P. Failli, A. Pezzatini, E. Pelo, F. Torricelli, C. Crescioli, P. Ferruzzi, R. Salerno, M. Marini, C.M. Rotella and G.B. Vannelli 2004. Expression and function of gonadotropin-releasing hormone (GnRH) receptor in human olfactory GnRH-secreting neurons: An autocrine GnRH loop underlies neuronal migration. J. Biol. Chem. 279, 117-126.

459. Tatko, Chad D., Waters, Marcey L. 2003. The geometry and efficacy of cation-pi interaction in a diagonal position of a designed beta-hairpin. Protein Sci. 12, 2443-2452.

460. Tsou, Lun K., Tatko, Chad D., Waters, Mercey L. 2002. Simple cation-pi interaction between a phenyl ring and a protonated amine stabilized an alpha-helix in water. J. Am. Chem. Soc. 124, 14917-14921.

461. Gruber, K., Zhou, B., Houk, K. N., Lerner, R. A., Shevlin, C. G., and Wilson, I. A. 1999. Biochemistry., 7062-7074.

462. Waters, M. L. 2004. Aromatic interactions in peptides: Impact on structure and function. Biopolymers. 76, 435-445.

463. Singh, J. T., J.M. 1990. SIRIUS : An automated method for the analysis of the preferred packing arrangements between protein groups. J. Mol. Biol. 211, 595-615.

464. Russell, S.J. and Cochran, A.G. 2002. Designing stable beta-hairpins: Energetic contributions from cross-strand residues. J. Am. Chem. Soc., 12600-12601.

465. Syud, F.A., Stanger, H.E., and Gellman, S.H. 2001. Interstrand side chain–side chain interactions in a designed beta-hairpin: Significance of both lateral and diagonal pairings. J. Amer. Chem. Soc., 8667-8677.

466. Fisk, J.D., Powell, D.R., and Gellman, S.H. 2000. Control of hairpin formation via proline configuration in parallel beta-sheet model systems. J. Am. Chem. Soc., 5443-5447.

467. Distefano, M.D., Zhong, A., and Cochran, A.G. 2002. J. Mol. Biol., 179-188.

468. Gallivan, J.P., and Dougherty, D.A. 1999. Cation-pi interactions in structural biology. Proc. Natl. Acad. Sci. U. S. A. 96, 9459-9464.

469. Waters, M. L. 2004. Aromatic interactions in peptides: Impact on structure and function. Biopolymers. 76, 435-445.

470. Du, Q. S., S.Y. Long, J.Z. Meng and R.B. Huang 2012. Empirical formulation and parameterization of cation-pi interactions for protein modeling. J. Comput. Chem. 33, 153-162.

471. Crowley, P. B. and A. Golovin 2005. Cation-pi interactions in protein-protein interfaces. Proteins. 59, 231-239.

472. John P. Perdew, Matthias Ernzerhof, and Kieron Burke 1996. Rationale for mixing exact exchange with density functional approximations. J. Chem. Phys. 105, 9982.

473. Mecozzi, S., A.P. West Jr and D.A. Dougherty 1996. Cation-pi interactions in aromatics of biological and medicinal interest: Electrostatic potential surfaces as a useful qualitative guide. Proc. Natl. Acad. Sci. U. S. A. 93, 10566-10571.

474. Dougherty, D. A. 2007. Cation-pi interactions involving aromatic amino acids. J. Nutr. 137, 1504S-1508S; discussion 1516S-1517S.

475. Dougherty, D. A. 1996. Cation-pi interactions in chemistry and biology: A new view of benzene, phe, tyr, and trp. Science. 271, 163-168.

476. Wu, G. and V. Terskikh 2008. A multinuclear solid-state NMR study of alkali metal ions in tetraphenylborate salts, M[BPh4] (M = na, K, rb and cs): What is the NMR signature of cation-pi interactions? J Phys Chem A. 112, 10359-10364.

477. Luhmer, M., K. Bartik, A. Dejaegere and Bovy, P.,Reisse, J. 1994. The importance of quadrupolar interactions in molecular recognition processes involving a phenyl group. Bull. Soc. Chim. Fr. 131, 603-606.

478. Bartik, K., A. Dejaegere, P. Bovy and J. Reisse 1994. The importance of quadrupolar interactions in molecular recognition processes involving a phenyl group. Bull. Soc. Chim. Fr. 131, 603-606.

479. Berry, B. W., M.M. Elvekrog and C. Tommos 2007. Environmental modulation of protein cation-pi interactions. J. Am. Chem. Soc. 129, 5308-5309.

480. Shepodd, T. J., M.A. Petti and D.A. Dougherty 1988. Molecular recognition in aqueous media: Donor-acceptor and ion-dipole interactions produce tight binding for highly soluble guests. J. Am. Chem. Soc. 110, 1985-1988.

481. Gallivan J.P., D. D. A. 1999. Cation-pi interactions in structural biology. Proc. Nat'l Acad Sci USA. 96, 9459-9464.

482. Kumpf, R. A. and D.A. Dougherty 1993. A mechanism for ion selectivity in potassium channels: Computational studies of cation-pi interactions. Science. 261, 1708-1710.

483. Callis, P. R. 1991. Molecular orbital theory of the 1Lb and 1La states of indole . J. Chem. Phys. 95, 4230.

484. Ricci, R. W. and J.M. Nesta 1976. Inter- and intramolecular quenching of indole fluorescence by carbonyl compounds. J. Phys. Chem. 80, 974-980.

485. Sillen, A., J.F. DÃ-az and Y. Engelborghs 2000. A step toward the prediction of the fluorescence lifetimes of tryptophan residues in proteins based on structural and spectral data. Protein Science. 9, 158-169.

486. Liu, T., P.R. Callis, B.H. Hesp, M. de Groot, W.J. Buma and J. Broos 2005. Ionization potentials of fluoroindoles and the origin of nonexponential tryptophan fluorescence decay in proteins. J. Am. Chem. Soc. 127, 4104-4113.

487. Qiu, W., L. Wang, W. Lu, A. Boechler, D.A. Sanders and D. Zhong 2007. Dissection of complex protein dynamics in human thioredoxin. Proc. Natl. Acad. Sci. U. S. A. 104, 5366-5371.

488. Chen, Y. and M.D. Barkley 1998. Toward understanding tryptophan fluorescence in proteins. Biochemistry. 37, 9976-9982.

489. Shinitzky, M. and R. Goldman 1967. Fluorometric detection of histiine-tryptophan complexes in peptides and proteins. Eur. J. Biochem. 3, 139-144.

490. Bushueva, T. L., E.P. Busel and E.A. Burstein 1978. Relationship of thermal quenching of protein fluorescence to intramolecular structural mobility. Biochim. Biophys. Acta. 534, 141-152.

491. Vos, R., Y. Engelborghs, J. Izard and D. Baty 1995. Fluorescence study of the three tryptophan residues of the pore-forming domain of colicin A using multifrequency phase fluorometry. Biochemistry. 34, 1734-1743.

492. Steiner, R. F. and E.P. Kirby 1969. The interaction of the ground and excited states of indole derivatives with electron scavengers. J. Phys. Chem. 73, 4130-4135.

493. Yuan, T., A.M. Weljie and H.J. Vogel 1998. Tryptophan fluorescence quenching by methionine and selenomethionine residues of calmodulin: Orientation of peptide and protein binding. Biochemistry. 37, 3187-3195.

494. Chen, Y. and M.D. Barkley 1998. Toward understanding tryptophan fluorescence in proteins. Biochemistry. 37, 9976-9982.

495. Sobolewski, A. L., W. Domcke, C. Dedonder-Lardeux and C. Jouvet 2002. Excited-state hydrogen detachment and hydrogen transfer driven by repulsive 1[small pi][sigma]* states: A new paradigm for nonradiative decay in aromatic biomolecules. Phys.Chem.Chem.Phys. 4, 1093-1100.

496. Bismuto, E., P.L. Martelli, R. Casadio and G. Irace 2000. Tryptophanyl fluorescence lifetime distribution of hyperthermophilic beta-glycosidase from molecular dynamics simulation: A comparison with the experimental data. Protein Sci. 9, 1730-1742.

497. Elber, R. and M. Karplus 1990. Enhanced sampling in molecular dynamics: Use of the time-dependent hartree approximation for a simulation of carbon monoxide diffusion through myoglobin. J. Am. Chem. Soc. 112, 9161-9175.

498. Eftink, M. R. 1986. Quenching of the intrinsic fluorescence of liver alcohol dehydrogenase by the alkaline transition and by coenzyme binding. Biochemistry. 25, 6620-6624.

499. Vos, R., Y. Engelborghs, J. Izard and D. Baty 1995. Fluorescence study of the three tryptophan residues of the pore-forming domain of colicin A using multifrequency phase fluorometry. Biochemistry. 34, 1734-1743.

500. Harris, D. L. and B.S. Hudson 1991. Fluorescence and molecular dynamics study of the internal motion of the buried tryptophan in bacteriophage T4 lysozyme: Effects of temperature and alteration of nonbonded networks. Chem. Phys. 158, 353.

501. Kim, S. J., F.N. Chowdhury, W. Stryjewski, E.S. Younathan, P.S. Russo and M.D. Barkley 1993. Time-resolved fluorescence of the single tryptophan of bacillus stearothermophilus phosphofructokinase. Biophys. J. 65, 215-226.

502. Albani, J., B. Alpert, D.T. Krajcarski and A.G. Szabo 1985. A fluorescence decay time study of tryptophan in isolated hemoglobin subunits. FEBS Lett. 182, 302-304.

503. Szabo, A. G. and D.M. Rayner 1980. Fluorescence decay of tryptophan conformers in aqueous solution. J. Am. Chem. Soc. 102, 554-563.

504. Schlau-Cohen, G. S., A. Ishizaki, T.R. Calhoun, N.S. Ginsberg, M. Ballottari, R. Bassi and G.R. Fleming 2012. Elucidation of the timescales and origins of quantum electronic coherence in LHCII. Nat. Chem. 4, 389-395.

505. Engelborghs, Y. 2003. Correlating protein structure and protein fluorescence. J. Fluoresc. 13, 9-16.

**Cation-π Interactions Contribute to the Stability of the Fibroblast Growth Factor Receptor D2 Domain**

Ryan D. Thurman[1], Dakshinamurthy Rajalingam[1], Dan Davis[1], Igor Prudovsky[2] and Thallapuranam Krishnaswamy Suresh Kumar[1]*

1. *Department of Chemistry and Biochemistry, University of Arkansas, Fayetteville, AR 72701*
2. *Center for Molecular Medicine, Maine Medical Center, Scarborough, ME 04074*

**Abstract**

Activation of the Fibroblast growth factor receptors (FGFR) is a key step in important cellular processes such as, angiogenesis, cell differentiation and tumor growth. The extracellular D2 domain of the FGFR is the binding site for both FGF and heparin. CaPTURE prediction program identified a cation-π interaction in both the crystal and NMR solution structure of the D2 domain of FGFR2. Interestingly, the CapTURE predicted lone cation-π interaction is located in distinctly different locations in the crystal (R152-Tyr155) and solution (Trp191-Arg203) structures of the D2 domain. The significance of the lone cation-π interaction, in terms of stability and heparin affinity, was studied by site-directed mutagenesis and in conjunction with a

variety of biophysical studies. Results of the far-UV, steady-state fluorescence, and 1-anilino naphthalene 8-sulfonate binding suggest that the mutations which are designed to potentially disrupt the predicted cation-π interaction only cause subtle conformational changes in the D2 domain. Limited trypsin digestion data show that disruption of the predicted cation-π interaction increases the backbone flexibility of the protein. Differential scanning calorimetry (DSC) data show that loss of the predicted cation-π interaction causes a significant decrease in the thermodynamic stability of the D2 domain. DSC data unambiguously support the existence of a cation-π interaction between Trp191 and Arg203 predicted in the NMR solution structures. However, DSC results conclusively show that the electrostatic interaction, observed in the crystal structures of the D2 domain, between the positively charged guanido group of Arg203 and the negatively charged β-carboxyl of Asp225 is irrelevant in solution. Isothermal titration calorimetry data show that disruption of the cation-π interaction (Arg152-Tyr155) predicted in the crystal structure does not significantly affect the binding affinity of the D2 domain to heparin. In the contrary, loss of the predicted Trp191-Arg203 cation-π interaction in solution causes a ~ 20-fold decrease in the heparin-D2 domain binding interaction. $^{1}H$-$^{15}N$ chemical shift perturbation data suggest that disruption of the predicted Trp191-Arg203 cation-π interaction causes subtle but clear long-range structural effects resulting in increase in the overall flexibility of the backbone of the D2 domain. The results of this study, for the first time, demonstrate the presence of cation-π interaction between Trp191 and Arg203 and also show that it plays an important role in the thermodynamic stability and in ligand binding affinity of the D2 domain of FGFR2.

## Introduction

Protein structures are stabilized by non-covalent forces such as electrostatic interactions, hydrogen bonds, hydrophobic forces, and cation-π interactions (1). The least understood of these forces are the cation-π interactions. Cation-π interactions are a subset of electrostatic attractions between positively charged amino acids, such as lysine and arginine, and the quadrupole moment generated by the π-cloud of aromatic amino acids (2). A survey of X-ray structures of proteins deposited in the **P**rotein **D**ata **B**ank (PDB, http://www.pdb.org) revealed that cation-π interactions are a common feature of protein structures and occur at an average of one in 77 residues (3). In recent years, cation-π interactions have garnered considerable interest due to their role in structure, stability, folding and interactions of proteins (4-9). For example, cation-π energy has been demonstrated to be correlated with the gating efficiency of the nicotinic acetylcholine receptor (10-20). In addition, cation-π interactions are implicated as an important structural force in DNA-protein complex formation, oligomerization of transmembrane helices, self-assembly of collagen peptides, enzyme catalysis, enhancement of stability of thermophilic proteins, ligand recognition, and enzyme catalysis (21, 22). The energetic significance of the cation-π interaction(s) has been demonstrated in model peptide systems as well as in protein structures by site-directed mutagenesis studies (4, 23-26). Cation-π interaction energy involving lysine and arginine range from -3.3 ± 1.5 kcal/mol to -2.9 ± 1.4 kcal/mol (3, 27-37).

CaPTURE (Cation-π Trends Using Realistic Electrostatics) has been successfully used to predict cation-π interactions in proteins (3). Studies have shown occurrence of cation-π interactions in a number of protein structures deposited in the Protein Data Bank (3). In particular, cation-π interactions are more prevalent in membrane proteins and thermophilic proteins. (21, 22)The accuracy of prediction of cation-π interaction in crystal structures using the

CapTURE algorithm is well documented (38). However, the studies focused on examination of accuracy of CaPTURE prediction(s) based on the three-dimensional solution structures of proteins determined by NMR spectroscopy is sparse. In this context, it will be interesting to compare the strength of the cation-π interactions predicted in the X-ray and NMR solution structures of proteins by the CaPTURE algorithm. This is important because the strength of the cation-π interactions have been shown to be significantly influenced by the presence of aqueous solvents (39-43). The conformational distributions in the ensemble of NMR structures allow for flexible snapshots of a protein's allowed conformations. In this context, it is possible that flexible conformations determined by NMR involve important stabilizing interactions which are not observed by the more rigid x-ray structures.

Fibroblast growth factors (FGFs) are approximately 16 kDa heparin-binding proteins that regulate key cellular processes such as angiogenesis, cell differentiation, morphogenesis, wound healing and tumor growth.(44-50). FGF receptors consist of three extracellular ligand binding domains (D1, D2, D3), a single transmembrane helix, and cytoplasmic tyrosine kinase domain. Cell surface-bound heparan sulfate proteoglycans (HSPG) that support dimerization or oligomerization of the FGFRs are thought to be crucial for activation of the signaling pathway (51, 52). The D2 domain is suggested to bind to both HSPGs and FGFs to form a ternary complex. [4] The structure of the FGF binding complex of the FGFR has been well characterized by Platnikov *et. al* to include FGF: FGFR: heparin in a 2: 2: 2 complex (53). Within the D2 domain there exist non-covalent interactions that stabilize the structure enabling it to interact with FGF and heparin. In this context, it will be interesting to examine if the 3D structure of the D2 domain contains potential cation-π interactions and also the role these interactions play in the stability and ligand binding interactions.

In this study, cation-π interactions in the D2 domain of x-ray and NMR solution structures were identified using the CAPTURE program (54). Interstingly, both the x-ray and NMR structures of the D2 domain predict a potential cation-π interaction. However, interestingly, the residues participating in the cation-π interaction are diferent in the crystal and solution structures. The authenticity of the prediction of cation-π interaction in the crystal and solution structures of the D2 domain was verified using site-directed mutagenesis and a variety of biophysical studies, including multidimensional NMR. Results of this study clearly suggest that the cation-π interaction, W191-R203, observed in the solution structure of the D2 domain is accurate. Comparison of ligand binding affinity and stability of wild type and mutants of the D2 domain indicate that W191-R203 Cation-π interaction is important for both heparin and FGF.

## Material and Methods

### *Mutagenesis, Expression and Protein Purification*

All mutations on the FGFR D2 were made using the Quikchange protocol (Stratagene). The designed mutations were confirmed by DNA sequencing. The mutations were all made to the D2 domain contained in the pET20b vector.

BL-21(DE3) pLysS E. *coli* strain was used to overexpress the wild type and mutants of the D2 domain. Bacteria were grown under controlled shaking conditions (270 rpm) at 37 °C in LB medium containing 100mg/ml ampicillin and 100mg/ml chloramphenicol. Bacterial cells were induced using IPTG at a $O.D._{600}$ value of 0.6. After induction the bacterial cells were allowed to grow incubated at 37 °C for another 5 hours. The cell culture was centrifuged at 6000 rpm to pellet the cells. Cell samples were sonicated using a Microson XL unit with the power setting adjusted to 12. The samples were sonicated 60 times at 1-second interval. The cell lysate was

centrifuged at 16K rpm to pellet the cell debris. Following centrifugation, the pellet was resuspended in 5M NaCl and centrifuged at 10K rpm. The pellet was then resuspended using 1M urea and centrifuged at 10K rpm. Finally, the pellet was resuspended using 8M urea and centrifuged at 10K rpm. The supernatant was dialyzed against 10mM phosphate buffer, 100mM NaCl and 50mM ammonium sulfate (pH 6.5) in order to refold the protein. Dialysis was carried out multiple rounds of buffer with a minimum of 3 hours per exchange. The dialyzed sample was loaded onto a heparin sepharose column and eluted using a salt gradient between 0.3 – 1.5 M NaCl. The purity of each fraction was assessed by 10% SDS gel electrophoresis.

***Cation-π Binding Interactions***

The CaPTURE program was used to predict cation-$\pi$ interactions in the available crystal (PDB codes -1EV2, 1DJS and 1E0o) and solution (PDB code – 1WVZ) of D2 domain of the FGF receptor-2 (FGFR2). The CaPTURE program identifies the potential cation-π (aromatic) side-chain interactions. The cation- $\pi$ interaction energetic potentials were determined using OPLS (optimized potentials for liquid simulations) force fields. The methodology for execution of the CaPTURE calculation has been previously reported (55).

***Circular Dichroism***

Far UV CD measurements on the wild type and mutants of the D2 domain were acquired in 10mM phosphate buffer containing 100 mM NaCl and 50 mM ammonium sulfate (pH 6.5). All CD spectra were acquired on a Jasco J-710 spectrometer at room 25 $^{o}$C. Wavelength scans were set to 250-190 nm. Samples were approximately 90- 100 μM in concentration and a 0.1 cm path length cuvette was used for data acquisition. Each spectrum is an average of 10 scans.

***Steady-state Fluorescence***

All steady state fluorescence measurements were made using a Hitachi F2500 fluorimeter. A 1.0 cm path length cell was used and concentration of each sample was adjusted to ~50 uM. The excitation wavelength was set to 280 nm and acquisition from 300 to 450 nm. For the ANS binding experiments, excitation wavelength was set at 390 nm and the emission was monitored from 450 nm to 600 nm. ANS titration was carried out by addition of 3 μl. aliquots of 10mM ANS to a fixed volume of protein in 10mM phosphate buffer containing 100 mM NaCl and 50 mM ammonium sulfate at a pH of 6.5.

***Differential Scanning Calorimetry***

Differential scanning calorimetric measurements were performed using a DASM-1M calorimeter. The concentration of the protein was was between 1.0 – 1.5 mg/ml in 10 mM phosphate buffer containing 50 mM ammonium sulfate and 100 mM NaCl (pH ~6.5). All samples were degassed prior to loading into the microcalorimeter. The temperature scanning rate was set to 1 °C/min and the protein melting profiles were monitored scanned from 10 °C - 90°C. The $T_m$ values were determined using Origin DSC software provided by Microcal Inc. The entropic or enthalpic energies are not reported because D2 domain does not completely refold back to its native conformation on cooling the sample from 90°C to 10°C.

***Isothermal Titration Calorimetry***

Isothermal titration calorimetry measurements were performed using a Microcal VP titration calorimeter (Northhampton, MA, USA). The concentration of the D2 domain used was 50 μM in 10 mM phosphate buffer containing 50 mM ammonium sulfate and 100 mM NaCl (pH ~6.5).

Titrations consisted of 5-10µl injections of 0.5 mM sucrose octasulfate (heparin analog)/FGF-1 delivered into 0.050 mM concentration of D2. Injections were delayed 3.5 minutes to allow the titration peak to return to a baseline prior to additional injections. All titrations were corrected for background heat changes. The raw data was fit using the available (Origin software supplied by the vendor) binding models and the $\chi 2$ values were used as a guide to decide on the accuracy of the fitting model.

***NMR Spectroscopy***

1H-15N HSQC experiments were acquired using $^{15}N$ isotope enriched D2 domain sample. The concentration of the protein(s) was in the range of 0.15 – 0.5 mM. in 10 mM phosphate buffer (95% $H_2O$ + 5 %$D_2O$, pH 6.5) containing 50 mM ammonium sulfate and 100 mM NaCl. All NMR experiments were conducted at 298°K. All experiments were conducted using Bruker Avance 700 mHz or Bruker Avance 500 mHz NMR. All NMR data were referenced to the $^{1}H$ resonance frequency of DSS.

**Results and discussion**

***Prediction of cation-$\pi$ interactions***- 3D structures of the ternary FGF signaling complex, consisting of, FGF (ligand), heparin/SOS, and FGFR, shows that the D2 domain contributes significantly to the binding of heparin as well as FGF (56) Deletion of the D2 domain completely abolishes the FGF signaling process. To-date, multiple crystal structures of the extracellular domains of FGFR, D2-D3, are available available (57-59)However, only one NMR solution structure of the D2 domain has been reported (60). The 3D structure of the D2 domain of FGFR2

has an immunoglobulin-like fold consisting of 10 antiparallel β-strands arranged in a β-sandwich structure. Potential cation-π interactions in the D2 domain of FGFRs using the CaPTURE program (http://capture.caltech.edu/) (3). Table-1 shows the cation-π interactions predicted in the crystal and solution structures of the D2 domain of FGFR. The CaPTURE program predicts one cation-π in the crystal and solution structures of D2 domain. However, interestingly, the location of the predicted lone cation-π interaction is different in the crystal and solution structures of the D2 domain (Fig. 2.1). The crystal structures consistently show a cation-π interaction between Arg152 (located in β-strand A) and Tyr155 (located in β-strand A). The center of the phenolic ring of Tyr155 is separted from the alpha-carbon atom of Arg152 by a spatial distance of 3.7-4.2 Å and planes of disposition of their side-chain subtend an angle of ~91°. The predcited average electrostatic and van der Waals energies of the Arg152-Tyr155 cation-π interaction are quite favorable and are ~ -3.8 kcal.mol.$^{-1}$ and -3.5 kcal.mol.$^{-1}$ , respectively. These predicted energies values are in good aggreement with the experimentally determined values reported for different types of cation-π interactions (3, 27, 28). The R152-Y155 interaction site occurs in the x-ray structures of the D2 domain. The W191-R203 cation-π interaction is observed in the D2 NMR structure. Interestingly, the CaPTURE program does not predict the presence of the Arg152-Tyr155 cation-π interaction in any of the structures constituting the ensemble of the NMR solution structures of the D2 domain. In the contrary, a cation-π interaction between Trp191 (located in β-strand C) and Arg203 (located in β-strand D) is predicted in the ensemble of the solution structures of the D2 domain determined by multidimensional NMR spectroscopy (60). The average distance between the center of the indole ring of Trp191 and the alpha-carbon atom of Arg203 ~3.5 – 5.4 Å in the NMR structures of the D2 domain. It should be mentioned that due to lack of sufficient side-chain NOE distance constraints, the spatial distance between

Trp191 and Arg203 in the individual structures (constituting the ensemble of NMR structures) was observed to show significant variation. The angle subtended by the side-chains of Trp191 and R203, involved in the cation-π interaction, is ~ 94° - 99° . The average electrostatic energy for the Trp191-Arg203 cation-π interaction is ~ 3.87 kcal. mol.$^{-1}$ (Table 2.2)

To our knowledge, cation-π interactions predicted in the crystal and solution structures of a protein have not been directly compared. In this context, the observed disparity in the cation-π interactions predicted in the crystal and solution structures of the D2 domain of FGFR2 is interesting.

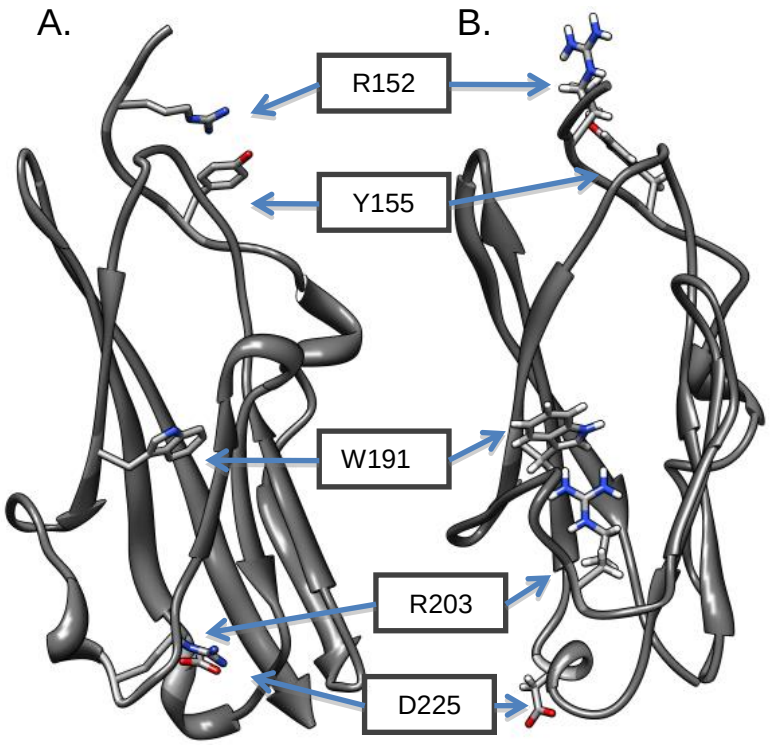


**Figure-2.1.** ***Depiction of the*** x-ray (Panel A, PDB: 1EV2) and NMR solution structures (Panel-B, **PDB:** 1WVZ) of the D2 domain of FGFR2. The residues labeled indicate sites that are predicted to form cation-pi interactions.

Therefore, we verified the authenticity of the predicted cation-π interactions in the 3D structure of the D2 domain by mutating specific residues and monitoring the consequence of the site-

specific mutations on the structure, stability, and ligand binding properties. In this context, several site-specific mutations (K151E, K151L, K151R, R152E, R152L, R152K, F198A, R203E, R203L, Y155A, W191A, and R203L/W191L, D225A), which can potentially disrupt the predicted cation-π interactions in the crystal and solution structures of the D2 domain of FGFR, were generated.

| FGFR2 D2 PDB | Pi residue | Cation residue | ES (kcal/mol) | VDW (kcal/mol) |
|---|---|---|---|---|
| 1WVZ #5 | W191 | R203 | -6.28 | -0.12 |
| 1WVZ #7 | W191 | R203 | -1.2 | -1.78 |
| 1WVZ #10 | W191 | R203 | -4.14 | -2.04 |
| 1EV2 | Y155 | R152 | -4.64 | -3.86 |
| 1DJS | Y155 | R152 | -2.98 | -3.04 |
| 1E0o | Y155 | R152 | -3.73 | -3.04 |

***Table 2.2.*** Cation-π interactions predicted by the CAPTURE program in the 3D structures of the D2 domain of FGFR2. ES and VDW refer to the electrostatic (ES) and van der Waals energies for each cation –π interaction. The NMR solution structures of FGFR2 D2 are represented by the pdb code 1WVZ and the and the crystal structures of the D2 domain of FGFR2 are represented by the pdb codes 1EV2, 1DJS and 1E0o.

***Secondary structure is not perturbed by the disruption of the predicted cation-π interactions***

It is important to assess if disruption of potential cation-π interactions would cause significant changes in the backbone conformation of the D2 domain. Far UV CD provides useful information on the backbone conformation of proteins (61). The far-UV circular dichroism spectra of the wild type and the designed mutants of the D2 domain are shown in Figure 2.2. The far UV CD spectra show a positive and negative ellipticity bands centered at around 205 nm and

225 nm, respectively. These spectral features are reminiscent of a protein with beta-sandwich architecture (60). Interestingly, the far UV CD spectra of the wild type and the designed mutants of the D2 domain superimpose quite well suggesting the disruption of the potential cation-π interactions, caused due to the designed mutations, does not have significant effect(s) on the backbone conformation of the protein.

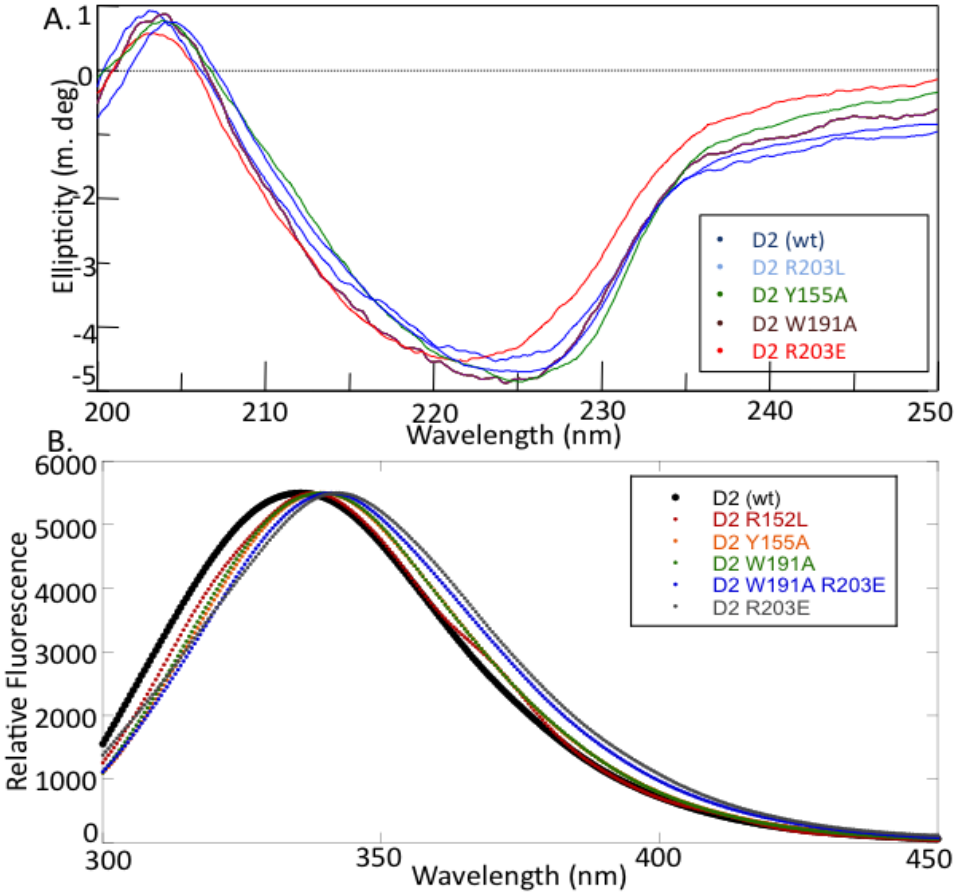


**Figure-2.3 Panel A** - shows the circular dicroism spectra of the mutants shown to have significant changes in flexibility or stability. **Panel B** shows the steady state fluorescence of wild type and selected mutants of the D2 domain. The mutant proteins only minor red shift in their wavelength of maximum emission.

***Disruption of cation-π interactions only causes minor tertiary structural changes***: Monitoring changes in the intrinsic steady state tryptophan fluorescence spectrum of a protein yields valuable information on the tertiary structural changes that can potentially occur as a result of

site-specific mutation(s). The D2 domain contains three tryptophan residues at positions W156, W214 and W191. Trp191 is buried in the interior of the structure of the D2 domain and the other two tryptophans, Trp156 and Trp214, are moderately exposed at the surface of the protein. Steady state fluorescence spectrum of the wild type D2 domain shows an emission maximum of ~ 339 nm and is reflective of the presence of partially buried indole chains in the protein (Figure-2.3). The fluorescence spectra of all the designed mutations show a minor red-shift in the wavelength of emission maximum (Figure-2.3). The W191L/R203E shows a maximum red shift of ~ 5 nm (Figure-2.3). These results indicate that only subtle changes in the tertiary structure occur when the predicted cation-π interaction(s) in the D2 domain are disrupted.

***Subtle conformational change leads to increase in solvent- exposed non-polar surface***: ANS (8-anilino-1-napthalene sulfonate) is a hydrophobic dye that exhibits weak emission in aqueous solutions. However, the emission of ANS increases significantly when it binds to solvent-exposed non-polar pockets in the protein. Therefore, ANS is an useful probe to monitor subtle conformational changes which lead to increased exposure of solvent-exposed non-polar surface(s) in proteins. In this context, we performed ANS binding studies to probe the potential tertiary structural changes caused due to mutations disrupting the cation-π interaction. Titration of wild type D2 domain with ANS shows an emission maximum at around 510nm. The emission intensity (at 510 nm) increases very moderately when wild type D2 domain is titrated with ANS in the concentration range of 0 – 250 μM (Figure-2.4). All the mutations which potentially disrupt the predicted cation-π interaction(s), such as, Y155A, R203E, R203L, R203K and W191A, consistently show higher emission intensity than wild type D2 domain suggesting that the designed mutations cause a subtle conformational change resulting in greater solvent-

exposure of the hydrophobic surface(s) in the protein. ANS emission intensity changes are most pronounced for the mutations, which potentially disrupt the Trp191-Arg203 cation – π interaction than those, which cause loss of the R152-Y155 interaction. These results plausibly suggest that loss of the Trp191-Arg203 cation-π interaction predicted in the NMR structure(s) of the D2 domain causes more discernible changes in the tertiary structure than the R152-Y155 cation-π interaction predicted in the crystal structures.

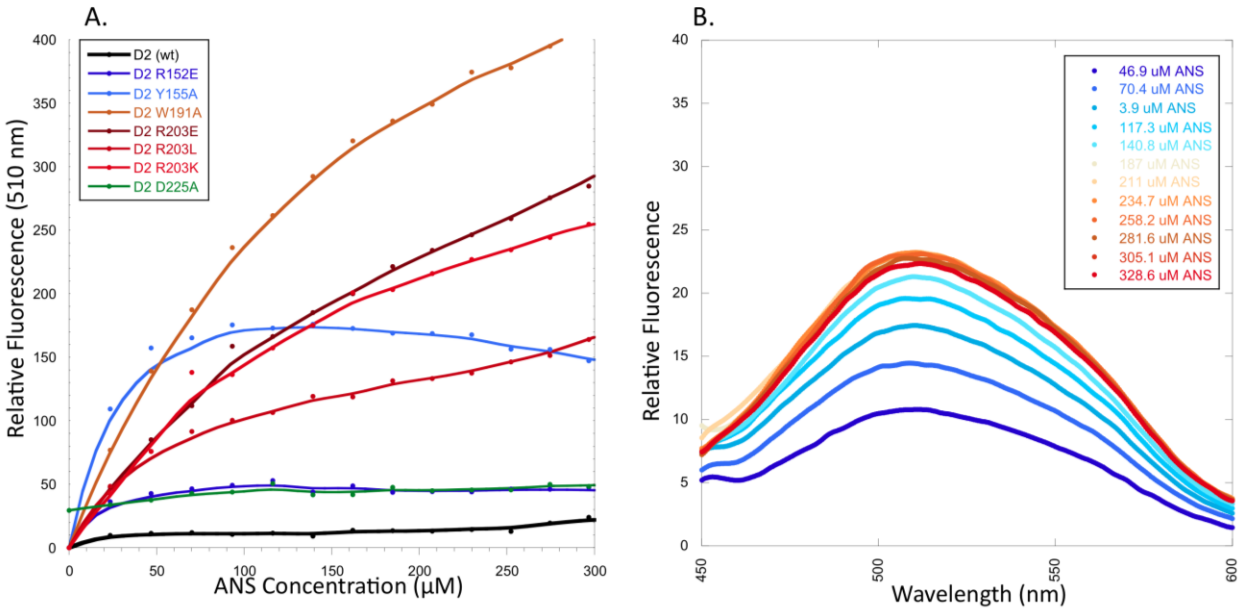


**Figure 2.4**: **Panel A -** ANS titration of the mutants and the wild type D2 domain monitored at 490 nm. Mutants D2 Y155A, W191A and R203E, L and K showed significant increases in fluorescence when titrated with ANS. The D2 K151 is an example of an insignificant change in the fluorescence when titrated with ANS. **Panel B** – Steady-state fluorescence titration of D2 (wt) with ANS.

***Loss of cation-π interaction increases the conformational flexibility of the D2 domain*:** Limited trypsin digestion is a common method to evaluate the flexibility of a protein (62, 63). There are nine lysines and six arginines in the D2 domain making trypsin an apt choice for monitoring the effect of the designed mutations on the conformational flexibility of the D2 domain. Densitometric scan of the intact ~12 kDa D2 domain band on SDS-PAGE shows about ~50% of

the D2 domain band is digested in the first five minutes of incubation with the enzyme (Figure-2.5). Interestingly, R203E, W191A and Y155A mutants of the D2 domain are completely digested within the first five minutes (Figure-2.5). These results suggest that designed mutations cause a subtle conformational chain, which increases the flexibility of the protein backbone and consequently rendering it more susceptible to trypsin cleavage. Therefore, the results of the limited trypsin digestion corroborate the ANS fluorescence data that indicate a subtle tertiary structural change in the R203E, W191A and Y155A mutants.

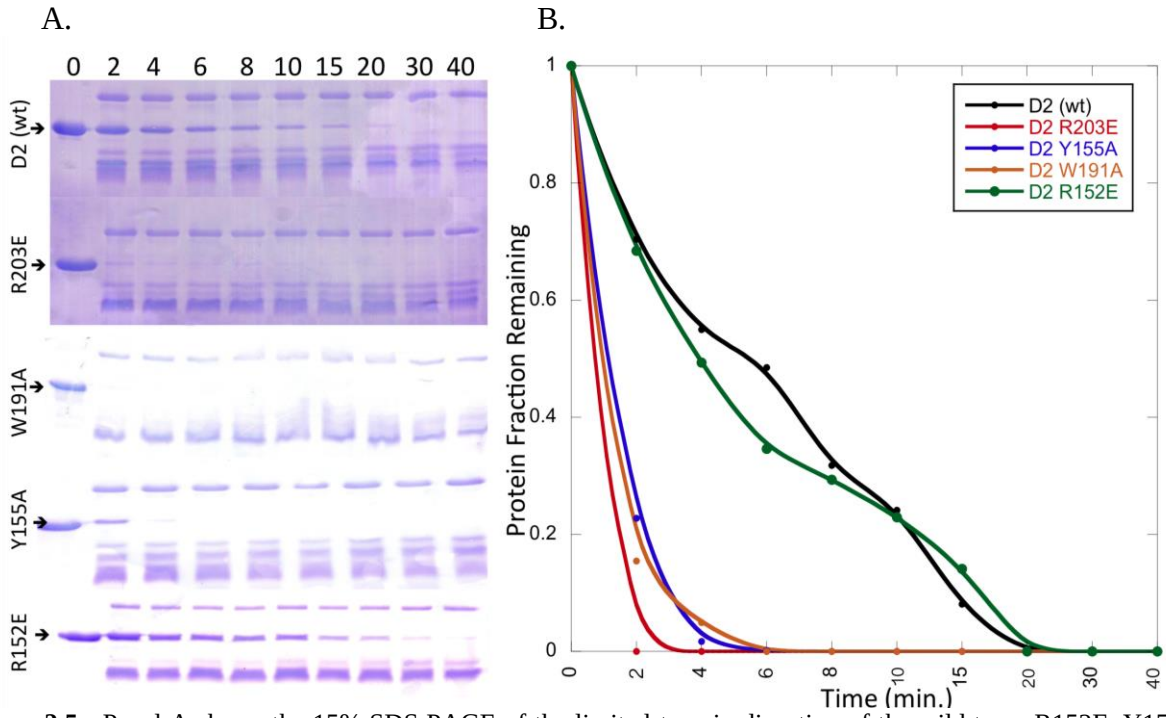


**Figure 2.5** - Panel A shows the 15% SDS PAGE of the limited-trypsin digestion of the wild type, R152E, Y155A, W191A and R203E mutants of the D2 domain after 0, 2, 4, 6, 8, 10, 15, 20, 30 and 40 min of incubation of the protein domain with trypsin. Panel B shows the densitometric plot of the limited-trypsin digestion of wild type (black), R203E (red), Y155A (blue), W191A (orange) and R152E (green).

flexibility of the D2 domain. Densitometric scan of the intact ~12 kDa D2 domain band on SDS PAGE shows about ~50% of the D2 domain band is digested in the first five minutes of incubation with the enzyme (Figure-2.5). Interestingly, the designed mutants of the D2 domain are completely digested within the first five minutes (Figure-2.5). These results suggest that

designed mutations cause a subtle conformational chain, which increases the flexibility of the protein backbone and consequently rendering it more susceptible to trypsin cleavage. Therefore, the results of the limited trypsin digestion corroborate the fluorescence data, which indicate a subtle tertiary structural change in the designed mutants.

***Cation-π interactions contribute significantly to the thermodynamic stability of the D2 domain:*** Differential scanning calorimetry (DSC) is a popular technique for the direct measurement of the thermodynamic stability of proteins (64, 65). DSC facilitates the measurement of melting temperatures ($T_m$), the temperature at which 50% of the population of protein molecules are in the denatured state(s)]. Least-square fitting the individual DSC profiles reveals that the $T_m$ of wild type D2 domain is ~ 52.0 ° C. The $T_m$ values of Y155A, R103E, R203L, R203K, W191A and W191L/R203L mutants of the D2 domain are about 10°C lower than that of the wild type (Figure-2.6). These results indicate that the predicted cation-π interactions contribute significantly to the thermodynamic stability of the protein.

Pitteloud et al reported that D225-R203 mutations result in a loss-of-function (66). It is believed that a mutation of D225 or R203 favors destabilization of the D2 domain, which consequently results a loss-of-function. Interestingly, one of the notable differences between the crystal and solution structures of the D2 domain is the interaction forged by Arg203 with residue W191 (60). The aspartate group of D225 is projected in opposite directions in the crystal and solution structures of the D2 domain. While in the solution structure(s), the positively charged arginine side chain group is involved in a cation-π interaction with the indole side-chain of Trp191, it is paired in an electrostatic interaction with the negatively charged β-carboxyl group of Asp225. We designed an Asp225Ala mutation to probe the presence of an electrostatic

interaction between Arg203 and Asp225. Interestingly, results of the DSC experiments indicate the $T_m$ of the Asp225Ala mutant is in the same range ($T_m$ ~ 51°C) as that of the wild type D2 domain (Figure-2.6). These results clearly demonstrate that the electrostatic interaction which is observed consistently in the crystal structures between Arg203 and Asp225 is not relevant in solution. On the other hand, it appears that guanido group of Arg203 is only involved in a cation-π interaction in solution.

| **D2 Mutation** | **Melting Temp. (~$T_m$)** | **D2 Mutation** | **Melting Temp. (~$T_m$)** |
|---|---|---|---|
| K151E | 50 °C | Y155F | 41 °C |
| K151L | 51 °C | W191A | 43 °C |
| K151R | 52 °C | W191L/R203L | 38 °C |
| R152E | 48 °C | R203E | 39 °C |
| R152L | 51 °C | R203L | 39 °C |
| R152K | 52 °C | R203K | 41 °C |
| R152A | 51 °C | D225A | 51 °C |
| Y155A | 41 °C | | |

**Table 2.6**: DSC melting temperature ($T_m$) for the wild type and mutants of the D2 domain.

***Disruption of Trp191-Arg203 Cation-π interaction decreases heparin binding***: Heparin is crucial for the activation of FGFR (67). Both FGFR and FGF bind to heparin and form the active FGF-heparin-FGFR ternary complex (68). Heparin is believed to increase the stability of the FGF signaling complex (68). Crystal structure data of FGF signaling complex suggests that heparin binds to a positively charged canyon formed through the dimerization of the D2 domain. In this context, it is important to assess if the predicted cation-π interactions affect the binding affinity of the D2 domain to heparin.

Isothermal titration calorimetry (ITC) is a versatile technique, which can be used for direct measurement of binding affinity ($K_d$) as well as the thermodynamics, which characterize protein-ligand interactions. We used ITC to measure the binding affinity of the wild type and designed mutants of the D2 domain and heparin/sucrose octasulfate (SOS). In our hands, commercially available heparin (both low as well as high molecular weight heparin) was highly heterogeneous both in terms of the length and the contaminants. In this context, we did not use heparin in our ITC experiments because the accuracy of the binding affinity and stoichiometry measurements significantly rely on the purity of both the ligand as well as the protein (69). We used sucrose octasulfate (SOS) as a surrogate ligand for heparin in our ITC experiments. SOS is a good structural and functional mimic of heparin. (70). SOS has been shown to support the cell proliferation activity of FGF to the same extent as heparin (70). Isothermogram representing the titration of SOS with wild type D2 domain is exothermic and sigmoidal (Figure-2.7, provides raw ITC curves for wild type D2, R203E, W191A, Y155A and D225A) The binding stoichiometry between the D2 domain and SOS is 1:1 and the binding affinity to SOS is ~ 2.2 μM (Figure-2.7). These values are consistent with those reported earlier for the FGFR-heparin/SOS interaction(s). (60). In marked contrast, the mutations affecting the predicted Trp191-Arg203 cation-π interaction show significant decrease in the binding affinity to SOS (Table-2). These results clearly suggest that disruption of the Trp191-R203 cation-π interaction, predicted in the solution structures of the D2 domain, affects the heparin binding of the D2 domain. On the other hand, ITC data show that the SOS binding affinity of the Arg152-Tyr155

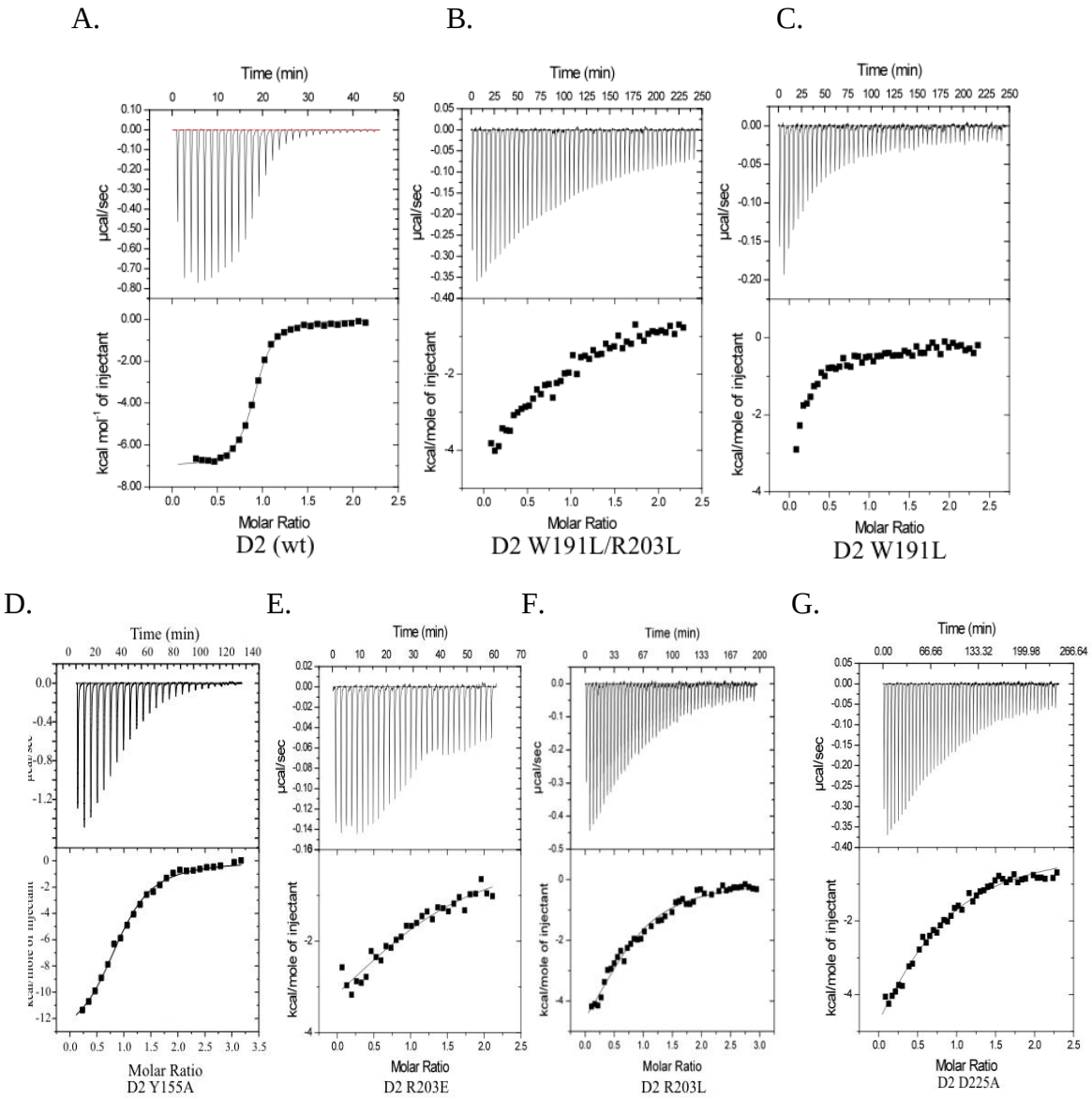


**Figure 2.7** - shows the isothermal titrations of each of the mutants of D2 with SOS. The raw data was fitted to a one-site binding model. The lower panel depicts the raw data of the µmol/s of heat release at various molar ratios of the lipid to protein. The binding affinity of D2 (wt) vs. SOS shows a moderate affinity ($K_D$ ~ 2.2 uM). The mutants showing the largest decreases in binding affinity to SOS include W191L/R203L ($K_D$ ~ 38 uM), W191L ($K_D$ ~ 31 uM), R203E ($K_D$ ~ 30 uM) and R203L ($K_D$ ~ 33. uM). Minor decreases in binding affinity were determined for mutants D2 Y155A ($K_D$ ~ 4 uM) and D2 D225A ($K_D$ ~ 3. uM).

mutant is not significantly affected ($K_d$ ~ 4µM, Table-2). These results indicate that the mutation

A.

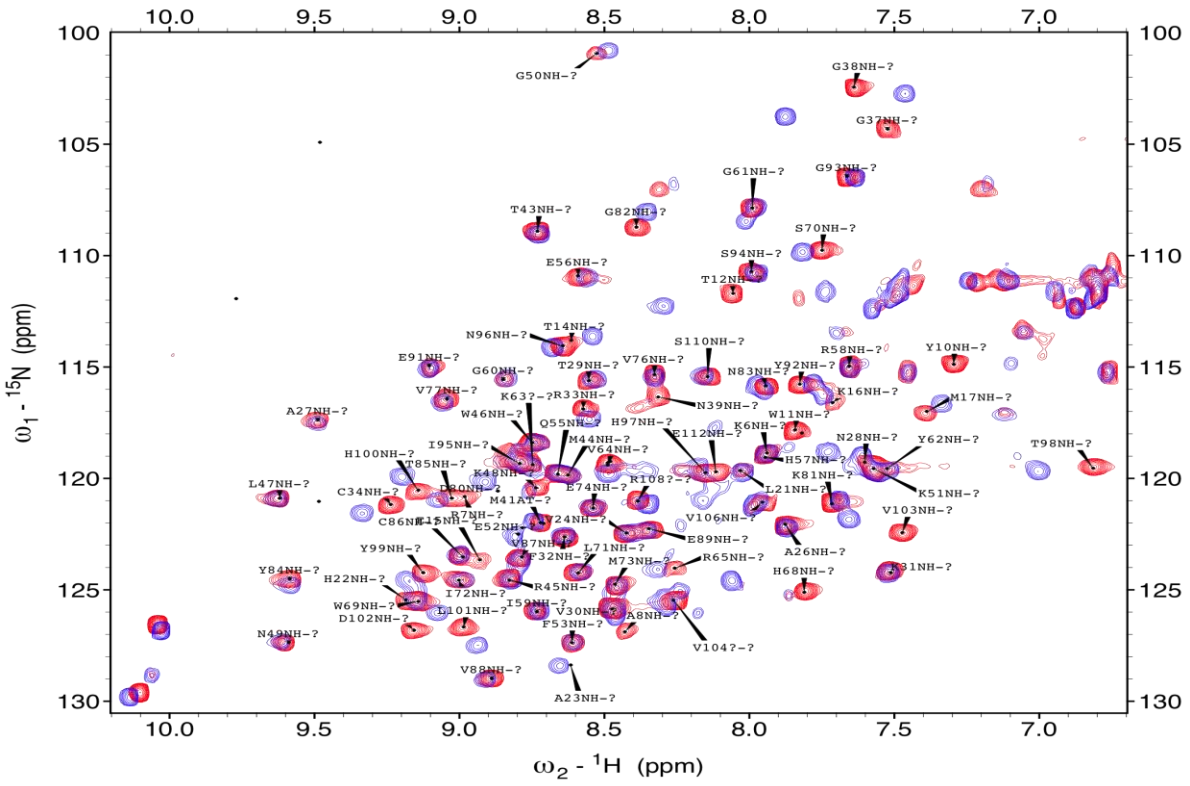


B.

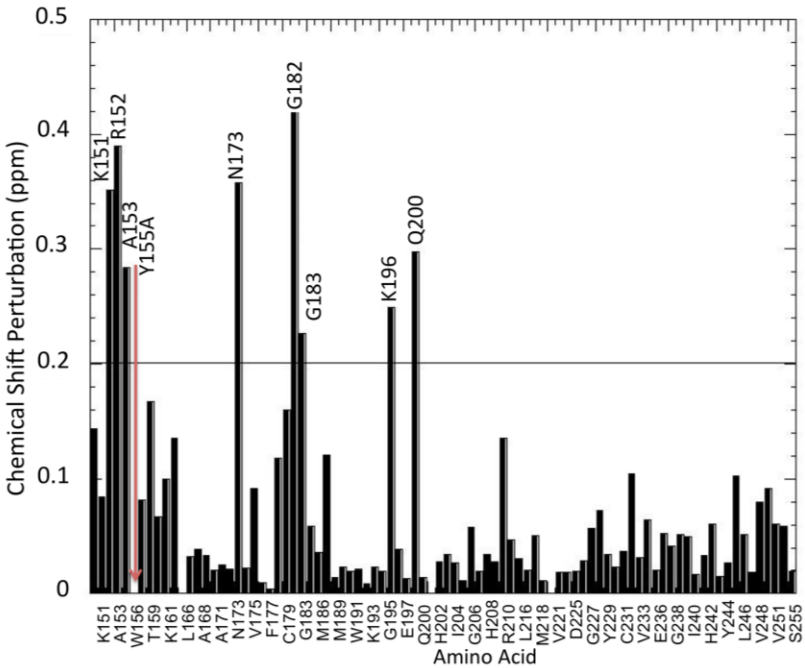


C.

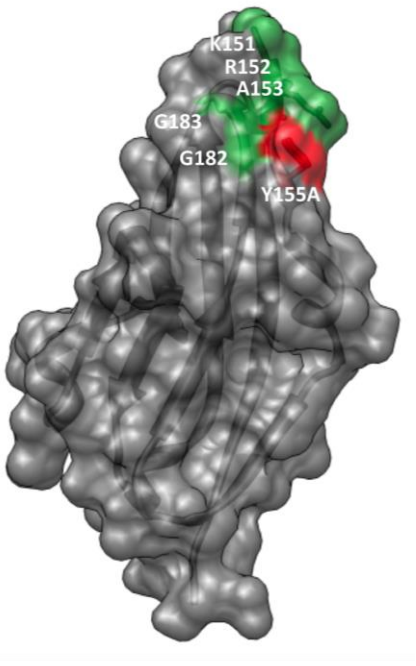


**Figure 2.8 – Panel A –** shows the $^{1}H$-$^{15}N$ HSQC of the D2 Y155A mutant of D2 (blue) overlaid on wild type D2 (red). **Panel B** – is the chemical shift perturbation plot for D2 Y155A. **Panel C** - is a structural representation highlighting the most perturbed residues on the D2 Y155A domain.
**A.**

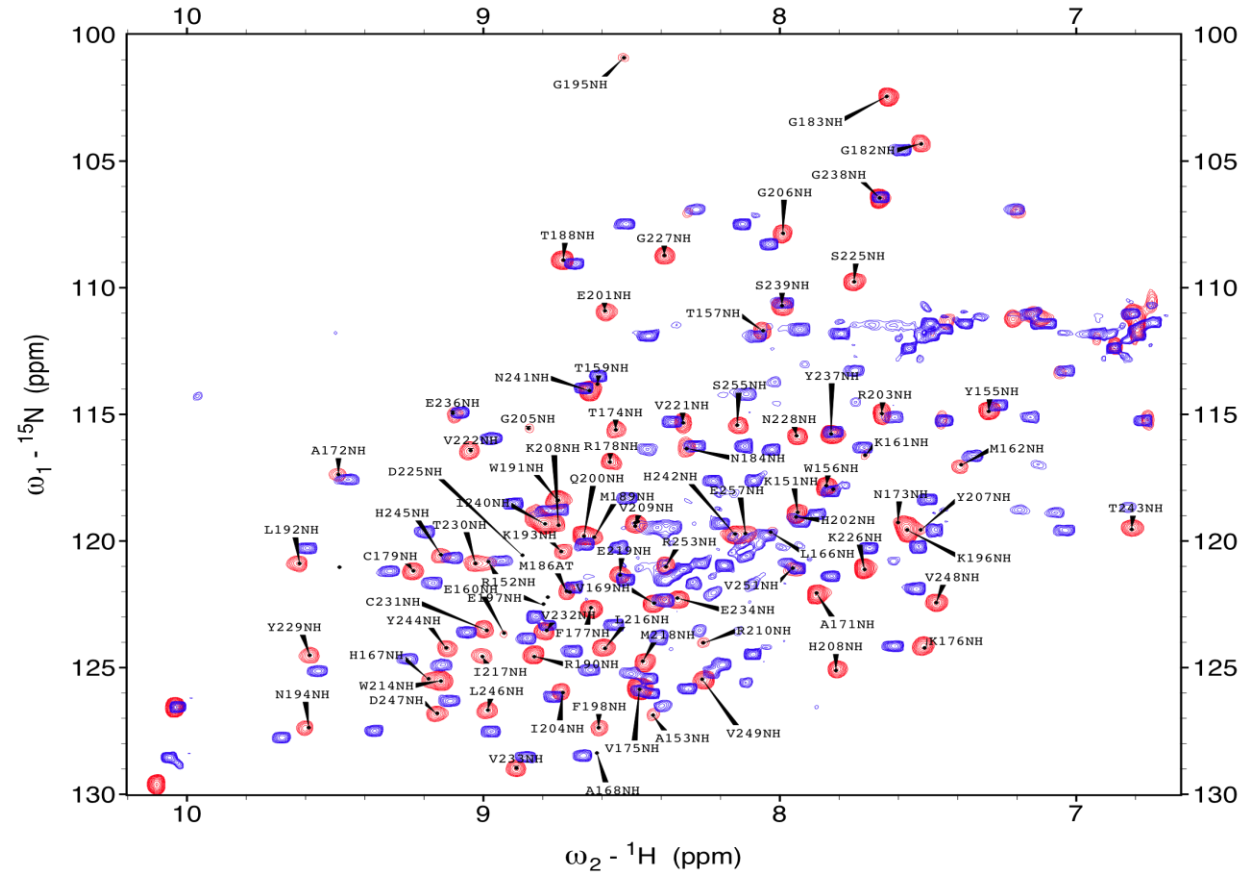


**B.** **C.**

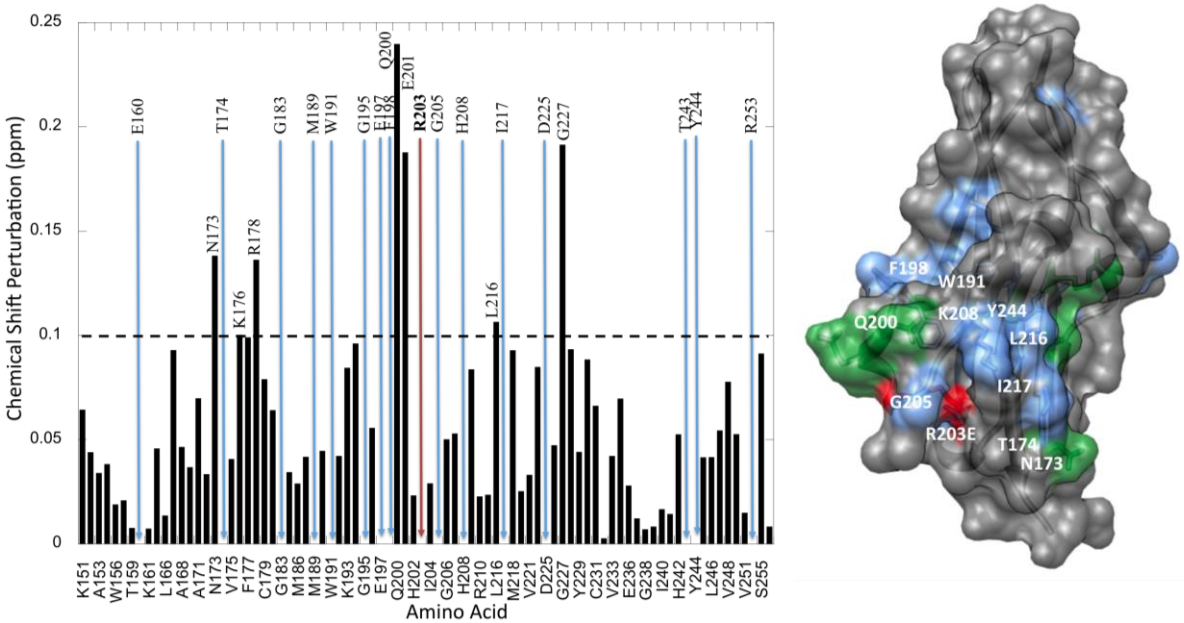


**Figure 2.9 – Panel A –** shows the $^{1}H$-$^{15}N$ HSQC of the D2 R203E mutant of D2 (blue) overlaid on wild type D2 (red). **Panel B** – is the chemical shift perturbation plot for D2 R203E. **Panel C** - is a structural representation highlighting the most perturbed residues on the D2 R203E domain.

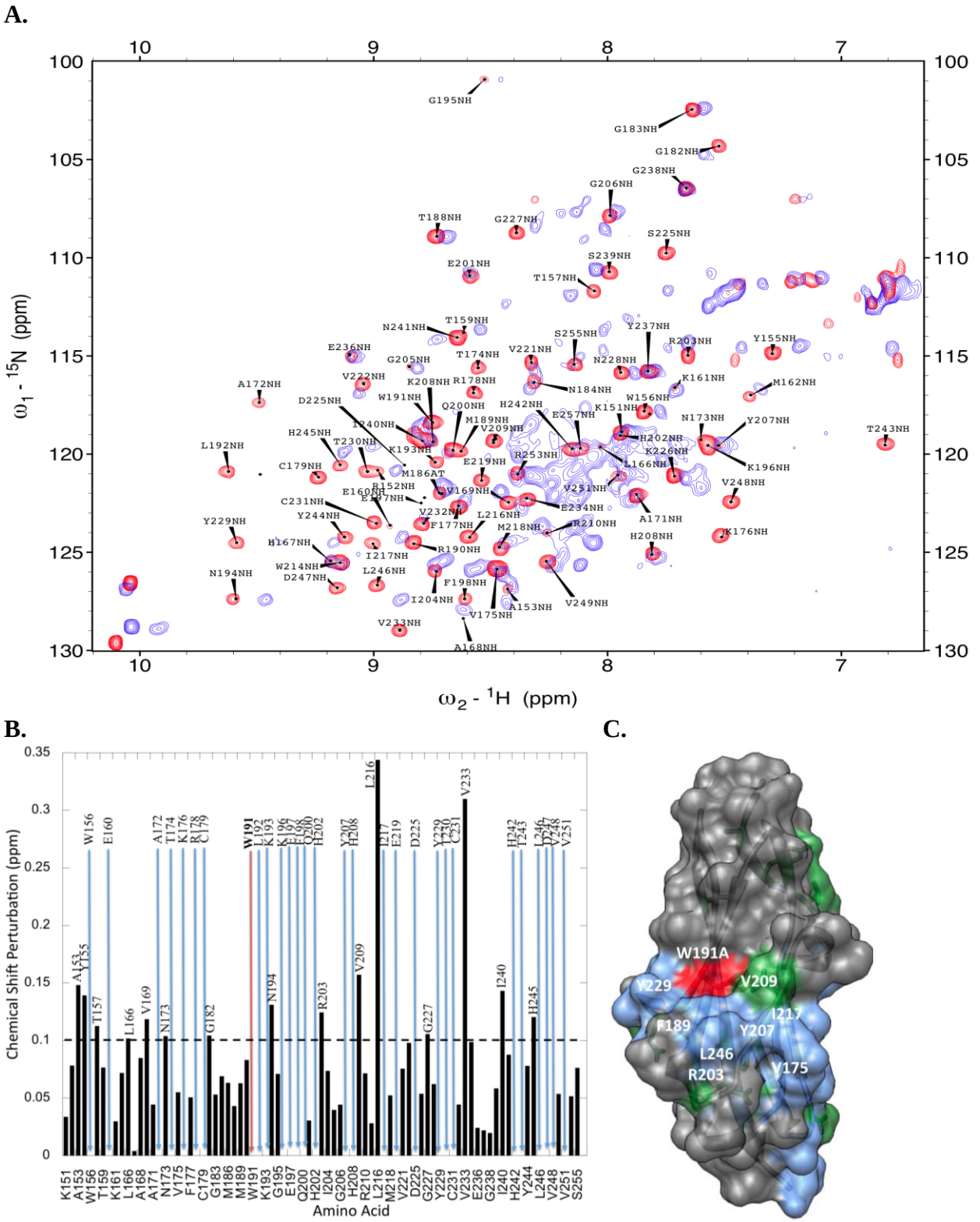


**Figure 2.10 – Panel A –** shows the $^{1}H$-$^{15}N$ HSQC of the D2 R203E mutant of D2 (blue) overlaid on wild type D2 (red). **Panel B** – is the chemical shift perturbation plot for D2 R203E. **Panel C -** is a structural representation highlighting the most perturbed residues on the D2 R203E domain.

(Y155A) potentially affecting the stability of the K151-Y155 cation-π interaction, predicted in the crystal structures, does not affect heparin-binding affinity of the D2 domain.

***Disruption of the Trp191-Arg203 interaction causes significant $^{1}$H-$^{15}$N chemical shift perturbation***: Two-dimensional $^{1}$H-$^{15}$N **h**eteronuclear **s**pin **q**uantum **c**oherence ($^{1}$H-$^{15}$N HSQC) is a finger-print of the backbone conformation of a protein. Each $^{1}$H-$^{15}$N crosspeak in the HSQC spectrum represents an amino acid in a particular backbone conformation of a protein. Therefore, $^{1}$H-$^{15}$N chemical shift perturbation provides atomic level information on the backbone structural changes that occur in a protein due to mutation or ligand binding. In this context, we monitored the potential conformational changes, which plausibly occur due to the disruption of the predicted cation-π interactions. $^{1}$H-$^{15}$N crosspeaks in the HSQC spectrum of the wild type D2 domain are spread-out suggesting that the protein is well structured (**Figure-2.8, Panel-A**). Overlay of the HSQC spectra of the Tyr155Ala mutant on that of the wild D2 domain suggests that most $^{1}$H-$^{15}$N chemical shift perturbed residues are located in close spatial vicinity of the mutation site. The most perturbed residues (R152, A153, G182, G183 and T157) are located in beta-strands A and B. These results suggest that disruption of the Arg152-Tyr155 cation-π interaction, predicted in the crystal structures of the D2 domain, does not result in a global structural change(s).

It is important to understand the cause of the significant loss ($\Delta T_m$~ 10°C) in the thermodynamic stability of the Tyr1551Ala mutant as observed from the DSC data (Figure-2.6). 3D crystal structures of the D2 domain show that Tyr155 is involved in a pi-pi stacking interaction with Trp156. Therefore, substitution of Tyr with Ala (as in the Tyr155Ala mutation) appears to weaken the pi-pi stacking interaction resulting in a significant loss in the thermodynamic

stability of the protein. Based on the DSC and HSQC data obtained on Tyr155Ala and Arg152Glu it appears that the cation-π interaction predicted in the crystal structures of the D2 domain is either non-existent in solution or its presence makes no significant contribution to the structural stability of the protein domain.

Overlay of the $^{1}H$-$^{15}N$ HSQC spectrum of the Trp191Ala on that of the wild type D2 domain shows that several crosspeaks in the HSQC spectrum of the Trp191Ala mutant have shifted significantly from their orginal position. Therefore, owing to large chemical shifts we could not completely assign all the $^{1}H$-$^{15}N$ crosspeaks in the HSQC spectrum of the Trp191Ala mutant. In addition, some regions are severely overlapped suggesting that the conformational flexibility of certain portion(s) of the D2 domain are increased due to the mutation. In addition, the Trp191Ala mutation appears to cause a mild conformational heterogeneity in D2 domain. This is obvious from the presence of two/multiple sets of $^{1}H$-$^{15}N$ crosspeaks ($^{15}N$ chemical shift range from 127 ppm to 130 ppm & $^{1}H$ chemical shift range from 9.75 ppm to 10.25 ppm) in the HSQC spectrum (Figure-2.8, Panel-C). These results are consistent those of steady state flurescence, ANS binding and DSC experiments and support the prediction of the presence of a cation – π interaction in the D2 domain involving Trp191 and Arg203.

Superimposition of the $^{1}H$-$^{15}N$ HSQC spectra of the Arg203Glu mutant and the wild type D2 domain show that disruption of the predicted Trp191-Arg203 cation-π interaction causes a significant change in the backbone folding of the protein (Figure-2.8, Panel-D). Despite the prominent shift of the $^{1}H$-$^{15}N$ crosspeaks, the HSQC spectrum appears well-dispersed. These results suggest that the Arg203Glu mutation does not disorganize the native β-sandwich architecture of the D2 domain. The conclusions drawn from the NMR data are in good agreement with those obtained from other biophysical experiments.

***Significance of the predicted cation-π interactions in solution***: The results of this study overwhelmingly support the presence of the Trp191-Arg203 cation-π interaction present in the solution structures but not the one predicted in the crystal structures between Arg152 and Tyr155. The experimental evidence against the presence of the Arg152-Tyr155 cation-π interaction could imply, 1. The predicted Arg152-Tyr155 is non-existent under solution conditions and its existence is an artifact of the crystallization conditions used, 2. the predicted cation-pi interaction, even if present, does not contribute significantly to the stability of the protein or 3. the cation-pi interaction is only induced when the D2 domain interacts with its ligands (FGF/heparin), or it is only formed in the dimeric state of D2 domain. The latter two possibilities are relevant because, in all the crystal structures, of FGFR (pdb code – 1EV2 )/FGFR-heparin binary complex (pdb code - 1EV2) the D2 domain is present with along with the other extracellular domain (D3 domain) and exists as a dimer with direct structural contacts between the D2 domains. In marked contrast the lone NMR solution structure reported of the isolated D2 domain is a monomer. The solution structure of the FGF signaling complex is not yet available. However, the results of this study clearly support the presence of the Trp191-Arg203 cation-π interaction in the D2 domain under solution conditions. In addition, this cation-π interaction appears to confer thermodynamic stability to the D2 domain and also affects the heparin binding affinity of the protein domain.

**Supplementary data:**

A.

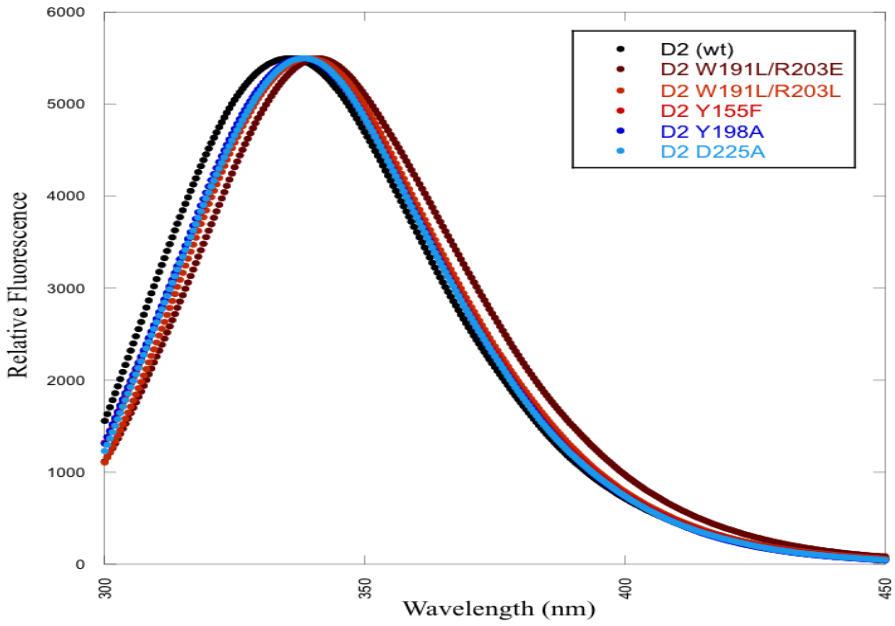


B.

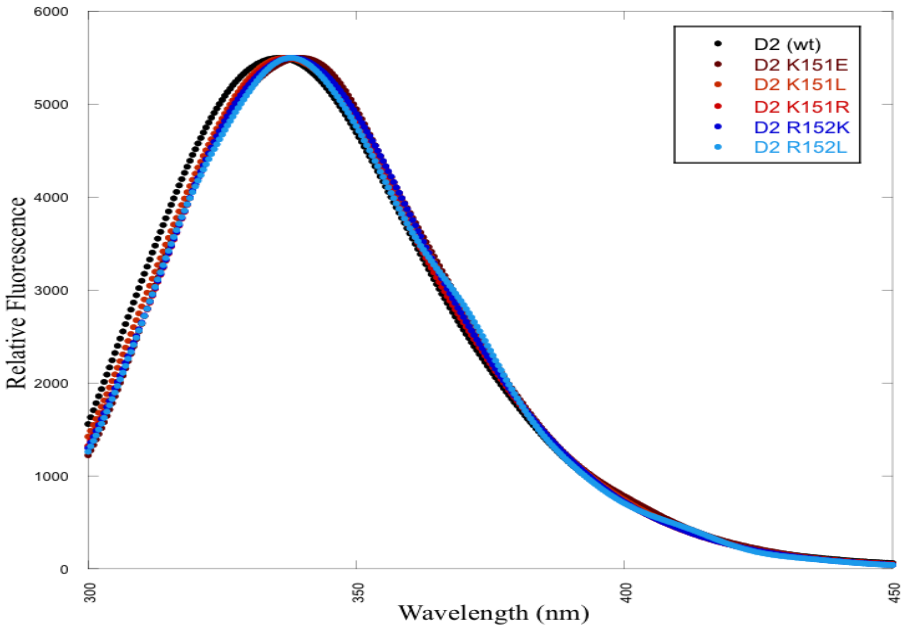


**Figure S2.11 – Panel A and B** show the relative steady-state fluorescence of mutants of D2. Each of the mutants showed very minor shifts in the maximum wavelength. Most mutants exhibit 1-3 nm red shift in maximum wavelength.

A.

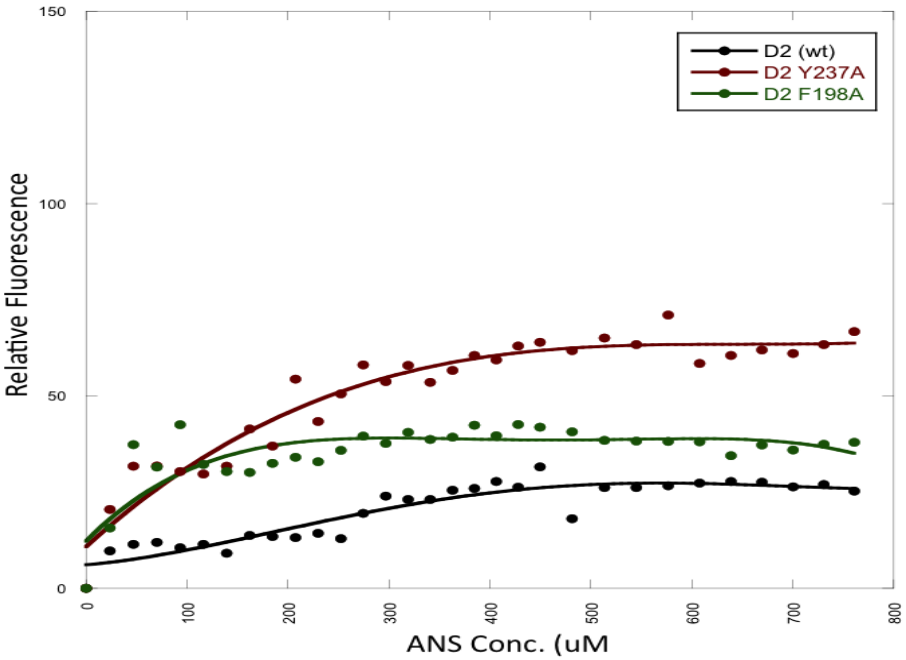


B.

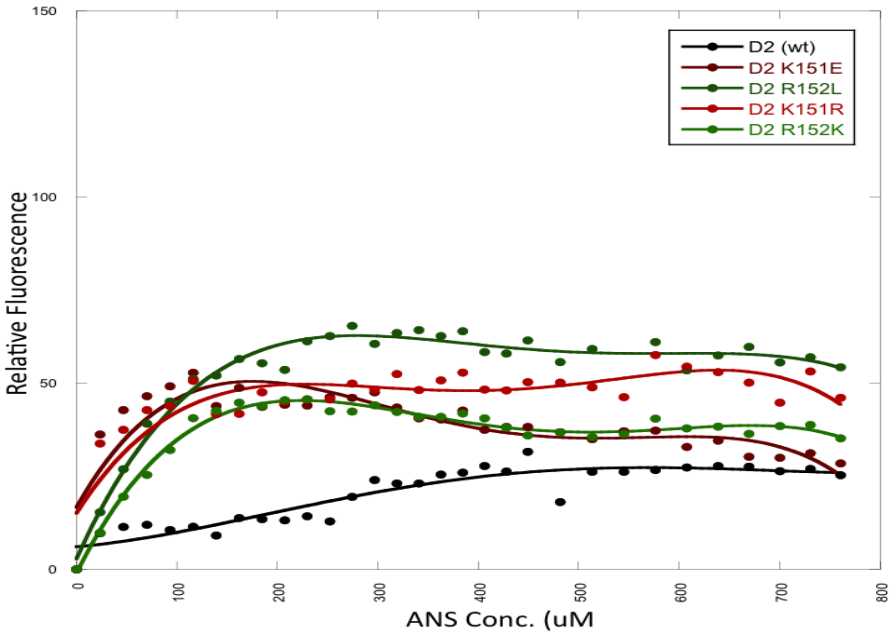


**Figure S2.12** – **Panels A and B** show mutants ANS titration of mutants of D2. The relative fluorescence of the mutants of D2 shown suggests only minor increases in hydrophobic residue exposure.

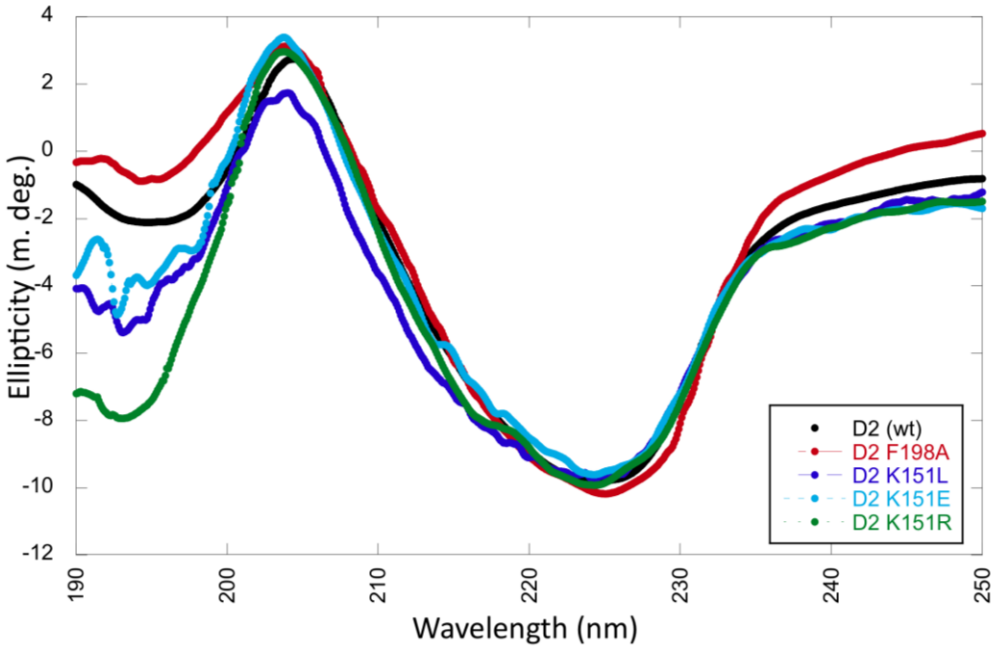


**Figure S2.13 -** Overlay of the far-UV circular dichroism spectra of the wild type (black) and mutants of D2.

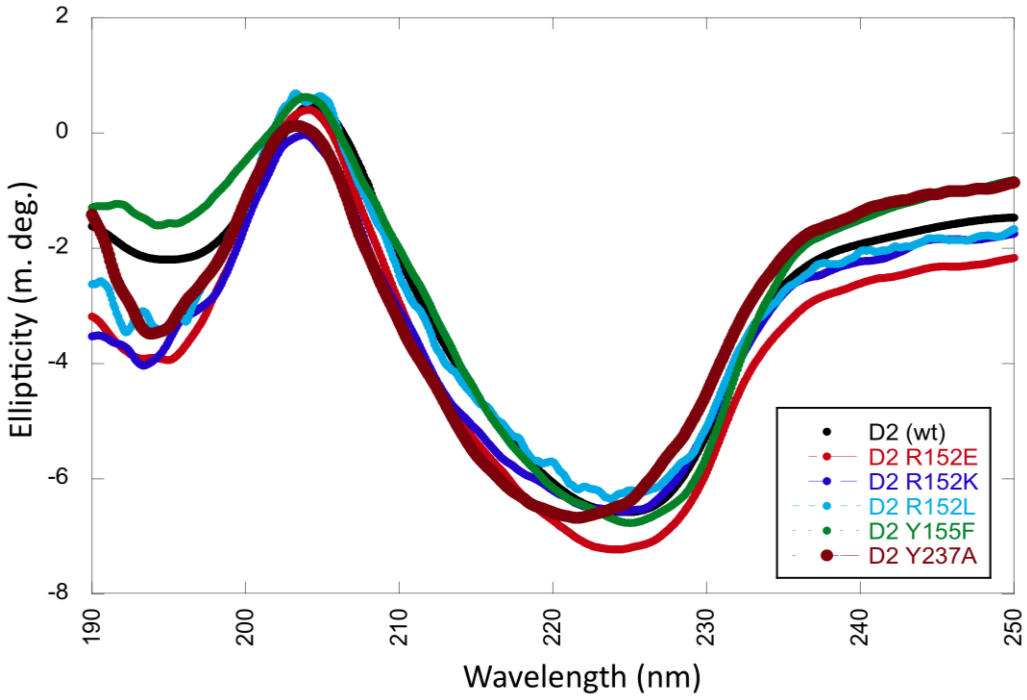


**Figure S2.14 -** Overlay of the far-UV circular dichroism spectra of the wild type (black) and mutants of D2.

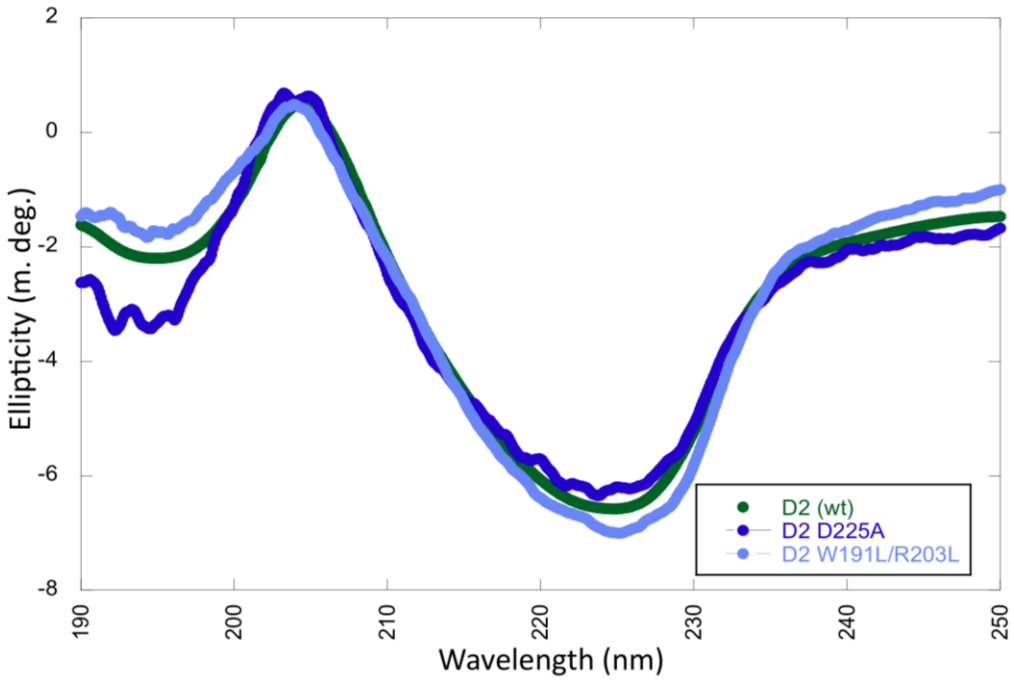


**Figure S2.15 -** Overlay of the far-UV circular dichroism spectra of the wild type (black) and mutants of D2.

**Literature Cited**


1.Gruber, K., B. Zhou, K.N. Houk, R.A. Lerner, C.G. Shevlin and I.A. Wilson 1999. Structural basis for antibody catalysis of a disfavored ring closure reaction. Biochemistry (N. Y. ). 38, 7062-7074.

2. Garau, C., A. Frontera, D. Quionero, P. Ballester, A. Costa and P.M. Dey 2004. Cation-π versus anion-π interactions: energetic, charge transfer, and aromatic aspects. The Journal of Physical Chemistry A. 108, 9423-9427.

3. Gallivan J.P., D. D. A. 1999. Cation-pi interactions in structural biology. Proc. Nat'l Acad Sci USA. 96, 9459-9464.

4. Russell, S.J. and Cochran, A.G. 2002. Designing stable beta-hairpins: Energetic contributions from cross-strand residues. J. Am. Chem. Soc., 12600-12601.

5. Burghardt, T. P., N. Juranic, S. Macura and K. Ajtai 2002. Cation-pi interaction in a folded polypeptide. Biopolymers. 63, 261-272.

6. Gustiananda, M., J.R. Liggins, P.L. Cummins and J.E. Gready 2004. Conformation of prion protein repeat peptides probed by FRET measurements and molecular dynamics simulations. Biophys. J. 86, 2467-2483.

7. Andersen, N. H., K.A. Olsen, R.M. Fesinmeyer, X. Tan, F.M. Hudson, L.A. Eidenschink and S.R. Farazi 2006. Minimization and optimization of designed beta-hairpin folds. J. Am. Chem. Soc. 128, 6101-6110.

8. Barbaras, D. and K. Gademann 2008. Stable beta turns of tripeptides in water through cation-pi interactions. Chem. biochem. 9, 2398-2401.

9. Zheng, X., C. Wu, J.W. Ponder and G.R. Marshall 2012. Molecular dynamics of beta-hairpin models of epigenetic recognition motifs. J. Am. Chem. Soc. 134, 15970-15978.

10. Pan, J., Q. Chen, D. Willenbring, K. Yoshida, T. Tillman, O.B. Kashlan, A. Cohen, X.P. Kong, Y. Xu and P. Tang 2012. Structure of the pentameric ligand-gated ion channel ELIC cocrystallized with its competitive antagonist acetylcholine. Nat. Commun. 3, 714.

11. Kombo, D. C., A. Mazurov, K. Tallapragada, P.S. Hammond, J. Chewning, T.A. Hauser, M. Vasquez-Valdivieso, D. Yohannes, T.T. Talley, P. Taylor and W.S. Caldwell 2011. Docking studies of benzylidene anabaseine interactions with alpha7 nicotinic acetylcholine receptor (nAChR) and acetylcholine binding proteins (AChBPs): Application to the design of related alpha7 selective ligands. Eur. J. Med. Chem. 46, 5625-5635.

12. Blum, A. P., H.A. Lester and D.A. Dougherty 2010. Nicotinic pharmacophore: The pyridine N of nicotine and carbonyl of acetylcholine hydrogen bond across a subunit interface to a backbone NH. Proc. Natl. Acad. Sci. U. S. A. 107, 13206-13211.

13. Tantama, M. and S. Licht 2009. Functional equivalence of the nicotinic acetylcholine receptor transmitter binding sites in the open state. Biochim. Biophys. Acta. 1788, 936-944.

14. Tantama, M. and S. Licht 2008. Use of calculated cation-pi binding energies to predict relative strengths of nicotinic acetylcholine receptor agonists. ACS Chem. Biol. 3, 693-702.

15. Tantama, M., W.C. Lin and S. Licht 2008. An activity-based protein profiling probe for the nicotinic acetylcholine receptor. J. Am. Chem. Soc. 130, 15766-15767.

16. Rana, S., B. Kundu and S. Durani 2007. A mixed-alpha,beta miniprotein stereochemically reprogrammed to high-binding affinity for acetylcholine. Biopolymers. 87, 231-243.

17. Artursson, E., P.O. Andersson, C. Akfur, A. Linusson, S. Borjegren and F. Ekstrom 2013. Catalytic-site conformational equilibrium in nerve-agent adducts of acetylcholinesterase: Possible implications for the HI-6 antidote substrate specificity. Biochem. Pharmacol. 85, 1389-1397.

18. McMenimen, K. A., D.A. Dougherty, H.A. Lester and E.J. Petersson 2006. Probing the Mg2+ blockade site of an N-methyl-D-aspartate (NMDA) receptor with unnatural amino acid mutagenesis. ACS Chem. Biol. 1, 227-234.

19. Petraglio, G., M. Bartolini, D. Branduardi, V. Andrisano, M. Recanatini, F.L. Gervasio, A. Cavalli and M. Parrinello 2008. The role of li+, na+, and K+ in the ligand binding inside the human acetylcholinesterase gorge. Proteins. 70, 779-785.

20. Samson, A., T. Scherf, M. Eisenstein, J. Chill and J. Anglister 2002. The mechanism for acetylcholine receptor inhibition by alpha-neurotoxins and species-specific resistance to alpha-bungarotoxin revealed by NMR. Neuron. 35, 319-332.

21. Gromiha, M. M., S. Thomas and C. Santhosh 2002. Role of cation-pi interactions to the stability of thermophilic proteins. Prep. Biochem. Biotechnol. 32, 355-362.

22. Chakravarty, S. and R. Varadarajan 2002. Elucidation of factors responsible for enhanced thermal stability of proteins: A structural genomics based study. Biochemistry. 41, 8152-8161.

23. Syud, F.A., Stanger, H.E., and Gellman, S.H. 2001. Interstrand side chain–side chain interactions in a designed beta-hairpin: Significance of both lateral and diagonal pairings. J. Amer. Chem. Soc., 8667-8677.

24. Fisk, J.D., Powell, D.R., and Gellman, S.H. 2000. Control of hairpin formation via proline configuration in parallel beta-sheet model systems. J. Am. Chem. Soc., 5443-5447.

25. Distefano, M.D., Zhong, A., and Cochran, A.G. 2002. J. Mol. Biol., 179-188.

26. Rao, J. S. and G.N. Sastry 2009. Structural and energetic preferences of bidentate cation binding (Li+, Na+, and Mg2+) to aromatic amines (phCH2)NH2, n = 2âˆ’5): A theoretical study. The Journal of Physical Chemistry A. 113, 5446-5454.

27. Liu, T., J. Gu, X. Tan, W. Zhu, X. Luo, H. Jiang, R. Ji, K. Chen, I. Silman and J.L. Sussman 2001. Theoretical insight into the interactions of TMA-benzene and TMA-pyrrole with B3LYP density-functional theory (DFT) and ab initio second order M Plesset perturbation theory (MP2) calculations. The Journal of Physical Chemistry A. 105, 5431-5437.

28. Kar, T., R. Ponec and A.B. Sannigrahi 2001. Electronic structure, stability, and nature of bonding of the complexes of C2H2 and C2H4 with H+, li+, and na+ ions. extensive ab initio and density functional study. The Journal of Physical Chemistry A. 105, 7737-7744.

29. Priyakumar, U. D., M. Punnagai, G.P. Krishna Mohan and G.N. Sastry 2004. A computational study of cation–π interactions in polycyclic systems: Exploring the dependence on the curvature and electronic factors. Tetrahedron. 60, 3037-3043.

30. Chourasia, M., G.M. Sastry and G.N. Sastry 2011. Aromatic-aromatic interactions database, A(2)ID: An analysis of aromatic pi-networks in proteins. Int. J. Biol. Macromol. 48, 540-552.

31. Moreno, D. V., S.A. Gonzalez and A. Reyes 2010. Secondary hydrogen isotope effects on the structure and stability of cation-π complexes (cation = Li+, Na+, K+ and Ï€ = acetylene, ethylene, benzene). The Journal of Physical Chemistry A. 114, 9231-9236.

32. Wei, Y., G.N. Sastry and H. Zipse 2008. Methyl cation affinities of commonly used organocatalysts. J. Am. Chem. Soc. 130, 3473-3477.

33. Tsuzuki, S., M. Mikami and S. Yamada 2007. Origin of attraction, magnitude, and directionality of interactions in benzene complexes with pyridinium cations. J. Am. Chem. Soc. 129, 8656-8662.

34. Priyakumar, U. D. and G.N. Sastry 2000. Structures, energetics, relative stabilities, and out-of-plane distortivities of skeletally disubstituted benzenes, (CH)4X2 (X = N, P, C-, si-, O+, and S+): an ab initio and DFT study. J. Am. Chem. Soc. 122, 11173-11181.

35. Duan, M., B. Song, G. Shi, H. Li, G. Ji, J. Hu, X. Chen and H. Fang 2012. CationâŠ—3Ï€: Cooperative interaction of a cation and three benzenes with an anomalous order in binding energy. J. Am. Chem. Soc. 134, 12104-12109.

36. Watt, M., J. Hwang, K.W. Cormier and M. Lewis 2009. Preference for Na+ binding over Na+ Dipole binding in Na+ Arene interactions. The Journal of Physical Chemistry A. 113, 6192-6196.

37. Liu, T., J. Gu, X. Tan, W. Zhu, X. Luo, H. Jiang, R. Ji, K. Chen, I. Silman and J.L. Sussman 2002. The relationship between binding models of TMA with furan and imidazole and the

molecular electrostatic potentials: DFT and MP2 computational studies. The Journal of Physical Chemistry A. 106, 157-164.

38. Berry, B. W., M.M. Elvekrog and C. Tommos 2007. Environmental modulation of protein cation-pi interactions. J. Am. Chem. Soc. 129, 5308-5309.

39. Larrucea, J., E. Rezabal, T. Marino, N. Russo and J.M. Ugalde 2010. Ab initio study of microsolvated Al3+-aromatic amino acid complexes. J Phys Chem B. 114, 9017-9022.

40. Gilis, D., C. Biot, E. Buisine, Y. Dehouck and M. Rooman 2006. Development of novel statistical potentials describing cation-pi interactions in proteins and comparison with semiempirical and quantum chemistry approaches. J. Chem. Inf. Model. 46, 884-893.

41. Berry, B. W., M.M. Elvekrog and C. Tommos 2007. Environmental modulation of protein cation-pi interactions. J. Am. Chem. Soc. 129, 5308-5309.

42. Remko, M. and S. Soralova 2012. Effect of water coordination on competition between pi and non-pi cation binding sites in aromatic amino acids: L-phenylalanine, L-tyrosine, and L-tryptophan li+, na +, and K+ complexes. J. Biol. Inorg. Chem. 17, 621-630.

43. Capp, M. W., L.M. Pegram, R.M. Saecker, M. Kratz, D. Riccardi, T. Wendorff, J.G. Cannon and M.T. Record Jr 2009. Interactions of the osmolyte glycine betaine with molecular surfaces in water: Thermodynamics, structural interpretation, and prediction of m-values. Biochemistry. 48, 10372-10379.

44. Ornitz, D. M. 2005. FGF signaling in the developing endochondral skeleton. Cytokine Growth Factor Rev. 16, 205-213.

45. Thisse, B. and C. Thisse 2005. Functions and regulations of fibroblast growth factor signaling during embryonic development. Dev. Biol. 287, 390-402.

46. Thisse, B. and C. Thisse 2005. Functions and regulations of fibroblast growth factor signaling during embryonic development. Dev. Biol. 287, 390-402.

47. Itoh, N. 2007. The fgf families in humans, mice, and zebrafish: Their evolutional processes and roles in development, metabolism, and disease. Biol. Pharm. Bull. 30, 1819-1825.

48. Itoh, N., R. Linhardt and M. Mohammadi 2004. Biochemical analysis of pathogenic ligand-dependent FGFR2 mutations suggests distinct pathophysiological mechanisms for craniofacial and limb abnormalities. Human Molecular Genet. 13(19) 2313-2324.

49. Itoh, N. and D.M. Ornitz 2004. Evolution of the fgf and fgfr gene families. TRENDS in Genetics., 1-7.

50. Baird, K., S. Davis, C.R. Antonescu, U.L. Harper, R.L. Walker, Y. Chen, A.A. Glatfelter, P.H. Duray and P.S. Meltzer 2005. Gene expression profiling of human sarcomas: Insights into sarcoma biology. Cancer Res. 65, 9226-9235.

51. Furdui, C. M., E.D. Lew, J. Schlessinger and K.S. Anderson 2006. Autophosphorylation of FGFR1 kinase is mediated by a sequential and precisely ordered reaction. Mol. Cell. 21, 711-717.

52. Mohammadi, M., I. Dikic, A. Sorokin, W.H. Burgess, M. Jaye and J. Schlessinger 1996. Identification of six novel autophosphorylation sites on fibroblast growth factor receptor 1 and elucidation of their importance in receptor activation and signal transduction. Mol. Cell. Biol. 16, 977-989.

53. Schlessinger J, Plotnikov AN, Ibrahimi OA, Eliseenkova AV, Yeh BK, Yayon A, Linhardt RJ and Mohammadi M 2000. Crystal structure of a ternary FGF-FGFr-heparin complex reveals a dual role for heparin in FGFr bindin and dimerization. Mol Cell. 6, 743-750.

54. Gallivan, J.P., and Dougherty, D.A. 1999. Cation-pi interactions in structural biology. Proc. Natl. Acad. Sci. U. S. A. 96, 9459-9464.

55. Crowley, P. and A. Golovin 2005. Cation--interactions in protein--protein interfaces. PROTEINS: Structure.

56. Schlessinger, J., A.N. Plotnikov, O.A. Ibrahimi, A.V. Eliseenkova, B.K. Yeh, A. Yayon, R.J. Linhardt and M. Mohammadi 2000. Crystal structure of a ternary FGF-FGFR-heparin complex reveals a dual role for heparin in FGFR binding and dimerization. Mol. Cell. 6, 743-750.

57. Stauber, D. J., A.D. DiGabriele and W.A. Hendrickson 2000. Structural interactions of fibroblast growth factor receptor with its ligands. Proc. Natl. Acad. Sci. U. S. A. 97, 49-54.

58. Pellegrini, L., D.F. Burke, F. von Delft, B. Mulloy and T.L. Blundell 2000. Crystal structure of fibroblast growth factor receptor ectodomain bound to ligand and heparin. Nature. 407, 1029-1034.

59. Plotnikov, A.N., Hubbard, S.R., Schlessinger, J., Mohammadi, M. 2000. Crystal structure of FGF2 in complex with the extracellular lignad binding domain of FGF receptor 2 (FGFR2). Cell. 101, 413-424.

60. Hung KW, Kumar TK, Kathir KM, Xu P, Ni F, Ji HH, Chen MC, Yang CC, Lin FP, Chiu IM, Yu C. 2005. Solution structure of the ligand binding domain of the fibroblast growth factor receptor: Role of heparin in the activation of the receptor. Biochemistry., 15787-15798.

61. Adler, A. J., N.J. Greenfield and G.D. Fasman 1973. Circular dichroism and optical rotatory dispersion of proteins and polypeptides. Methods Enzymol. 27, 675-735.

62. Fontana, A., P.P. de Laureto, B. Spolaore, E. Frare, P. Picotti and M. Zambonin 2004. Probing protein structure by limited proteolysis. Acta Biochim. Pol. 51, 299-321.

63. Fontana, A., P. Polverino de Laureto, V. De Filippis, E. Scaramella and M. Zambonin 1997. Probing the partly folded states of proteins by limited proteolysis. Fold. Des. 2, R17-26.

64. Scholtz, J. M., S. Marqusee, R.L. Baldwin, E.J. York, J.M. Stewart, M. Santoro and D.W. Bolen 1991. Calorimetric determination of the enthalpy change for the alpha-helix to coil transition of an alanine peptide in water. Proc. Natl. Acad. Sci. U. S. A. 88, 2854-2858.

65. Taylor, J. W., N.J. Greenfield, B. Wu and P.L. Privalov 1999. A calorimetric study of the folding-unfolding of an alpha-helix with covalently closed N and C-terminal loops. J. Mol. Biol. 291, 965-976.

66. Pitteloud, N., A. Meysing, R. Quinton, J.S. Acierno Jr, A.A. Dwyer, L. Plummer, E. Fliers, P. Boepple, F. Hayes, S. Seminara, V.A. Hughes, J. Ma, P. Bouloux, M. Mohammadi and W.F. Crowley Jr 2006. Mutations in fibroblast growth factor receptor 1 cause kallmann syndrome with a wide spectrum of reproductive phenotypes. Mol. Cell. Endocrinol. 254-255, 60-69.

67. Ornitz, D. M., A. Yayon, J.G. Flanagan, C.M. Svahn, E. Levi and P. Leder 1992. Heparin is required for cell-free binding of basic fibroblast growth factor to a soluble receptor and for mitogenesis in whole cells. Mol. Cell. Biol. 12, 240-247.

68. Pantoliano, M. W., R.A. Horlick, B.A. Springer, D.E. Van Dyk, T. Tobery, D.R. Wetmore, J.D. Lear, A.T. Nahapetian, J.D. Bradley and W.P. Sisk 1994. Multivalent ligand-receptor binding interactions in the fibroblast growth factor system produce a cooperative growth factor and heparin mechanism for receptor dimerization. Biochemistry. 33, 10229-10248.

69. Pantoliano, M. W., R.A. Horlick, B.A. Springer, D.E. Van Dyk, T. Tobery, D.R. Wetmore, J.D. Lear, A.T. Nahapetian, J.D. Bradley and W.P. Sisk 1994. Multivalent ligand-receptor binding interactions in the fibroblast growth factor system produce a cooperative growth factor and heparin mechanism for receptor dimerization. Biochemistry. 33, 10229-10248.

70. Yeh, B. K., A.V. Eliseenkova, A.N. Plotnikov, D. Green, J. Pinnell, T. Polat, A. Gritli-Linde, R.J. Linhardt and M. Mohammadi 2002. Structural basis for activation of fibroblast growth factor signaling by sucrose octasulfate. Mol. Cell. Biol. 22, 7184-7192.

Appendix

UNIVERSITY OF ARKANSAS

J. William Fulbright College of Arts and Sciences
*Chemistry and Biochemistry*

**To Whomsoever it may concern**

This is to certify that Mr. Ryan Thurman is the first author of the papers mentioned below and has completed about 75% of the work reported in these papers,

1. "Cation-π Interactions Act to Stabilize FGF Receptor D2 "
2. "Molecular Basis for the Kallmann Syndrome-Linked Fibroblast Receptor Mutation A168"

Suresh K. Thallapuranam

Major Advisor

CHEM 119 • 1 University of Arkansas • Fayetteville, AR 72701-1201 • 479-575-4601 • Fax: 479-575-4049 • http://chemistry.uark.edu/

**Molecular Basis for the Kallmann Syndrome-Linked Fibroblast Growth Factor Receptor Mutation A168S**

Ryan D. Thurman,[a] Karuppanan Muthusamy Kathir[a,#], Dakshinamurthy Rajalingam[a,$] and Thallapuranam K. Suresh Kumar [a, *]

[a]*Department of Chemistry and Biochemistry, University of Arkansas, Fayetteville, AR 72701.*

*(* Corresponding author,* ***Email:*** *sthalla@uark.edu,****Tel:*** *1-479-575-5646;* ***Fax****: 1-479-575-4049)*

[#] *Present address: Regeneron Pharmaceuticals Inc., 777 Old Saw Mill River Rd. Tarrytown, NY 10591*

[$]*Present address: Department of Chemistry, University of Western Kentucky, Bowling Green, KY, 42101.*

**Abstract**: Kallmann syndrome (KS) is a developmental disease that expresses in patients as hypogonadotropic hypogonadism and anosmia. KS is commonly associated with mutations in the extracellular D2 domain of the fibroblast growth factor receptor (FGFR). In this study, for the first time, the molecular basis for the FGFR associated KS mutation (A168S) is elucidated using a variety of biophysical experiments, including multidimensional NMR spectroscopy. Secondary and tertiary structural analysis using far UV circular dichroism, fluorescence and limited trypsin digestion assays suggest that the KS mutation induces subtle tertiary structure change in the D2 domain of FGFR. Results of isothermal titration calorimetry experiments show the KS mutation causes a 10-fold decrease in heparin binding affinity and also a complete loss in ligand (FGF-1) binding. $^{1}H$-$^{15}N$ chemical perturbation data suggest that complete loss in the ligand (FGF) binding affinity is triggered by a subtle conformational change that disrupts crucial structural interactions in both the heparin and the FGF binding sites in the D2 domain of FGFR. The novel findings reported in this study are expected to provide valuable clues toward a complete understanding of the other genetic diseases linked to mutations in the FGFR.

**Introduction:** Kallmann syndrome (KS) is a form of idiopathic hypogonadotropic hypogonadism (IHH) that expresses phenotypically with anosmia (1). Most commonly, KS is expressed with synkinesia, hearing loss, labial or palentine cleft, dental anomalies and inhibited puberty development. An estimated 10% of KS cases are attributed to mutations in the fibroblast growth factor receptor 1 (FGFR1) (2).

Fibroblast growth factors (FGFs) are a family of heparin-binding proteins that regulate key cellular processes such as angiogenesis, cell differentiation, morphogenesis, wound healing and

tumor growth (3-10). FGF receptors consist of three extracellular ligand-binding domains (D1, D2, and D3), a single transmembrane helix, and a cytoplasmic tyrosine kinase domain. Cell surface-bound heparan sulfate proteoglycans (HSPGs) that support dimerization or oligomerization of the FGF receptors (FGFRs) are believed to be required for the activation of the FGF signaling pathway (11, 12). The FGF signaling is shown to be modulated by anosmin-1, a KAL-1 gene product underlying X-linked KS. (13). Anosmin-1 is a 680-amino acid glycoslylated protein, which directly binds to HSPG and FGFR and regulates the assembly and activity of the FGF signaling complex (13-16).

The extracellular D2 domain of FGFRs is suggested to bind with both HSPGs and FGFs to form a ternary FGF signaling complex. Mutations in the D2 domain of FGFR1 have been associated with families carrying Kallmann syndrome phenotypes (17). The A168S mutation in the D2 domain of FGFR is one of the common KS mutations. Knockout mutational studies in mice have established A168S as a loss-of-function mutation resulting in the inactivation of FGFR. Inactivation of FGFR in mice telencephalon tissue results in the failure of olfactory bulb formation- a phenotype manifestation commonly observed in KS (17). The molecular basis for the observed loss-of-function associated with KS mutations is still unclear. It is believed that KS mutations either disrupt the anosmin-1/FGFR interaction(s) or cause a drastic structural change in FGFR leading to loss in the binding affinity to the ligand (FGF) (17). However, very little experimental evidence exists in support or in contradiction of this proposal. In this study for the first time the structural basis for the A168S associated KS is elucidated. The results of the present study are expected to trigger intensive studies leading to a comprehensive understanding of the molecular mechanism underlying the different FGFR mutation related diseases.

**Materials and Methods**

***Mutagenesis, overexpression and protein purification:*** The A168S mutation on the FGFR2 D2 domain (residues, 145-255) was generated using the *Quikchange* kit (Stratagene). The mutation was confirmed by automated DNA sequencing. Wild type and the A168S mutant of the D2 domain were overexpressed and purified from *Escherichia coli* [BL21 (pLysS) strain] according to the method reported previously [18].

***Far UV Circular Dichrosim (CD):*** Data on the wild type D2 and the A168S mutant were acquired using a Jasco J-710 spectropolarimeter. Protein solutions (90-100 μM) were prepared in 10 mM phosphate buffer containing 100 mM NaCl and 50 mM ammonium sulfate (pH 6.5). Wavelength scans were set to 250-190 nm. CD measurements were made using a 0.1 cm pathlength cuvette. A total of 10 scans were averaged for each sample.

***Fluorescence spectroscopy:*** Measurements were made using a Hitachi F-2500 fluorimeter. Fluorescence measurements were made using a 1.0 cm path length and the concentration of each protein sample was adjusted to ~50 μM. Excitation wavelength was set to 280 nm and intrinsic tryptophan emission was measured from 300 nm to 450 nm. 8-anilino-1-napthalene sulphonate (ANS) binding experiments were performed using an excitation wavelength of 390 nm and an emission wavelength range of 450 nm - 600 nm. In the ANS titration experiments, protein samples were titrated with 3 μl aliquots of 10 mM ANS in 10 mM phosphate buffer containing 100 mM NaCl and 50 mM ammonium sulfate at pH 6.5.

***Differential scanning calorimetry (DSC):*** DSC measurements were performed using a N-DSC III calorimeter. Protein concentration used was in the range of 1.0 – 1.5 mg/ml in 10 mM phosphate buffer containing 50 mM ammonium sulfate and 100 mM NaCl (pH ~6.5). The scan

rate was set to 1 °C/min and protein samples were heated from 10 °C - 90°C. Data were analyzed using the CpCalc software provided by the manufacturer.

***Isothermal titration caolorimetry (ITC):*** ITC measurements were performed using Microcal VP titration calorimeter (Northhampton, MA, USA). Titrations consisted of 5-10 µl injections of 0.5 mM sucrose octasulfate (a heparin analog) delivered into 0.050 mM concentration of the D2 domain. Injections were delayed for 1.5 - 3.5 minutes to allow the titration peak to return to the baseline prior to additional injections. The titrations curves were analyzed using Origin software supplied by Microcal Inc.

***NMR spectroscopy:*** $^{1}H$-$^{15}N$ HSQC data were acquired at 298 °K using 0.5 mM $^{15}N$ labeled D2 domain in 10 mM phosphate buffer (prepared in 95% $H_2O$ + 5 %$D_2O$, pH 6.5) containing 50 mM ammonium sulfate and 100 mM NaCl. All experiments were performed using Bruker Avance 700 MHz and 500 MHz NMR spectrometers equipped with cryoprobes. NMR data were referenced to the $^{1}H$ resonance frequency of 2,2-dimethyl-2-silapentane-5-sulfonic acid (DSS).

**Results**

The secondary structure of the D2 domain of FGFR includes 12 antiparallel β-strands arranged in a β-sandwich fold. A168 is well conserved in all four isoforms of the human FGF receptor. Ala168 is located in the middle of a hydrophobic core of residues consisting of L165, P170, V248 and V249 (Fig. 3.1). In addition, A168 along with L165 and V248 has been shown to contribute to the binding of the ligand (FGF) (18).

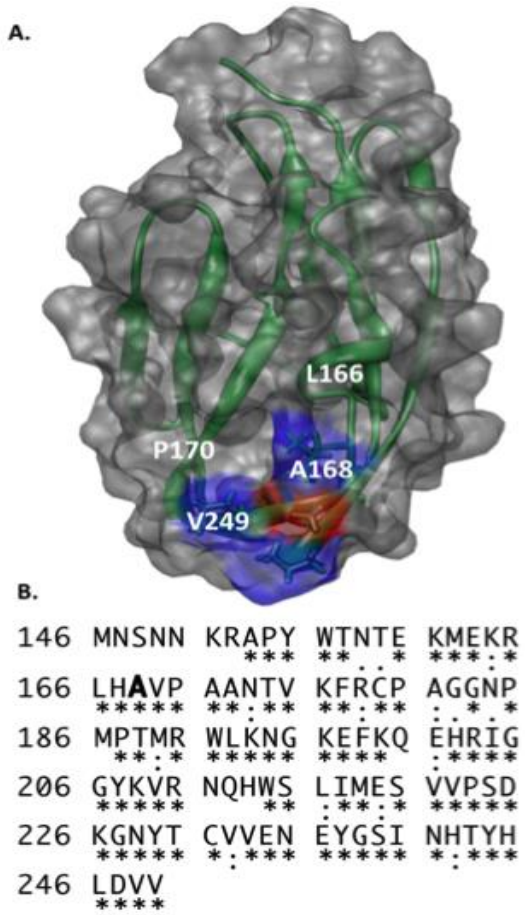


**Figure 3.1**: Panel-**A**, Depiction of the three-dimensional structure of the D2 domain Worldwide Protein Data Bank (PDB ID: 1WVZ) of FGFR2. The residues forming hydrophobic interactions with FGF include A168 (red), L166 (blue), P170 (blue) and V249 (blue). A168 of the D2 domain contacts Tyr-24 and Met- 142 of FGF. Panel-**B** Amino acid sequence of the D2 domain of FGFR2. The conserved residues in the D2 domain of FGFRs are indicated by an asterix. Ala168 is conserved in FGFRs and is highlighted in bold.

***A168S mutation does not significantly perturb the backbone conformation of the D2 domain***:

Far UV CD spectrum of the wild type D2 domain shows a strongly negative ellipticity band around 220 nm and a positive ellipticity peak centered at 205 nm. These features of the far UV CD spectrum are typical of β-sheets arranged in a β-sandwich structure. Interestingly, the far UV CD spectrum of the A168S mutant superimposes quite well with that of the wild type of the D2 domain suggesting that the A168S mutation causes no or minimal perturbations in the secondary structure of the receptor domain (Supplementary Fig. S3.1). These observations are quite

surprising because introduction of a polar serine residue in a hydrophobic core can be expected to significantly perturb the backbone conformation of the protein.

***A168S mutation causes a subtle but crucial tertiary structural change in the receptor domain***: Intrinsic fluorescence serves as a useful and sensitive spectral probe to monitor tertiary structural changes in proteins. D2 domain has three well-conserved tryptophan residues that are partially buried in the interior of the protein (19). The 339 nm emission maximum suggests that the tryptophan residues in the wild type D2 domain are partially exposed to the solvent (Supplementary Fig. S3.1). The emission maximum of the A168S mutant shows a modest red shift of 3 nm (339 nm to 342 nm) indicating that the mutation causes a subtle tertiary conformational change (Supplementary Fig. S3.1) resulting in greater solvent exposure of the indole rings of tryptophan residues in the receptor domain.

ANS is a popular fluorescent hydrophobic dye, which is commonly used to monitor solvent-exposed hydrophobic surfaces in proteins (6). ANS in the presence of the wild type D2 domain shows weak emission with an emission maximum centered at 508 nm. (Fig. 3.2A) However, the emission maximum of the dye when bound to the A168S mutant shows a red shift of 4 nm (from 508 nm to 512 nm) with a very moderate increase in the emission intensity relative to the wild type protein. These fluorescence characteristics suggest that substitution of alanine with serine (A168S) causes a subtle conformational change resulting in increased solvent exposure of hydrophobic surface(s) in the protein.

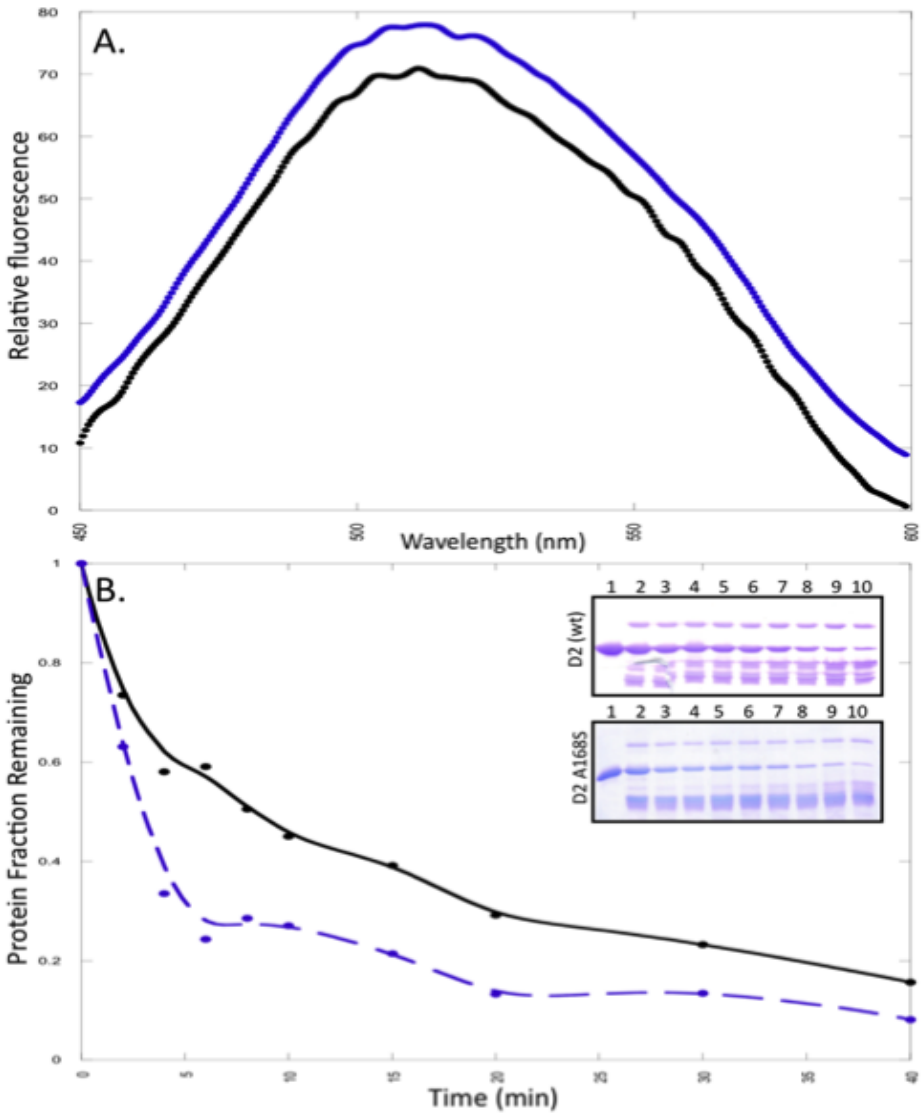


**Figure 3.2** – **Panel A** represents the ANS spectra in the presence of the wild type (black) and theA168S mutant of the D2 domain (blue). The concentration of ANS is 150 μM. **Panel B** shows the densitometric plot of the limited-trypsin digestion of wild type (black) and the A168S (blue) mutant of D2 domain. **Panel B** insert shows the 15% SDS PAGE of the limited-trypsin digestion of the wild type and A168S mutant of the D2 domain after 0, 2, 4, 6, 8, 10, 15, 20, 30 and 40 minutes of incubation of the protein domain with trypsin.

***The A168S mutation does not significantly affect the thermodynamic stability but increases the conformational flexibility of the D2 domain:*** Differential scanning calorimetry is a versatile technique that can be used to directly probe the themodynamic stability of proteins.(20) The melting thermogram of the wild type D2 domain shows a relatively sharp melting transition

($T_m$~52 ºC), from the folded to the unfolded state (Supplementary Fig. S3.5). The $T_m$ value does not appear to change due to the A168S mutation (Supplementary Fig. S3.5; $T_m$~51.5 ºC). These results suggest that the thermodynamic stability of the receptor domain is not significantly affected by the mutation.

Limited trypsin digestion is a useful technique to obtain information on the backbone flexibility of proteins (21, 22). Lysine and arginine residues located in the flexible and solvent-accessible regions of the protein are more susceptible to trypsin cleavage than when they are located in the interior or the rigid portions of proteins. Therefore, differences in the susceptibility to trypsin cleavage can be expected to provide valuable information on the changes in the backbone flexibility caused by subtle conformational changes induced in the protein due to the A168S mutation.

The D2 domain contains nine lysine residues and six arginine residues. The wild type protein is rapidly cleaved by trypsin in the first few minutes of initiation of the cleavage reaction (Fig. 3.2). About 40% of the band ($M_r$ ~13.7 kDa) corresponding to the intact D2 domain remains after 10 minutes of initiation of cleavage (Fig. 3.2). Interestingly more than 80% of the A168S mutant protein is cleaved within the same time period (Fig. 3.2). These results in conjunction with those obtained from the fluorescence data suggest that the alanine to serine substitution at position 168 causes subtle conformational change, which significantly increases the backbone flexibility and solvent-accessibility of the hydrophobic surface(s) in the protein.

***A168S mutation decreases heparin-binding affinity and causes a complete loss of FGF binding:*** D2 domain is the most important structural module of the fibroblast growth factor receptor as it provides binding surface to both heparin and the ligand (FGF). Isothermal titration

calorimetry (ITC) experiments were performed to examine the effect(s) of the Kallmann mutation (A168S) on the heparin and FGF binding affinities of the D2 domain. ITC is a useful technique to characterize the protein-protein/ligand interactions as it relies on the heat evolved or absorbed during binding interactions.

Heparin is polydisperse and therefore it is challenging to obtain an accurate estimation of its binding affinity to proteins. In this context, we used polyanionic sucrose octasulfate (SOS) to represent heparin binding interactions with the D2 domain. Sucrose octasulfate, unlike heparin, is monodisperse and can be obtained in the pure form (>99% purity). In addition, SOS has been demonstrated to be a good structural and functional mimic for heparin.

The isothermogram representing the binding of wild type D2 domain to SOS is sigmoidal and the binding constant ($K_d$) characterizing the SOS-D2 domain interaction(s) is ~ 2.2 μM (Fig. 3.3A). SOS and D2 domain bind to each other in a 1:1 stoichiometry. Interestingly, in marked contrast, the A168S *versus* SOS titration curve is hyperbolic and the binding affinity between A168S mutant and SOS is about 10 times ($K_d$ ~22 μM) weaker than that of the wild type D2 domain (Fig. 3).

The lowering of the heparin binding affinity is unexpected because the mutation site (A168S) is spatially remote from the heparin-binding site in the D2 domain. Wild type D2 domain binds strongly ($K_d$~ 2 μM) to FGF. The binding affinity ($K_d$) of the isolated D2 domain is in the same range as that of the intact extracellular portion of FGFR suggesting that D2 domain is critical for FGF binding.

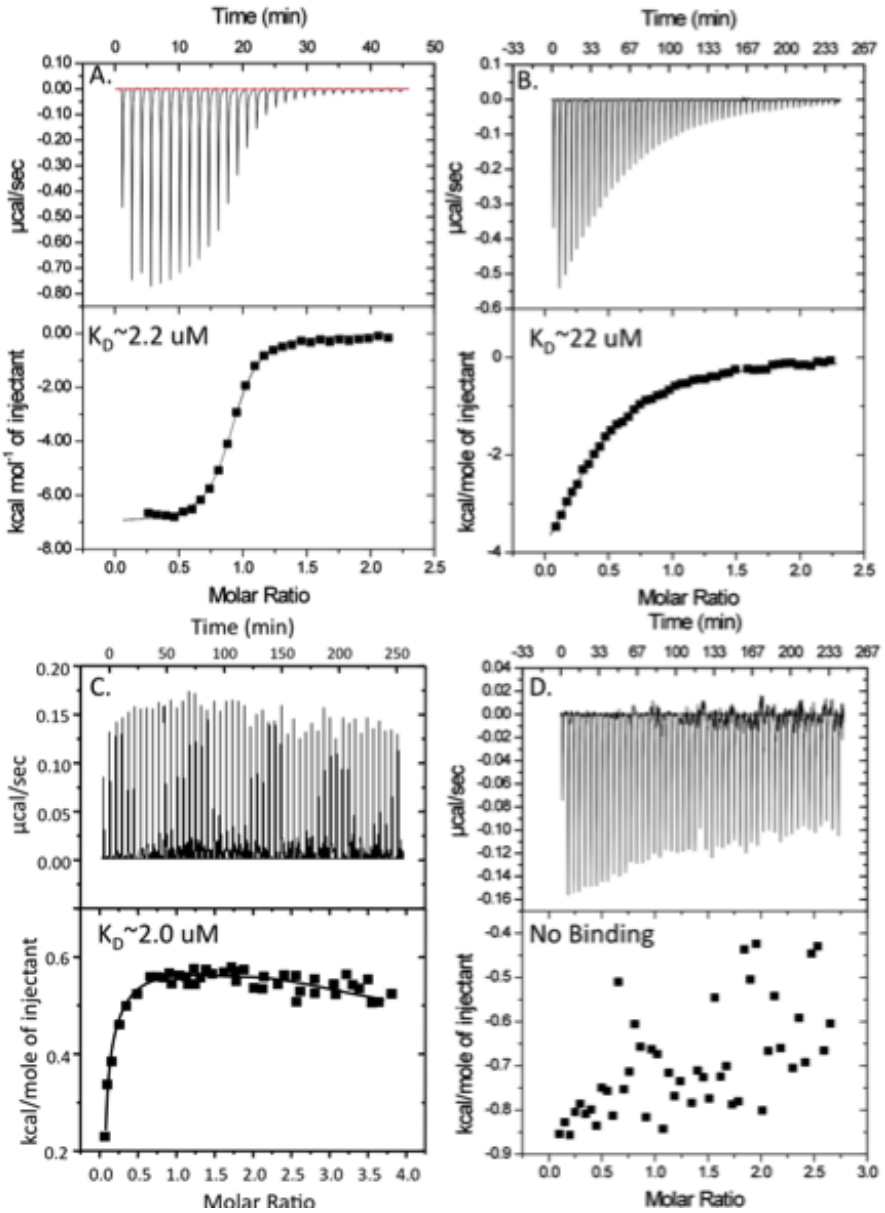


**Figure 3.3** – Binding isotherm representing the titration of the wild type and the A168S mutant of the D2 domain with SOS and FGF. The top panel shows the raw data from the titration. The bottom panel shows the integrated data derived from the raw data. Panels **A** and **B** show the titration of the wild type and the A168S mutant of the D2 domain with SOS. Panels **C** and **D** show the isothermogram of the wild type and A168S mutant of the D2 domain titrated with FGF.

Interestingly, the A168S mutant of the D2 domain exhibits no or very insignificant binding to FGF. These results suggest that loss-of-function associated with the KS (A168S) mutation is due to complete loss of interaction between the ligand and the receptor.

***Structural basis for Kallmann syndrome*:** A clear picture of the molecular basis for Kallmann syndrome would only emerge when the effects of the mutation on the conformation are understood at an atomic level. In this context, multidimensional NMR experiments were performed to assess the plausible structural changes induced by the KS mutation and also understand the consequences of the conformational change on both heparin and FGF binding.

Two-dimensional $^{1}H$-$^{15}N$ HSQC spectrum is a finger-print of the backbone conformation of proteins. Each crosspeak in the $^{1}H$-$^{15}N$ HSQC spectrum represents an amino acid in a particular backbone conformation of the protein. In this context, we monitored the backbone conformational changes induced due to the Kallmann mutation (A168S) using the $^{1}H$-$^{15}N$ chemical shift perturbation ($\delta$) observed in the HSQC spectra (Fig. 3.4A).

Most of the perturbed residues are located in the vicinity of the mutated residue (A168). Interestingly, residues located in the β-strand G (residues, H242 to V248) located at the C-terminal end of the D2 domain are also significantly perturbed (23). The observed $^{1}H$-$^{15}N$ chemical shift perturbation of residues in β-strand G is plausibly because of their spatial proximity to mutation site (A168) in the three-dimensional structure of the D2 domain (23). It appears that the Kallmann mutation causes a subtle conformational change resulting in the disruption of the structural topology of the FGF binding pocket, which consequently leads to complete loss in ligand (FGF) binding. Although several residues in the D2 domain are involved in the stabilization of the FGF-D2 domain complex, the intramolecular and intermolecular structural interactions contributed by A168 appear to be quite critical for the formation and

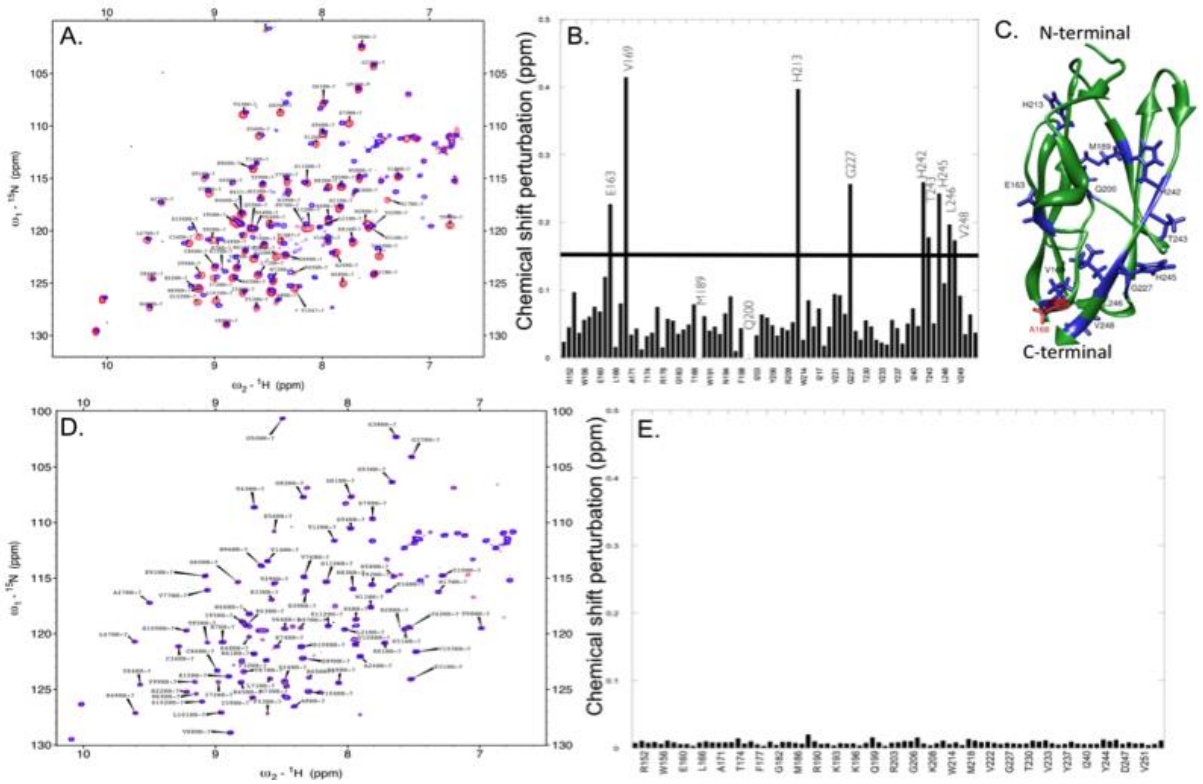


**Figure 3.4:** Structural changes induced due to the Kallmann (A168S) mutation. Panel **A** shows an overlay of the $^{1}H$-$^{15}N$ HSQC spectra of the wild type (red) and the A168S (blue) mutant of the D2 domain of FGFR. Panel **B** shows the composite $^{1}H$-$^{15}N$ chemical shift perturbation (δ) calculated from the data shown in Panel **A**. The horizontal bar represents an arbitrarily set threshold to identify the residues, which show the most significant $^{1}H$-$^{15}N$ chemical shift perturbation. Panel **C** depicts a structural of the D2 domain (PDB ID: 1WVZ) highlighting the A168S mutation site (red) and the most perturbed residues (blue).[18] $^{1}H$-$^{15}N$ HSQC spectra of the A168S mutant of the D2 domain in the presence (**red)** and absence (**blue)** of FGF is shown in Panel **D**. Composite $^{1}H$-$^{15}N$ chemical perturbation of the A168S mutant calculated from the $^{1}H$-$^{15}N$ HSQC data (Panel **E).** The data suggest that the A168S mutant of the D2 domain does not bind to FGF.

stabilization of the ligand-receptor complex. The complete loss in ligand binding affinity of the Kallmann mutant is evident from the insignificant $^{1}H$-$^{15}N$ chemical shift perturbation [composite 1H-15N chemical shift (δ <0.02 ppm)] of residues observed when $^{15}N$ enriched A168S mutant of the D2 domain is titrated with unlabeled FGF (Fig. 3.4D). The lack of binding affinity of the

A168S mutant to the ligand is also corroborated by the ITC results discussed earlier (Figs. 3C & 3D).

ITC results, discussed earlier, revealed that the A168S mutant exhibits 10-fold lower affinity to bind to heparin than wild type D2 domain (Figs. 3.3A & 3.3B). In this context, the structural basis for the decrease in heparin binding of the Kallmann mutant was assessed by comparing the composite $^{1}H$-$^{15}N$ chemical shift perturbation ($\delta$) of the A168S mutant and wild type D2 domain on binding to heparin/SOS. Comparison of the composite $^{1}H$-$^{15}N$ chemical shift perturbation plots of the wild type and A168S mutant in the presence of SOS show that residues such as, K161, K174, K196, K208 and R210 in the wild type D2 domain show significant $^{1}H$-$^{15}N$ chemical shift perturbation (Supplementary Fig. S3.3). 3D structures of the FGF-heparin-receptor complex show that these residues located in the D2 domain constitute the heparin-binding pocket (24). Interestingly, the extent of the composite $^{1}H$-$^{15}N$ chemical shift perturbation for residues in the heparin binding pocket are significantly less in the A168S mutant than observed in the wild type D2 domain (Supplementary Fig. S3.7). These results suggest that the subtle conformational change caused due to the A168S mutation alters the orientation of side-chains of residues involved in electrostatic interaction with heparin and consequently causes the decrease (~ 10-fold) in affinity to the polysulfated proteoglycan.

**Discussion**

Kallmann syndrome mutations have been detected in all major structural modules located in the extracellular portion of the FGFR (25). KS mutations invariably cause a loss-of-function. Several proposals are made to account for the loss-of-function observed in KS. Anosmin-1, a glycosylated protein, encoded by the KAL-1 gene modulates FGF signaling by directly

interacting with FGFR (25). It is believed that the KS mutations cause a disruption of the putative anosmin-1 / FGFR interaction and consequently inhibits the FGF signaling process. Alternatively, it is also believed that the loss-of-function of the KS mutations is due to a drastic conformational change leading to the misfolding and plausibly aggregation of the receptor. Contrary to these proposals, the results of the present study clearly suggest that the loss-of-function of the KS (A168S) mutation is due to a subtle conformational change that results in complete disruption of binding interactions between FGF and the receptor. We believe that structure-function studies in the future with other KS mutations can be expected to provide valuable information to understand the general molecular mechanisms underlying FGFR-linked genetic diseases.

Supplementary Data:

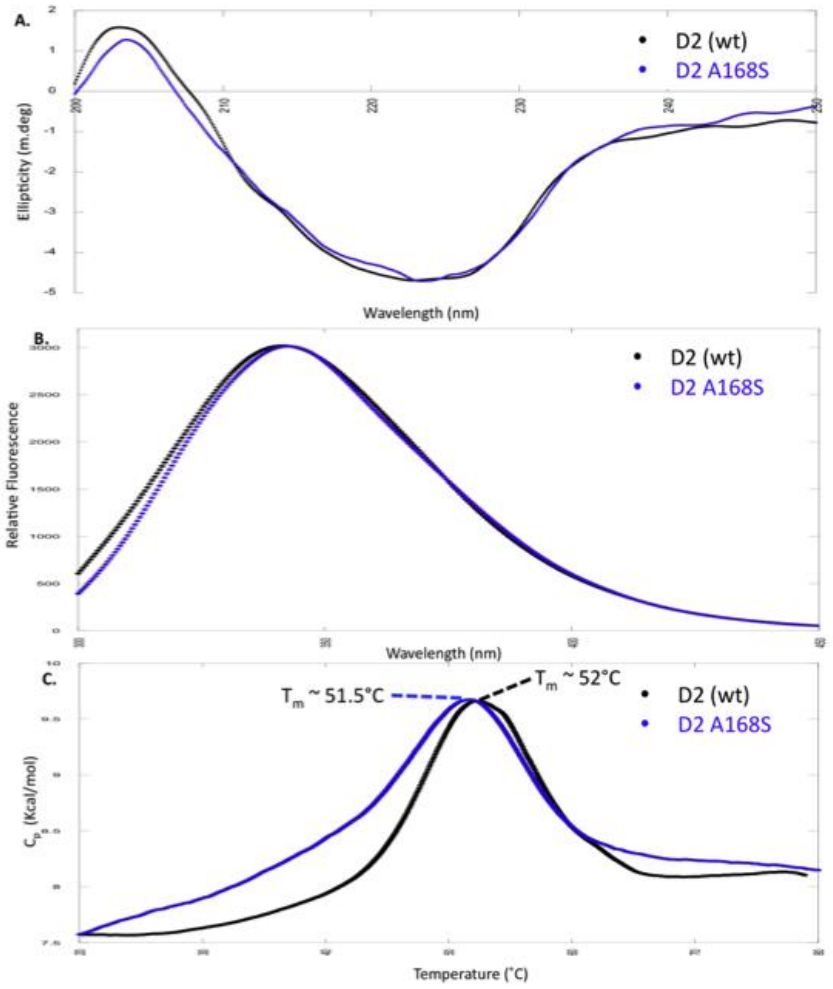


**Figure S3.5** Panel **A,** Overlay of the far-UV circular dichroism spectra of the wild type (black) and the A168S (blue) mutant of D2. Panel **B,** The steady-state intrinsic fluorescence spectra of wild type (black) and the A168S mutant of the D2 domain (blue). Panel **C**, Overlay of the DSC scans of the D2 wild type (black) and A168S mutant of D2 (blue).

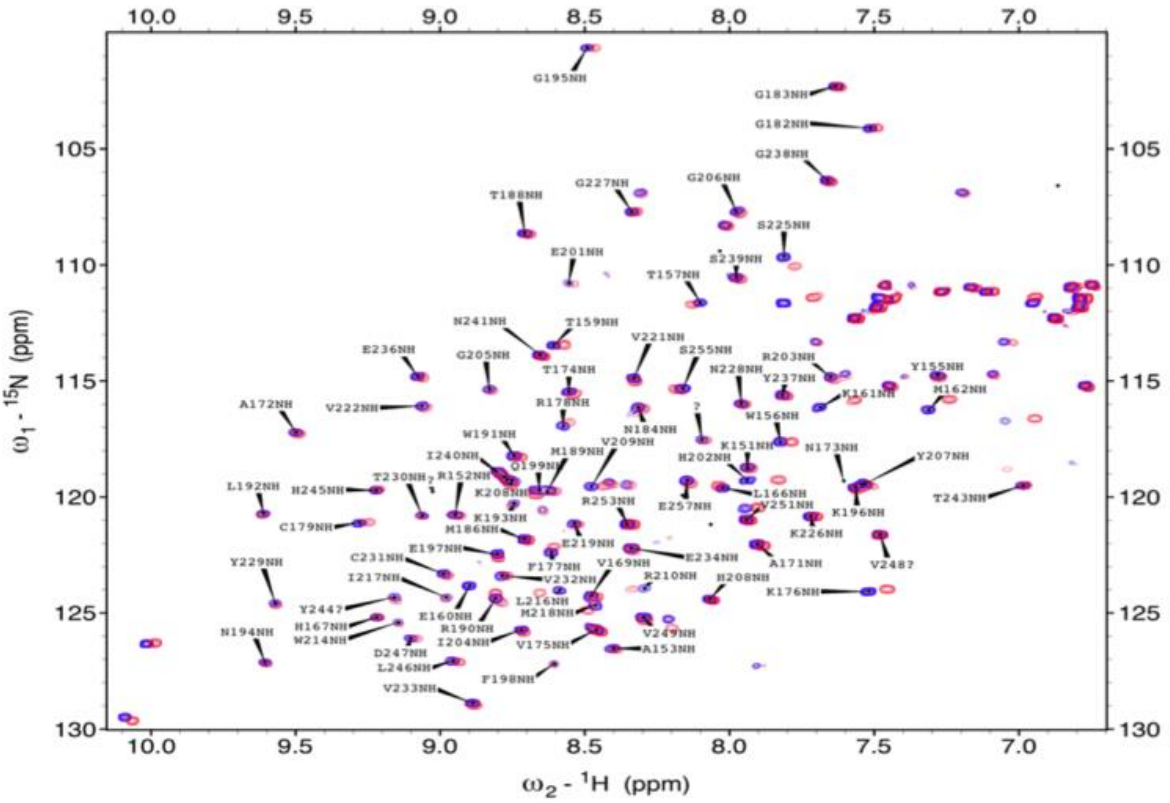


**Figure S3.6** - shows an overlay of the $^{1}H$-$^{15}N$ HSQC spectra of the A168S mutant in the presence (red**)** and absence (blue) of SOS at protein to SOS ratio of 1:1.

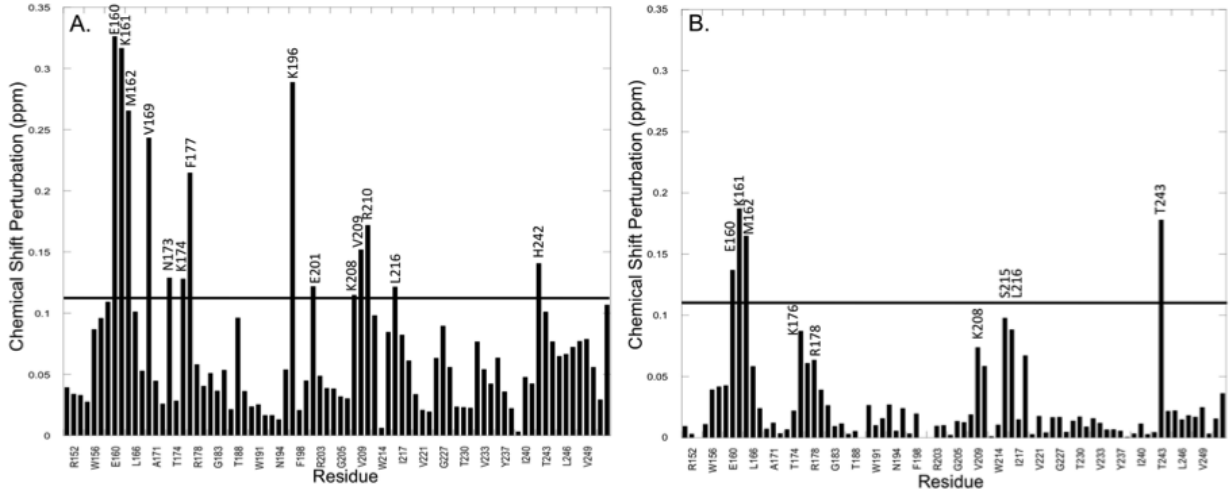


**Figure S3.7** - shows the $^{1}H$-$^{15}N$ chemical shift perturbation observed on titration of the wild type (Panel –**A**) and the A168S mutant (Panel –**B**) of the D2 domain individually with SOS. The decrease in the magnitude of the composite $^{1}H$-$^{15}N$ chemical shift perturbation observed in the A168S mutant of the D2 domain (in the presence of SOS) appears to corroborate with the ITC results which show a 10-fold loss in heparin binding affinity of the KS mutant.

**Literature Cited**


1. Naftolin, F., G. Harris and M. Bobrow 1971. Effect of purified luteinizing hormone releasing factor on normal and hypogonadotrophic anosmic men. Nature. 232, 496-497.

2. Zenaty, D., P. Bretones, C. Lambe, I. Guemas, M. David, J. Leger and N. de Roux 2006. Paediatric phenotype of kallmann syndrome due to mutations of fibroblast growth factor receptor 1 (FGFR1). Mol. Cell. Endocrinol. 254, 78-83.

3. Albuisson, J., C. Pecheux, J.C. Carel, D. Lacombe, B. Leheup, P. Lapuzina, E. Legius, G. Matthijs, M. Wasniewska, M. Dwlpech, J. Young, J.P. Hardelin and C. Dode 2005. Kallmann syndrome: 14 novel mutations in KAL1 and FGFR1 (KAL2). Hum. Mutat. 25, 98-99.

4. Gill, J., S.M. Moenter and P.S. Tsai 2004. Developmental regulation of gonadotropin-releasing hormone neurons by fibroblast growth factor signaling. Endocrinology. 145, 3839.

5. Raivio, T., Y. Sidis, L. Plummer, H. Chen, J. Ma, A. Mukherjee, E. Jacobson-Dickman, R. Quinton, G. Van Vliet, H. Lavoie, V.A. Hughes, A. Dwyer, F.J. Hayes, S. Xu, S. Sparks, U.B. Kaiser, M. Mohammadi and N. Pitteloud 2009. Impaired fibroblast growth factor receptor 1 signaling as a cause of normosmic idiopathic hypogonadotropic hypogonadism. Jcem., 4380-4390.

6. Pedersen-White, J., L.P. Chorich, D.P. Bick, R.J. Sherins and L.C. Layman 2008. The prevalence of intragenic deletions in patients with idiopathic hypogonadotropic hypogonadism and kallmann syndrome. Molecular Human Reprod. 14, 367-370.

7. Pitteloud, N., R. Quinton, S. Pearce, T. Raivio, J. Acerno, A. Dwyer, L. Plummer, V. Hughes, S. Seminara, Y. Cheng, W. Li, G. Maccoll, A.V. Eliseenkova, S.K. Olsen, O. Ibrahimi, F.J. Hayes, P. Boepple, J.E. Hall, P. Bouloux, M. Mohammadi and W.J. Crowley 2007. Digenic mutations account for variable phenotypes in idiopathic hypogonadotropic hypogonadism. J. Clin. Invest. 117, 457-463.

8. Sato, N., T. Hasegawa, N. Hori, M. Fukami, Y. Yoshimura and T. Ogata 2005. Gonadotrophin therapy in kallmann syndrome caused by heterozygous mutations of the gene for fibroblast growth factor receptor 1: Report of three families: Case report. Eshre., 2173-2178.

9. Trarbach, E., E. Costa, B. Versiani, M. de Castro, M.T. Baptista, H.M. Garmes, B.B. de Mendonca and A.C. Latronico 2006. Novel fibroblast growth factor receptor 1 mutations in patients with congenital hypogonadotropic hypogonadism with and without anosmia. J. Clin. Endocrinol Metab., 91(10):4006-12

10. Pitteloud, N., J.A. Jr, A.U. Meysing, A.A. Dwyer, F.J. Hayes and W.F. Crowley Jr. 2005. Reversible kallmann syndrome, delayed puberty, and isolated anosmia occurring in a single

family with a mutation in the fibroblast growth factor receptor 1 gene. J. Clin. Endocrinol Metab., 90(3):1317-22

11. Colvin, J., A. White, S. Pratt and D. Ornitz 2001. Lung hypoplasia and neonatal death in Fgf9-null mice identify this gene as an essential regulator of lung mesenchyme. Development. 128, 2095-2106.

12. Feldman, B, Poueymirou, W., Papaioannou, V.E., DeChiara, T.M. and Goldfarb, M. 1995. Requirement of FGF-4 for postimplantation mouse development. Science. 267, 246-249.

13. Dode, C., J. Levilliers, J.M. Dupont, A.D. Paepe, N.L. Du, N. Soussi-Yanicostas, R.S. Coimbra, S. Delmaghani, S. Compain-Nouaille and F. Baverel 2003. Loss-of-function mutations in FGFR1 cause autosomal dominant kallmann syndrome. Nat. Genet. 33, 463-465.

14. Trokovic, N., R. Trokovic, P. Mai and J. Partanen 2003. Fgfr1 regulates patterning of the pharyngeal region. Genes Dev. 17(1):141-53.

15. Andrea Ballabio and Generoso Andria 1992. Deletions and translocations involving the distal short arm of the human X chromosome: Review and hypotheses. Hum. Mol. Genet. 1(4):221-7.

16. Hebert, J. M., M. Lin, J. Partanen, J. Rossant and S.K. McConnell 2003. FGF signaling through FGFR1 is required for olfactory bulb morphogenesis. Development. 130, 1101.

17. Hebert,J., Lin,M., J. Partanen and Rossant J. 2003. FGF signaling through FGFR1 is required for olfactory bulb morphogenesis. Development. 130(6):1101-11.

18. Plotnikov, A.N., Hubbard, S.R., Schlessinger, J., Mohammadi, M. 2000. Crystal structure of FGF2 in complex with the extracellular lignad binding domain of FGF receptor 2 (FGFR2). Cell. 101, 413-424.

19. Hung KW, Kumar TK, Kathir KM, Xu P, Ni F, Ji HH, Chen MC, Yang CC, Lin FP, Chiu IM, Yu C. 2005. Solution structure of the ligand binding domain of the fibroblast growth factor receptor: Role of heparin in the activation of the receptor. Biochemistry., 15787-15798.

20. Lepock, J. R. 2005. Measurement of protein stability and protein denaturation in cells using differential scanning calorimetry. Methods. 35, 117-125.

21. Fontana, A., P.P. de Laureto, B. Spolaore, E. Frare, P. Picotti and M. Zambonin 2004. Probing protein structure by limited proteolysis. Acta Biochim. Pol. 51, 299-321.

22. Fontana, A., P. Polverino de Laureto, V. De Filippis, E. Scaramella and M. Zambonin 1997. Probing the partly folded states of proteins by limited proteolysis. Fold. Des. 2, R17-26.

23. Hung, K. W., T.K. Kumar, K.M. Kathir, P. Xu, F. Ni, H.H. Ji, M.C. Chen, C.C. Yang, F.P. Lin, I.M. Chiu and C. Yu 2005. Solution structure of the ligand binding domain of the fibroblast growth factor receptor: Role of heparin in the activation of the receptor. Biochemistry. 44, 15787-15798.

24. Ibrahimi, O.A., Zhang, F., Eliseenkova, A.V., Itoh, N., Linhardt, R.J. and Mohammadi, M. 2004. Biochemical analysis of pathogenic ligand dependent FGFR2 mutations suggests distinct pathophysiological mechanisms for craniofacial and limb abnormalities. Hum Mol. Genet. 13(19):2313-24

25. Nelly Pitteloud, Richard Quinton, Simon Pearce, Taneli Raivio, James Acierno, Andrew Dwyer, Lacey Plummer, Virginia Hughes,Stephanie Seminara, Yu-Zhu Cheng, Frances J. Hayes, Paul Boepple, Janet E. Hall, Pierre Bouloux Moosa Mohammadi, William Crowley Jr. 2007. Digenic mutations account for variable phenotypes in idiopathic hypogonadotropic hypogonadismJ. of Clinical Investigations. 117, 457-463.

## Appendix I

**ELSEVIER LICENSE**
**TERMS AND CONDITIONS**

Jun 07, 2013

This is a License Agreement between Thallapuranam K Suresh Kumar ("You") and Elsevier ("Elsevier") provided by Copyright Clearance Center ("CCC"). The license consists of your order details, the terms and conditions provided by Elsevier, and the payment terms and conditions.

**All payments must be made in full to CCC. For payment instructions, please see information listed at the bottom of this form.**

| | |
|---|---|
| Supplier | Elsevier Limited<br>The Boulevard,Langford Lane<br>Kidlington,Oxford,OX5 1GB,UK |
| Registered Company Number | 1982084 |
| Customer name | Thallapuranam K Suresh Kumar |
| Customer address | Department of Chemistry & Biochemistry<br>FAYETTEVILLE, AR 72701 |
| License number | 3159370668562 |
| License date | May 31, 2013 |
| Licensed content publisher | Elsevier |
| Licensed content publication | Biochemical and Biophysical Research Communications |
| Licensed content title | Molecular basis for the Kallmann syndrome-linked fibroblast growth factor receptor mutation |
| Licensed content author | Ryan D. Thurman,Karuppanan Muthusamy Kathir,Dakshinamurthy Rajalingam,Thallapuranam K. Suresh Kumar |
| Licensed content date | 31 August 2012 |
| Licensed content volume number | 425 |
| Licensed content issue number | 3 |
| Number of pages | 6 |
| Start Page | 673 |
| End Page | 678 |
| Type of Use | reuse in a thesis/dissertation |
| Portion | full article |
| Format | both print and electronic |
| Are you the author of this Elsevier article? | Yes |
| Will you be translating? | No |

| | |
|---|---|
| Expected completion date | Jun 2013 |
| Estimated size (number of pages) | 250 |
| Elsevier VAT number | GB 494 6272 12 |
| Permissions price | 0.00 USD |
| VAT/Local Sales Tax | 0.0 USD / 0.0 GBP |
| Total | 0.00 USD |
| Terms and Conditions | |

## INTRODUCTION

1. The publisher for this copyrighted material is Elsevier. By clicking "accept" in connection with completing this licensing transaction, you agree that the following terms and conditions apply to this transaction (along with the Billing and Payment terms and conditions established by Copyright Clearance Center, Inc. ("CCC"), at the time that you opened your Rightslink account and that are available at any time at http://myaccount.copyright.com).

## GENERAL TERMS

2. Elsevier hereby grants you permission to reproduce the aforementioned material subject to the terms and conditions indicated.

3. Acknowledgement: If any part of the material to be used (for example, figures) has appeared in our publication with credit or acknowledgement to another source, permission must also be sought from that source. If such permission is not obtained then that material may not be included in your publication/copies. Suitable acknowledgement to the source must be made, either as a footnote or in a reference list at the end of your publication, as follows:

"Reprinted from Publication title, Vol /edition number, Author(s), Title of article / title of chapter, Pages No., Copyright (Year), with permission from Elsevier [OR APPLICABLE SOCIETY COPYRIGHT OWNER]." Also Lancet special credit - "Reprinted from The Lancet, Vol. number, Author(s), Title of article, Pages No., Copyright (Year), with permission from Elsevier."

4. Reproduction of this material is confined to the purpose and/or media for which permission is hereby given.

5. Altering/Modifying Material: Not Permitted. However figures and illustrations may be altered/adapted minimally to serve your work. Any other abbreviations, additions, deletions and/or any other alterations shall be made only with prior written authorization of Elsevier Ltd. (Please contact Elsevier at permissions@elsevier.com)

6. If the permission fee for the requested use of our material is waived in this instance, please be advised that your future requests for Elsevier materials may attract a fee.

## Appendix II

UNIVERSITY OF ARKANSAS

J. William Fulbright College of Arts and Sciences
*Chemistry and Biochemistry*

**To Whomsoever it may concern**

This is to certify that Mr. Ryan Thurman is the first author of the papers mentioned below and has completed about 75% of the work reported in these papers,

1. "Cation-π Interactions Act to Stabilize FGF Receptor D2 "
2. "Molecular Basis for the Kallmann Syndrome-Linked Fibroblast Receptor Mutation A168"

Suresh K. Thallapuranam

Major Advisor

CHEM 119 • 1 University of Arkansas • Fayetteville, AR 72701-1201 • 479-575-4601 • Fax: 479-575-4049 • http://chemistry.uark.edu/

**Characterization of a Kallmann Syndrome Mutations of the Fibroblast Growth Factor Receptor D2 Domain**

Ryan D. Thurman, Karuppanan Muthusamy Kathir and T.K.S Kumar

**Abstract:** Kallmann syndrome expresses in patients as hypogonadotrpic hypogonadism and anosmia. Common symptoms of KS include cleft palate, corpus callosum agenesis, and fusion of the fourth and fifth metacarpal bones. Fibroblast growth factor receptor 1 is a gene that mutations commonly occur resulting in KS. Additionally, mutations found in the FGF receptor may also result in Pfeiffer syndrome – a disease resulting in craniosynostosis, retardation and limb abnormalities. We have assessed the biophysical characteristics of both Kallmann syndrome and Pfeiffer syndrome. Kallmann syndrome mutations in the D2 domain include C179S, W214G, D225H, and G238D. The Pfeiffer syndrome mutation in the D2 domain includes A172F. Isothermal titration calorimetry and $^{1}H - ^{15}N$ HSQC experiments of the KS related mutants of the D2 domain suggest a significant decreased FGF and heparin binding interaction with the D2 domain and increased perturbation at the FGF binding site. Additionally, the Pfeiffer syndrome mutation resulted in only moderately decreased interactions with FGF and heparin with the D2 domain. This data combines to provide biophysical evidence that KS may result from a loss of signaling from the FGFR1 protein.

## Introduction

Kallmann syndrome (KS) is a form of idiopathic hypogonadotrpic hypogonadism (IHH) that expresses phenotypically with anosmia(1). Most commonly KS is expressed with synkinesia, hearling loss, labial or palentine cleft, dental anomalies and inhibited puberty development (2, 2). KS occurs in approximately 1:10,000 males and 1:50,000 females (3). An estimated 10% of KS cases are attributed to mutations in fibroblast growth factor receptor 1 (FGFR1) (4). The remaining cases are KS caused by mutations in KAL1 gene or sporadic mutations. KS cases caused by FGFR1 mutations are an autosomal dominant form of KS. The mutations found in FGFR1 include missense, nonsense, frameshift and deletion mutations (5-12)

Fibroblast growth factors (FGFs) are approximately 16 kDa heparin-binding proteins that regulate key cellular processes such as angiogenesis, cell differentiation, morphogenesis, wound healing and tumor growth (13, 14). FGF receptors consist of three extracellular ligand-binding domains (D1, D2, D3), a single transmembrane helix, and cytoplasmic tyrosine kinase domain. Cell surface-bound HSPGs (heparan sulfate proteoglycans) that support dimerization or polymerization of the FGFRs are thought to be required to activate the signaling pathway (15, 16). The D2 domain is suggested to bind both HSPGs and FGFs to form a ternary complex. The dimerization complex of the FGFR has been well characterized by Platnikov et. al to include FGF: FGFR: heparin in a 2: 2: 2 complex. Mutations found in FGFR1 in the D2 domain have been associated with families carrying Kallmann syndrome phenotypes (17).

The FGFR D2 C179S, W214G, D225H and G238D mutations have been associated with Kallmann syndrome (18, 19). The role of FGFR1 plays in the development of KS is postulated to be the result of decreased signal transduction (18, 20-22)The decrease in FGFR1 signaling resulting from KS linked mutations has been termed the loss-of-function mechanism. The loss-

of-function mechanism has been established through structure analysis and through knockout mice. FGFR1 inactivation in mice telencephalon tissue results in a failure of olfactory bulb formation (22). Analysis of the structure of FGFR suggests either a decreased interaction of the receptor with the ligand (FGF) or the destabilization of the structure caused due to mutations in a diseased state. However, very little structural information is available to rationalize the results of the knockout studies in mice. Kallmann syndrome linked mutations D2 G238D and D225H have been characterized using structural analysis of x-ray structures of the D2 domain. The D2 G238D has been postulated to destabilize the D2 domain. Glycine 238 occurs in a turn located between β-strand F and β-strand G. Replacement of glycine 238 with aspartic acid is suggested to result in unfavorable steric clashes with neighboring residues. Structural assessment using x-ray crystallography structures of the D225H mutation has been postulated to disrupt a charge-charge interaction with nearby R203 (23). This interaction is shown to occur in the x-ray crystal structure solved by Plotinikov et. al.(24)However, the orientation of these residues in the D2 NMR solution structure suggests these interactions are not present. (25). The loss-of-function theory and decrease structural competency as a result of KS mutations were both assessed. In this study we use biophysical experiments to determine the structural changes in D2 and the changes in D2-ligand interactions.

## Material and Methods

***Mutagenesis, Expression and Protein Purification.*** All mutations on the FGFR2 D2 were made using the quikchange protocol. (Stratagene). The mutations were confirmed using DNA sequencing. The mutations were all made to the D2 domain contained in the PET20b vector. All experiments were conducted using only the D2 domain.

BL-21(DE3) pLysS E. *coli* strain was used to express the wild type and mutants of the D2 domain. The cells were grown in LB medium containing 100mg/ml ampicillin and 100mg/ml chloramphenicol. The cells were grown and 37 °C and induced using IPTG when the O.D.600 value was 0.6. After induction the cells were incubated at 37 °C for 5 hours. The culture was centrifuged at 6000 rpm to pellet the cells. Cell samples were sonicated using a Microson XL unit with the power setting adjusted to 12. The samples were sonicated 60 times for 1-second intervals. The cell lysate was centrifuged at 16K rpm to pellet the sample. Following centrifugation the pellet was resuspended in 5M NaCl and centrifuged at 10K rpm. The pellet was then resuspended using 1M urea and centrifuged at 10K rpm. Finally, the pellet was resuspended using 8M urea and centrifuged at 10K rpm. The supernatant was dialyzed against 10mM phosphate buffer, 100mM NaCl and 50mM ammonium sulfate (pH 6.5) in order to refold the protein. The buffer exchange was repeated four times with a minimum of 3 hours per exchange. The dialyzed sample was loaded onto a heparin sepharose column and eluted using a salt gradient between 0.3 – 1.5 M NaCl. The purity of each fraction was assessed using a 10% SDS gel followed by Coomassie Brilliant Blue staining.

***Fluorescence and CD*** measurements of the D2 (wt) and mutants were acquired in a 10 mM phosphate buffer containing 100 mM NaCl and 50 mM ammonium sulfate (pH 6.5). CD spectra were acquired on a Jasco J-710 spectropolarimeter. Wavelength scans were set to 250-190 nm. Samples were approximately 90- 100 uM in concentration and a 0.1 cm path length cuvette was used for data acquisition. A total of 10 scans were averaged for each sample. Fluorescence measurements were acquired using a Hitachi F2500 fluoremeter. A 1.0 cm path length quartz cell was used and each sample was adjusted to ~50 uM. The excitation wavelength was set to 280 nm and acquisition from 300 to 450 nm. The ANS titration excitation wavelength was 390 nm while the acquisition was from 450 nm to 600 nm. During the ANS titration protein samples were titrated with 3 ul. aliquots of 10mM ANS in 10mM phosphate buffer containing 100 mM NaCl and 50 mM ammonium sulfate at a pH of 6.5.

***Differential scanning calorimetric*** measurements were performed using a DASM-1M calorimeter. Each sample concentration was between 1.0 – 1.5 mg/ml. The buffer used was 10 mM phosphate containing 50 mM ammonium sulfate and 100 mM NaCl (pH ~6.5) and degassed prior to loading into the microcalorimeter. The scanning rate was set to 1 °C/min and scanned from 10 °C - 90°C. The $T_m$ values were determined using Origin DSC software provided by Microcal Inc. The entropic or enthalpic energies were not reported because the D2 domain does not undergo complete refolding by reducing the temperature.

***Isothermal Titration Calorimetry*** measurements were performed using a Microcal VP titration calorimeter (Northhampton, MA, USA). Titrations consisted of 5-10µl injections of 0.5 mM sucrose octasulfate (heparin analog) delivered into 0.050 mM concentration of D2. Injections

were delayed 3.5 minutes to allow the titration peak to return to a baseline prior to additional injections.

***NMR spectroscopy*** data on the D2 domain was acquired using a protein concentration of 0.15-0.5 mM concentrations in 10 mM phosphate buffer (95% H2O + 5 %D2O, pH 6.5) containing 50 mM ammonium sulfate and 100 mM NaCl. NMR experiments were conducted at 298°K. All experiments were conducted using Bruker Avance 700 mHz or Bruker Avance 500 mHz NMR. All NMR data were referenced to the 1H resonance frequency of DSS.

**Results and Discussion**

***Structure Analysis of the D2 G238*** mutation is located in the ßF-ßG turn of FGFR1. G238 is highly conserved in each of the FGF receptors. The location of G238 stabilizes the ßF-ßG turn through hydrogen bonds formed from the backbone oxygen of G238 with the backbone amide of N234. (Figure 4.1)

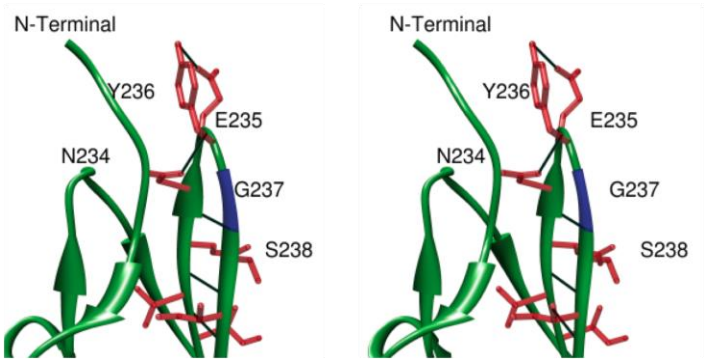


**Figure 4.1** - shows a stereo view of the N-terminal region of FGFR1. Connecting black lines highlight the hydrogen bonds formed in the ßF-ßG strands. The mutations site G237 is highlighted in blue and contains one backbone hydrogen bond formed with N234.

Conservation of glycine 237 is critical for the FGF receptors. Gly234 is involved in interactions with closely placed residues in ß-sheet ßA. Replacement of G237 with a bulky sidechain

containing amino acid would result in the sidechain residue extending towards the ß-sheet ßA at the N-terminal of D2. Side-chain containing mutations at G234 is postulated to destabilize the D2 fold. Additionally, the expression of D2 G238D has been shown to result in a large percentage of the protein entering into inclusion bodies. This change of expression of D2 G238D suggests a decreased ability of D2 to properly fold. The expression of the G238D mutant is lower than the expression of wild type D2. *Pitteloud et al.* suggest the lowered expression of the G238D mutant of D2 results from the retention of the misfolded protein in the endoplasmic reticulum(23).

***Structural analysis of FGFR2 A172F***: Ibrahami *et al.* studied the ligand binding characteristics of A172F using surface plasmon resonance binding and xray crytallography (figure 4.2) (26-28). A172 is located near the c-terminal end of the structure and is located at the ßA'-ßB loop. Dimeric structures of the the D2 domain reveals that A172 is situated in hydrophobic contact with the adjacent D2 A172 residue.

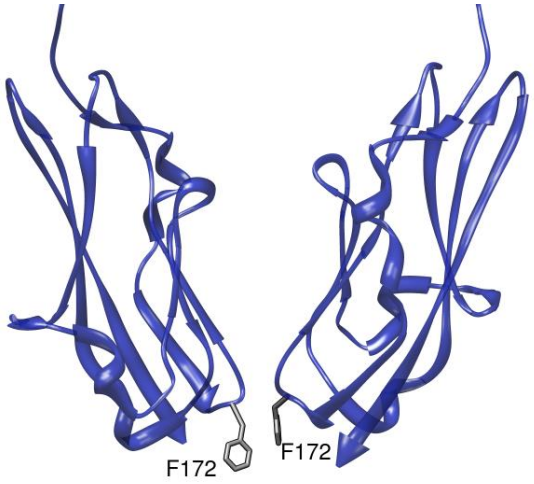


**Figure 4.2** - shows FGFR1 D2 showing the A172F mutation. The model shown replaces A172 with phenylalanine to give a representation of the possible orientation of the aromatic phenylalanine ring(29).

A172 also forms hydrogen bond contacts with serine 220 of the adjacent D2 domain. The x-ray structure of the D2 domain supports A172F forms a hyrophobic interactions with the A172F residue of the adjacent D2. The xray structure places the A172F residue of interacting D2 molecules 3.3 Å apart(26). The addition of these hydrophobic contacts is believed to contribute to the stability of the D2 dimeric structure required for FGF receptor signal transduction (26).

***Structural analysis of FGF receptor C179S:*** The D2 domain is a ß-sandwich structure of two layers of ß-sheets. One ß-sheet is composed of strands ßA, ßB, ßE and ßD and the second ß-sheet formed by strands ßA', ßG, ßF, ßC and ßC'**.** C179 is located between ßB and ßB' and forms a disulfde bond with C230 located on the ßF strand. C179 and C230 are highly conserved residues found in FGF receptors 1-4. In each of the receptors these residues form a disulfide bond that provides a stability to the ß-sandwich of D2. Although the C179S mutation is associated with KS the pathogenic mechanism resulting from this mutation is unknown(30). The disulfide bond is suggested to stabilize the D2 domain (29). It is likely that the C179S mutation will destabilize the D2 domain and inhibit it interactions with heparin and/or FGF. This would contribute to the proposed loss-of-function mechanis common in KS mutations.

***Structural analysis of FGFR1 D225H*** was conducted by Pitteloud *et. al* through the analysis of existing xray structures of the FGF receptor(31). The D225H mutation is located in a loop region between ßE and ßF strands Pitteloud *et.al.* assert the mutation would result in the deformation of a saltbridge formed between D225 and R203 (figure 4.3) (29). The x-ray structure of the D2 domain used to support this assertion places the D225 and R203 in close proximity.

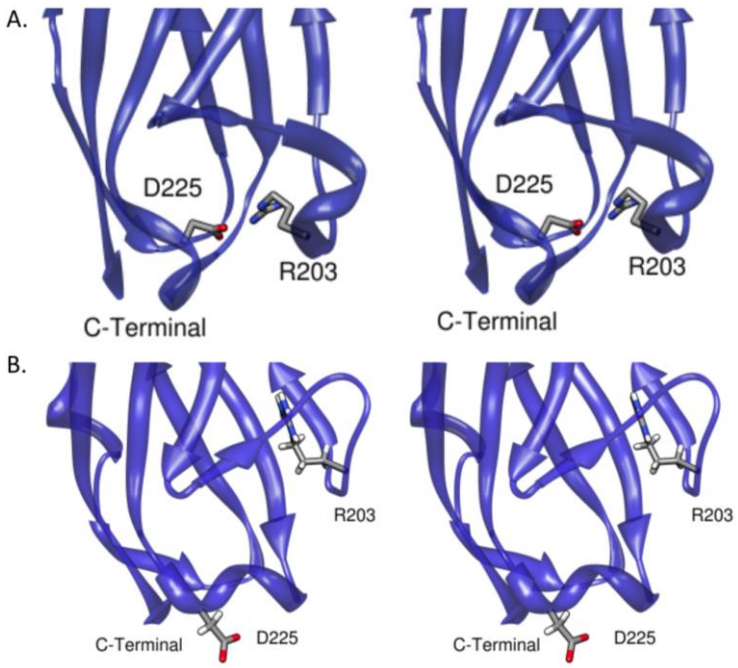


**Figure 4.3 -** Panel A is a stereo view of the x-ray structure of FGF receptor D2 (PDB – 1FQ9). Highlighted is aspartic acid 225 and R203(15). Panel B is a stereo view of the NMR solution structure (PDB – 1WVZ) of FGF receptor D2(25). Highlighted in this structure is the R203 and aspartic acid 225.

However, FGFR2 D2 NMR solution structures provide a contradictory orientation of D225 and R203. The D2 solution structure shows R203 in a vertical orientation placing it in close proximity to W191. Additionally, D225 is rotated away from R203. Rotation of D225 places it in a more solvent exposed orientation when compared to the x-ray structural models (25).

***Structural analysis of W214G*** in the FGF receptor places the site of the mutation between strands ßD – ßE (figure 4.4). W214 extends into a hydrophobic pocket formed by P180, A181, P187, V233 and I 240. The size of the cavity formed allows for W214 to extend into the pocket and stabilize the loop by hydrophobic interactions.

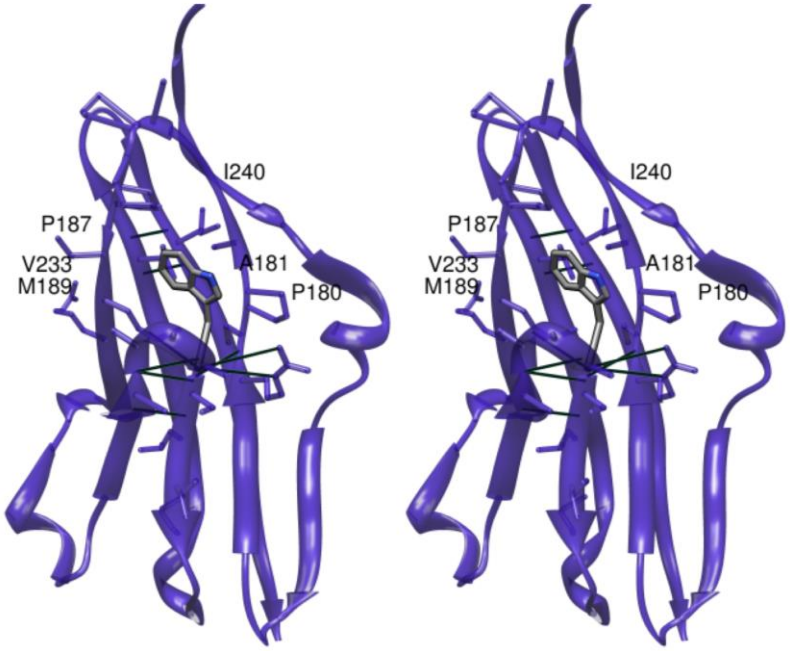


**Figure 4.4** - shows the stereo view of the xray structure of the D2 domain (PDB 1FQ9)(15). The hydrogen bonds formed by strands ßD – ßE are shown in black. The residues forming a hydrophobic pocked containg the W214 residue are include P180, A181, P187, M189, V233 and I240.

The W214G mutation is expected to increase the the flexibility of the ßD – ßE strands and decreae the stability of the D2 structure. Additionally, the heparin binding site extends across the W214 location. As a result it is expected that the heparin binding interactions may be reduced as a result of the increased flexibility caused by the W214G mutation.

***The secondary structures*** of the mutants of D2 were assessed using far-UV CD. The far-UV circular dichroism spectra are shown to overlay with the β-structure formed in D2 (wt). D2 wild type shows a negative ellipticity band centered near 225 nm and a positive ellipticity peak near 205 nm. This profile is consistent with the β sheet formed by the nine β-strands of the D2 domain (figure 4.5). The D2 G238D and D2 C179S mutations expected to show significant

changes in the structure of the D2 domain, resulted in no significant changes in the CD spectra. The CD spectra of the D2 D225H and W214G mutations were consistent with the wild type D2

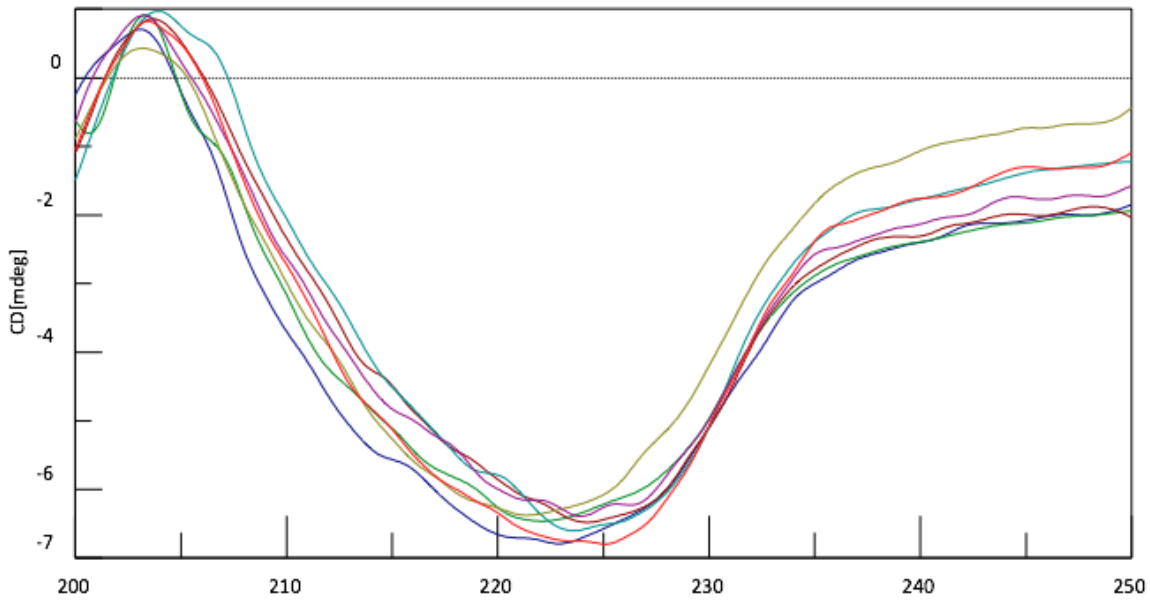


CD spectra.

**Figure 4.5** - Circular dichroism measurements from 200-250 nm suggests a ß-sheet structure for each of the mutants. The spectrum overlay includes wild type (green), A172 (yellow), W214 (purple), D225H (red) and G238D (light blue) mutant of D2.

The D2 domain contains one tryptophan residue in a hydrophobic environment and two tryptophan residues that are moderately exposed at the surface of the D2 domain. Using steady-state fluorescence the maximum fluorescence wavelength of the tryptophan residues in the D2 domain may indicate conformational changes in the domain. The fluorescence spectrum of wild type D2 shows of a wavelength maximum at 339 nm (Figure 4.6). The wavelength maximum for D2 C179S, D225H and D2 G238D exhibited a slight red shift to 342 nm. The D2 W214G mutation exhibited the largest wavelength maximum shift. The D2 W214G fluorescence

maximum shift is the result of the remaining two tryptophans, W156 and W191. The remaining tryptophans are in buried environments resulting in a large blue shift for the maximum wavelength of D2 W214G ($\lambda_{Max}$ - 308 nm).

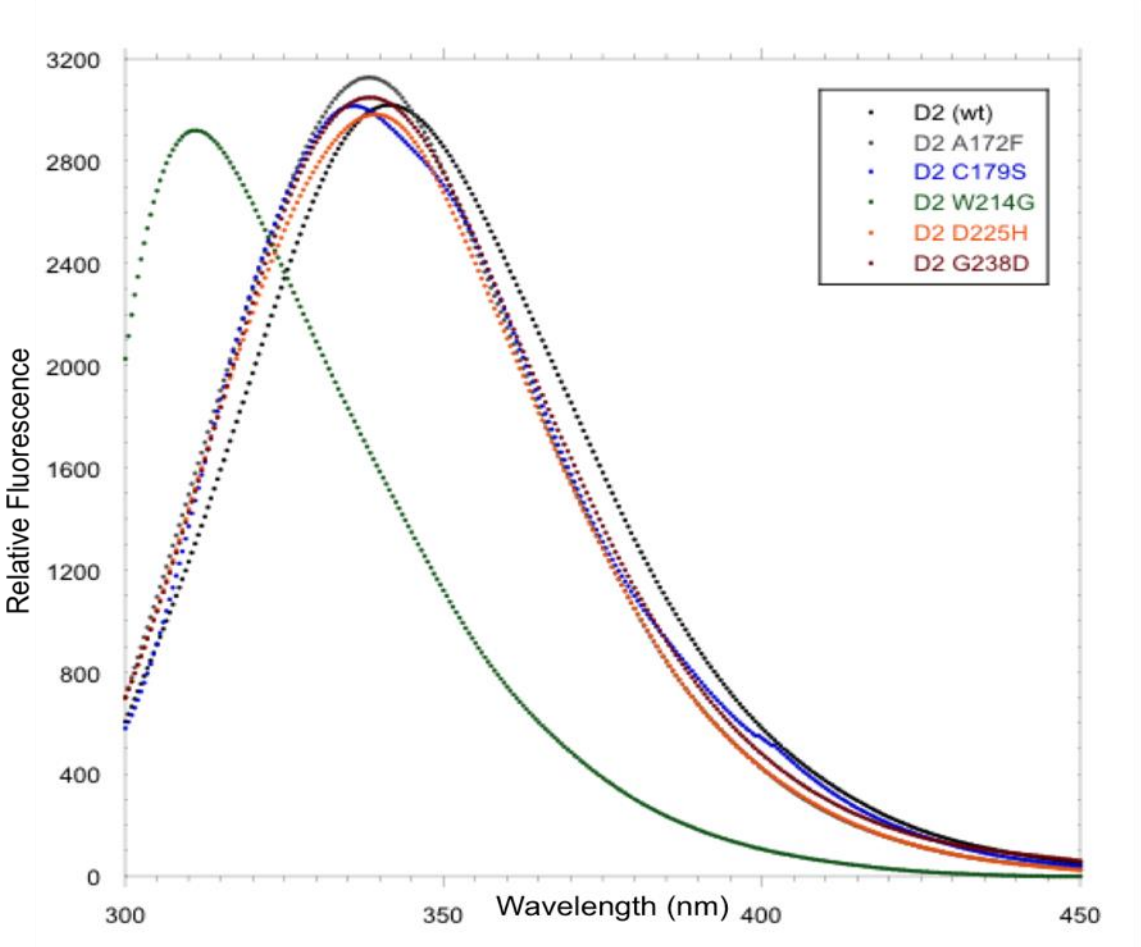


**Figure 4.6** - Shows the steady-state fluorescence of each of the mutants of D2. The excitation wavelength was 280nm. D2 W214G (green) shows the greatest shift in the maximum wavelength ($\lambda_{max}$-308 nm)

Differential scanning calorimetry (DSC) was used to determine changes in the melting temperature ($T_m$) as a result the mutations in the D2 domain. The $T_m$ values were determined for each sample in the presence and absence of sucrose octasulphate (SOS). SOS is a heparin sulfate proteoglycan used to mimic the binding of heparin to the D2 domain. The D2 (wt) melting

temperature is 52.0 ° C and increased to 55.0 °C in the presence of SOS (figure 4.7). The melting temperature for D2 D225H closely matched the $T_m$ value of D2 (wt) at ~51°C and 52 °C in the presence of SOS. This data suggests the aspartic acid to histidine mutation results in minor decreases in the stability of the D2 domain. The greatest $T_m$ value decrease resulted from the D2 C179S and G238D mutation. The D2 C179S $T_m$ value was ~28 ºC without SOS (figure 4.8). Additionally, the G238D mutation of D2 resulted in a significant destabilization of the D2 domain ($T_m$~34 ºC). This significant change in the structural stability was predicted by *Plotnikov et. al* (17). The addition of SOS to the G238D mutant stabilized the D2 domain increasing the melting temperature ($T_m$-40 ºC).

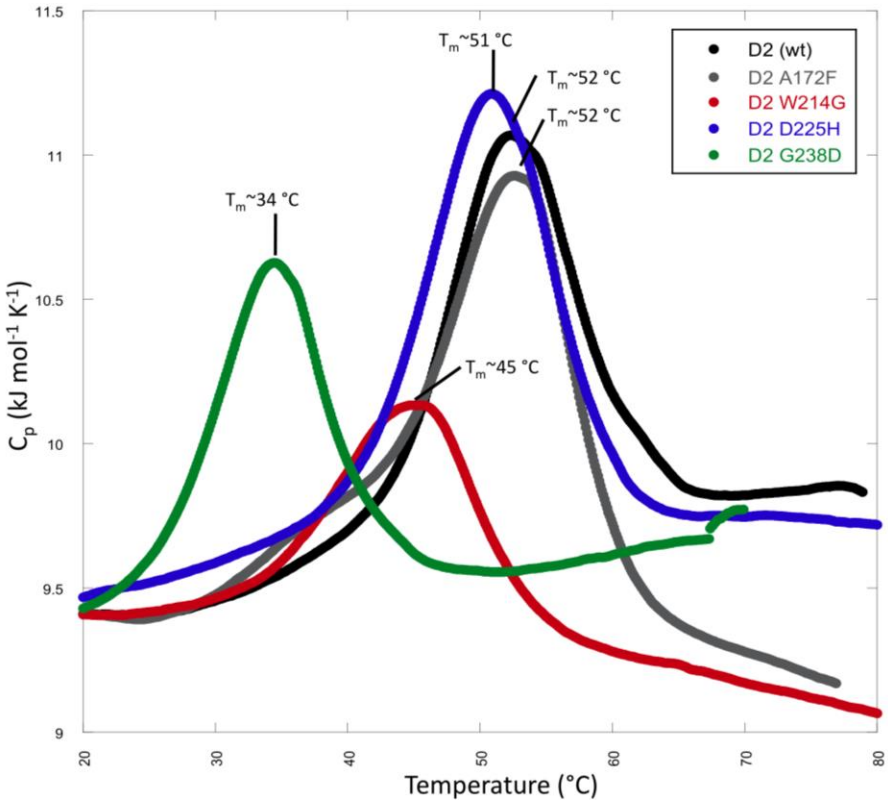


**Figure 4.7** - Differential scanning calorimetry thermogram showing the thermal denaturation of each of the mutants of D2. The mutants showing the greatest decrease in $T_m$ is the G238D ($T_m$~34 ºC) mutant of D2. Protein concentrations were 1-1.5 mg/ml in 10 mM phosphate buffer containing 100 mM NaCl and 50 mM ammonium sulfate (pH – 6.5).

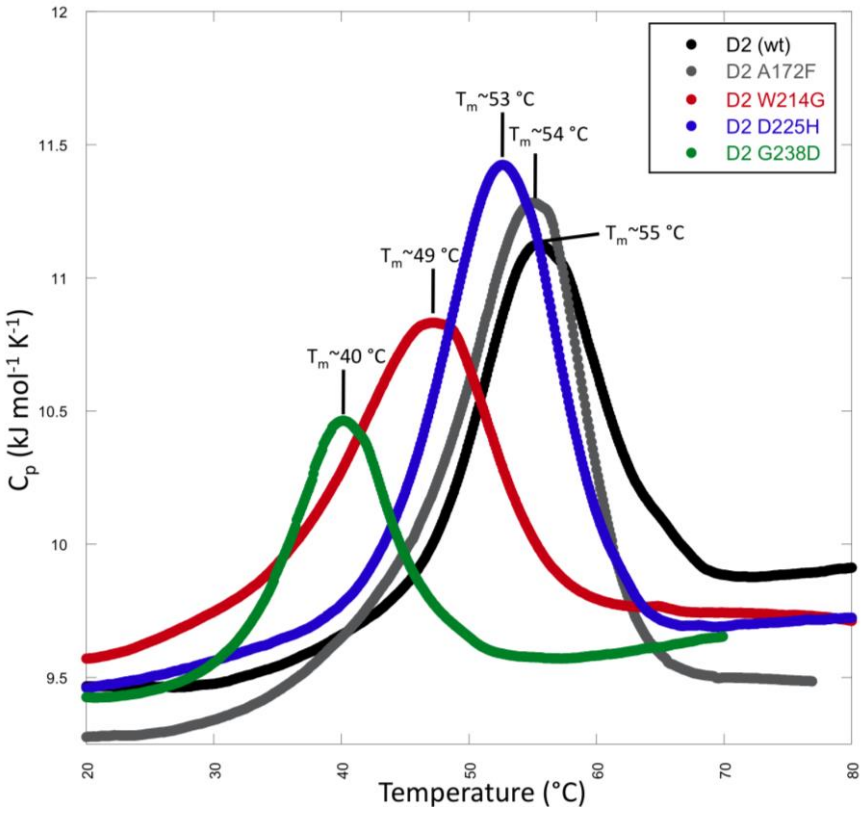


**Figure 4.8** - shows the differential scanning calorimetry thermogram of the KS and PS mutants of D2 in the presence of SOS. The D2:SOS were added in a 1:1 molar ratios in 10 mM phosphate buffer containing 100 mM NaCl and 50 mM ammonium sulfate (pH ~6.5).

The D2 W214G mutation also produced a moderate decrease in the $T_m$ value ~45 ºC in the absence of SOS and the melting temperature increased in the presence of SOS ($T_m$ ~47 ºC) **.** This data suggests the disulfide bond formed by C179-C230 plays a significant role in stabilizing the D2 domain.

ANS (8-anilino-1-napthalene sulfonate) is a hydrophobic molecule that shows an increase in fluorescence emission upon binding to hydrophobic surfaces on a protein. Mutants of D2 that result in increased exposure of hydrophobic surfaces are expected show increased fluorescence intensity when titrated with ANS. Figure 4.9 shows the relative fluorescence (RF) of each of the

mutants of D2 when titrated with ANS. Titration of D2 C179S with ANS produced highest relative fluorescence when compared to D2 (wt). The increase of fluorescence intensity suggests a significant exposure of hydrophobic residues on the surface of the protein when compared to D2 wild type (figure 4.9). W214G and G238D produced moderate increases in the RF upon titration with ANS. The A172F and D225H mutants also showed minor increases in RF up titration with ANS. These minor increases suggest only minor structural perturbations caused due to these mutations. The relative increase in fluorescence also suggests an increased exposure of hydrophobic residues as a result of the mutation.

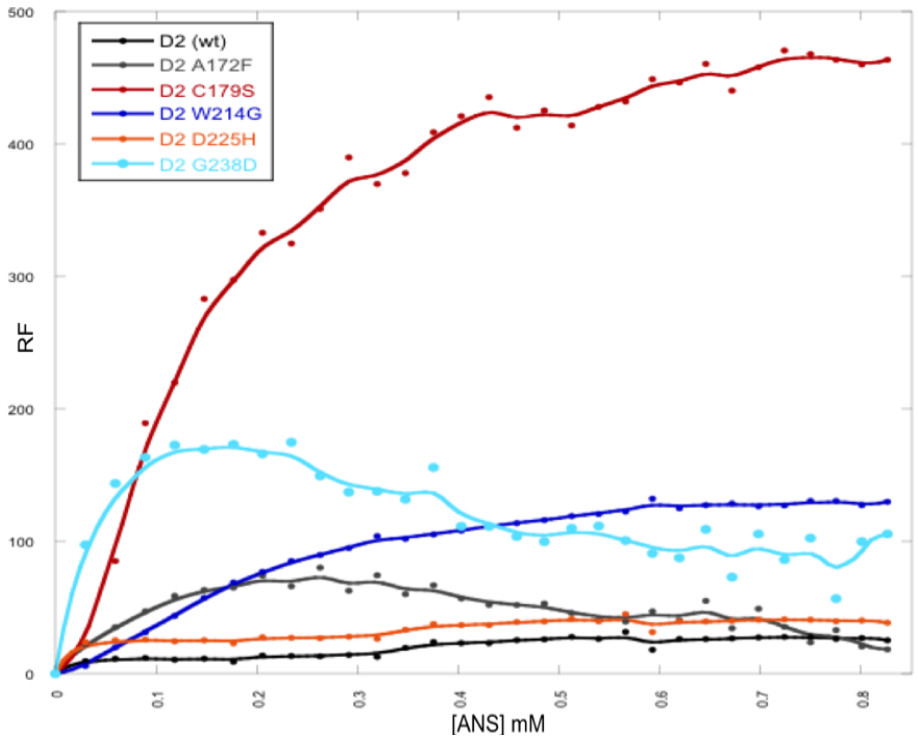


**Figure 4.9** – shows the ANS titration of each of the mutants of D2. This data suggests mutants C179S, G238D and W214G posses significant exposure of hydrophobic residues.

Flexibility of the backbone: Limited trypsin digestion is a common method to evaluate the flexibility of a protein. The D2 domain is abundant in both lysine (9) and arginine (6)

residues, making trypsin an ideal proteolytic enzyme to probe the flexibility of wild type and mutants of D2 (figure 4.10). The rate of the proteolytic digestion reflects the relative increased backbone flexibility caused as a result of the mutation. Densitometric scan is representative of the percentage of protein that remains uncleaved (Figure 4.11). Analysis of the SDS page of the limited trypsin digestion of D2 D225H and D2 G238D suggest each of these mutants result in a

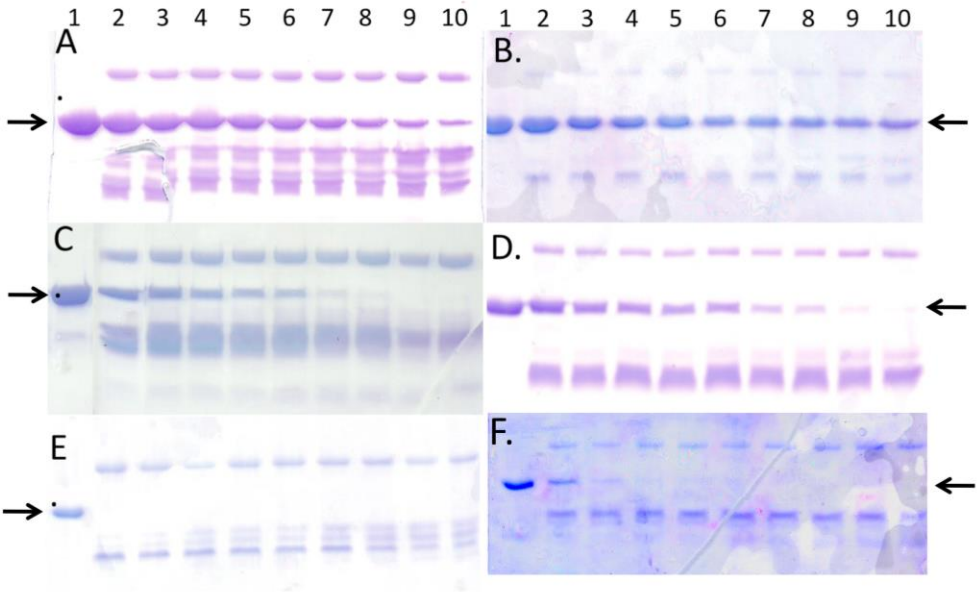


**Figure 4.10** - Time dependent trypsin digestion of the wild type (A) and mutants of D2 include C179S (E), A172F (B) W214G (C), D225H (D), and G238D (F). The D2 protein band is indicated by the arrow. Lanes 1 through 10 represent the trypsin digestion products formed after 0 min. (lane 1), 2 min (lane 2), 4 min (lane 3), 6 min (lane 4), 8 min (lane 5), 10 min (lane 6), 15 min. (lane 7), 20 min (lane 8), 30 min (lane 9) and 40 min (lane 10)

significant increase in the backbone flexibility. Additionally the D2 W214G mutation also shows a significantly-increased rate of proteolytic degradation. This data also suggests an increased backbone flexibility resulting from this mutation. Additionally, the C179S mutant showed a rapid cleavage rate suggesting a significant increase in the backbone flexibility of the protein.

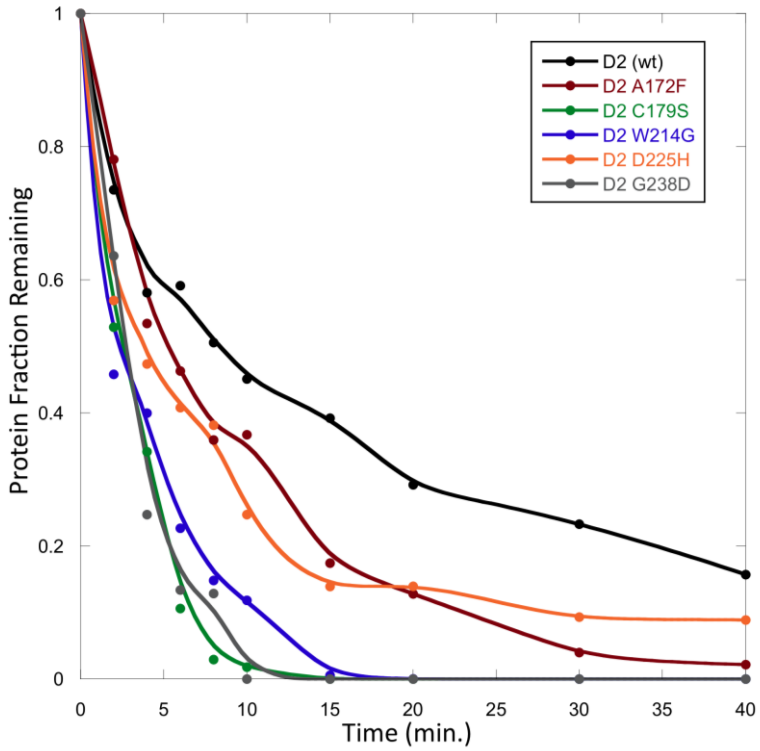


**Figure 4.11** shows the densitometric plot of the limited-trypsin digestion of wild type (black) and each of the disease mutations of D2.

Heparin and FGF receptor binding affinity: Isothermal titration calorimetry is a technique used to measure the heat of binding events occurring during protein and ligand interactions. Isothermogram also provides information on the binding affinity ($K_D$) value associated with the protein-ligand interactions. FGF-1 and sucrose octasulfate are both capable of binding to the D2 domain. Sucrose octasulfate (SOS) is a heparin analog that binds to the D2 domain. Isothermogram characterizing the binding interactions of the wild type and mutants with FGF-1 and SOS are shown in figure 4.12. The binding interactions of D2 W214G (51.35 μM ± 1.35), D2 D225H (13.0 μM) D2 G238D (47.14 ±2.01 μM) with SOS were significantly reduced when compared to D2 wild type (0.97 μM ± 0.02). Additionally, the D2 C179S binding interaction was most significantly inhibited of the mutants. The D2 C179S interaction was reduced to $K_d$ = 1.76 ±0.03 mM, suggesting there to be only minimal interactions formed with

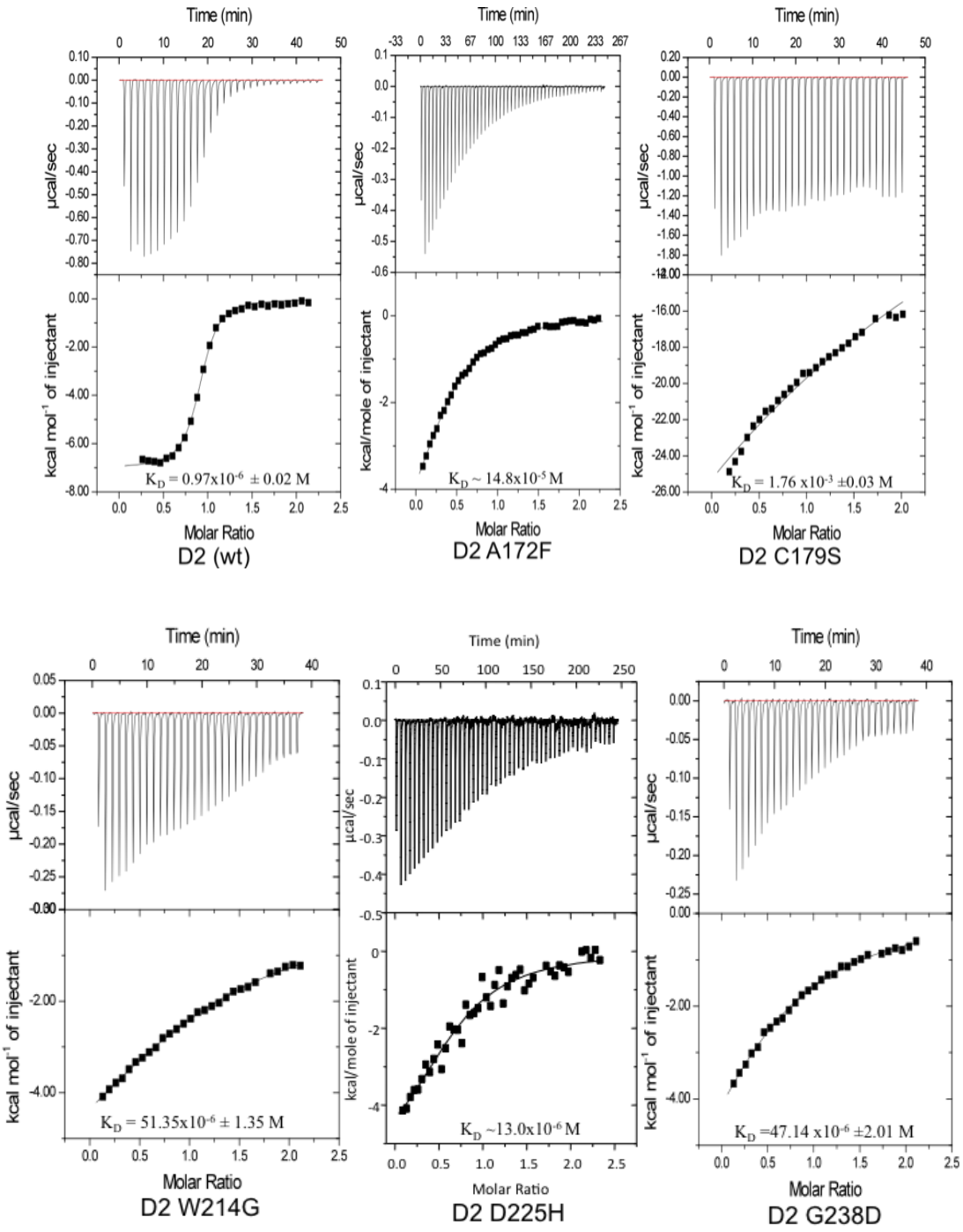


**Figure 4.12** - shows the isothermal titration calorimetry data of each of wild type and the mutants of D2 with SOS. The raw data was fitted to a two-site binding model. The lower panel depicts the raw data of the µmol/s of heat release at various molar ratios of the lipid to protein. The concentration of protein used was ~50 µM and the ligand was ~0.5 mM. 10mM phosphate buffer containing 50 mM ammonium sulfate and 100 mM NaCl was used in each of the titrations.

SOS. The Pfeiffer syndrome (PS) mutation A172F of D2 showed a 7-fold decrease ($K_D$) in the interaction with heparin. The position of the A172F residue is not directly involved in the binding of heparin. However, the binding pocket of heparin on the D2 domain stretches across the β-strand wherein the A172F mutation site is located. Increased flexibility of residues around A172 may result in higher flexibility of residues that interact with heparin. This result is expected to reduce the signaling efficiency of the D2 domain as heparin contributes to the stabilization of the 2: 2: 2 complex formed with FGF.

The isothermal titration calorimetry data of each of the D2 mutants with FGF was also measured to determine changes in the binding interaction (fig. 4.13). FGF binds to wild type D2 with a binding affinity 2.2 μM. The isothermograms shown in figure 4.12 suggests this interaction is significantly decreased for each of the mutants of the D2 domain. The interaction of C179S, W214G, D225H and G238D were reduced to insignificant binding. The PS mutation, D2 A172F, showed a decreased binding interaction resulting in a moderate affinity for FGF-1 ($K_D$ ~91μM).

Monitoring the structural changes caused due to mutations in the D2 domain: Superposition of the $^{1}H$-$^{15}N$ HSQC spectrum of C179S mutant overlaid on D2 (wt) shows consistent with local structural changes caused at the mutation site. Crosspeaks show significant $^{1}H$-$^{15}N$ chemical perturbations (>1ppm) and could not be unambiguously traced are highlighted in blue. This data suggests the disulfide bond formed between residues C179 and C230 significantly stabilize the D2 domain. The chemical perturbations of D2 C179S mapped onto the structure of D2 shows a patch of perturbed residues near the c-terminal of the D2 domain.

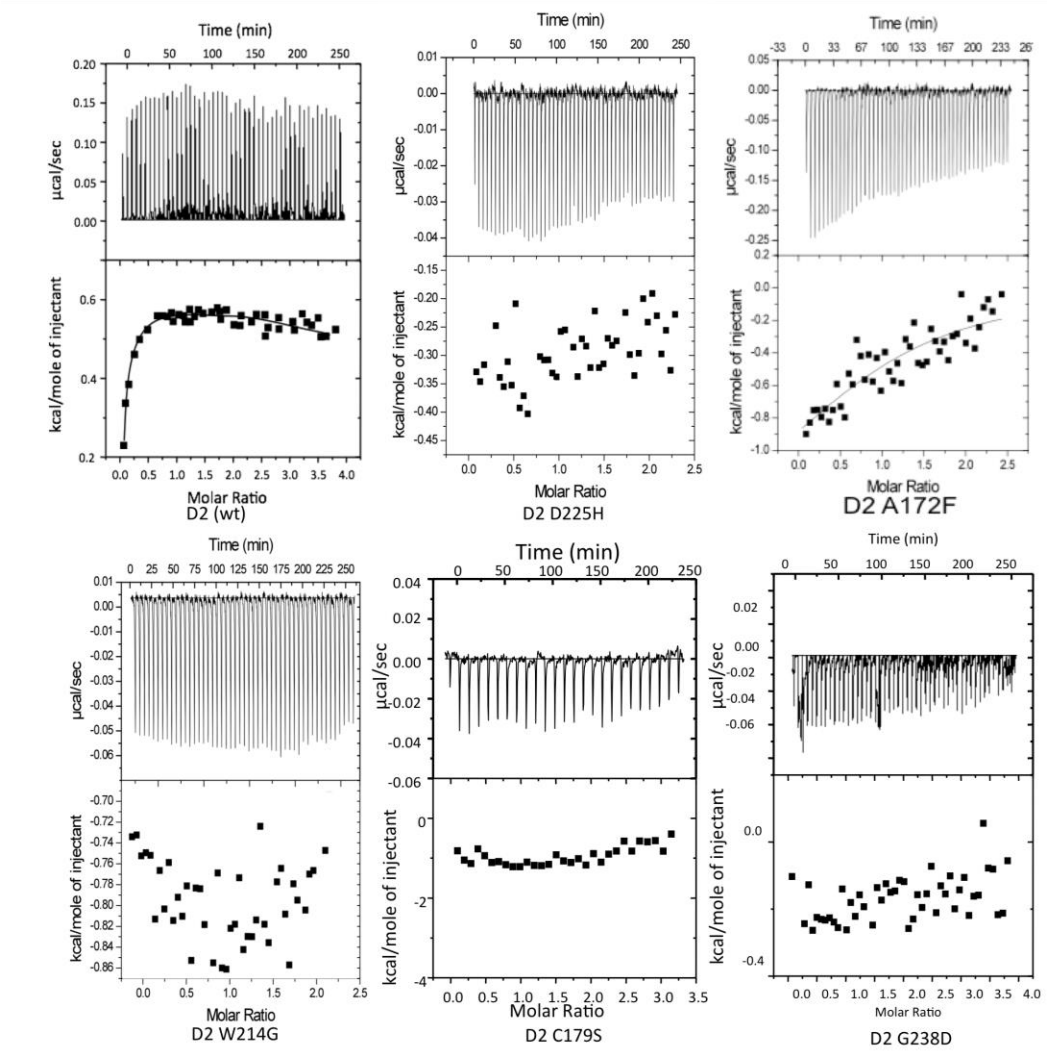


**Figure 4.13** – Binding isotherm for the titration of D2 and the D2 mutants with FGF. The top panel shows the raw data from the titration. The bottom panel shows the integrated data derived from the raw data. Kallmann syndrome mutants of D2 (C179S, W214G, D225H and G238D) exhibit typical isothermograms supporting a loss-of-binding with the FGF-1 ligand. The Pfeiffer syndrome mutant (D2 A172F) showed a reduced interaction with FGF-1 ($K_D$ ~ 90 µM).

Hydrophobic c-terminal residues H166, A168, V170, L246 and V248 are required for interactions with FGF-1. Residues H245, L246, D247 and V248 are significantly perturbed in the $^{1}H$-$^{15}N$ HSQC of D2 C179S.

Figure 4.16 shows the overlay of the $^{1}H$-$^{15}N$ HSQC spectra of the W214G mutant and wild type D2 domain. Several $^{1}H$-$^{15}N$ crosspeaks in the HSQC spectrum of the W214G mutant show significant chemical shift perturbations. Most of these correspond to residues located in the β-strands βD and βE. Incidentally, several of these residues constitute the binding site for heparin. Interestingly, some of the residues, which show significant 1H-15N chemical shift perturbations are located in β-strand G and constitute the FGF binding interface.

Effect of mutations on the D2-SOS interaction: The $^{1}H$-$^{15}N$ HSQC of W214G in the presence of SOS (fig. 4.16) shows a significant number of chemical shifts. The residues that show significant chemical shift perturbations in the presence of SOS include K161, K176 and K208. However, residues R210 and H213 that provide interactions to SOS in D2 (wt) are not visibly perturbed in the W214G mutant. The lower affinity of the W214G mutant to SOS/heparin is plausibly caused due to increased flexibility of the amino acid segment involved in SOS binding. Interestingly, the lower binding of the W214G mutant is corroborated by ITC results.

Overlay of $^{1}H$-$^{15}N$ HSQC spectra of the D225H mutant on that of the D2 (wt) reveals moderate perturbations in the D225H mutant (fig. 4.17). The chemical shift perturbation plot of D225H reveals the most perturbed residues are located in the central and -terminal portions of the D2 structure. The amino acid sequence spanning residues H245-L249 are significantly perturbed and located in the FGF binding site of the D2 domain. These residues are located in the βG strand, which is adjacent to the βD stand where the D225H mutation is located. Additionally, residues in the amino acid segment Y207 – H213 are also prominently perturbed. These residues occur in the flexible loop portion of D2. It appears that the D225H disrupts structural interactions with the Y207 – H213 segment also.

Superposition of $^{1}H$-$^{15}N$ HSQC spectra of D225H in the presence of SOS is shown in figure 4.17. Minor perturbations occur at the N-terminal and central regions of the D2 structure. The most perturbed residues include E160, K161, M162 and K176. The residues of D2 (wt) that form the heparin-binding site include K208, K161, R210, H213 and K176. Residues K208, R210 and H213 are not significantly perturbed in the D2 domain. Additionally, the $^{1}H$-$^{15}N$ HSQC of the D225H mutant shows moderate perturbations in the amino acid sequence Y207-H213. Residues K208 and R210 are in the perturbed regions of D225H and contribute to the binding site of heparin. The lack of chemical shifts during the $^{1}H$-$^{15}N$ HSQC titration of D225H using SOS suggests the flexibility in this region may decreases the interaction of K208 and R210 with SOS.

$^{1}H$-$^{15}N$ HSQC spectrum of G238D overlaid on wild type shows moderate perturbations across the D2 domain (figure 4.19). The D2 G238D mutation occurs at the turn between strands βF-βG strands. $^{1}H$-$^{15}N$ HSQC spectrum of the G238D mutation reveals the aspartic acid mutation causes the most significant perturbations in the amino acid segment E236 –S239. Residues in this segment are situated in close proximity to the G238 mutation site. Additionally, moderately perturbed residues extend down the β-strand G. The βG- strand extends to the C-terminus of the D2 domain and constitutes a significant portion of the FGF binding site. Therefore, perturbations in β-strand G likely causes local structural change that plausibly leads to loss-of-binding to the ligand, FGF-1. The loss of FGF-1 binding is supported by the ITC data. The G238D mutation prominent changes observed in the $^{1}H$-$^{15}N$ HSQC spectrum of G238D suggest that native β-sandwich structure of the D2 domain is significantly disrupted.

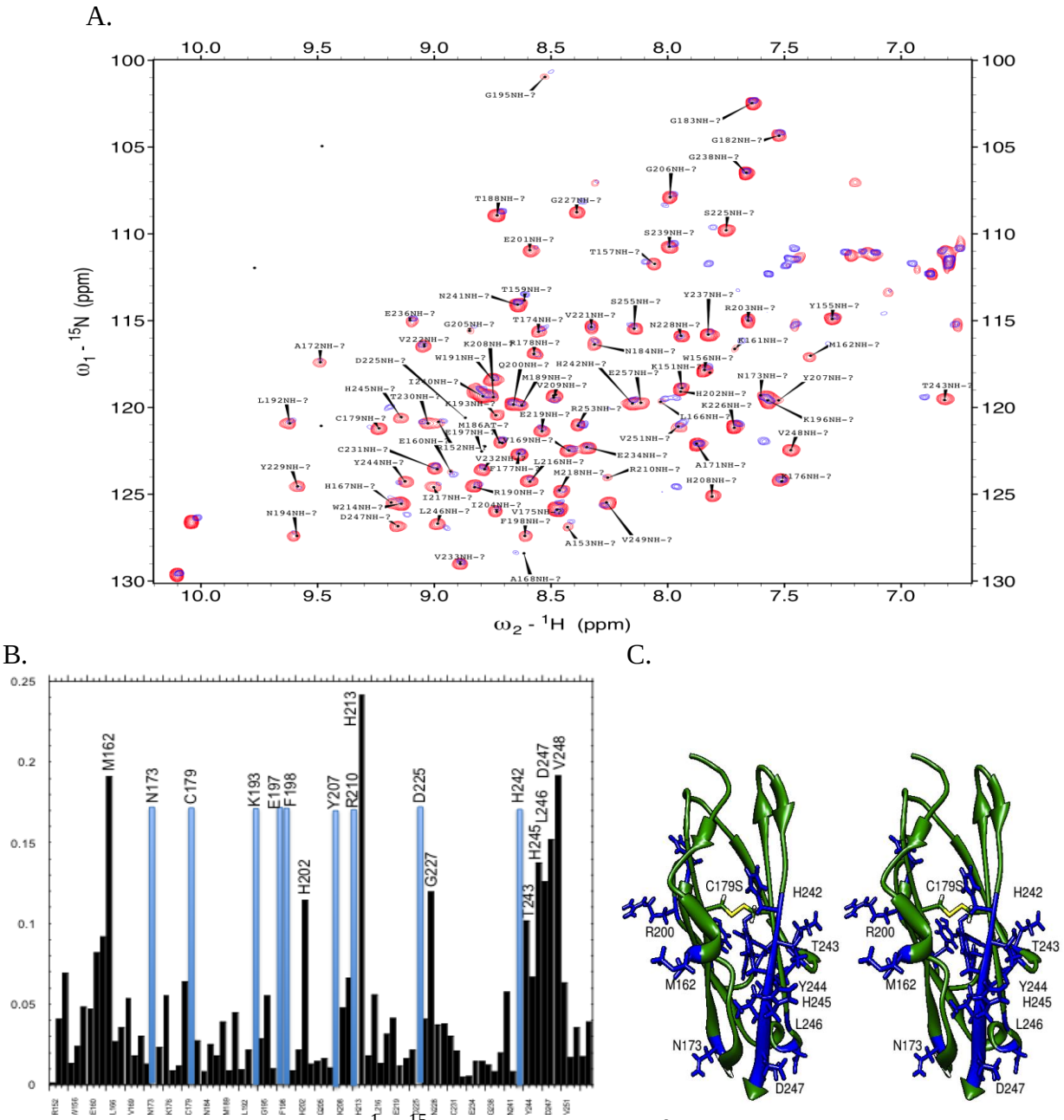


**Figure 4.14**– **Panel A** shows an $^{1}H$-$^{15}N$ HSQC spectrum of D2 C179S (blue) mutant overlaid on wild type D2 (red). **Panel B** The weighted average (of $^{1}H$ and $^{15}N$) chemical-shift perturbation [$\Delta\delta = \sqrt{((\delta H)^2 + 0.2(\delta^{15}N)^2)}$] of residues in the C179S mutant compared to wild type D2. The blue bars indicate crosspeaks in the C179S mutant of D2 that were significantly shifted and could not be unambiguously identified. The horizontal line arbitrarily set at 0.1 ppm to highlight residues which show significant chemical-shift perturbations. **Panel C** is a structural stereo-view representation (pdb -1wvz) of the D2 domain highlighting the residues (blue) which show $^{1}H$-$^{15}N$ chemical perturbation greater than 0.10 ppm. The site of the C179S mutation is colored in red. Most perturbed residues resulting from the C179S mutation is located on β-strand F and the C-terminal beta strand G.

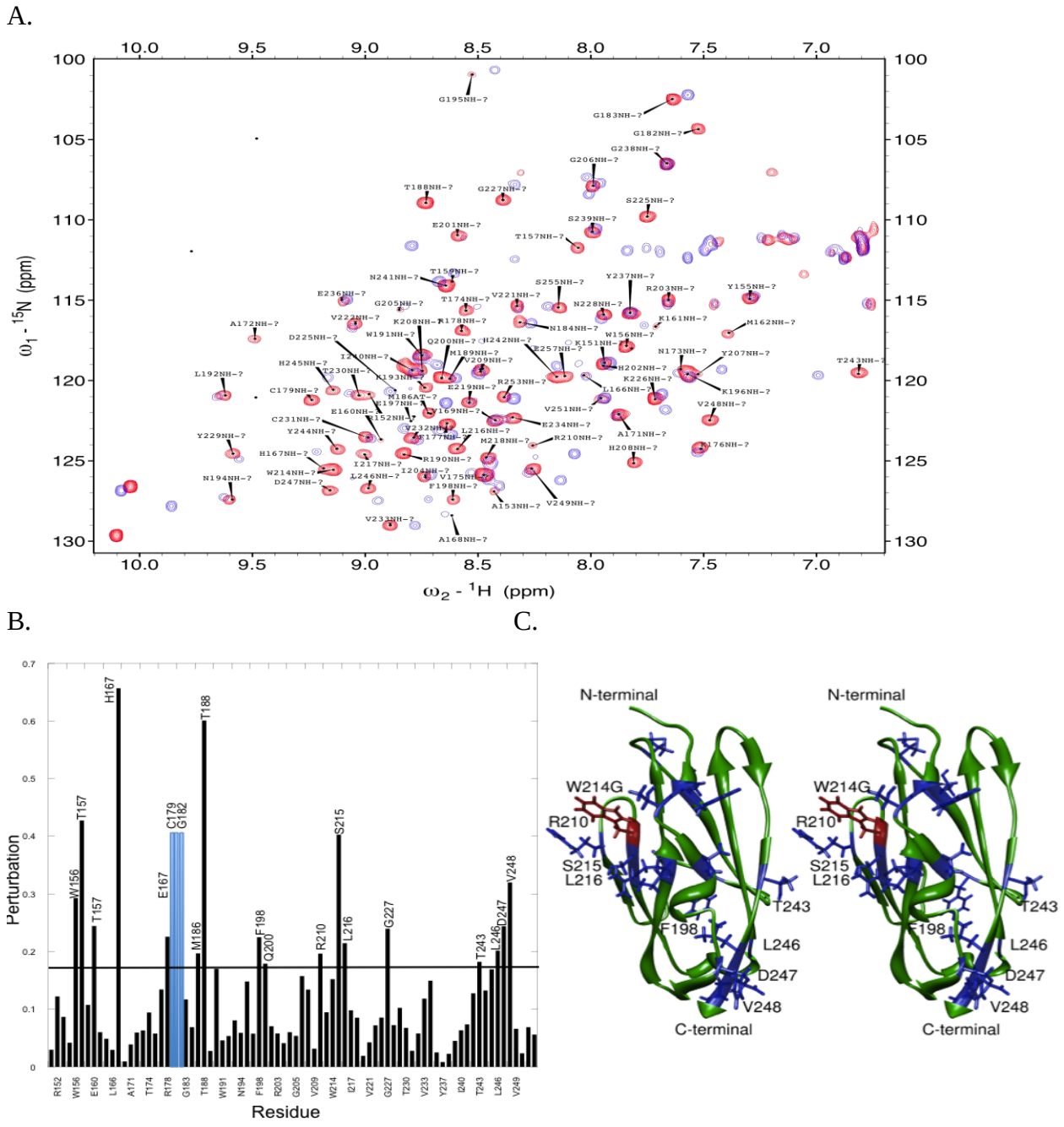


**Figure 4.15**– **Panel A** shows an $^1$H-$^{15}$N HSQC spectrum of W214G (blue) mutant overlaid on wild type D2 (red). **Panel B** The weighted average (of $^1$H and $^{15}$N) chemical-shift perturbation [$\Delta\delta = \sqrt{((\delta H)^2 + 0.2(\delta^{15}N)^2)}$] of residues in the W214G mutant compared to wild type D2. The blue bars indicate crosspeaks in the W214G mutant of D2 that were significantly shifted and could not be unambiguously identified. The horizontal line arbitrarily set at 0.1 ppm to highlight residues, which show significant chemical-shift perturbations. **Panel C** is a structural stereo-view representation (pdb -1wvz) of the D2 domain highlighting the residues (blue) which show $^1$H-$^{15}$N chemical perturbation greater than 0.10 ppm. The site of the W214G mutation is colored in red.

A.

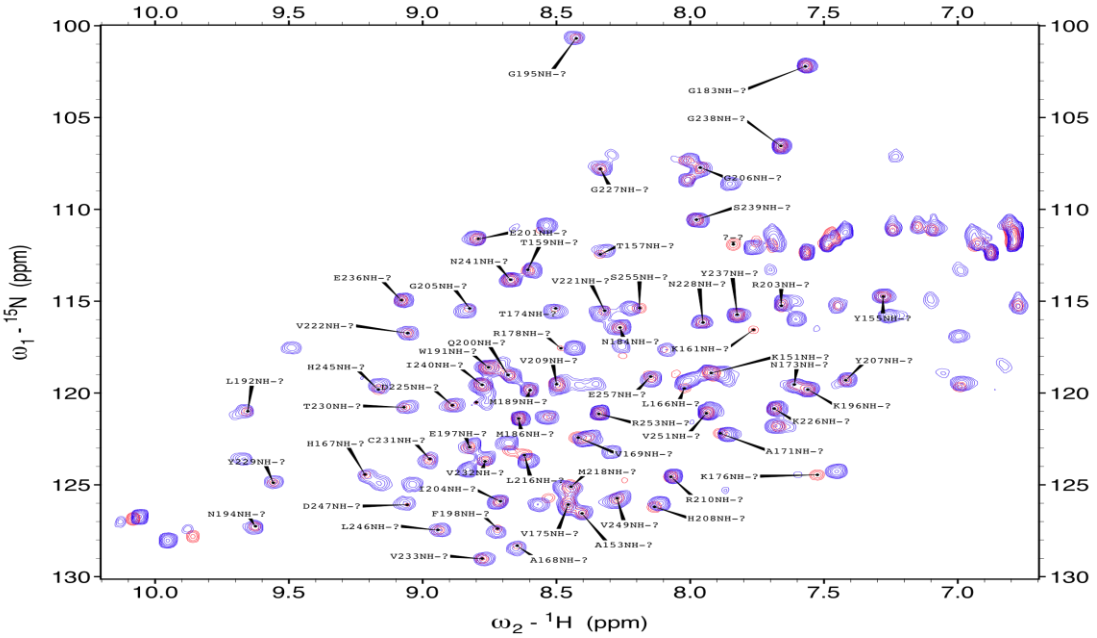


B.

C.

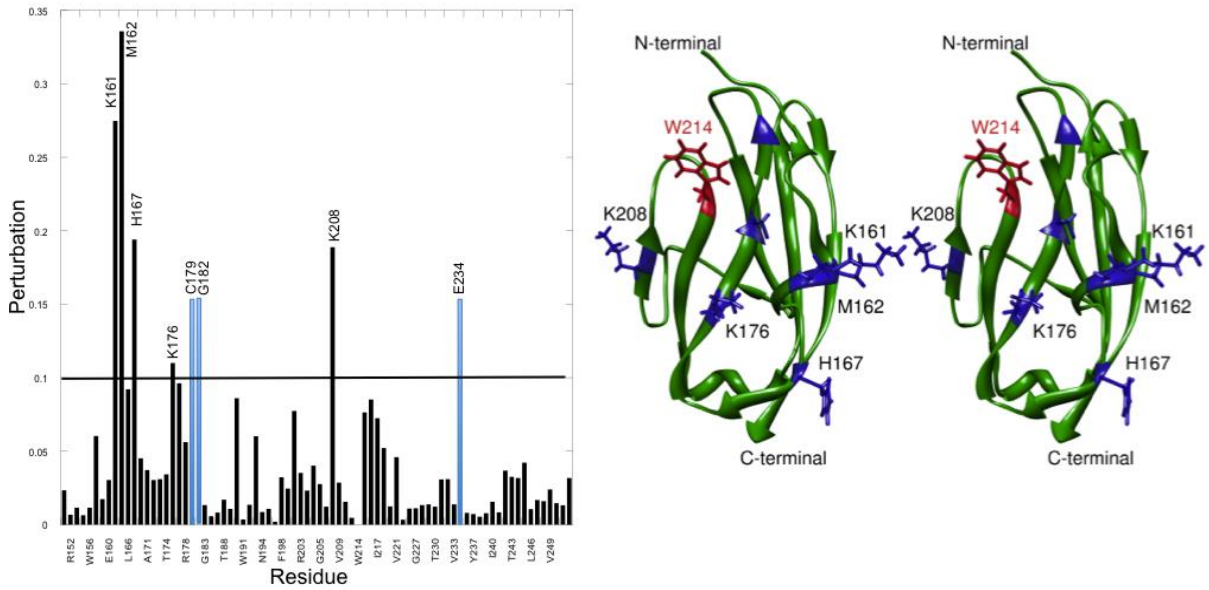


**Figure 4.16 – Panel A** shows the $^1$H-$^{15}$N HSQC of D2 W214G + SOS (blue) overlaid on wild type D2 W214G (red). **Panel B** The weighted average (of $^1$H and $^{15}$N) chemical-shift perturbation [$\Delta\delta = \sqrt{((\delta H)^2 + 0.2(\delta^{15}N)^2)}$] of residues in the W214G mutant of D2 compared to wild type D2. The horizontal line arbitrarily set at 0.1 ppm to indicate the significant chemical-shift perturbations from those that show insignificant chemical perturbations (< 0.1 ppm). **Panel C** is a structural stereo view representation (pdb -1wvz) of D2 highlighting the residues (blue) with chemical perturbations greater than 0.1 ppm. The site of the W214G mutation is colored in red. Many of the most perturbed residues resulting from the addition of SOS to the W214G mutation of D2 is located at the residues (K161, H167, K176 and K208) responsible for interacting with heparin on the wild type D2 domain.

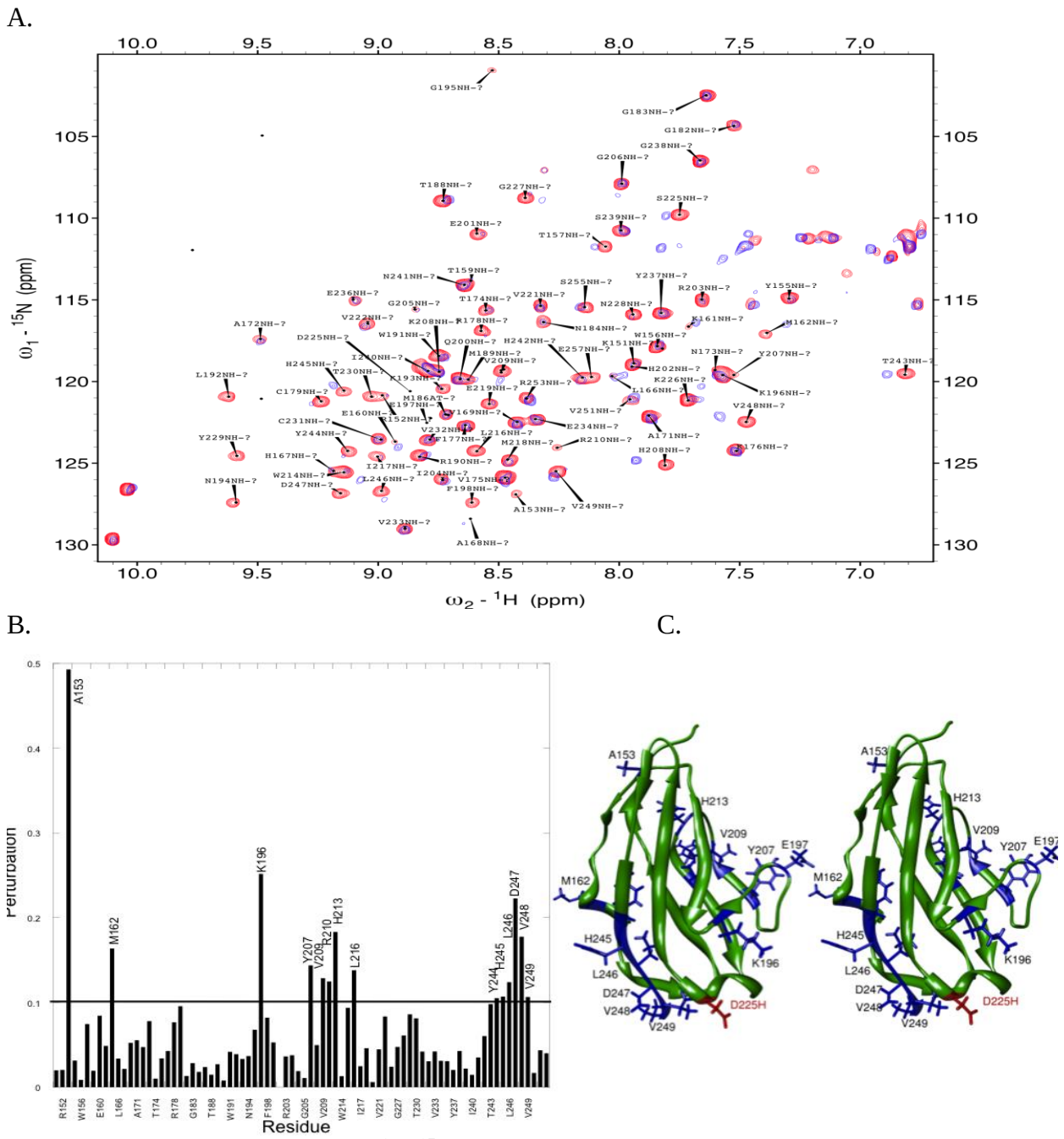


**Figure 4.17**– **Panel A** shows an $^{1}H$-$^{15}N$ HSQC spectrum of D225H (blue) mutant overlaid on wild type D2 (red). **Panel B** The weighted average (of $^{1}H$ and $^{15}N$) chemical-shift perturbation [$\Delta\delta = \sqrt{((\delta H)^2 + 0.2(\delta^{15}N)^2)}$] of residues in the D225H mutant compared to wild type D2. The blue bars indicate crosspeaks in the D225H mutant of D2 that were significantly shifted and could not be unambiguously identified. The horizontal line arbitrarily set at 0.1 ppm to highlight residues which show significant chemical-shift perturbations. **Panel C** is a structural stereo-view representation (pdb -1wvz) of the D2 domain highlighting the residues (blue) which show $^{1}H$-$^{15}N$ chemical perturbation greater than 0.10 ppm. The site of the D225H mutation is colored in red.

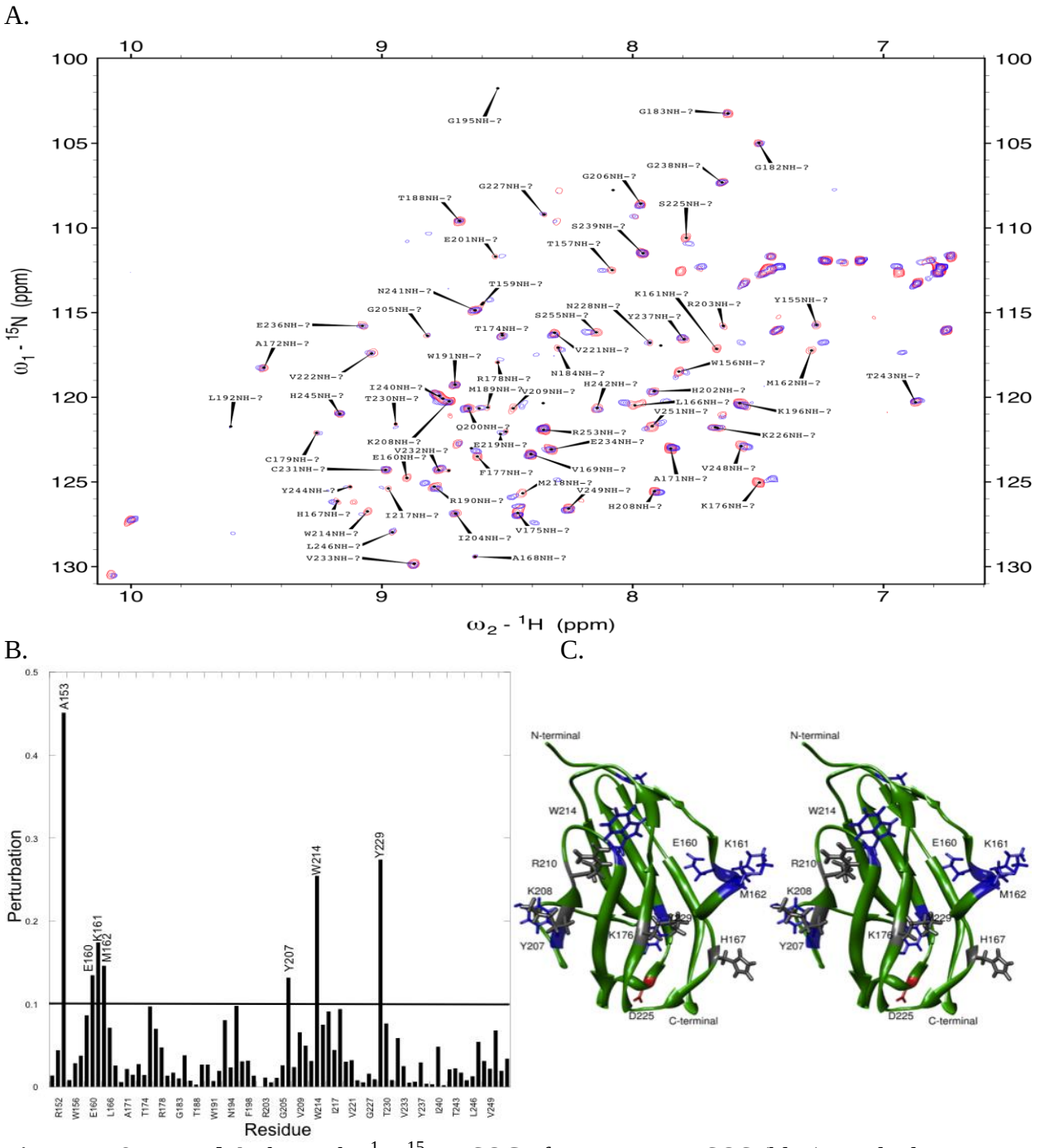


**Figure 4.18 – Panel A** shows the $^{1}$H-$^{15}$N HSQC of D2 D225H + SOS (blue) overlaid on D225H (red). **Panel B** The weighted average (of $^{1}$H and $^{15}$N) chemical-shift perturbation [$\Delta\delta = \sqrt{((\delta H)^2 + 0.2(\delta^{15}N)^2)}$] of residues in the D225H mutant with SOS compared to D225H. The horizontal line arbitrarily set at 0.1 ppm to indicate the significant chemical-shift perturbations from those that show insignificant chemical perturbations (< 0.1 ppm). **Panel C** is a structural stereo view representation (pdb -1wvz) of D2 highlighting the residues (blue) with chemical perturbations greater than 0.1 ppm. The site of the G238D mutation is colored in red. Many of the most perturbed residues resulting from the D225H mutation of D2 is located on charged residues (K161, K176, K208 and R210) responsible or interacting with SOS.

A.

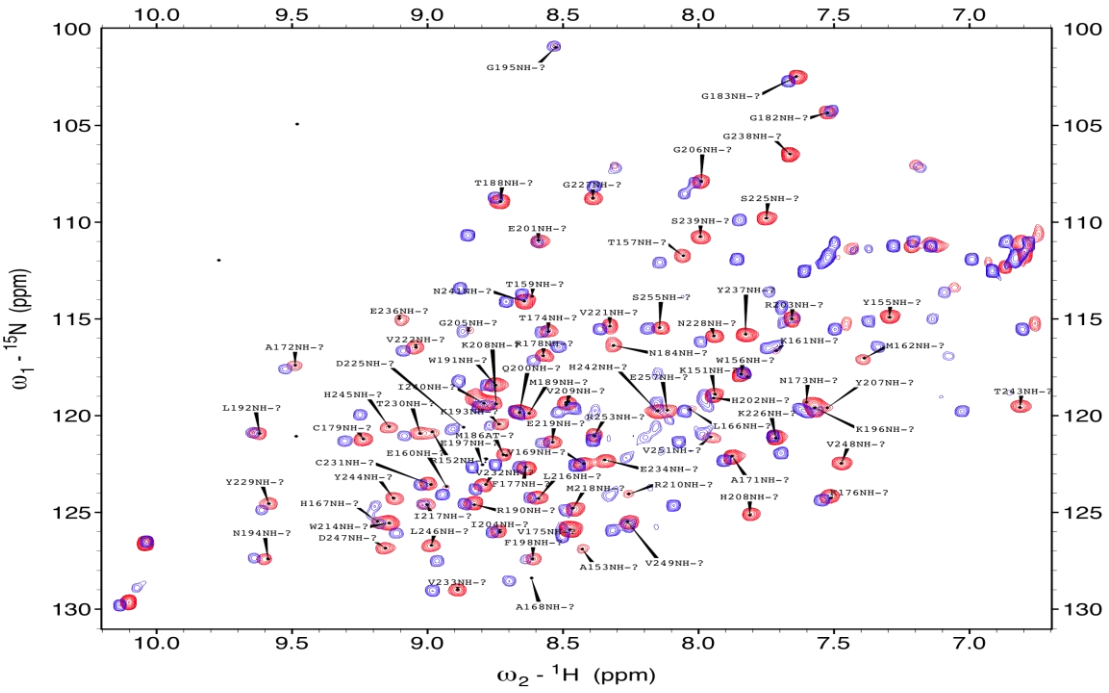


B.

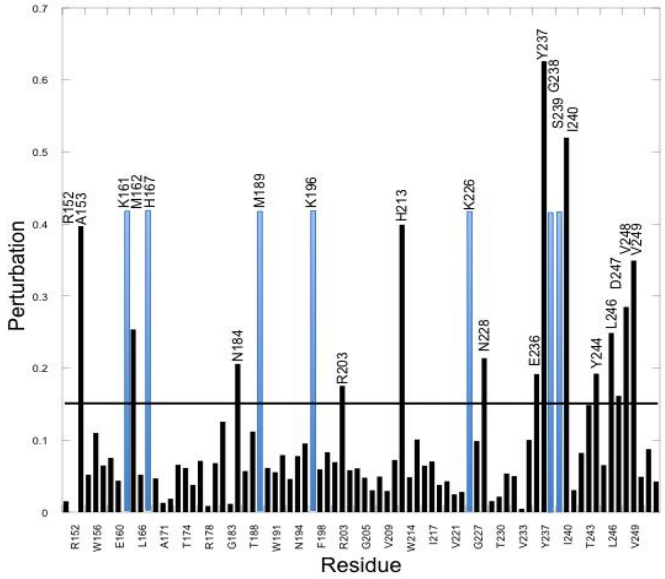


C.

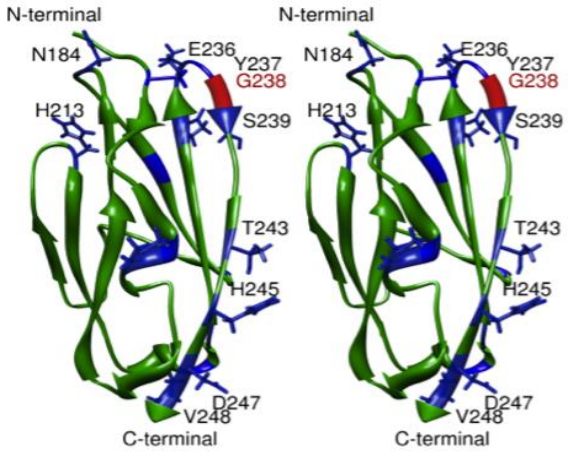


**Figure 4.19**– **Panel A** shows an $^{1}$H-$^{15}$N HSQC spectrum of G238D (blue) mutant overlaid on wild type D2 (red). **Panel B** The weighted average (of $^{1}$H and $^{15}$N) chemical-shift perturbation [$\Delta\delta = \sqrt{((\delta H)^2 + 0.2(\delta^{15}N)^2)}$] of residues in the G238D mutant compared to wild type D2. The blue bars indicate crosspeaks in the G238D mutant of D2 that were significantly shifted and could not be unambiguously identified. The horizontal line arbitrarily set at 0.1 ppm to highlight residues which show significant chemical-shift perturbations. **Panel C** is a structural stereo-view representation (pdb -1wvz) of the D2 domain highlighting the residues (blue) which show $^{1}$H-$^{15}$N chemical perturbation greater than 0.10 ppm. The site of the G238D mutation is colored in red. Most perturbed residues resulting from the G238D mutation is located on β-strand F and the C-terminal beta strand G.

## Discussion

Kallmann's syndrome may be associated numerous mutations that occur in the fibroblast growth factor receptor 1. The FGFR1 loss-of-function theory has been postulated for mutations in the receptor resulting in Kallmann's syndrome. The mutations C179S, W214G, D225H and G238D of D2 showed many different biophysical changes with some specific similarities.

***C179S Mutation of D2 shows a significant change in the thermodynamic stability and it interactions with heparin and FGF-1.*** Disruption of the disulfide bond formed by C179 and C230 resulted in very significant changes in the stability of the D2 domain. The increased flexibility upon disruption of the disulfide bond is most notably observed by the rapid cleavage during the limited trypsin digestion and the low melting temperature ($T_m$ ~28 ºC) determined using differential scanning calorimetry. Despite these significant stability changes in the D2 structure the secondary structure appears not to be significantly changes. The circular dichroism measurements of the C179S mutant of D2 suggest the mutation does not disrupt the native ß-sheet structure observed in wild type D2. Additionally, this data is supported by the steady-state fluorescence maximum wavelength that very closely matches the maximum wavelength of wild type D2. The steady-state fluorescence suggests the only subtle structural changes result from the C179S mutant. The isothermal titration calorimetry data supports ligand binding experiments suggest the C179S mutant significantly hinders the interaction with both FGF-1 and heparin. The isothermal titration thermogram supports negligible binding occurs between the C179S mutant of D2 and heparin. Additionally, results of the isothermal titration calorimetry experiments support that the ligand, FGF-1, binding is lost upon disruption of the disulfide bond. Although it is no yet known if heparin is required for signaling, the D2 domain must interact with FGF for signal transduction to occur. $^{1}H$-$^{15}N$ HSQC perturbation plots of the C179S mutant of D2 shows

significant perturbations occurring at the c-terminal domain of ß-strand G. Additionally, significant structural perturbations result across the middle portion of the D2 domain and between the two ß-sheets that form the ß-sandwich of D2. This data plausibly supports a partial opening of the D2 domain structure, separating the positively charged residues responsible for the interaction with heparin. The perturbation of the central portion of the structure of the D2 domain as well as the perturbations of the C-terminal domain residues supports the loss-of-binding of the D2 domain to heparin and FGF.

***W214G mutation of D2 results in a significant reduction in its interaction with FGF.*** The W214 is located between strands ßD – ßE in the structure of the D2 domain. In Addition, W214 has several residues which are located in lose vicitinity. The W214G mutation of D2 results in very little changes in secondary structural as supported by the circular dichroism data. The steady-state fluorescence shows a signficant shift in the wavelength maximum of 339 nm observed in wild type D2 to 308 nm for the W214G mutant of D2. Although the maximum wavelength shift is very large the shift may be a result of the removal of one of the three tryptophans in D2. The decrease in the stability of the D2 domain as a result of the W214G mutation can be inferred from the differential scanning calorimetry and limited trypsin digestion experiments. The limited trypsin digestion experiment support an increase in the backbone flexibility. The differential scanning calorimetry data support a moderate decrease in the stability of the D2 domain (decrease in $T_m$ ~ 5 ºC). The isothermogram shows the ligand binding interactions of the W214G mutant results in a 25-fold decrease in the binding interaction with heparin. Additionally, results of the isothermal titration calorimetry experiment of the W214G

mutant of D2 with FGF-1 shows no significant binding interactions. $^{1}H$-$^{15}N$ chemical shift perturbation plots of the W214G mutant shows significant perturbations in the heparin binding region, surrounding the W214 as well as in the C-terminal region of the D2 molecule. The C-terminal domain is responsible for the hydrophobic interactions required for FGF binding. Significant $^{1}H$-$^{15}N$ chemical shift perturbations in the c-terminal domain support the loss-of-binding to FGF. The $^{1}H$-$^{15}N$ HSQC spectrum of W214G in the presence of SOS shows prominent perturbations at residues K208, K176 and K161. However, significant perturbations are not observed at residues R210 and H213 which are located in the heparin binding site of wild type D2. The close proximity of these residues to the W214G mutation appears to weaken interactions with heparin due to increase flexibility or moderate structural perturbations.

***D225H mutant of D2 results in a significant decrease in affinity to FGF.*** D225H does not cause significant change in the secondary structure. The circular dichroism and steady-state fluorescence closely resemble the data acquired on wild type D2. The limited trypsin digestion data suggests there is an increase in the backbone flexibility as a result of the D225H mutant of D2. Although there is increased flexibility, differential scanning calorimetry experiments suggests that the stability of the D225H mutant is comparable to wild type ($\Delta T_m$ ~ 1 ºC). The minor decrease in melting temperature of the D225H mutant of D2 does not support a significant charge-charge interaction with R203. The isothermal titration calorimetry data suggests the heparin binding affinity of D225H is decreased seven-fold compared to wild type D2. Additionally the isothermal titration calorimetry indicate that binding interaction of the D225H mutant of D2 with FGF-1 is completely inhibited. $^{1}H$-$^{15}N$ HSQC perturbation plot of the D225H mutant of D2 compared to wild type suggests the mutation most signficantly perturbs the strand ßD-ßE and at the C-terminal ßG strand. The hydrophobic FGF binding pocket formed by the ßA'

and ßG strands. The loss of FGF binding by the D225H mutant of D2 is further supported by the pertrubations occuring in the ßG strand.

***G238D mutant of D2decreases the stability of the D2 domain and also reduces the binding interaction with FGF:*** *Pitteloud et al.* previousy proposed that the lowered expression of the G238S mutant of D2 results from the retention of the misfolded protein in the endoplasmic reticulum(23). Circular dichroism and steady-state fluorescence structural studies suggest the ß-sheet formation and the tertiary structure formation of the D2 domain are not due to the G238D mutation. Limited trypsin digestion and ANS titration experiments suggest the D238G mutation increases the backbone flexibility and the exposure of hydrophobic residues. Additionally, the differential scanning calorimetry experiments suggest the mutation results in a significant decrease in the stability of the D2 domain ($\Delta T_m$ ~12 ºC). Isothermal titration calorimetry binding experiments suggest the G238D mutant of D2 significantly reduces the interaction with heparin by 25-fold. Additionally, ITC rsults suggests that the G238D mutantion causes a loss-of-binding to FGF-1. $^{1}H$-$^{15}N$ HSQC chemical perturbation plots of the G238D mutation of D2 compared to wild type suggest the most prominent structural peturbations occur at ß-strands F and G. The perturbation of ß-strand G is centered at the FGF binding site on the D2 domainIt appears that introduction of a negatively charged residue in the middle of β-strand F cuases a subtle conformations changes which causes loss-of-binding to the lignad, FGF-1.

In conclusion, Kallmann syndrome mutations appear to induce critical local structural changes at the heparin and FGF-1 binding sites, which in turn effect the FGF-signalling process.

***Pfeiffer syndrome mutations have been suggested to result in an increased signaling.*** A172F mutation did not cause major changes in the stability of the D2 domain. Steady-state fluorescence and circular dichroism data suggests that the A172F mutation retains most of the native secondary structural interactions. Additionally, ANS titration and limited trypsin digestion support a minor increase in the backbone flexibility and a greater exposure of the solvent-exposed non-polar surfaces. Interestingly the ligand binding interaction of the A172F mutant of D2 and heparin is decreased 7-fold compared with the wild type. Heparin plays an important role in the formation of the 2: 2: 2 ternary signaling complex composed of heparin: D2: FGF. Destabilization of the interaction of the D2 domain with heparin would also be expected to decrease the signaling of the receptor. Therefore, the results of this study are not consistent with the gain-of-function proposed for the Pfeiffer syndrome mutations. Results of phosphorylation assays of the A172F mutant of D2 reported by Ibrahami et. al showed that A172F mutation enhances the tyrosine phosphorylation activity(26). These results suggest that pfeiffer mutation cause increased activation of the FGF receptor. Crystal structure of the D2-D3 homodimer of FGFR shows that phenylalanine 172 in one monomeric unit of the D2 domain is involved in a positive pi-stacking interaction with the complementary monomeric unit of the D2 domain. This pi-stacking interaction acts to stabilize the dimeric structure of the FGF receptor and consequently activates the FGF receptor even in the absence of the ligand, FGF (26). Interestingly, ITC results obtained in this study do not support the hypothesis proposed by Ibrahimi et al. ITC data suggests that the A172F mutant has ~45-fold lower affinity to FGF than the wild type D2 domain. At the present juncture, the reasons for the observed disparity in the results between this study and the published report is not clear. More detailed experiments including tyrosine kinase assays comparing the autophosphorylation potency of the wild type and

the A172F need to be performed in the future to understand the structure-function relationship of the A172F Pfeiffer sydrome mutation.

**Literature Cited**


1. Naftolin, F., G. Harris and M. Bobrow 1971. Effect of purified luteinizing hormone releasing factor on normal and hypogonadotrophic anosmic men. Nature. 232, 496-497.

2. Zenaty, D., P. Bretones, C. Lambe, I. Guemas, M. David, J. Leger and N. de Roux 2006. Paediatric phenotype of kallmann syndrome due to mutations of fibroblast growth factor receptor 1 (FGFR1). Mol. Cell. Endocrinol. 254, 78-83.

3. Pawlowitzki, I. H., P. Diekstall, A. Schadel and P. Miny 1987. Estimating frequency of kallmann syndrome among hypogonadic and among anosmic patients. Am. J. Med. Genet. 26, 473-479.

4. Bianco, S. D. and U.B. Kaiser 2009. The genetic and molecular basis of idiopathic hypogonadotropic hypogonadism. Nat. Rev. Endocrinol. 5, 569-576.

5. Albuisson, J., C. Pecheux, J.C. Carel, D. Lacombe, B. Leheup, P. Lapuzina, E. Legius, G. Matthijs, M. Wasniewska, M. Dwlpech, J. Young, J.P. Hardelin and C. Dode 2005. Kallmann syndrome: 14 novel mutations in KAL1 and FGFR1 (KAL2). Hum. Mutat. 25, 98-99.

6. Gill, J. C., S.M. Moenter and P.S. Tsai 2004. Developmental regulation of gonadotropin-releasing hormone neurons by fibroblast growth factor signaling. Endocrinology. 145, 3830-3839.

7. Raivio, T., Y. Sidis, L. Plummer, H. Chen, J. Ma, A. Mukherjee, E. Jacobson-Dickman, R. Quinton, G. Van Vliet, H. Lavoie, V.A. Hughes, A. Dwyer, F.J. Hayes, S. Xu, S. Sparks, U.B. Kaiser, M. Mohammadi and N. Pitteloud 2009. Impaired fibroblast growth factor receptor 1 signaling as a cause of normosmic idiopathic hypogonadotropic hypogonadism. Jcem., 4380-4390.

8. Pedersen-White, J. R., L.P. Chorich, D.P. Bick, R.J. Sherins and L.C. Layman 2008. The prevalence of intragenic deletions in patients with idiopathic hypogonadotropic hypogonadism and kallmann syndrome. Mol. Hum. Reprod. 14, 367-370.

9. Pitteloud, N., R. Quinton, S. Pearce, T. Raivio, J. Acerno, A. Dwyer, L. Plummer, V. Hughes, S. Seminara, Y. Cheng, W. Li, G. Maccoll, A.V. Eliseenkova, S.K. Olsen, O. Ibrahimi, F.J. Hayes, P. Boepple, J.E. Hall, P. Bouloux, M. Mohammadi and W.J. Crowley 2007. Digenic mutations account for variable phenotypes in idiopathic hypogonadotropic hypogonadism. J. Clin. Invest. 117, 457-463.

10. Sato, N., T. Hasegawa, N. Hori, M. Fukami, Y. Yoshimura and T. Ogata 2005. Gonadotrophin therapy in kallmann syndrome caused by heterozygous mutations of the gene for fibroblast growth factor receptor 1: Report of three families: Case report. Hum. Reprod. 20, 2173-2178.

11. Trarbach, E. B., E.M. Costa, B. Versiani, M. de Castro, M.T. Baptista, H.M. Garmes, B.B. de Mendonca and A.C. Latronico 2006. Novel fibroblast growth factor receptor 1 mutations in patients with congenital hypogonadotropic hypogonadism with and without anosmia. J. Clin. Endocrinol. Metab. 91, 4006-4012.

12. Pitteloud, N., J.S. Acierno Jr, A.U. Meysing, A.A. Dwyer, F.J. Hayes and W.F. Crowley Jr 2005. Reversible kallmann syndrome, delayed puberty, and isolated anosmia occurring in a single family with a mutation in the fibroblast growth factor receptor 1 gene. J. Clin. Endocrinol. Metab. 90, 1317-1322.

13. Colvin, J., A. White, S. Pratt and D. Ornitz 2001. Lung hypoplasia and neonatal death in Fgf9-null mice identify this gene as an essential regulator of lung mesenchyme. Development. 128, 2095-2106.

14. Feldman, B, Poueymirou, W., Papaioannou, V.E., DeChiara, T.M. and Goldfarb, M. 1995. Requirement of FGF-4 for postimplantation mouse development. Science. 267, 246-249.

15. Plotnikov, A.N., Hubbard, S.R., Schlessinger, J., Mohammadi, M. 2000. Crystal structure of FGF2 in complex with the extracellular lignad binding domain of FGF receptor 2 (FGFR2). Cell. 101, 413-424.

16. Raivio, T., Y. Sidis, L. Plummer, H. Chen, J. Ma, A. Mukherjee, E. Jacobson-Dickman, R. Quinton, G. Van Vliet, H. Lavoie, V.A. Hughes, A. Dwyer, F.J. Hayes, S. Xu, S. Sparks, U.B. Kaiser, M. Mohammadi and N. Pitteloud 2009. Impaired fibroblast growth factor receptor 1 signaling as a cause of normosmic idiopathic hypogonadotropic hypogonadism. J. Clin. Endocrinol. Metab. 94, 4380-4390.

17. Plotnikov, A. N., J. Schlessinger, S.R. Hubbard and M. Mohammadi 1999. Structural basis for FGF receptor dimerization and activation. Cell. 98, 641-650.

18. Dode, C., J. Levilliers, J.M. Dupont, A.D. Paepe, N.L. Du, N. Soussi-Yanicostas, R.S. Coimbra, S. Delmaghani, S. Compain-Nouaille and F. Baverel 2003. Loss-of-function mutations in FGFR1 cause autosomal dominant kallmann syndrome. Nat. Genet. 33, 463-465.

19. Plotnikov, A. N., J. Schlessinger, S.R. Hubbard and M. Mohammadi 1999. Structural basis for FGF receptor dimerization and activation. Cell. 98, 641-650.

20. Trokovic, N., R. Trokovic, P. Mai and J. Partanen 2003. Fgfr1 regulates patterning of the pharyngeal region. Genes Dev. 17, 141-153.

21. Ballabio, A. and G. Andria 1992. Deletions and translocations involving the distal short arm of the human X chromosome: Review and hypotheses. Hum. Mol. Genet. 1, 221-227.

22. Hebert, J. M., M. Lin, J. Partanen, J. Rossant and S.K. McConnell 2003. FGF signaling through FGFR1 is required for olfactory bulb morphogenesis. Development. 130, 1101-1111.

23. Pitteloud, N., J.S. Acierno Jr, A. Meysing, A.V. Eliseenkova, J. Ma, O.A. Ibrahimi, D.L. Metzger, F.J. Hayes, A.A. Dwyer, V.A. Hughes, M. Yialamas, J.E. Hall, E. Grant, M. Mohammadi and W.F. Crowley Jr 2006. Mutations in fibroblast growth factor receptor 1 cause both kallmann syndrome and normosmic idiopathic hypogonadotropic hypogonadism. Proc. Natl. Acad. Sci. U. S. A. 103, 6281-6286.

24. Plotnikov, A. N., S.R. Hubbard, J. Schlessinger and M. Mohammadi 2000. Crystal structures of two FGF-FGFR complexes reveal the determinants of ligand-receptor specificity. Cell. 101, 413-424.

25. Hung, K. W., T.K. Kumar, K.M. Kathir, P. Xu, F. Ni, H.H. Ji, M.C. Chen, C.C. Yang, F.P. Lin, I.M. Chiu and C. Yu 2005. Solution structure of the ligand binding domain of the fibroblast growth factor receptor: Role of heparin in the activation of the receptor. Biochemistry. 44, 15787-15798.

26. Ibrahimi, O. A., B.K. Yeh, A.V. Eliseenkova, F. Zhang, S.K. Olsen, M. Igarashi, S.A. Aaronson, R.J. Linhardt and M. Mohammadi 2005. Analysis of mutations in fibroblast growth factor (FGF) and a pathogenic mutation in FGF receptor (FGFR) provides direct evidence for the symmetric two-end model for FGFR dimerization. Mol. Cell. Biol. 25, 671-684.

27. Beenken, A., A.V. Eliseenkova, O.A. Ibrahimi, S.K. Olsen and M. Mohammadi 2012. Plasticity in interactions of fibroblast growth factor 1 (FGF1) N terminus with FGF receptors underlies promiscuity of FGF1. J. Biol. Chem. 287, 3067-3078.

28. Yeh, B. K., M. Igarashi, A.V. Eliseenkova, A.N. Plotnikov, I. Sher, D. Ron, S.A. Aaronson and M. Mohammadi 2003. Structural basis by which alternative splicing confers specificity in fibroblast growth factor receptors. Proc. Natl. Acad. Sci. U. S. A. 100, 2266-2271.

29. Schlessinger, J., A.N. Plotnikov, O.A. Ibrahimi, A.V. Eliseenkova, B.K. Yeh, A. Yayon, R.J. Linhardt and M. Mohammadi 2000. Crystal structure of a ternary FGF-FGFR-heparin complex reveals a dual role for heparin in FGFR binding and dimerization. Mol. Cell. 6, 743-750.

30. Zenaty, D., P. Bretones, C. Lambe, I. Guemas, M. David, J. Leger and N. de Roux 2006. Paediatric phenotype of kallmann syndrome due to mutations of fibroblast growth factor receptor 1 (FGFR1). Mol. Cell. Endocrinol. 254-255, 78-83.

31. Pitteloud, N., A. Meysing, R. Quinton, J.S. Acierno Jr, A.A. Dwyer, L. Plummer, E. Fliers, P. Boepple, F. Hayes, S. Seminara, V.A. Hughes, J. Ma, P. Bouloux, M. Mohammadi and W.F. Crowley Jr 2006. Mutations in fibroblast growth factor receptor 1 cause kallmann syndrome with a wide spectrum of reproductive phenotypes. Mol. Cell. Endocrinol. 254-255, 60-69.

**Structure and Functional Characterization of the R203C Mutation of D2 Commonly Found in Breast Cancer**

**Abstract:**

Fibroblast growth factor signaling mediates key cellular processes including cell differentiation, mitogenesis, angiogenesis, neuron development and tumor growth. Mutations found in the FGF receptor are associated with 5- 10% of human breast cancer cases (1-3). Associated with these single nucleotide polymorphisms is the R203C mutation located in the FGF receptor D2 domain (3). Using a variety of biophysical methods including multidimensional NMR techniques we have shown that the R203C mutation in the D2 domain of FGFR2 decreases the binding affinity between FGF and heparin. The loss-of-binding suggests a decrease in the FGF induced activation of the R203C mutant of FGFR2.

**Introduction**:

Cancerous cells are the combination of accumulated mutations and/or the overexpression of proteins resulting in a malignancy (4). Characterization of malignant cells shows six properties required to maintain tumor growth. Malignant cancer cells require: insensitivity of anti-growth signals, self-sufficiency in growth signals, unlimited replicative potential, uncontrolled cell proliferation, invasive metastasis of distant tissues and sustained supply to nutrients and oxygen to promote growth (4). Cancer cells often have a significant number of mutations that have accumulated over a prolonged period of time. Among the many cell growth and regulatory genes, receptor tyrosine kinases are highlighted as protein accumulating mutations that may result in changes in the cellular regulations (4).

Fibroblast growth factors (FGFs) are approximately 16 kDa heparin-binding proteins that regulate key cellular processes such as angiogenesis, cell differentiation, morphogenesis, wound healing and tumor growth (5, 6). FGF receptors consist of three extracellular ligand binding domains (D1, D2, D3), a single transmembrane helix, and cytoplasmic tyrosine kinase domain. Cell surface-bound HSPGs (heparan sulfate proteoglycans) that support dimerization or oligomerization of FGFRs, which are activated during cellular processes (7). The D2 domain of the FGF receptor is suggested to bind with both HSPGs and FGFs to form a ternary complex (8). The dimerization complex of the FGFR has been well characterized by Platnikov et. al to include FGF: FGFR: heparin in a 2: 2: 2 complex (8). Formation of the dimeric complex results in autophosphorylation of seven-conserved cytoplasmic tyrosine residues (9). Subsequently, autophosphorylation of the tyrosine residues recruits SH2 domain containing proteins allowing for downstream signaling (10). FRS2 (FGF receptor substrate 2) is an SH2 domain containing

protein that docks on the FGF receptor. Phosphorylation of FRS2 results in downstream signaling and the activation of the MAPK (mitogen activated protein kinase) pathway mediating proliferation, gene expression, differentiation, apoptosis and other cellular events (11). Fibroblast growth factor receptors act as a point of activation for the MAPK pathway allowing for mutations in the FGF receptor to result in disease states (12, 13).

The R203C mutant of the FGF receptor D2 domain has been indicated as a mutation occurring in breast cancer tumors (14, 15). Fibroblast growth factor receptor 2 activated proliferation and invasion of terminal end buds of the developing breast in mice (16). Single nucleotide polymorphisms have been located in the FGFR2 gene and associated with the increased risk of breast cancer (17). FGF receptor 2 shows increased expression in breast cancer cell lines and in tumoral breast tissue (18, 19). SNPs associated with breast cancer commonly occur in the intron 2 of the FGF receptor 2 (3). Additionally, the R203C mutant of the D2 domain has been determined to be associated with breast cancer (14, 15). The R248C (bladder cancer), S249C (cervical cancer) and W290C (lung cancer) mutations result in ligand-independent dimer formations (20-23). The autodimerization and subsequent autophosphorylation result from intermolecular disulfide bonds formed between adjacent FGF receptors (24-26). The cell takes up phosphorylated fgf receptors so the protein may be recycled through proteolytic degredation in the lysosome following endocytosis (27). The enhanced stability of the interdisulfide bond inhibits protein degradation in the lysosome (28). The added lifetime of the phosphorylated FGF receptor is postulated to result in reinsertion into the membrane to continue signaling (29, 30). In this study we use multidimensional nmr and biophysical techniques to characterize the structural properties of the R203C mutant of the D2

domain. Additionally, mutants R203E, R203L and R203K were assessed to determine the wild type interactions formed by R203.

**Materials and Methods**

***Mutagenesis, overexpression and protein purification:*** The R203 mutations on the FGFR2 D2 domain (residues, 145-255) was generated using the *Quikchange* kit (Stratagene). The mutation was confirmed by automated DNA sequencing. Wild type and the R203 mutants of the D2 domain were overexpressed and purified from *Escherichia coli* [BL21 (pLysS) strain] according to the method reported previously [18].

***Far UV Circular Dichrosim (CD):*** Data on the wild type D2 and the R203 mutants were acquired using a Jasco J-710 spectropolarimeter. Protein solutions (90-100 μM) were prepared in 10 mM phosphate buffer containing 100 mM NaCl and 50 mM ammonium sulfate (pH 6.5). Wavelength scans were set to 250-190 nm. CD measurements were made using a 0.1 cm pathlength cuvette. A total of 10 scans were averaged for each sample.

***Fluorescence spectroscopy:*** Measurements were made using a Hitachi F-2500 fluorimeter. Fluorescence measurements were made using a 1.0 cm path length and the concentration of each protein sample was adjusted to ~50 μM. Excitation wavelength was set to 280 nm and intrinsic tryptophan emission was measured from 300 nm to 450 nm. 8-anilino-1-napthalene sulphonate (ANS) binding experiments were performed using an excitation wavelength of 390 nm and an emission wavelength range of 450 nm- 600 nm. In the ANS titration experiments, protein samples were titrated with 3 μl aliquots of 10 mM ANS in 10 mM phosphate buffer containing 100 mM NaCl and 50 mM ammonium sulfate at pH 6.5.

***Differential scanning calorimetry (DSC):*** DSC measurements were performed using a N-DSC III calorimeter. Protein concentration used was in the range of 1.0 – 1.5 mg/ml in 10 mM phosphate buffer containing 50 mM ammonium sulfate and 100 mM NaCl (pH ~6.5). The scan rate was set to 1 °C/min and protein samples were heated from 10 °C - 90°C. Data were analyzed using the CpCalc software provided by the manufacturer.

***Isothermal titration caolorimetry (ITC):*** ITC measurements were performed using Microcal VP titration calorimeter (Northhampton, MA, USA). Titrations consisted of 5-10 µl injections of 0.5 mM sucrose octasulfate (a heparin analog) delivered into 0.050 mM concentration of the D2 domain. Injections were delayed for 1.5 - 3.5 minutes to allow the titration peak to return to the baseline prior to additional injections. The titrations curves were analyzed using Origin software supplied by Microcal Inc.

***NMR spectroscopy:*** $^{1}H$-$^{15}N$ HSQC data were acquired at 298 °K using 0.5 mM $^{15}N$ labeled D2 domain in 10 mM phosphate buffer (prepared in 95% $H_2O$ + 5 %$D_2O$, pH 6.5) containing 50 mM ammonium sulfate and 100 mM NaCl. All experiments were performed using Bruker Avance 700 MHz and 500 MHz NMR spectrometers equipped with cryoprobes. NMR data were referenced to the $^{1}H$ resonance frequency of 2,2-dimethyl-2-silapentane-5-sulfonic acid (DSS).

**Results:**

Structure and sequence analysis shows R203 to be conserved in FGF receptors 1 – 4. Analysis of the 3D x-ray and NMR structure of the D2 domain reveal differences in the structural interactions involving R203. The x-ray crystal structure shows the side chain of R203 is directed towards the interior of the structure. The side chain non-covalent interactions formed by R203 includes a charge-charge interaction with aspartic acid 225, which is located on beta strand F.

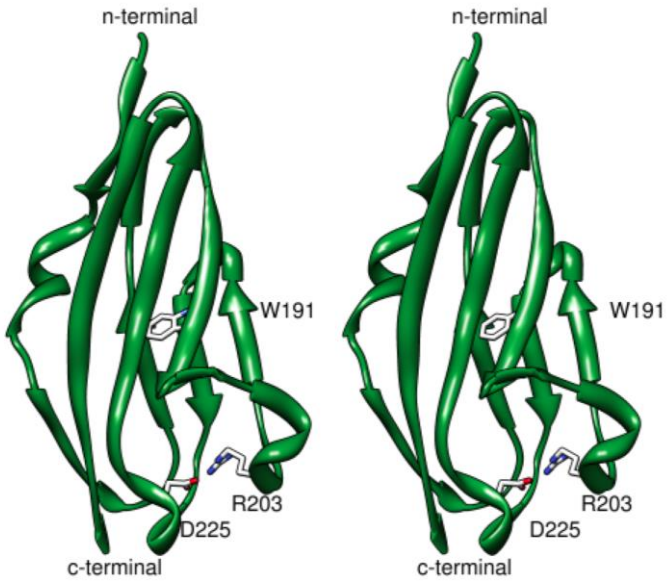


**Figure 5.1** shows the x-ray crystal stereo view structure of the D2 domain (pdb – 1ev2) (31). Aspartic acid 225 is oriented towards R203 allowing for an electrostatic interaction between side chains.

The distance of the interacting side chains of D225 and R203 are less than 5 Å. However, the NMR solution structure of the D2 domain does not place R203 – D225 within close spatial proximity to allow for an electrostatic interaction. The distance of separation between the side chain residues of R203 and D225 is approximately 12 Å(32). The distance of separation is too large for an effective electrostatic interaction. Additionally, the mutational studies support the formation of a cation-π interaction with W191 in the absence of a ligand (Supporting information in chapter 1).

*The R203 mutation of D2 only causes subtle tertiary changes in the D2 domain.* Intrinsic fluorescence serves as a useful and sensitive spectral probe to monitor tertiary structural changes in proteins. D2 domain has three well-conserved tryptophan residues that are partially buried in the interior of the protein. The microenvironment of the tryptophan is obvious from the emission maximum of the wild type D2 domain at 339 nm (fig. 5.3). The emission maximum of the R203

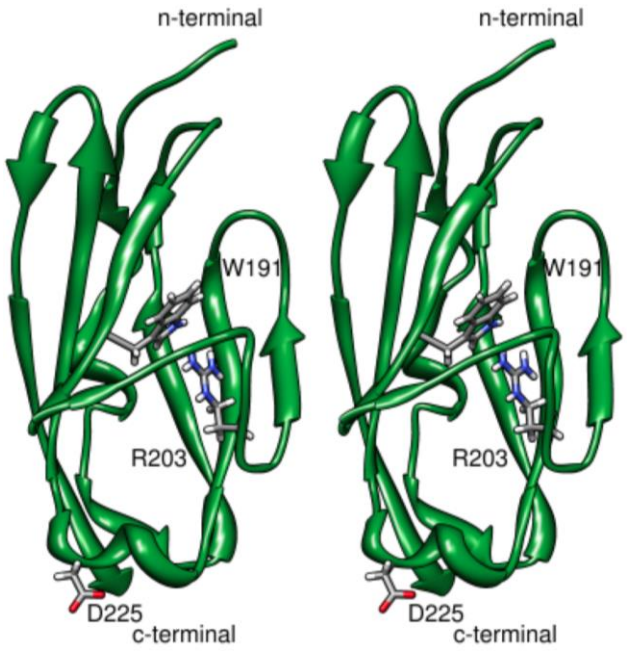


**Figure 5.2** Stereoview of the NMR solution structure of the D2 domain (pdb: 1wvz) (32).Labeled residues include R203, W191 and D225. Side chain of aspartic acid 225 shown to be projected towards the exterior of the D2 structure. Additionally, the sidechain of R203 is displaced vertically to be in close proximity to the indole ring of W191.

mutant of D2 is a modest red shift by 2-3 nm ($\lambda_{max}$ – 339 nm – 342 nm) indicating the mutation causes only a subtle tertiary conformational change (fig. 5.3). The red shift in wavelength maximum suggests an increased solvent exposure of the tryptophan indole rings of tryptophan residues found in the D2 domain.

***Tertiary structural changes:*** ANS is a popular fluorescent hydrophobic dye, which is commonly used to monitor solvent-exposed hydrophobic surfaces in proteins. ANS in the presence of the wild type D2 domain shows weak emission with an emission maxima centered at 510 nm (Fig. 5.4). However, the emission maximum of the dye shows a red shift of 4 nm (508 nm to 512 nm)

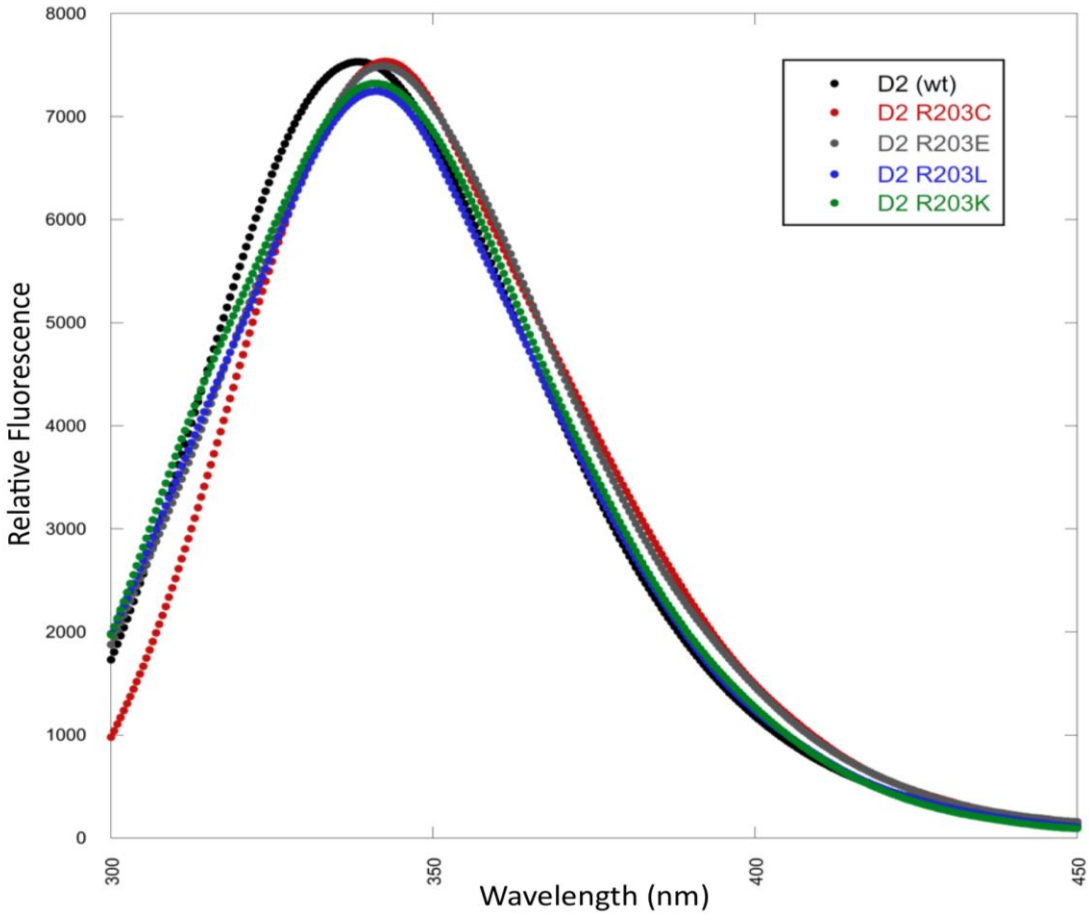


**Figure 5.3** The steady-state fluorescence spectrum of the R203 mutants of the D2 domain. The wavelength of maximum emission of the mutants of D2 show a slight red shift when compared to that of wild type D2.

with a concomitant 6-fold increase in the emission intensity. These fluorescence characteristics suggest that substitution of R203 with lysine and glutamic acid results in significant increase in the solvent exposure of hydrophobic residues.

The R203C and R203L mutants of D2 showed significant increases in relative fluorescence intensity (at 510 nm), but were considerably less than the glutamic acid and lysine mutants of D2. These results suggest that a mutation at the R203 site results in the moderate to significant solvent exposure of hydrophobic residues.

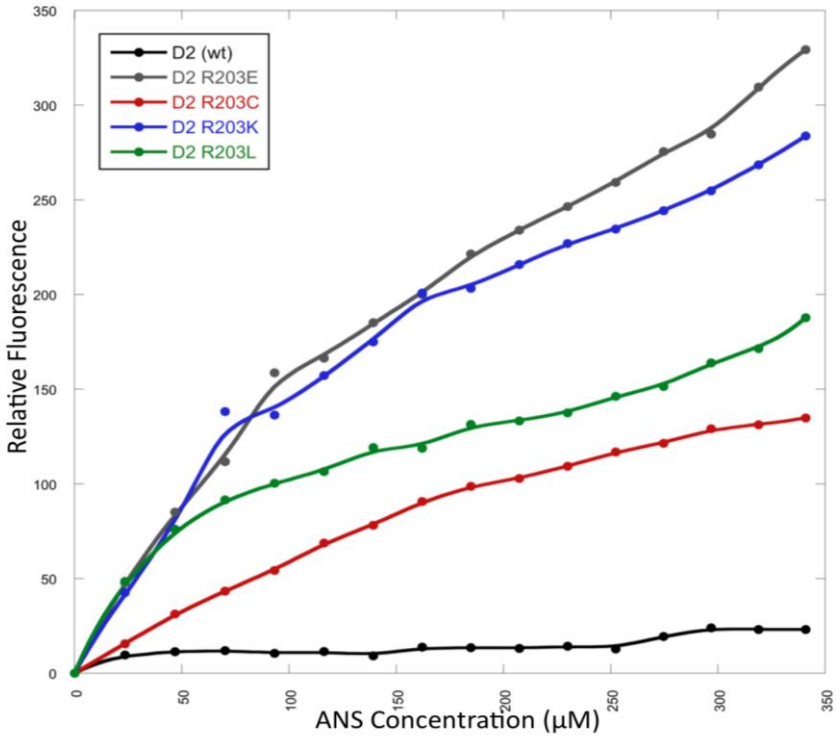


**Figure 5.4** ANS titration of the mutants of D2 and wild type. The maximum fluorescence of R203E and R203K mutants of D2 is eight fold than that of the wild type. The relative fluorescence measurements were recorded at 510 nm.

***The R203 mutation significantly decreases the thermodynamic stability and increase in the conformational flexibility of the FGF receptor domain****:* Differential scanning calorimetry is a versatile technique to directly probe the themodynamic stability of proteins. Melting thermograms of wild type D2 show a relatively sharp melting transition ($T_m$~52 ºC), from the folded to the unfolded state. (Fig. 5.5) These results suggest that mutations R203E ($T_m$ ~39 °C), R203L ($T_m$ ~42 °C) and R203K ($T_m$ ~42 °C) result in a significant decrease in the stability of the

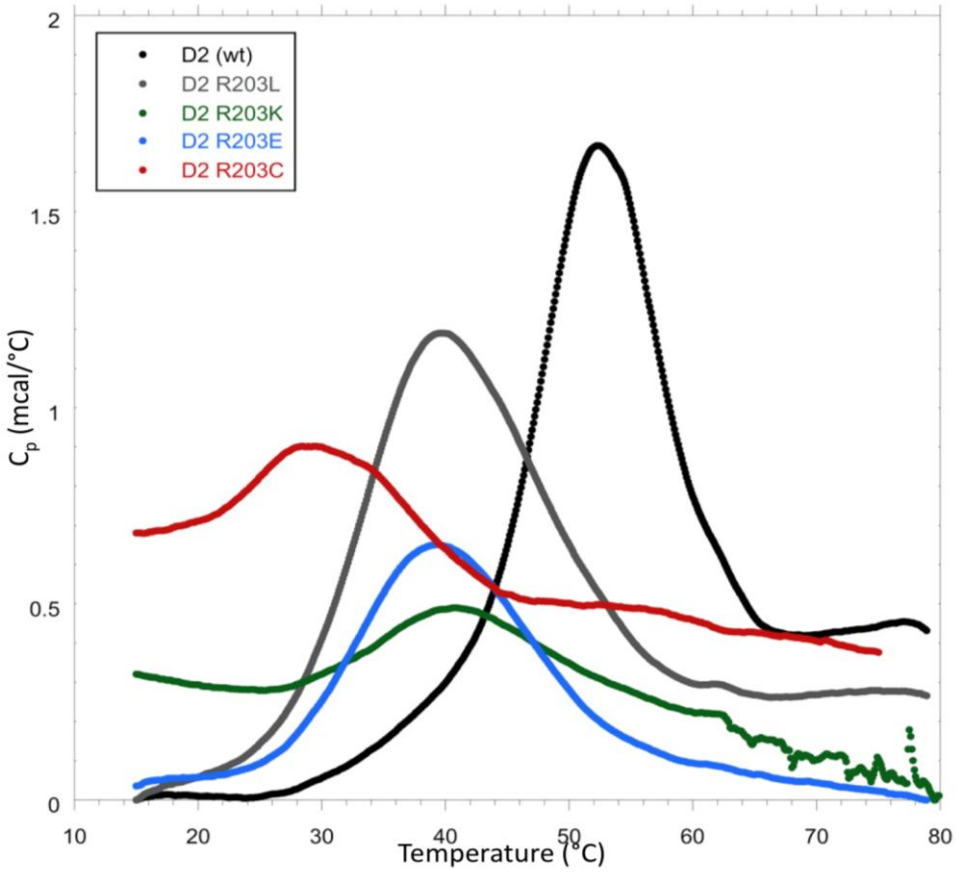


**Figure 5.5** shows an overlay of the differential scanning calorimetry thermograms of the wild type and R203 mutants of the D2 domain.

D2 domain. Additionally, the R203C mutant of D2 showed the greatest decrease in melting temperature ($T_m$ ~34 °C). The thermogram suggests the R203C mutant of D2 is moderately less stable that the other R203 mutants.

Limited trypsin digestion is a useful technique to obtain information on the backbone flexibility of proteins. Lysine and arginine residues located in flexible and solvent-accessible regions of the protein are more susceptible to trypsin cleavage than when these residues are located in the rigid portions of protein molecules. Therefore, differences in the susceptibility to trypsin cleavage can be expected to provide valuable information on the changes in the backbone flexibility due to conformational changes in the protein.

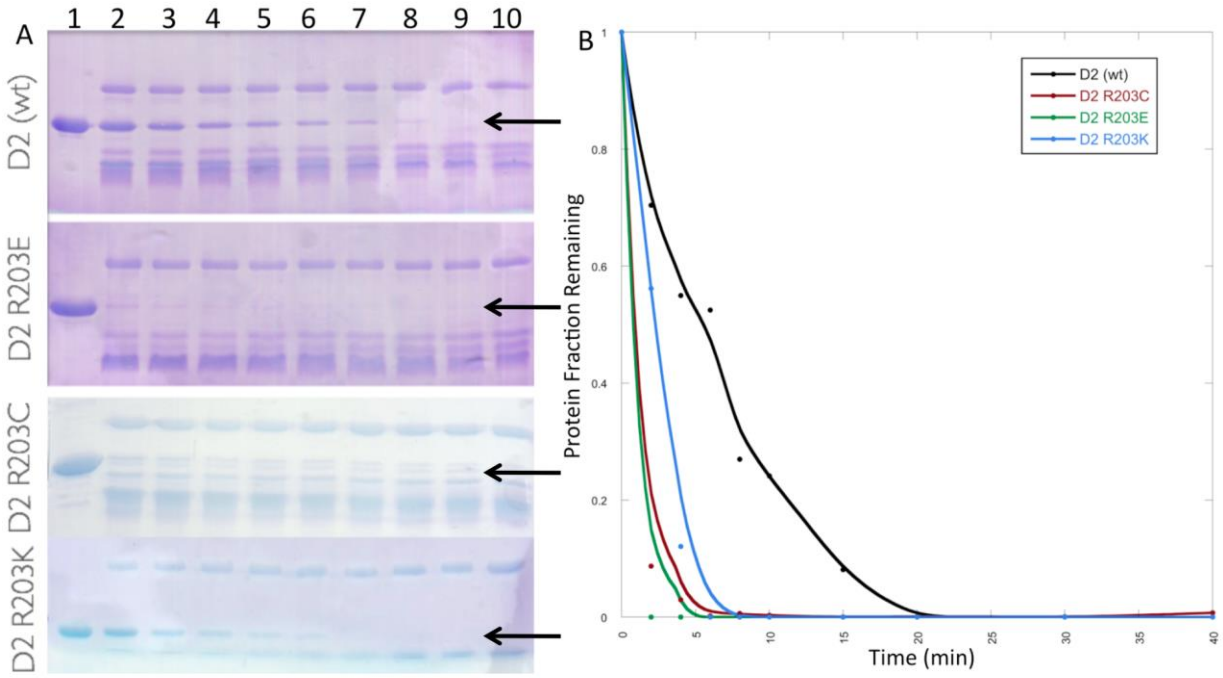


**Figure 5.6 Panel A** - shows the 15% SDS PAGE of the limited-trypsin digestion of the wild type and R203E, R203C and R203K mutants of D2 after 0, 2, 4, 6, 8, 10, 15, 20, 30 and 40 min.). The arrow indicates the protein band**. Panel B** – shows the densitometric scan of the limited-trypsin digestion of the mutants of D2 and wild type.

D2 domain of FGFR2 contains nine lysine residues and six arginine residues. The wild type protein is rapidly cleaved by trypsin in the initial few minutes of initiation of the cleavage reaction (Fig. 5.6). About 45% of the D2 parent band (MW~13.7 kDa) corresponding to the intact D2 domain remains after 10 minutes of cleavage. (Fig. 5.6) Interestingly, more than 80% of the R203K mutant protein and 90% of the R203C and R203E mutants are cleaved within the same time period (of 5 minutes; Fig. 5.6). These results in conjunction with those obtained using the far UV CD and fluorescence data suggest that the lysine substitution at position 203 only causes subtle conformational changes.

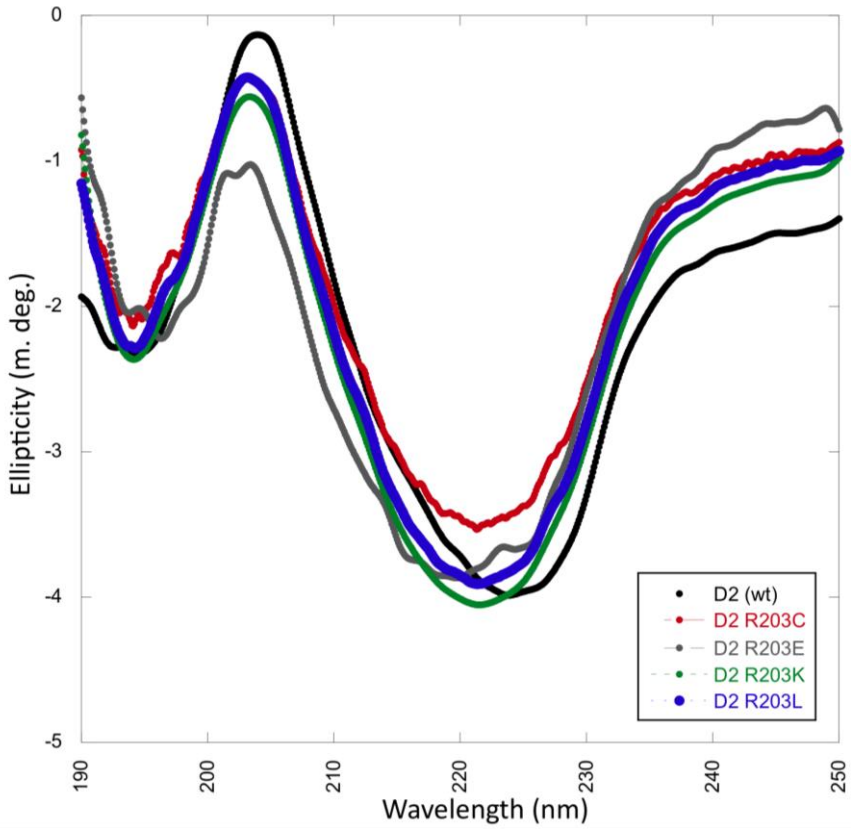


**Figure 5.7** – Far UV circular dichroism spectral overlay for the R203 mutants of D2. Wild-type D2 (black) and mutants R203C (red), R203E (grey), R203K (green) and R203L (blue).

Heparin is polydisperse and therefore, it is challenging to obtain an accurate estimation of their binding to proteins. In this context, we used sucrose octasulfate (SOS) to represent heparin binding interactions with the D2 domain. In addition, sucrose octasulfate, unlike heparin, is monodisperse and can be obtained in the pure form (>99% purity). SOS has been demonstrated to be a good structural and functional mimic of heparin.

Isothermogram representing the binding of wild type D2 domain to SOS is sigmoidal and the binding consistent ($K_d$) characterizing the SOS-D2 domain interactions is ~ 2.2 uM (Fig. S5.1). SOS and D2 domain bind to each other in a 1:1 stoichiometry. Interestingly, results of the ITC experiments performed under similar conditions show that the binding affinity of the R203C mutant for SOS is about 15 times lower than that of the wild type D2 protein. The lowering of

the heparin binding is unexpected because the mutation site (R203) is remote from the heparin-binding site in the D2 domain. However, R203 is shown to stabilize the interaction with heparin through the cation-π interaction formed with W191.

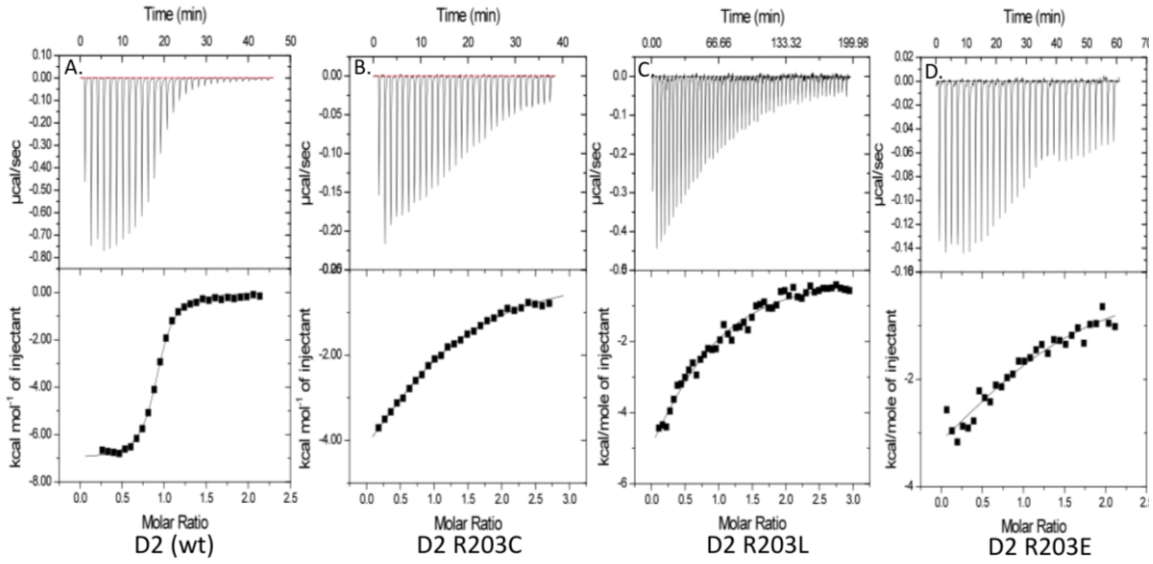


**Figure 5.8** – Binding isotherm representing the titration of D2 and D2 R203C, R203L and R203E with SOS. The top panel shows the raw data from the titration. The bottom panel shows the integrated data derived from the raw data.

The ITC experiments show the R203L and R203E mutations in D2 significantly reduce the binding interaction with SOS (fig. 5.8). The binding affinity of the R203L mutant for SOS is about 15 times lower than that of the wild type D2 protein. Additionally, the binding affinity of the R203E mutant of D2 for SOS is about 25 times lower than the interaction with D2 wild type.

Wild type D2 domain binds strongly ($K_d$~ 2 µM) to FGF-1. The binding affinity ($K_d$) of the isolated D2 domain is in the same range as that of the intact extracellular portion of FGFR suggesting that D2 domain is critical for FGF binding (fig. 5.9). Interestingly, the R203C mutant of the D2 domains exhibits a 45-fold decrease in affinity for FGF-1. These results suggest that loss-of-function from the R203C mutation.

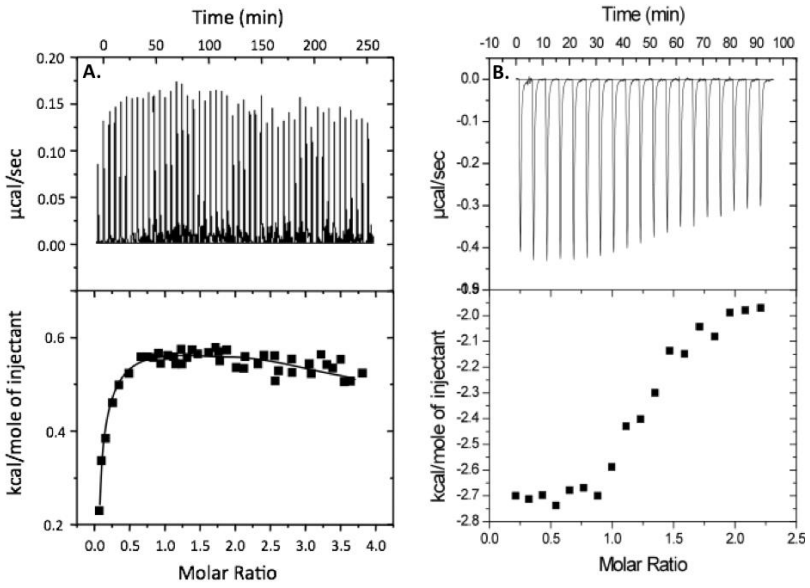


**Figure 5.9** - Binding isotherm representing the titration of the wild type and the R203C mutant of the D2 domain with FGF. The top panel shows the raw data of the titration. The bottom panel shows the integrated data derived from the raw data. Panels **A** and **B** show the titration of the wild type and the R203C mutant of the D2 domain with FGF.

***Loss of ligand binding affinity occurs due to subtle conformational changes to the D2 domain:***

Two-dimensional $^{1}H$-$^{15}N$ HSQC spectrum is a finger-print of the backbone conformation of proteins. Each crosspeak in the $^{1}H$-$^{15}N$ HSQC spectrum represents an amino acid in a particular backbone conformation of the protein. In this context, we monitored the backbone conformational changes induced due to the breast cancer related R203C mutant of D2. The $^{1}H$-$^{15}N$ HSQC spectrum overlaid on wild type shows a significant amount of overlay. However, the amino acids in close proximity to the R203C mutation site show significant perturbations. The $^{1}H$-$^{15}N$ chemical shift perturbation plot (fig 5.9) shows the most significant perturbations occurring on the C-terminal β-strand G (which is the binding site of FGF). Additionally, the structural view of the 3D structure of the D2 domain of FGFR shows that residues such as F198, K193 and K196 are also significantly perturbed in the R203C mutant. Loss-of-binding of the cation-π interactions formed by R203 and W191 appears to result in the increased flexibility of

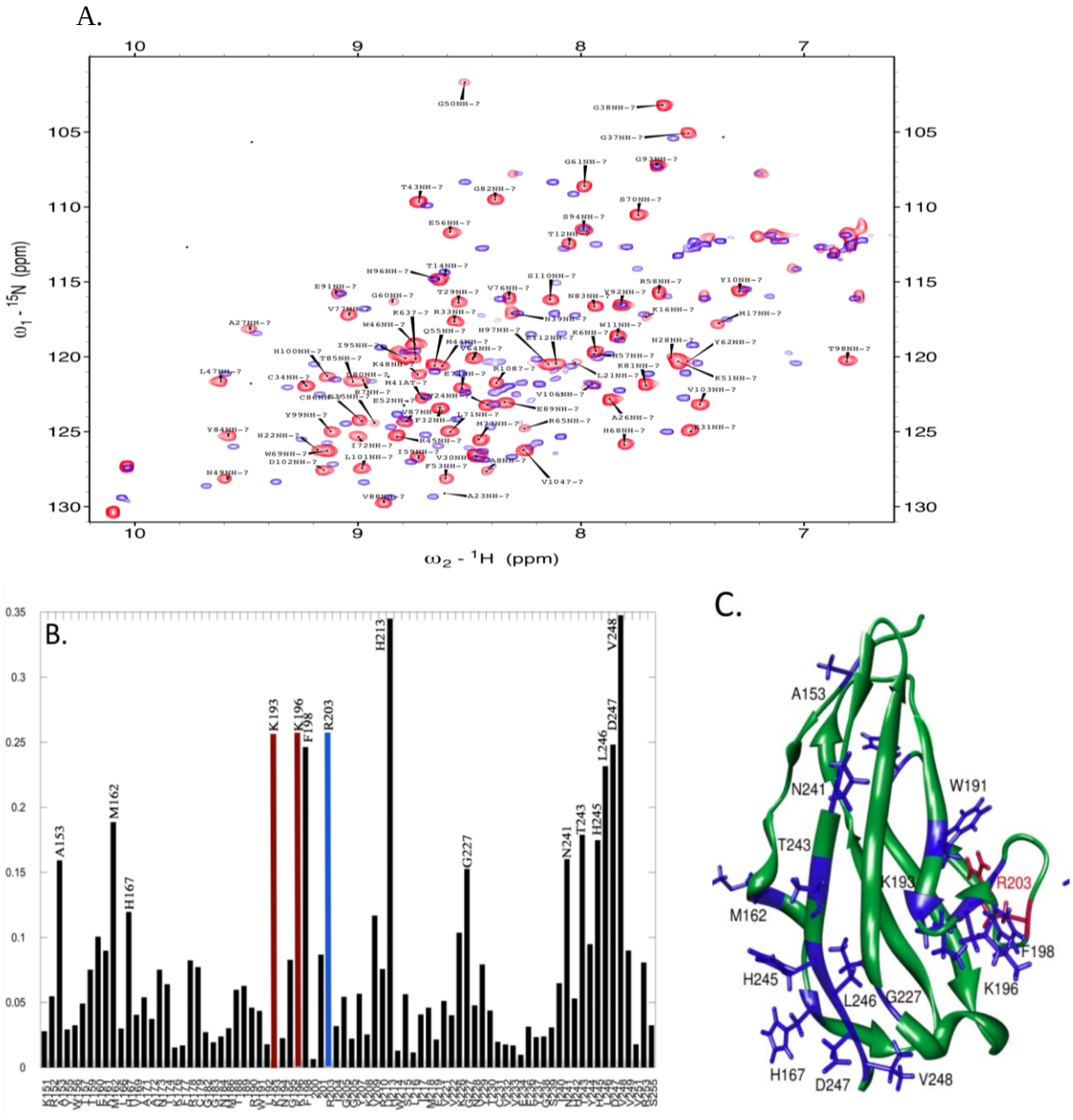


**Figure 5.10 - Panel A** shows an overlay of $^1$H-$^{15}$N HSQC spectra of D2 R203C (blue) on that of wild type D2 (red). **Panel B** The weighted average (of $^1$H and $^{15}$N) chemical-shift perturbation [$\Delta\delta = \sqrt{((\delta H)^2 + 0.2(\delta^{15}N)^2)}$] of residues in the R203C mutant of D2 compared to wild type D2. The horizontal line arbitrarily set at 0.1 ppm to indicate the significant chemical-shift perturbations from those that show insignificant chemical perturbations (< 0.1 ppm). **Panel C:** 3D structural depiction of D2 (pdb -1wvz) highlighting the residues (blue) with chemical perturbations greater than 0.1 ppm. The site of the R203C mutation is colored in red. Most of the most perturbed residues resulting from the R203C mutation of D2 is located on the C-terminal beta strand G.

the βC' – βC strands. In addition, the $^{1}H$-$^{15}N$ chemical shift perturbation plot of the R203C mutant also suggests that residues in β-strands F and G are also significantly perturbed due to the R203C mutation.

**Conclusion**

Results of the biophysical experiments on the R203C mutant do not fully support R203C is a gain-of-function mutation. The R203 side-chain extends into a hydrophobic pocket consisting of residues in β-strand C and C'. The side-chain of arginine 203 form a cation-π interaction with the indole group of W191 (chapter 2). The R203E, R203L and R203K mutants showed a consistent decrease in the melting temperature ($T_m$ ~9 –ll °C). The mutations at the 203 site produce similar structural changes. All the R203 mutants appear to lack the cation-π interaction observed between R203 and W191. Results of ANS titration reveal that both R203E and R203K enhanced solvent –exposed non-polar surfaces. Introduction of negatively charged glutamic acid residue plausibly disrupts the potential cation-π with W191. Similarly, introduction of a lysine side-chain (R203K) may not be favorable for the formation of a cation-π interaction with W191. It appears that disruption of the native R203-W191 interaction in the R203E and R203K mutants slightly opens-up the 3D structure of the D2 domain. In this context the increased solvent exposed non-polar surfaces results in R203E and R203K is supported by the ANS binding data. The R203L and R203C mutations also showed a significant decrease in melting temperature. ANS titration also suggests that there are significant solvent-exposed non-polar surfaces due to conformational change induced by these mutations (R203L and R203C). The conformational change induced in the R203L and R203C appears to be likely due to the disruption of the native cation-π interaction.

The isothermal titration calorimetry binding study shows a 15-25-fold decrease in the interaction of the mutants with heparin. This significant decrease in binding affinity to heparin suggests the heparin interaction partially is stabilized by the r203 cation-π interaction. Additionally, results from the isothermal titration calormetry characterization of the binding of R203C with FGF-1 show a 45-fold decrease in the binding affinity. The significant loss-of-interaction with both FGF-1 and heparin is further supported by the $^{1}H$-$^{15}N$ HSQC chemical shift perturbation data obtained on he R203C mutant. The R203C mutation resulted in significantly perturbed residues across both the heparin and FGF-1 binding regions. The location of the perturbed residues corroborates the significant decrease in binding affinity of both heparin and FGF-1.

Most cancers linked to the FGF receptor are believed to be due to enhanced activation of the receptor-ligand (FGF) binding. Although, R203C mutation is associated with breast cancer the same mechanism does not appear to be valid for breast cancer associated with the R203C mutation in the D2 domain of the FGF receptor. The results obtained with the R203C mutants clearly show that the mutants exhibit significantly decreased binding affinity to both heparin and FGF. Based on these results, it is reasonable to assume that the R203C mutation linked breast cancer is not due to enhanced FGF-mediated cell signaling events. Alternatively, it appears that substitution of arginine with cysteine at position 203 (R203C) induces dimerization of adjacently placed FGF receptors through formation of intermolecular disulfide bonds involving cysteine at position 203. Dimerization of FGF receptor causes its activation, triggering a sequence of down stream events resulting in unregulated proliferation of cells. However, in the absence of experimental evidence supporting dimerization of the FGF receptor through intermolecular disulfide bond formation, this mechanism should be considered as largely speculative.

**Literature Cited**


1. Gelsi-Boyer, V., B. Orsetti, N. Cervera, P. Finetti, F. Sircoulomb, C. Rouge, L. Lasorsa, A. Letessier, C. Ginestier, F. Monville, S. Esteyries, J. Adelaide, B. Esterni, C. Henry, S.P. Ethier, F. Bibeau, M.J. Mozziconacci, E. Charafe-Jauffret, J. Jacquemier, F. Bertucci, D. Birnbaum, C. Theillet and M. Chaffanet 2005. Comprehensive profiling of 8p11-12 amplification in breast cancer. Mol. Cancer. Res. 3, 655-667.

2. Chin, K., S. DeVries, J. Fridlyand, P.T. Spellman, R. Roydasgupta, W.L. Kuo, A. Lapuk, R.M. Neve, Z. Qian, T. Ryder, F. Chen, H. Feiler, T. Tokuyasu, C. Kingsley, S. Dairkee, Z. Meng, K. Chew, D. Pinkel, A. Jain, B.M. Ljung, L. Esserman, D.G. Albertson, F.M. Waldman and J.W. Gray 2006. Genomic and transcriptional aberrations linked to breast cancer pathophysiologies. Cancer. Cell. 10, 529-541.

3. Letessier, A., F. Sircoulomb, C. Ginestier, N. Cervera, F. Monville, V. Gelsi-Boyer, B. Esterni, J. Geneix, P. Finetti, C. Zemmour, P. Viens, E. Charafe-Jauffret, J. Jacquemier, D. Birnbaum and M. Chaffanet 2006. Frequency, prognostic impact, and subtype association of 8p12, 8q24, 11q13, 12p13, 17q12, and 20q13 amplifications in breast cancers. BMC Cancer. 6, 245.

4. Hanahan, D. and R.A. Weinberg 2000. The hallmarks of cancer. Cell. 100, 57-70.

5. Colvin, J.S., Green, R.P., Schmahl, J., Capel, B. and Ornitz, D.M. 2001. Male-to-female sex reversal in mice lacking fibroblast growth factor 9. Cell. 104, 875-889.

6. Feldman, B, Poueymirou, W., Papaioannou, V.E., DeChiara, T.M. and Goldfarb, M. 1995. Requirement of FGF-4 for postimplantation mouse development. Science. 267, 246-249.

7. Thornton, S.C., Mueller, S.N. and Levine, E.M. 1983. Human endothelial cells: Use of heparin in cloning and long-term serial cultivation. Science. 222, 623-625.

8. Plotnikov, A. N., J. Schlessinger, S.R. Hubbard and M. Mohammadi 1999. Structural basis for FGF receptor dimerization and activation. Cell. 98, 641-650.

9. Mohammadi, M., I. Dikic, A. Sorokin, W.H. Burgess, M. Jaye and J. Schlessinger 1996. Identification of six novel autophosphorylation sites on fibroblast growth factor receptor 1 and elucidation of their importance in receptor activation and signal transduction. Mol. Cell. Biol. 16, 977-989.

10. Martinez, N., C.A. Garcia-Dominguez, B. Domingo, J.L. Oliva, N. Zarich, A. Sanchez, S. Gutierrez-Eisman, J. Llopis and J.M. Rojas 2007. Sprouty2 binds Grb2 at two different proline-rich regions, and the mechanism of ERK inhibition is independent of this interaction. Cell. Signal. 19, 2277-2285.

11. Beenken, A. and M. Mohammadi 2009. The FGF family: Biology, pathophysiology and therapy. Nat. Rev. Drug Discov. 8, 235-253.

12. Turner, N. and R. Grose 2010. Fibroblast growth factor signalling: From development to cancer. Nat. Rev. Cancer. 10, 116-129.

13. Wesche, J., K. Haglund and E.M. Haugsten 2011. Fibroblast growth factors and their receptors in cancer. Biochem. J. 437, 199-213.

14. Stephens, P., S. Edkins, H. Davies, C. Greenman, C. Cox, C. Hunter, G. Bignell, J. Teague, R. Smith, C. Stevens, S. O'Meara, A. Parker, P. Tarpey, T. Avis, A. Barthorpe, L. Brackenbury, G. Buck, A. Butler, J. Clements, J. Cole, E. Dicks, K. Edwards, S. Forbes, M. Gorton, K. Gray, K. Halliday, R. Harrison, K. Hills, J. Hinton, D. Jones, V. Kosmidou, R. Laman, R. Lugg, A. Menzies, J. Perry, R. Petty, K. Raine, R. Shepherd, A. Small, H. Solomon, Y. Stephens, C. Tofts, J. Varian, A. Webb, S. West, S. Widaa, A. Yates, F. Brasseur, C.S. Cooper, A.M. Flanagan, A. Green, M. Knowles, S.Y. Leung, L.H. Looijenga, B. Malkowicz, M.A. Pierotti, B. Teh, S.T. Yuen, A.G. Nicholson, S. Lakhani, D.F. Easton, B.L. Weber, M.R. Stratton, P.A. Futreal and R. Wooster 2005. A screen of the complete protein kinase gene family identifies diverse patterns of somatic mutations in human breast cancer. Nat. Genet. 37, 590-592.

15. Easton, D. F., K.A. Pooley, A.M. Dunning, P.D. Pharoah, D. Thompson, D.G. Ballinger, J.P. Struewing, J. Morrison, H. Field, R. Luben, N. Wareham, S. Ahmed, C.S. Healey, R. Bowman, SEARCH collaborators, K.B. Meyer, C.A. Haiman, L.K. Kolonel, B.E. Henderson, L. Le Marchand, P. Brennan, S. Sangrajrang, V. Gaborieau, F. Odefrey, C.Y. Shen, P.E. Wu, H.C. Wang, D. Eccles, D.G. Evans, J. Peto, O. Fletcher, N. Johnson, S. Seal, M.R. Stratton, N. Rahman, G. Chenevix-Trench, S.E. Bojesen, B.G. Nordestgaard, C.K. Axelsson, M. Garcia-Closas, L. Brinton, S. Chanock, J. Lissowska, B. Peplonska, H. Nevanlinna, R. Fagerholm, H. Eerola, D. Kang, K.Y. Yoo, D.Y. Noh, S.H. Ahn, D.J. Hunter, S.E. Hankinson, D.G. Cox, P. Hall, S. Wedren, J. Liu, Y.L. Low, N. Bogdanova, P. Schurmann, T. Dork, R.A. Tollenaar, C.E. Jacobi, P. Devilee, J.G. Klijn, A.J. Sigurdson, M.M. Doody, B.H. Alexander, J. Zhang, A. Cox, I.W. Brock, G. MacPherson, M.W. Reed, F.J. Couch, E.L. Goode, J.E. Olson, H. Meijers-Heijboer, A. van den Ouweland, A. Uitterlinden, F. Rivadeneira, R.L. Milne, G. Ribas, A. Gonzalez-Neira, J. Benitez, J.L. Hopper, M. McCredie, M. Southey, G.G. Giles, C. Schroen, C. Justenhoven, H. Brauch, U. Hamann, Y.D. Ko, A.B. Spurdle, J. Beesley, X. Chen, kConFab, AOCS Management Group, A. Mannermaa, V.M. Kosma, V. Kataja, J. Hartikainen, N.E. Day, D.R. Cox and B.A. Ponder 2007. Genome-wide association study identifies novel breast cancer susceptibility loci. Nature. 447, 1087-1093.

16. Lu, P., A.J. Ewald, G.R. Martin and Z. Werb 2008. Genetic mosaic analysis reveals FGF receptor 2 function in terminal end buds during mammary gland branching morphogenesis. Dev. Biol. 321, 77-87.

17. Hunter, D. J., P. Kraft, K.B. Jacobs, D.G. Cox, M. Yeager, S.E. Hankinson, S. Wacholder, Z. Wang, R. Welch, A. Hutchinson, J. Wang, K. Yu, N. Chatterjee, N. Orr, W.C. Willett, G.A. Colditz, R.G. Ziegler, C.D. Berg, S.S. Buys, C.A. McCarty, H.S. Feigelson, E.E. Calle, M.J. Thun, R.B. Hayes, M. Tucker, D.S. Gerhard, J.F. Fraumeni Jr, R.N. Hoover, G. Thomas and

S.J. Chanock 2007. A genome-wide association study identifies alleles in FGFR2 associated with risk of sporadic postmenopausal breast cancer. Nat. Genet. 39, 870-874.

18. Tannheimer, S. L., A. Rehemtulla and S.P. Ethier 2000. Characterization of fibroblast growth factor receptor 2 overexpression in the human breast cancer cell line SUM-52PE. Breast Cancer Res. 2, 311-320.

19. Adnane, J., P. Gaudray, C.A. Dionne, G. Crumley, M. Jaye, J. Schlessinger, P. Jeanteur, D. Birnbaum and C. Theillet 1991. BEK and FLG, two receptors to members of the FGF family, are amplified in subsets of human breast cancers. Oncogene. 6, 659-663.

20. Munro, N. P. and M.A. Knowles 2003. Fibroblast growth factors and their receptors in transitional cell carcinoma. J. Urol. 169, 675-682.

21. Black, P. C. and C.P. Dinney 2008. Growth factors and receptors as prognostic markers in urothelial carcinoma. Curr. Urol. Rep. 9, 55-61.

22. Lajeunie, E., S. Heuertz, V. El Ghouzzi, J. Martinovic, D. Renier, M. Le Merrer and J. Bonaventure 2006. Mutation screening in patients with syndromic craniosynostoses indicates that a limited number of recurrent FGFR2 mutations accounts for severe forms of pfeiffer syndrome. Eur. J. Hum. Genet. 14, 289-298.

23. Robertson, S. C., A.N. Meyer, K.C. Hart, B.D. Galvin, M.K. Webster and D.J. Donoghue 1998. Activating mutations in the extracellular domain of the fibroblast growth factor receptor 2 function by disruption of the disulfide bond in the third immunoglobulin-like domain. Proc. Natl. Acad. Sci. U. S. A. 95, 4567-4572.

24. Dutt, A., H.B. Salvesen, T.H. Chen, A.H. Ramos, R.C. Onofrio, C. Hatton, R. Nicoletti, W. Winckler, R. Grewal, M. Hanna, N. Wyhs, L. Ziaugra, D.J. Richter, J. Trovik, I.B. Engelsen, I.M. Stefansson, T. Fennell, K. Cibulskis, M.C. Zody, L.A. Akslen, S. Gabriel, K.K. Wong, W.R. Sellers, M. Meyerson and H. Greulich 2008. Drug-sensitive FGFR2 mutations in endometrial carcinoma. Proc. Natl. Acad. Sci. U. S. A. 105, 8713-8717.

25. Pandith, A. A., Z.A. Shah and M.A. Siddiqi 2013. Oncogenic role of fibroblast growth factor receptor 3 in tumorigenesis of urinary bladder cancer. Urol. Oncol. 31, 398-406.

26. Pollock, P. M., M.G. Gartside, L.C. Dejeza, M.A. Powell, M.A. Mallon, H. Davies, M. Mohammadi, P.A. Futreal, M.R. Stratton, J.M. Trent and P.J. Goodfellow 2007. Frequent activating FGFR2 mutations in endometrial carcinomas parallel germline mutations associated with craniosynostosis and skeletal dysplasia syndromes. Oncogene. 26, 7158-7162.

27. Haugsten, E. M., J. Malecki, S.M. Bjorklund, S. Olsnes and J. Wesche 2008. Ubiquitination of fibroblast growth factor receptor 1 is required for its intracellular sorting but not for its endocytosis. Mol. Biol. Cell. 19, 3390-3403.

28. Belleudi, F., L. Leone, M. Maggio and M.R. Torrisi 2009. Hrs regulates the endocytic sorting of the fibroblast growth factor receptor 2b. Exp. Cell Res. 315, 2181-2191.

29. Haugsten, E. M., J. Malecki, S.M. Bjorklund, S. Olsnes and J. Wesche 2008. Ubiquitination of fibroblast growth factor receptor 1 is required for its intracellular sorting but not for its endocytosis. Mol. Biol. Cell. 19, 3390-3403.

30. Haugsten, E. M., V. Sorensen, A. Brech, S. Olsnes and J. Wesche 2005. Different intracellular trafficking of FGF1 endocytosed by the four homologous FGF receptors. J. Cell. Sci. 118, 3869-3881.

31. Schlessinger, J., A.N. Plotnikov, O.A. Ibrahimi, A.V. Eliseenkova, B.K. Yeh, A. Yayon, R.J. Linhardt and M. Mohammadi 2000. Crystal structure of a ternary FGF-FGFR-heparin complex reveals a dual role for heparin in FGFR binding and dimerization. Mol. Cell. 6, 743-750.

32. Hung, K. W., T.K. Kumar, Y.H. Chi, I.M. Chiu and C. Yu 2004. Molecular cloning, overexpression, and characterization of the ligand-binding D2 domain of fibroblast growth factor receptor. Biochem. Biophys. Res. Commun. 317, 253-258.

**Fluorescence Quenching Mechanism of Fibroblast Growth Factor 1**

**Introduction**: Tryptophan serves as a critical chromophore in biological fluorescence experiments that is sensitive to the surrounding electrostatic environment (1, 2). Tryptophan residues exhibit the largest fluorescence quantum yields of the naturally occurring amino acids. These characteristics allow tryptophan to be an excellent intrinsic fluorophore to probe the structural properties of proteins. The properties of a protein commonly monitored by fluorescence include folding/unfolding, ligand binding and external quencher accessibility. (3-6) Many fluorescence experiments take advantage of changes in fluorescence intensity, wavelength maximum ($\lambda_{max}$), fluorescence lifetimes, band shape and energy transfers. Tryptophan fluorescence experiments monitoring wavelength maximum and fluorescence intensity experiments are particularly sensitive to the microenvironment of the tryptophan residue. The fluorescence sensitivity of tryptophan to the local electrostatic environment is further explained by the Stokes shift.

The Stokes-shift is the difference between the wavelength of the maximal absorbance and maximal emission. Changes in the Stokes-shift are attributed to the rearrangement of dipoles around the tryptophan residue upon excitation of the tryptophan. Both the solvent and the protein environment may influence the Stokes-shift (7). Fluorescence intensity is determined by the excited state electron density shift from the indole ring to the electron acceptor (adjacent side chain, solvent or amide backbone).(8) The electron build-up on the tryptophan residues have two excited states, $^1L_a$ and $^1L_b$. The $^1L_a$ is the fluorescing state of tryptophan residues. (9) Rapidly quenched tryptophan residues results in a decrease in the electron build-up on the benzene ring of tryptophan. As a result, it is possible for proteins to contain a tryptophan but display diminished tryptophan fluorescence. Tryptophan fluorescence quenching mechanisms are critical towards understanding the fluorescence intensity of proteins.

Tryptophan fluorescence quenching may occur through both radiative and non-radiative mechanisms. The non-radiative contributors towards fluorescence quenching include intersystem crossing, solvent quenching, excited-state proton transfer and excited-state electron transfer (10-16). The quenching mechanism of buried tryptophan residues in proteins is commonly achieved though excited-state electron transfer. Tryptophan excited-state electron transfer occurs by the excited-state electron transferring from the indole ring to the benzene ring on the tryptophan residue (17). The electron may then be transferred to an electron acceptor of nearby amino acid side chain or to the peptide backbone of the protein. The side chains capable of quenching an excited state electron from tryptophan residues are limited. The electron-accepting amino acids include cysteine (oxidized and reduced), thiolate (deprotonated cysteine), histidine , glutamic acid (pH <5), aspartic acid (pH <5), N-acylated glutamine and asparagine (18). The efficiency of the excited-state electron transfer may be enhanced by the angle of the tryptophan relative to the electron acceptor as well as charges surrounding the tryptophan side chain (18).

The angle of the tryptophan relative to the electron acceptor changes the energy required for the electron transfer. The rotameric state of the tryptophan depends on the $\chi_1$ and $\chi_2$ angle. Rotation about $\chi_1$ and $\chi_2$ provide nondegenerate states of electron transfer (19). Tryptophan residues confined to angles decreasing the efficiency of electron transfer may lead to a build-up of excited-state electron population allowing for increased fluorescence. Likewise, tryptophan side chains allowed to freely rotate will be capable of allowing for efficient electron transfer to an electron acceptor. The second contributing factor to fluorescence lifetime is the charge distribution of amino acid side chains surrounding the tryptophan side chain.

Following excitation of the tryptophan residue, the excited-state electron is transferred from the indole ringe to the benzene ring of tryptophan. The excited-state electrons that do not

undergo radiative relaxation will be transferred to a side chain or to the peptide backbone of the protein. The rate of excited-state electron transfer is accelerated by placement of positively charged near the benzene ring of tryptophan (20-22). Accelerating the transfer of the excited-state electron to an electron acceptor prevents the build-up of excited-state electrons on the benzene ring of tryptophan side chains (23). Decreasing this population of excited state electrons decreases the fluorescence lifetime. Conversely, placement of negatively charged residues surrounding the benzene portion of a tryptophan can act to inhibit the transfer of the excited-state electrons to an electron acceptor (24).

This rare phenomenon of highly decreased tryptophan fluorescence may further be masked by tyrosine fluorescence (25-28). The occurrence of this phenomenon is observed in proteins azurin and fgf-1. Azurin has been highly studied, but the FGF-1 fluorescence has been given little explanation for the observed fluorescence.

Fibroblast growth factor-1 (fgf-1) is a critical tyrosine kinase binding protein that regulates key cellular functions. Interactions of fgf-1 with the fibroblast growth factor receptor domain D2 act to regulate angiogenesis, cell differentiation, neurogenesis and tumor growth. In addition to the FGF receptor the fgf protein binds to heparin. The heparin-fgf-1 interaction is believed to inhibit proteolysis of the fgf-1 protein on the cell surface. The fgf-1 protein is a 16-kDa protein composed of 12 antiparallel β-sheets in trefoil architecture. The fgf-1 protein sequence contains a single tryptophan residue and 8 tyrosine residues. The fluorescence spectrum of fgf-1 shows a wavelength maximum of ~307 nm.

**Materials and Methods**

***Mutagenesis, overexpression and protein purification:*** The mutations on the FGF domain (residues, 145-255) were generated using the *Quikchange* kit (Stratagene). The mutation was confirmed by automated DNA sequencing. Wild type and the FGF mutants were overexpressed and purified from *Escherichia coli* [BL21 (pLys) strain] according to the method reported previously.

***Far UV Circular Dichrosim (CD):*** data on the wild type FGF and the FGF mutants were acquired using a Jasco J-710 spectropolarimeter. Protein solutions (90-100 uM) were prepared in 10 mM phosphate buffer containing 100 mM NaCl and 50 mM ammonium sulfate (pH 6.5). Wavelength scans were set to 250-190 nm. CD measurements were made using a 0.1 cm pathlength cuvette. A total of 10 scans were averaged for each sample.

***Fluorescence spectroscopy:*** measurements were made using a Hitachi F-2500 fluorimeter. Fluorescence measurements were made using a 1.0 cm pathlength and the concentration of each protein sample was adjusted to ~50 μM. Excitation wavelength was set to 280 nm and intrinsic tryptophan emission was measured from 300 nm to 450 nm. 8-anilino-1-napthalene sulphonate (ANS) binding experiments were performed using an excitation wavelength of 390 nm and an emission wavelength range of 450 nm- 600 nm. In the ANS titration experiments, protein samples were titrated with 3 μl aliquots of 10 mM ANS in 10 mM phosphate buffer containing 100 mM NaCl and 50 mM ammonium sulfate at pH 6.5.

***Differential scanning calorimetry (DSC):*** DSC measurements were performed using a DASM-1M calorimeter. Protein concentration used was in the range of 1.0 – 1.5 mg/ml in 10 mM phosphate buffer containing 50 mM ammonium sulfate and 100 mM NaCl (pH ~6.5). The scan

rate was set to 1 °C/min and protein samples were heated from 10 °C - 90°C. Data were analyzed using the Origin DSC software provided by Microcal Inc.

***Isothermal titration caolorimetry (ITC):*** ITC measurements were performed using Microcal VP titration calorimeter (Northhampton, MA, USA). Titrations consisted of 5-10 µl injections of 0.5 mM sucrose octasulfate (a heparin analog) delivered into 0.050 mM concentration of the D2 domain. Injections were delayed for 3.5 minutes to allow the titration peak to return to the baseline prior to additional injections. The titrations curves were analyzed using Origin software supplied by Microcal Inc.

***NMR spectroscopy:*** $^{1}H$-$^{15}N$ HSQC data were acquired at 298 °K using 0.5 mM $^{15}N$ labeled D2 domain in 10 mM phosphate buffer (prepared in 95% $H_2O$ + 5 %$D_2O$, pH 6.5) containing 50 mM ammonium sulfate and 100 mM NaCl. All experiments were performed using Bruker Avance 700 MHz and 500 MHz NMR spectrometers equipped with cryoprobes. NMR data were referenced to the $^{1}H$ resonance frequency of 2,2-dimethyl-2-silapentane-5-sulfonic acid (DSS).

**Results**

The secondary structure of the FGF-1 domain is a 16 kDa protein that includes 12 antiparallel β-strands arranged in a trefoil fold to form a β-barrel structure (fig. 6.1). Tryptophan 121 is the only tryptophan residue in the FGF-1 structure. This tryptophan is highly conserved in the fgfs. Tryptophan 121 is placed between β-strand 9 and β-strand 10. The fgf-1 residues responsible for binding to heparin include Arg-20, Asn-94, Asn-116, Gln-117, Val-122, Lys-126, Gln-131, Lys-132 and Thr-133.

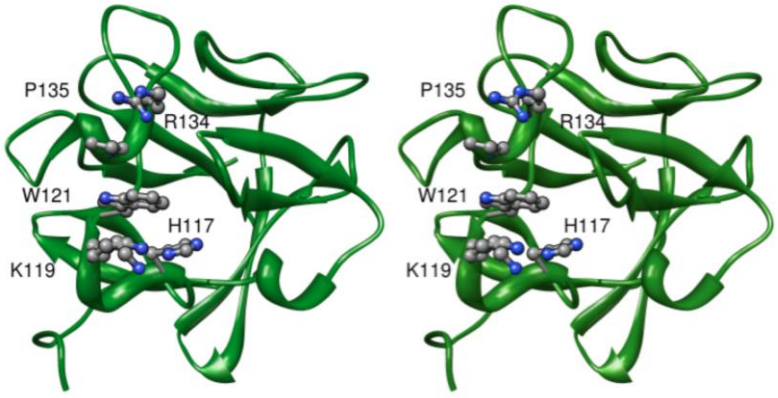


**Figure 6.1** – Stereo-view of the Ribbon structure of FGF-1. Tryptophan 121 is located centrally between residues P135 and H117.

Nearby strong quenching residue His-117 is placed ~3.7 Å in distance from Trp-122. Histidine is considered to be a strong fluorescent quenching side-chain. Additionally, placed adjacent to His-117 is Lys-120 that is only 4 Å in distance from the tryptophan side-chain. Positively charged residues placed near a fluorescent quenching side chain aids in the excited state electron transfer from the tryptophan to an electron-accepting residue. Additionally, the backbone of proline 135 is located ~3.75 Å in distance from the side chain of tryptophan. Proline 135 has been cited by Blaber et. al. as the quenching residue of tryptophan 121 (29) Located directly behind Pro-135 is Arg-133 that could aid in the excited-state electron transfer from the tryptophan residue to the backbone of Pro-135. This diversity of fluorescence quenching side chain residues surrounding Trp-122 has required the synthesis of multiple mutants to determine characterize the quenching mechanism. In order to address this multiple fluorescence quenching mechanisms we have made FGF H117A, K120E, W122Y, FGF P135G and FGF H117A/P135G.

***The steady-state fluorescence the mutants His-117 and P135G of fgf-1 contribute to the quenching mechanism in fgf-1.*** The steady-state fluorescence of wild type fgf-1 shows a wavelength maximum at ~306 nm. The fluorescence spectrum of wild-type fgf-1 in 6M urea results in a wavelength maximum of 346 nm. The shift in the maximum wavelength suggests the tryptophan side chain is efficiently quenched in the native fgf-1 structure. The W122L mutant of fgf-1 shows a wavelength maximum of ~306 nm. This spectrum suggests the fluorescence observed in fgf-1 is tyrosine fluorescence and not tryptophan fluorescence.

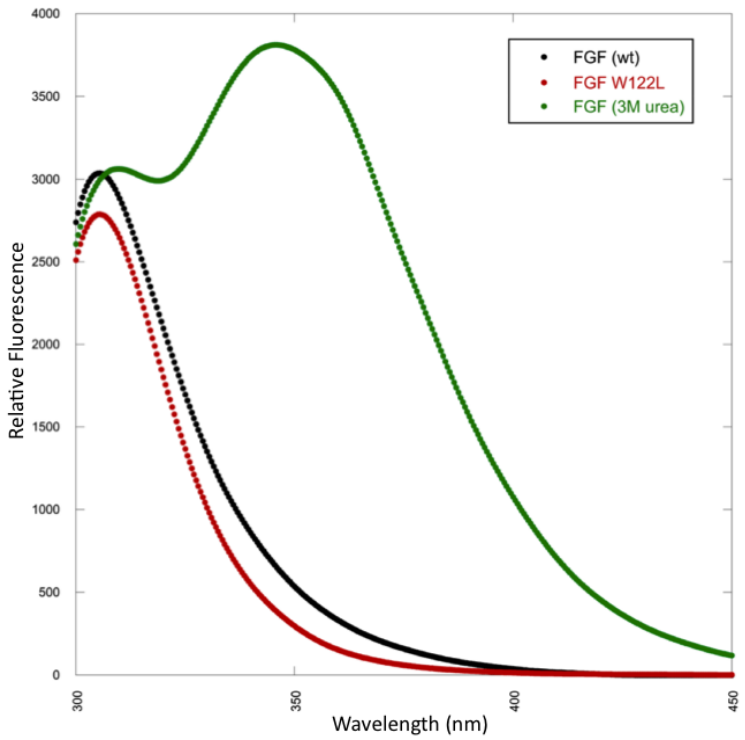


Figure 6.2 – steady-state fluorescence of fgf-1 (wt), fgf W122L and fgf-1 (3M urea). The steady state fluorescence excitation wavelength was 280nm and emission was measured from 300nm – 450nm.

The steady-state fluorescence spectrum (fig. 2) includes the mutants of fgf-1. The K120E mutant of fgf-1 exhibits only a slight red shift in the wavelength maximum. Mutants H117A and P135G both result in a wavelength maximum (~306 nm). However, the H117A and P135G mutants

show a moderate shoulder peak occurring near 350 nm. The H117A/P135G mutant shows the same maximum wavelength maximum as wild type fgf-1. However, the H117A/P135G mutant shows a significant shoulder peak occurring at ~347 nm. The increased fluorescence occurring at 347 nm suggests an increase in tryptophan fluorescence.

However, the fluorescence spectrum of the H117A/P135G mutant of fgf-1 does not reflect the denatured (3m urea) sample fluorescence. This data suggests the tryptophan fluorescence quenching mechanism is partially impaired by the H117A/P135G mutant.

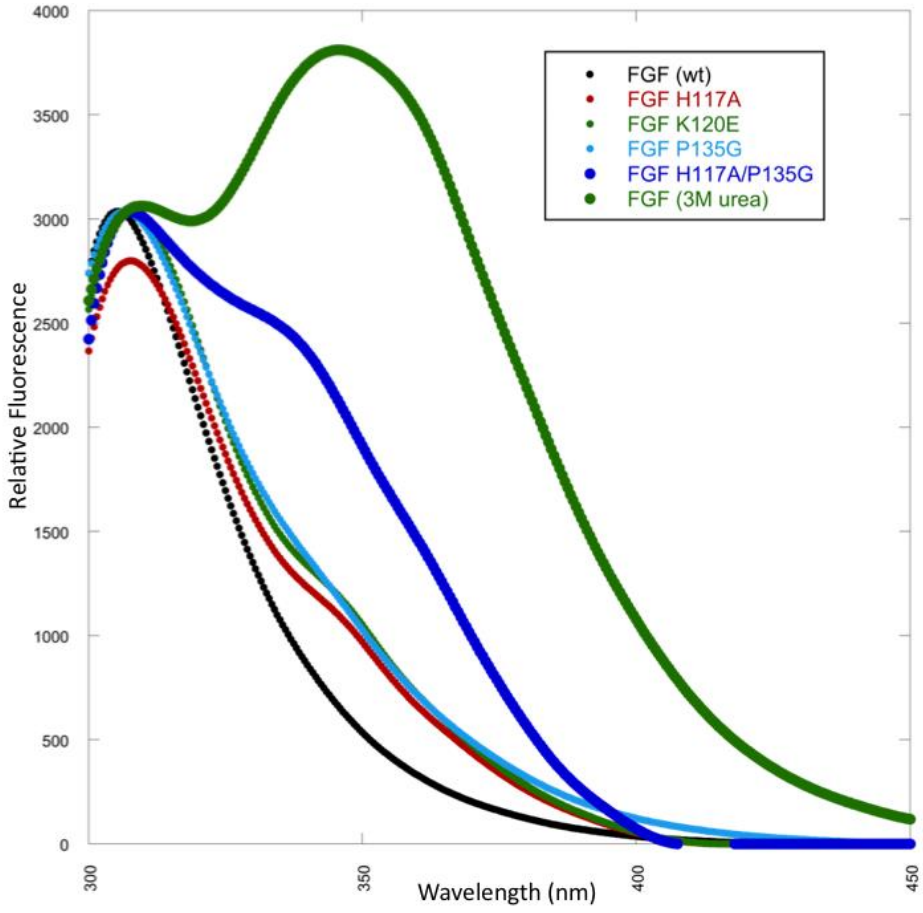


**Figure 6.3 –** Steady-state fluorescence spectrum of each of the mutants of fgf-1. The excitation wavelength was 280nm.

***The H117A and P135G mutations do not significantly perturb the backbone conformations of FGF-1.*** Far UV CD spectrum of the wild type FGF-1 domain shows a strongly negative ellipticity band around 220 nm and a positive ellipticity peak centered at 205 nm. These features of the far UV CD spectrum are typical of β-sheets arranged in a β-sandwich structure. Interestingly, the far UV CD spectrum of the H117A and P135G mutants superimpose quite well with that of the wild type of the D2 domain suggesting that these mutations causes no or minimal perturbations in the secondary structure of the receptor domain. Maintaining a wild type fold is critical to understand the fluorescence quenching mechanism of FGF-1. The CD suggests the secondary structure of the FGF-1 mutants is not significantly changed from that of wild type.

***The FGF-1 mutations do not significantly affect the stability of the FGF domain:*** Differential scanning calorimetry is a versatile technique that can be used to directly probe the thermodynamic stability of proteins. The melting thermogram of the wild type FGF domain shows a relatively sharp melting transition ($T_m$~48 ºC), from the folded to the unfolded state. The $T_m$ value does not appear to significantly change due to the W122L, P135G or K120E mutations. The W122L mutation resulted a decrease in $T_m$ value by 5 °C. The K120E and P135G mutants of FGF-1 resulted in a decrease of $T_m$ value of ~3°C compared to wild type. These results suggest that the thermodynamic stability of the receptor domain is not significantly affected by the mutation.

Differential scanning calorimetry was also used to determine the thermodynamic properties of the each of the FGF-1 mutants in the presence of SOS. The ligand SOS binds to wild type FGF-1 with relatively high affinity ($K_D$ ~ 7 μM). The DSC experiment of wild type FGF in the presence of SOS reflects the high affinity interaction through increased $T_m$ values.

The change in the wild type $T_m$ value with the addition of SOS results in an increase by 6 °C. Each of the mutants of FGF-1 resulted in similar increases in $T_m$ value when compared to wild type. However, the K120E mutant of FGF-1 resulted in a 10 °C increase in $T_m$ value in the presence of SOS. This data suggests the K120E mutant of FGF-1 may stabilize the interactions formed with SOS. Additionally, the W122L and P135G DSC $T_m$ values suggest the mutations do not significantly change the interactions with heparin.

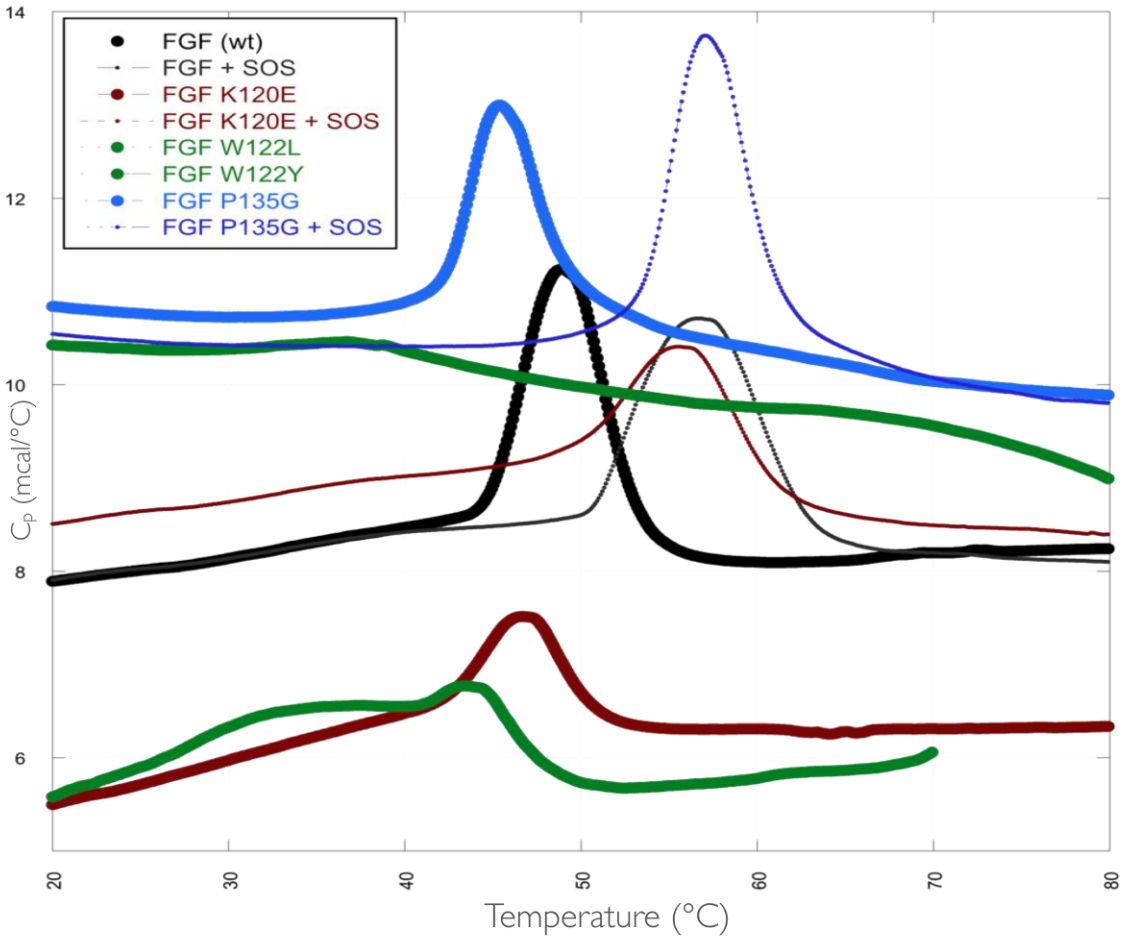


**Figure 6.4** – Shows the dsc scans for each of the mutants of FGF-1. The mutants W122L ($T_m$~37°C) and W122Y ($T_m$~45°C) show a significant decrease in stability when compared to FGF-1 wild-type ($T_m$~49°C).

***FGF-1 mutation decreases heparin-binding affinity:*** FGF-1 is forms binding interactions with both fibroblast growth factor receptor and heparin. Isothermal titration calorimetry (ITC) experiments were performed to examine the effect(s) of the mutation of FGF on the affinities with heparin. ITC is a useful technique to characterize the protein/ligand interactions as it relies on the heat evolved or absorbed during binding interactions.

Heparin is polydisperse and therefore it is challenging to obtain an accurate estimation of its binding affinity to proteins. In this context, we used polyanionic sucrose octasulfate (SOS) to represent heparin binding interactions with the FGF domain. Sucrose octasulfate, unlike heparin, is monodisperse and can be obtained in the pure form (>99% purity). In addition, SOS has been demonstrated to be a good structural and functional mimic for heparin.

Isothermogram representing the binding of wild type FGF domain to SOS is sigmoidal and the binding constant ($K_d$) characterizing the SOS-D2 domain interaction(s) is ~ 7.2 µM. SOS and D2 domain bind to each other in a 1:1 stoichiometry. Interestingly, each of the mutants show very similar binding affinities when compared to wild type interactions with SOS. This data suggests each of the mutation in the FGF-1 domain do not significantly change the binding interactions with SOS.

***Structural changes resulting from the mutants in the FGF-1 domain*:** The changes in fluorescence quenching were further investigated for any structural changes resulting from the mutations. In this context, multidimensional NMR experiments were performed to assess the plausible structural changes induced by the FGF mutations and also understand the consequences of the conformational change. Two-dimensional $^{1}H$-$^{15}N$ HSQC spectrum is a finger-print of the backbone conformation of proteins. Each crosspeak in the $^{1}H$-$^{15}N$ HSQC spectrum represents an

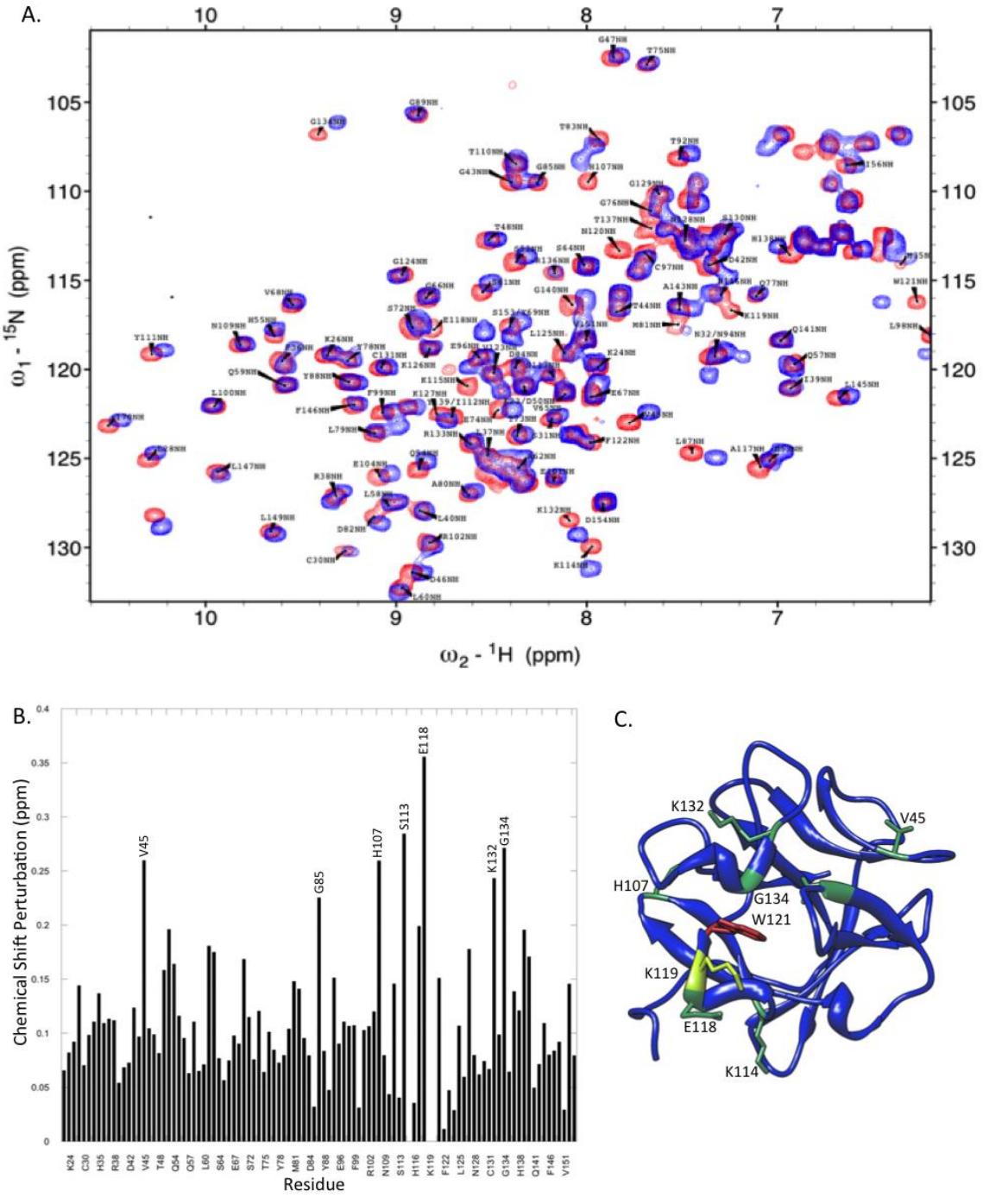


Figure 6.5 – Panel A shows the $^{1}$H-$^{15}$N HSQC of FGF K119E (blue) overlaid on FGF-1 wild type (red). Panel B shows the chemical shift perturbation of the K119E residues shown in the $^{1}$H-$^{15}$N HSQC. Panel C highlights the most perturbed residues (green) on the structure of FGF-1. The tryptophan (red) and mutated residue K119E are shown on the structure of FGF-1.

amino acid in a particular backbone conformation of the protein. In this context, we monitored the backbone conformational changes induced due to the FGF-1 mutations using the $^{1}H$-$^{15}N$ chemical shift perturbation (δ) observed in the HSQC spectra.

The $^{1}H$-$^{15}N$ HSQC of the K119E mutant of FGF-1 overlays the peaks of FGF-1 wild type very closely. The minor perturbations increase in residues neighboring the K119E mutation. The location of the most perturbed residues (K114, K132, G134 and V45) are located near K119, but they are not in the hydrophobic pocket containing W121. This data suggests the structural perturbations resulting from the K119E mutant do not change the chemical environment directly surrounding W121.

The $^{1}H$-$^{15}N$ HSQC of the P135G mutant of FGF-1 is shown in figure X. Panel B shown in figure x highlights the most perturbed residues in the $^{1}H$-$^{15}N$ HSQC. The most perturbed residues encircle the P135G residue. Interestingly, of the six most perturbed residues (T83, G84, L87, K132, G134 and T137) only the side chain of L87 is located in the hydrophobic pocket containing tryptophan 121. However, residues K132 – T137 are all located on the same β-sheet. The location of this β-sheet encloses the hydrophobic box that contains W121. The P135G mutant may significantly reduce the turn induced by proline 135. The current tryptophan fluorescence quenching mechanism suggests this the backbone of P135 acts as the excited-state electron acceptor. Perturbations in this β-sheet may then act to reduce the quenching efficiency.

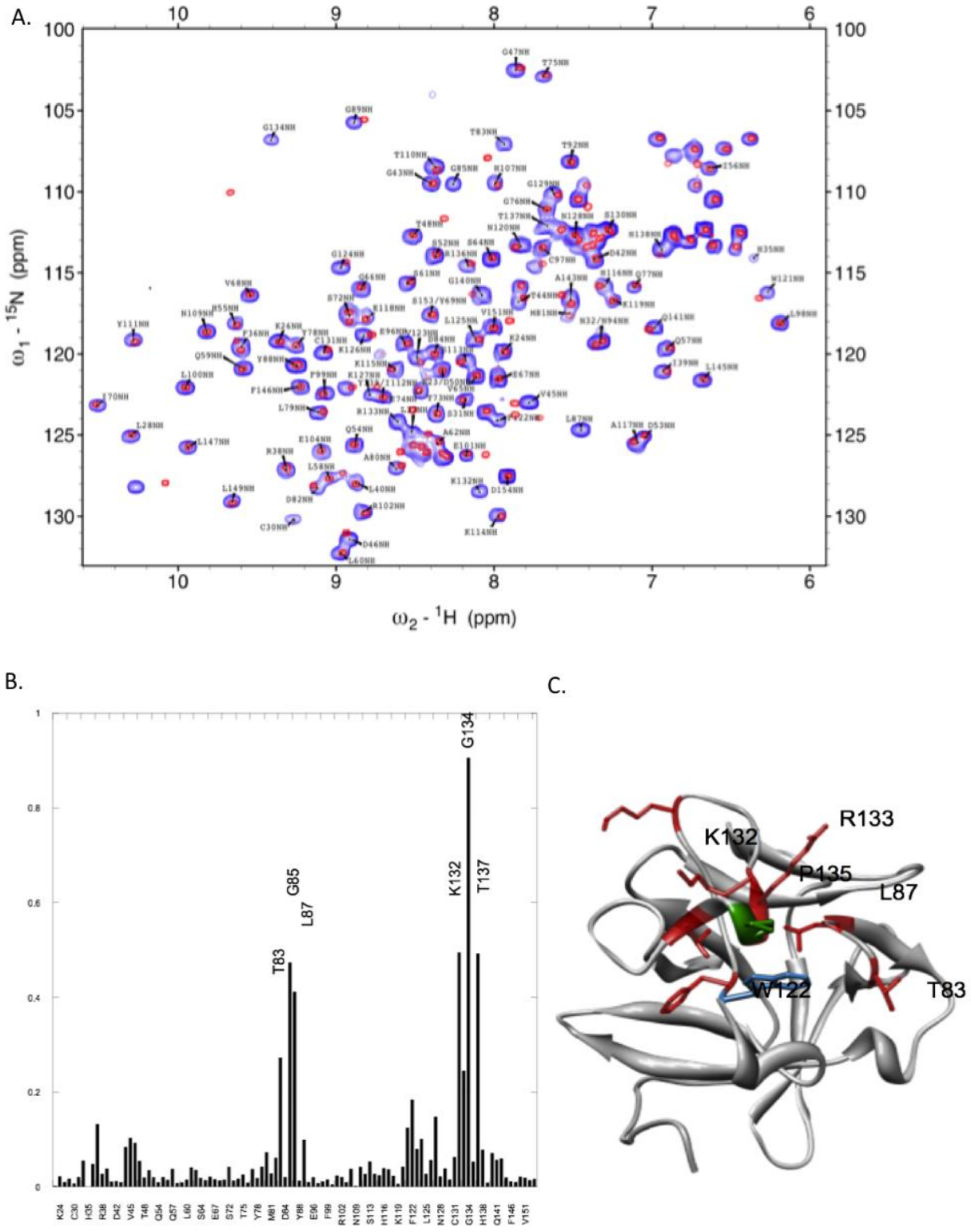


Figure 6.6 – Panel A shows the $^1$H-$^{15}$N HSQC of FGF P135G (red) overlaid on FGF-1 wild type (blue). Panel B shows the chemical shift perturbation of the mutant FGF-1 residues shown in the $^1$H-$^{15}$N HSQC. Panel C highlights the most perturbed residues (green) on the structure of FGF-1. The tryptophan (blue) and mutated residue P135G (green) are shown on the structure of FGF-1.

**Conclusion**

Tryptophan fluorescence of FGF-1 has previously studied, but the efficient fluorescence quenching mechanism is not yet fully understood (29). The first mechanism proposed by Blaber *et al.* suggests the backbone of P135 acts to quench tryptophan 121 (29). Site-directed mutagenesis suggests mutant K119E may not significantly contribute to the steady-state fluorescence quenching mechanism. However, mutant FGF H117A, P135G and H117A/P135G show minor and significant changes in the steady-state fluorescence intensity of tryptophan 121.

FGF P135 residue caused minor increases in the steady-state fluorescence of tryptophan. Thermal denaturation experiments suggest only minor decreases in protein stability result from the P135G mutant of FGF-1. $^{1}$H-$^{15}$N HSQC perturbation plots show perturbations centered at the residues adjacent to P135. $^{1}$H-$^{15}$N HSQC suggests no significant perturbation of the W121 residues as a result of the P135G mutant. The stead-state fluorescence of the P135G mutant shows a minor increase in relative fluorescence occurring near 350 nm. However, the observed tryptophan steady-state fluorescence is significantly less than the tryptophan fluorescence of denatured FGF-1. This suggests the fluorescence quenching mechanism of tryptophan 121 may be supplemented by additional tryptophan quenching mechanisms. Similar to P135, the H117 side chain is in close distance to W121 and capable of quenching tryptophan.

The H117 residue of FGF-1 is approximately 4 Å from the side chain of tryptophan 121. The close proximity of H117 to W121 makes it a possible quenching agent of tryptophan. The differential scanning calorimetry results suggest the H117A mutation does not significantly change the stability of the FGF domain. This data suggests the H117A mutant does not significantly destabilize the structure of the FGF domain. The H117A mutant of FGF-1 resulted

in minor increases in the fluorescence of W121. Steady-state fluorescence data of the H117A mutant shows a minor increase in relative fluorescence near a wavelength of 350 nm. This minor increase in relative fluorescence suggests the H117A mutant causes minor changes in the efficiency of the tryptophan fluorescence quenching mechanism. The role of both H117A and P135G mutants of FGF-1 were determined by introducing the double mutant into FGF.

The H117A/P135G mutant of FGF-1 shows the greatest increase in tryptophan fluorescence. This data suggests the H117 and P135 residues both play a role in the fluorescence quenching mechanism of FGF-1. However, unlike the single mutants the H117A/P135G mutant significantly destabilized the FGF-1 domain. The fluorescence denaturation curve suggests the $T_m$ value is reduced from 48 °C (FGF-1 wt) to ~29 °C for the H117A/P135G mutant of FGF. The denaturation data suggests that in each of these residues plays a significant role in the stability of the FGF domain. The distance of H117 (4 Å) and P135 (3.75 Å) from W121 and might allow for efficient electron transfer from the tryptophan to the backbone of P135 or side chain of H117. Additionally, the position of R134 and K119 are surrounding the electron acceptors (H117 and P135). The position of R134 and K119 introduces an electrostatic environment surrounding W121 that may stabilize excited-state electron transfer from the benzene ring to the electron acceptors. However, single mutation at the K119 residue is not sufficient to increase tryptophan intensity. This may be the result of electron transfer to P135 backbone or to H117.

Mutants P135G and H117A of FGF-1 are implicated in this study as significant contributors of the quenching of tryptophan 121. Two considerations that remain to be answered by this study include the structural changes of FGF-1 that result from each of the mutants and the degree of contribution residues H117A and P135G make toward the quenching of W121. The individual role of amino acids H117 and P135 may contribute toward the quenching of W121

has not been fully elucidated by this study. Steady-state fluorescence may indicate significant changes in the quenching of W121. However, the contribution H117A, P135G and H117A/P135G make individually to the overall rate of electron transfer ($K_{et}$) (quenching of W121) requires time resolved fluorescence experiments. Time-resolved fluorescence will provide the fluorescence lifetimes and the rate of electron transfer for each of the mutants. Additionally, structural information of the FGF-1 protein is required to determine if significant structural changes occurred as a result of the mutations.

The steady-state fluorescence of tryptophan side chains is sensitive to the chemical environment. Mutations made at amino acids known to make significant contributions to the backbone angles (Proline) are also most likely to result in structural changes in the secondary and possibly tertiary structure of FGF-1. Tryptophan-121 sits within a hydrophobic pocket allowing for efficient fluorescence quenching. Mutations resulting in significant structural perturbations of FGF-1 may expose W121 to the solvent and/or remove it from the native tryptophan-quenching environment. The structural changes resulting from a mutation might decrease fluorescence-quenching contributions of amino acids that were not mutated. As a result, the fluorescence quenching changes of FGF-1 that result from mutations must be shown not to significantly change the structure of FGF-1.

**Literature Cited**


1. Eftink, M. R. 1991. Fluorescence techniques for studying protein structure. Methods Biochem. Anal. 35, 127-205.

2. Eisinger, J., A.A. Lamola, J.W. Longworth and W.B. Gratzer 1970. Biological molecules in their excited states. Nature. 226, 113-118.

3. Kubelka, J., W.A. Eaton and J. Hofrichter 2003. Experimental tests of villin subdomain folding simulations. J. Mol. Biol. 329, 625-630.

4. Royer, C. A. 2006. Probing protein folding and conformational transitions with fluorescence. Chem. Rev. 106, 1769-1784.

5. Godoy-Ruiz, R., E.R. Henry, J. Kubelka, J. Hofrichter, V. Munoz, J.M. Sanchez-Ruiz and W.A. Eaton 2008. Estimating free-energy barrier heights for an ultrafast folding protein from calorimetric and kinetic data. J Phys Chem B. 112, 5938-5949.

6. Kimura, T., J.C. Lee, H.B. Gray and J.R. Winkler 2007. Site-specific collapse dynamics guide the formation of the cytochrome c' four-helix bundle. Proc. Natl. Acad. Sci. U. S. A. 104, 117-122.

7. Callis, P. R. 1997. $^{1}L_{a}$ and $^{1}L_{b}$ transitions of tryptophan: Applications of theory and experimental observations to fluorescence of proteins. Methods Enzymol. 278, 113-150.

8. Pan, C. P., P.R. Callis and M.D. Barkley 2006. Dependence of tryptophan emission wavelength on conformation in cyclic hexapeptides. J Phys Chem B. 110, 7009-7016.

9. Broos, J., K. Tveen-Jensen, E. de Waal, B.H. Hesp, J.B. Jackson, G.W. Canters and P.R. Callis 2007. The emitting state of tryptophan in proteins with highly blue-shifted fluorescence. Angew. Chem. Int. Ed Engl. 46, 5137-5139.

10. Kowalska-Baron, A., M. Chan, K. Galecki and S. Wysocki 2012. Photophysics of indole, tryptophan and N-acetyl-L-tryptophanamide (NATA): Heavy atom effect. Spectrochim. Acta A Mol. Biomol. Spectrosc. 98, 282-289.

11. Connolly, M. L. 1983. Solvent-accessible surfaces of proteins and nucleic acids. Science. 221, 709-713.

12. Chen, Y. and M.D. Barkley 1998. Toward understanding tryptophan fluorescence in proteins. Biochemistry. 37, 9976-9982.

13. Shinitzky, M. and R. Goldman 1967. Fluorometric detection of histiine-tryptophan complexes in peptides and proteins. Eur. J. Biochem. 3, 139-144.

14. Van Gilst, M. and B.S. Hudson 1996. Histidine-tryptophan interactions in T4 lysozyme: 'anomalous' pH dependence of fluorescence. Biophys. Chem. 63, 17-25.

15. Vos, R. and Y. Engelborghs 1994. A fluorescence study of tryptophan-histidine interactions in the peptide anantin and in solution. Photochem. Photobiol. 60, 24-32.

16. Hennecke, J., A. Sillen, M. Huber-Wunderlich, Y. Engelborghs and R. Glockshuber 1997. Quenching of tryptophan fluorescence by the active-site disulfide bridge in the DsbA protein from escherichia coli. Biochemistry. 36, 6391-6400.

17. Silvi Antonini, P., W. Hillen, N. Ettner, W. Hinrichs, P. Fantucci, S.M. Doglia, J.A. Bousquet and M. Chabbert 1997. Molecular mechanics analysis of tet repressor TRP-43 fluorescence. Biophys. J. 72, 1800-1811.

18. Alston, R. W., M. Lasagna, G.R. Grimsley, J.M. Scholtz, G.D. Reinhart and C.N. Pace 2008. Peptide sequence and conformation strongly influence tryptophan fluorescence. Biophys. J. 94, 2280-2287.

19. Adams, P. D., Y. Chen, K. Ma, M.G. Zagorski, F.D. Sonnichsen, M.L. McLaughlin and M.D. Barkley 2002. Intramolecular quenching of tryptophan fluorescence by the peptide bond in cyclic hexapeptides. J. Am. Chem. Soc. 124, 9278-9286.

20. Sobolewski, A. L. and W. Domcke 2000. Photoinduced charge separation in indole–water clusters. Chemical Physics Letters. 329, 130-137.

21. Sobolewski, A. L. and W. Domcke 1999. Ab initio investigations on the photophysics of indole. Chemical Physics Letters. 315, 293-298.

22. - Dedonder-Lardeux, C., C. - Jouvet, S. - Perun and A. L. - Sobolewski - External electric field effect on the lowest excited states of indole: Ab initio and molecular dynamics study. *Phys. Chem. Chem. Phys.* 5, 5118-5126.

23. Muino, P. L. and P.R. Callis 2009. Solvent effects on the fluorescence quenching of tryptophan by amides via electron transfer experimental and computational studies. J Phys Chem B. 113, 2572-2577.

24. Mak, C. C., Q.K. Timerghazin and G.H. Peslherbe 2012. Photoinduced electron transfer and solvation dynamics in aqueous clusters: Comparison of the photoexcited iodide-water pentamer and the water pentamer anion. Phys. Chem. Chem. Phys. 14, 6257-6265.

25. Finazzi-Agro, A., G. Rotilio, L. Avigliano, P. Guerrieri, V. Boffi and B. Mondovi 1970. Environment of copper in pseudomonas fluorescens azurin: Fluorometric approach. Biochemistry. 9, 2009-2014.

26. Petrich, J. W., J.W. Longworth and G.R. Fleming 1987. Internal motion and electron transfer in proteins: A picosecond fluorescence study of three homologous azurins. Biochemistry. 26, 2711-2722.

27. Gilardi, G., G. Mei, N. Rosato, G.W. Canters and A. Finazzi-Agro 1994. Unique environment of Trp48 in pseudomonas aeruginosa azurin as probed by site-directed mutagenesis and dynamic fluorescence spectroscopy. Biochemistry. 33, 1425-1432.

28. Mei, G., G. Gilardi, M. Venanzi, N. Rosato, G.W. Canters and A.F. Agro 1996. Probing the structure and mobility of pseudomonas aeruginosa azurin by circular dichroism and dynamic fluorescence anisotropy. Protein Sci. 5, 2248-2254.

29. Blaber, S. I., J.F. Culajay, A. Khurana and M. Blaber 1999. Reversible thermal denaturation of human FGF-1 induced by low concentrations of guanidine hydrochloride. Biophys. J. 77, 470-477.

Summary Conclusions:

Signaling through the fibroblast growth factor receptor is important for maintaining normal cellular functions and development. Critical receptor functions are modulated through non-covalent forces within the FGF receptor and between the D2 domain and FGF or heparin. Non-covalent interactions supported by disease-linked mutation sites emphasize the role many amino acids contribute to the function of the FGF receptor. The disease-linked mutation sites alter cation-π bonds, hydrogen bonds and hydrophobic binding sites.

R203 and W191 are engaged in a cation-π bond that contributes to the stability of the D2 domain. The R203C mutation within the D2 domain is also linked to breast cancer. We have shown mutations R203E, R203L, R203K and R203C in the D2 domain act to destabilize the FGF receptor. Additionally, point at the aromatic pi residue W191A and double mutation W191L/R203L result in decreased stability of the D2 domain. The biophysical characteristics of the W191 mutants reflect the results of the R203 mutations. These results support the NMR solutions structure (pdb: 1wvz). The electrostatic interaction formed by R203 and D225, supported by all published x-ray structures, within the D2 domain was not supported through site-directed mutagenesis data. Our site-directed mutagenesis and multidimensional NMR experiments provide a clarified structural picture of the D2 domain in solution and a new understanding for the contributions cation-π bonds provide to the structure of the FGF receptor.

The non-covalent interactions of Kallmann Syndrome-linked mutants of the FGF receptor are important for the stability and ligand-binding sites of the D2 domain. Differential scanning calorimetry, limited trypsin digestion and ANS titration experiments of KS-linked mutants C179S, W214G, and G238D show a significant decrease in stability and increased backbone flexibility. The increase flexibility of the D2 domain results in a significant decrease in binding

with both heparin and FGF-1. Mutants C179S, W214G and G238D show a loss-of-binding with FGF-1. KS-linked mutants A168S and D225H do no result in a significant decrease in stability of the D2 domain. The A168S and D225H mutants result in a moderate decrease in binding interaction with heparin and a loss-of-binding with FGF-1. The A168 residue forms critical hydrophobic interactions with FGF-1. The A168S mutation replaces a critical hydrophobic residue with a hydrophilic residue, causing a loss-of-binding with FGF-1. $^{1}H$-$^{15}N$ HSQC suggests the D225H mutant of D2 causes moderate perturbations at the C-terminus. The C-terminus of D2 forms a critical hydrophobic pocket required for FGF-1 binding. The D225H mutant results in a loss-of-binding with FGF-1.

The critical non-covalent interactions formed by cation and aromatic-π residues as well KS-linked mutation sites are critical for the ligand-binding and normal function of the FGF receptor.